157-0
176

October 9, 2006

Mark McClellan
Center for Medicare and Medicaid Services
Mail Stop 5-11-24
7500 Security Blvd.
Baltimore MD 21244-1850

Re: CMS-1321-P - Medicare Program; Revisions to Payment Policies Under the Physician Fee Schedule for Calendar Year 2007 and other Changes to Payment Under Part B

Dear Administrator McClellan:

We are survivors of gynecological cancers, their family members, and friends. We are writing to you because we have learned that the Medicare program may change the way it pays for tests that help oncologists choose the most effective chemotherapy for a patient. This type of testing is known as "chemoresponse testing" and is growing in use, particularly as the choice of chemotherapy becomes more complex.

Today, chemoresponse tests are widely used to guide the treatment of ovarian, epithelial and fallopian tube cancers. When a chemoresponse test has been incorporated into the treatment plan, women experience progression-free intervals two to three times longer than women whose treatment did not benefit from these tests.

Medicare has paid for these tests for years as a Part B service. Now, however, Medicare has apparently re-thought this practice and decided that these tests should be billed to the hospital as an inpatient service and included in the hospital's DRG payment. Hospitals, however, are understandably unwilling to pay for tests, which are done in an independent laboratory, after a patient has been discharged, for purposes of guiding treatment that will not be delivered in the hospital.

Perhaps this is being done to save money for Medicare, but the price to women will be high. Because hospitals will not pay, and Medicare rules forbid women to pay privately, this valuable service will become unavailable. We think that is wrong. Please continue the policy of paying for chemoresponse testing as a Part B service.

Sincerely,

GEORGIA ASSOCIATION
of
PATHOLOGISTS

158

Comments of the Georgia Association of Pathologists on the Revisions to Payment Policies Under the Physician Fee Schedule for Calendar Year 2007

[CMS–1321–P]

The Georgia Association of Pathologists (GAP) is pleased to have the opportunity to comment on the proposed revisions to payment policies under the physician fee schedule for calendar year 2007 (the "Proposed Rule"). 71 Fed. Reg. 48982 (Aug. 22, 2006). The GAP is a professional society of pathologists practicing in the state of Georgia. GAP members perform a variety of services that are reimbursed under the physician fee schedule. Thus, GAP members will be significantly affected by the changes in the Proposed Rule. The GAP's comments on the Proposed Rule focus on the revisions to the reassignment and physician self-referral rules, and changes to the rules governing how anatomic pathology services are billed.

PROVISIONS

REASSIGNMENT AND PHYSICIAN SELF-REFERRAL

The GAP is very pleased that CMS is taking action designed to curb the growth of so-called "pod" or condo laboratories. *Id.* at 49054. These arrangements give referring physicians the opportunity to earn revenues based on their own referrals for services performed by other physicians. The Medicare program has always expressed concern about such arrangements and has numerous provisions in place to curb such abuses. CMS is taking an important step in its revision to the reassignment rules and the Stark self-referral laws as a way of curbing these abusive arrangements. However, the GAP believes that in order to be effective in addressing the pod issue, CMS must implement not only the independent contractor reassignment revisions that pertain to the technical and professional components of anatomic pathology, but also measures that would limit the use of part-time employee pathologists in such arrangements.

As CMS recognizes, there are two different, but related, means of curbing these practices: first, clarify the provisions of the prohibition on reassignment, which is designed specifically to prevent Medicare from paying physicians for work performed by others, except in limited situations and second, modify the Stark self-referral law, which is designed to prevent physicians from profiting by referring business to entities with which they have a financial relationship. As CMS notes, many pod arrangements are established either in contravention of these requirements or by taking advantage of ambiguities that exist. Generally, the GAP is supportive of the changes that CMS is making, but we are aware of additional helpful proposals to clarify or more closely define the requirements set out by CMS, as well as to address the issue of part-time employees.

2612 Commons Blvd. • Augusta, Georgia 30909 • Office (706) 738-3119 • FAX (706) 736-8055

Changes to the Reassignment Rule

In the area of the changes to the prohibition on reassignment, CMS makes the following proposals:

- Clarify that physicians acting pursuant to the contractual arrangement exception must still meet the requirements applicable to the purchase of diagnostic testing, with regard to the professional component.

GAP position: **supports** applying current purchased-service limitations in situations of reassignment where the ordering physician that sees the patient is purchasing the professional interpretation from a pathologist, even if the service is reassigned under the contractual arrangement exception. Ordering physicians that bill for purchased diagnostic tests should not be able to circumvent the requirements by calling the purchased service a service performed under a contractual arrangement. However, the GAP does not support making the requirements across the board for all reassigned services under the contractual arrangement exception because of the potential unintended consequences for longstanding and legitimate practice arrangements among pathologists and pathology groups. Pathology groups that choose to engage another pathologist as an independent contractor and reassign payment rely on the contractual arrangement exception without risk of program abuse.

- CMS requests comments on what additional limitations should be put on the purchase of the professional component.

GAP position: **no additional limitations** are necessary on PC purchase, beyond the need to apply the purchased-service rules that already exist and clarifying that they apply in the contracted reassignment setting. But the GAP does not oppose an anti-markup provision for the PC, similar to the requirements for the purchase of the TC, to protect against other abuses by ordering physicians billing for diagnostic testing.

- CMS asks whether all diagnostic testing in the designated health services ("DHS") category should be covered or whether it should apply specifically to pathology; and whether any of the provisions should apply to services performed on the premises of the billing entity, and if so, how to define the premises appropriately.

GAP position: **no comment**

Stark Self Referral Provisions

As CMS recognizes, in order to limit these types of practices in all areas, it is also necessary to further clarify certain specific provisions or exceptions in the Stark self-referral law. The GAP agrees that this is imperative. We are especially concerned that in response to changes in the reassignment rules, discussed above, many pod

arrangements will simply restructure and hire pathologists as part-time employees, which could circumvent the purpose of many of these changes. The GAP believes that the Stark law may provide the most direct way of curbing these new abuses. Therefore, before discussing the other changes proposed by CMS to the Stark provisions, we wish to make one additional proposal designed to limit part-time pathologists.

Part-Time Employment of Pathologists

The GAP is concerned that in response to the provisions in the Proposed Rule, existing and new arrangements may be restructured so that pathologists will be retained as part-time employees rather than independent contractors. For example, a pathologist could become a part-time employee of several different groups under arrangements that potentially satisfy both the reassignment rules and the physician service or in-office ancillary services exceptions to the Stark self-referral provisions. From the standpoint of the group practice and the retained pathologist, the arrangement need not differ significantly from an independent contractor relationship. Thus, the GAP considers it to be essential that CMS address both structures in its rulemaking.

The GAP recognizes that some groups may decide to hire their own pathologist, but they should be required to make the same investment in salaries and capital that any other business would have to make in that endeavor and undertake the same type of business risk. They should not be able to avoid that requirement by re-characterizing an "independent contractor" pathologist as a "part-time employee" pathologist, without incurring the additional costs and risk attendant to hiring that person. Without some limitation on this practice, groups will simply restructure without any risk and continue to profit from their own referrals. The GAP believes that the part-time employee concern could be addressed through modifications in the "group practice" requirements under the Stark self-referral rules or, potentially, through changes in the employee reassignment provision.

We are aware of, and **support** suggested alternative regulatory proposals that would address this issue through the "substantially all" requirements for group practices under Stark. In essence, they would require that, in addition to the group practice as a whole having to perform at least 75% of its patient care services through the group, each individual member would need to perform at least one-half of its patient care services through the group. Such a provision could be limited to pathology services. Alternatively, CMS could, in the same provision of Stark establish a maximum number of group practices to which any one pathologist could belong. The GAP would strongly support this approach. These are more fully described in the comments of the American Clinical Laboratory Association, so they need not be repeated in detail here. Basically, if a pathologist arrangement did not meet this requirement, then the group practice would not be able to bill for pathology services that it refers to the pathologist. We believe that such a provision would limit restructuring that might be anticipated in response to the proposed changes in the contractor reassignment rules.

INDEPENDENT LAB BILLING

In the Proposed Rule, CMS states, "We continue to believe, however, that hospital prospective payment amounts already compensate hospitals for the TC of physician pathology tests and that additional payment under the PFS is inappropriate." *Id.* Therefore, CMS is proposing to amend § 415.130 to provide that, for services furnished after December 31, 2006, an independent laboratory may not bill the carrier for physician pathology services furnished to a hospital inpatient or outpatient.

The GAP believes that the proposed rule misstates the intention of the proposal to discontinue the Grandfather provision, where it states "For services furnished after December 31, 2006, an independent laboratory may not bill the carrier for physician pathology services furnished to a hospital inpatient or outpatient." We believe the intent was to state that "For services furnished after December 31, 2006, an independent laboratory may not bill the carrier for the technical component of physician pathology services furnished to a hospital inpatient or outpatient." We urge CMS to correct this language if this concept is to appear in the final rule.

Given this major change to these historical billing rules, we strongly urge CMS to help hospitals understand their new obligations and move forward to address them to ensure that Medicare beneficiaries have full access to necessary clinical laboratory testing services.

CONCLUSION

Thank you for the opportunity to submit these comments. We look forward to working with CMS to finalize and implement the proposed changes to the physician fee schedule. Please do not hesitate to contact us should you have any questions about this information or need any further information.

Respectfully submitted,

Matthew Fries, MD.

Matthew R. Fries, MD
President, Georgia Association of Pathologists
October 9, 2006

159

DePuy Mitek

a Johnson & Johnson company

October 4, 2006

Honorable Mark B. McClellan, M.D., Ph.D.
Administrator, Centers for Medicare and Medicaid Services
Department of Health & Human Services
Attention: CMS-1321-P
Mail Stop C4-26-05
7500 Security Boulevard
Baltimore, MD 21244-1850

Re: CMS-1321-P Medicare Program: Revisions to Payment Policies Under the Physician Fee Schedule for Calendar Year 2007 and Other Changes to Payment Under Part B

Dear Dr. McClellan:

On behalf of DePuy Mitek Inc., I am pleased to submit comments and recommendations in response to the Revisions to Payment Policies under the Physician Fee Schedule for Calendar Year 2007 and Other Changes to Payment under Part B issued by the Centers for Medicare & Medicaid Services (CMS) in the Federal Register on August 22, 2006. DePuy Mitek is a leading manufacturer of advanced orthopedic medical device technologies.

The FDA approved ORTHOVISC® in February 2004. Since that time, it has been without a permanent J code, which has caused significant access issues. Over the past 2-½ years, we have followed the process; completing three HCPCS applications and participating in two HCPCS panel reviews. To date, ORTHOVISC® remains with a temporary code. In the attached comment letter, we will make the following recommendations:

- Request a new unique code for ORTHOVISC® based on clinical differences, differences in cost of treatment and limited access to care by the Medicare population related to extreme administrative burdens caused by a Not Otherwise Classified (NOC) code.
- A new unique J code is necessary and appropriate for ORTHOVISC® under the established HCPCS process. Assignment of a new J code would recognize the unique characteristics of ORTHOVISC®, distinguish it from other viscosupplements, facilitate patient access and allow for appropriate payment for ORTHOVISC® and other hyaluronic acid (HA) products.
- The proposed 2007 Proposed OPPS Rule eliminates ORTHOVISC®'s existing C code, C 9220. Therefore, a permanent appropriate J code is needed for the use of ORTHOVISC® in the hospital outpatient clinic setting.
- We recommend J codes for sodium hyaluronate products be assigned based on dose ranges to accommodate existing and future products in this category:
  - Nineteen or less mg. per intra-articular injection - current J code 7320
  - Twenty to twenty-nine mg. per intra-articular injection - current J code 7317
  - Thirty and above mg. per intra-articular injection - **new** J code J**XXXX**

Overview

ORTHOVISC® (high molecular weight hyaluronan) is a high molecular weight, ultra-pure natural hyaluronan dissolved in physiological saline. It is used in the treatment of pain due to osteoarthritis (OA) of the knee for patients who have failed to respond adequately to conservative non-pharmacologic therapy and to simple analgesics (e.g. acetaminophen). The following represent the milestones and activity involved in attempting to obtain a unique J code since ORTHOVISC® obtained FDA approval in February 2004.

- J code application submitted in April 2004.
- Request for an OPPS pass through was submitted May 2004 and new C code approved November 2004.
- J code application was resubmitted December 2004 under the new HCPCS application process.
- DePuy Mitek presented clinical and economic information at the HCPCS Panel meeting in May 2005.
- The 2006 Physician Fee Schedule issued in November 2005 HCPCS panel created code 7318 to describe all sodium hyaluronate or derivatives products per mg including ORTHOVISC®.
- In November 2005, CMS reversed decision of the 2006 Final Physician Fee Schedule and previous coding was maintained placing ORTHOVISC® back in NOC and returned all HA products to previous pre-rule codes.
- DePuy Mitek resubmitted J code application for ORTHOVISC® December 2005.
- DePuy Mitek presented clinical, economic and market information at the HCPCS Panel meeting May 2006.

USA

PROUD PARTNER

325 Paramount Drive, Raynham, MA 02767, USA • Tel: +1 (508) 977-3800 • Toll-Free: +1 (800) 356-4835 • Fax: +1 (508) 977-6996

In the past 24 months, there have been over 100,000 ORTHOVISC® injections. Providers, who have determined that ORTHOVISC® is the appropriate treatment for their patients, have experienced severe payment issues due to lack of a specific code including:

- Automatic claim denials based on NOC code;
- Lengthy appeals process with some providers experiencing 1-4 months;
- Resubmission of claims adding an additional 2-4 weeks;
- Manual processing of claim which are more time consuming and results in delay in payment and
- ~46 % decrease in reimbursement from the ORTHOVISC® established Average Selling Price (ASP) due to carriers assigning ORTHOVISC® to J7317 resulting in inappropriate reimbursement.

Unique HCPCS Code for ORTHOVISC®

The request for a new unique code is based on clinical differences; differences in cost of treatment and limited access to care by the Medicare population related to extreme administrative burdens caused by the current NOC code.

Currently there are five FDA approved hyaluronans. Each agent has unique physical properties, dosing and administration schedules as outlined in Table I.

Table I

Brand Name	Generic name	Dose Per Injection	Number of weekly injections per treatment course	Molecular Weight ($X10^6$ D)	Hyaluronan Concentration (mg/ml)
ORTHOVISC®[v]	High Molecular Weight Hyaluronan	30 mg	3 or 4*	1.0 – 2.9	15
Synvisc®	Hylan G-F 20	16 mg	3	6 (Hylan A only)	8
Hyalgan®	Sodium Hyaluronate	20 mg	5	0.5 – 0.73	10
Supartz®	Sodium Hyaluronate	25 mg	3,4,5*	0.62 – 1.17	10
Euflexxa™	Sodium Hyaluronate	20 mg	3	2.4-3.6	10

Adapted from package inserts

*ORTHOVISC® is primarily used as a 3-injection treatment course. A majority of commercial Medical Policies defines ORTHOVISC® as a 3-injection treatment regime and Supartz and Hyalgan as 5-injection treatment regimes.

Aetna Clinical Policy Bulletin # 0179

Arkansas Blue Cross Blue Shield Coverage Policy: Viscosupplementation for the Treatment of Osteoarthritis of the Knee

CLINICAL DIFFERENCES:

In the osteoarthritic joint, the concentration as well as molecular weight of normal hyaluronate decreases in the synovial fluid, which compromises the viscoelastic properties of the joint fluid. The aim of viscosupplementation with hyaluronate products is to restore the elasticity and viscosity of the synovial fluid and provide symptomatic relief of osteoarthritic pain.[1]

Five agents have FDA approval for the intra-articular treatment of knee osteoarthritis. ORTHOVISC® (High Molecular Weight Hyaluronan) is unique from the other four products (Synvisc, Hyalgan, Supartz and Euflexxa) in the following ways:

- ORTHOVISC® is the only product with a 30-mg dose;
- ORTHOVISC® has a higher molecular weight than most other Hyaluronans. Cochrane Review [2] and JAMA Meta-Analysis [3] indicates higher molecular weight product may offer improved pain relief at early, mid and late time points; and

[1] Moreland LW *Arthritis Res Ther* (2003) 5:54-67
[2] Cochrane Group Review, Feb 2005
[3] JAMA, Dec 2003; 290: 3115 - 3121.

- ORTHOVISC® is supplied in the highest hyaluronic acid concentration (mg/ml) of the five products.

There are several reasons why placing ORTHOVISC® in one of the current existing codes is not appropriate.

- The use of code J7317 *Sodium hyaluronate, per 20 to 25 mg dose for intra-articular injection* to report ORTHOVISC® is inappropriate because it specifies a 20 to 25 mg dose and ORTHOVISC®can only be administered as a 30 mg dose.
- The use of code J7320 *Hylan G-F 20, 16 mg, for intra-articular injection* to report ORTHOVISC® is inappropriate because ORTHOVISC® is not Hylan G-F 20, which is a chemically modified Hyaluronan derivative viscosupplement. The brand name for J7320 *Hylan G-F 20* is Synvisc. ORTHOVISC® is a natural *product that is not described by code J7320.*

COST DIFFERENCES:

Table II compares the cost per injection and the cost for a typical complete course of therapy for the five FDA approved viscosupplements currently on the market.

Typically, ORTHOVISC® and Synvisc require a 3-injection treatment program (for a duration of pain relief of 26 weeks at a cost to the Medicare system of ~$800. Hyalgan and Supartz per FDA label require a 5-treatment program for duration of pain relief of 26 weeks for $876, a 10% increase in cost. Euflexxa requires a 3-injection treatment program for duration of pain relief of only 12 weeks at $714.69. While Euflexxa is not approved for repeat treatment, the cost of obtaining 24-week pain relief duration would be $1,429.38, a 79% increase in cost compared to an ORTHOVISC® or Synvisc 3-injection treatment program.

Table II

	ORTHOVISC®	Synvisc	Hyalgan	Supartz	*Euflexxa
	J3590 Per 30 mg	J7320 16mg	J7317 per 20-25 mg	J7317 per 20-25 mg	**J7317 per 20-25 mg
Reimbursement per injection***	$201.08	$198.74	$ 106.71	$ 106.71	106.71
Injection Fee	$ 68.00	$ 68.00	$ 68.00	$ 68.00	$ 68.00
# Injections****	3	3	5	5	3
Duration of Pain Relief	26 weeks	26 weeks	26 weeks	26 weeks	12 weeks
Total Reimbursement w/injection fees	$807.24	$800.22	$873.55	$873.55	$524.13

***Euflexxa - not considered a comparable treatment with only 12 weeks of pain relief is included in analysis to encompass all FDA approved Sodium Hyaluronates**

**Aligned with J7317 by manufacturer ***Q4 ASP 2006 rates

**** # of injections used to obtain state duration of pain relief as stated in package insert

Access Issues

It is important that ORTHOVISC® be assigned a product-specific code to allow Medicare and other payers to seamlessly update coverage guidelines to include ORTHOVISC®and the appropriate product-specific code that should be used to bill ORTHOVISC®. The use of miscellaneous coding continues to result in claims processing delays or denials and increases administrative costs for both physicians and payers. In many carrier environments, the use of an NOC code automatically denies the claim and requires the providers to file an appeal.

We have experienced Medicare carrier environments that are refusing the use of a NOC and requiring the use of J3717. Some carriers are requesting the use of a multiplier depending on the multiplier (1.5 or 2) the product may or may not be adequately reimbursed. Placing ORTHOVISC® in J3717 will impact future ASP for this J code where the products currently assigned to J3717 are similarly priced. Some claim systems require whole integers in the quantity in order to process electronically requiring a 1.5 multiplier to be billed and processed manually. The following examples of how ORTHOVISC® has been treated in the marketplace demonstrate the administrative burden and inadequate reimbursement that an NOC code creates.

Trailblazers (TX, MD, VA, DE, DC)

Trailblazers requires the use of J3717 and responded to inquiry from DePuy Mitek that 2 units should be billed. Trailblazers' rationale is that the code J3717 represents up to a 25mg dose, therefore a 26-mg to 50-mg dose would be considered 2 units. Since ORTHOVISC® is a 30-mg dose it would qualify as 2 units.

Without instructions from Trailblazers (Trailblazers communicated to DePuy Mitek that they do not plan to proactively notify their providers of these instructions) providers are reluctant to document 2 units.

Pinnacle (OK, NM, RI, LA, MO, AR)

In early 2006, Pinnacle was reimbursing ORTHOVISC®, as J3590, which initiated an automatic denial of claim, required provider to appeal and required manual processing. To streamline the process, Pinnacle changed the code for ORTHOVISC® to J3717 and was reimbursed at the ASP of $113.10, 43% below the established ASP for ORTHOVISC® of $199.50. Pinnacle increased the reimbursement to 1.5 units, only to discover that claim could not be processed electronically. In May 2006, Pinnacle reverted to accepting the NOC code, but this continues to cause difficulties in securing timely reimbursement for many providers.

CAHABA (AL, GA, MS)

Reimbursing ORTHOVISC® as J3590 (NOC code), initiates an automatic denial of claim, requires provider to appeal and requires manual processing, causing difficulties in securing timely treatment and reimbursement.

In summary, as noted in the above carrier examples, all of these factors lead to excessive administrative burdens, delays in reimbursement and under reimbursement. Combined, all of these factors lead to barriers to access for the Medicare population and unnecessary inefficiencies in the delivery of care.

Analysis of Proposed J Code Assignment for Sodium Hyaluronates

There are several proposals on possible J code assignment that have been discussed by the HCPCS panel review or previous proposed rules. We have listed several of these proposals below and outlined some of the significant issues that need to be considered in the evaluation of each of these options. It is very important to note that the wrong assignment of codes for these HA products, results in Medicare beneficiary access issues, inappropriate reimbursement by Medicare and inappropriate co-pays by Medicare beneficiaries.

I. Single J Code Bundle Proposal

The **single J Code bundle** proposal advocates assigning all of the current and future sodium hyaluronate products to one J Code. We believe that this is not an adequate or appropriate proposed course of action for the reasons outlined below.

CMS could experience increased expenditures if a single J Code were adopted:

- Increased office visits
- Increased claims processing
- Increased utilization driven by per dose payment proposal
- The current payment for a treatment course of a 3-injection regime (for 26-pain relief duration) is less than a treatment course of a 5-injection regime.

Table III demonstrates the change in ASP based on market share allocation to ASP if a single J code was adapted.

Table III
Estimated ASP + 6% calculation for FY, 2007
(Based upon 2006 Q4 ASP +6% / market share)

HCPCS Code	Description	Brand name	Mg/ Dose	Maximum Allowable ASP +6% Q4 2006	Market Share	Contribution to ASP (ASP*Market Share)
J7317	Sodium hyaluronate injection	Hyalgan	20	$106.71	22%	$ 23.48
J7317	Sodium Hyaluronate injection	Supartz	25	$106.71	11%	$ 11.74
J7317	Sodium Hyaluronate injection	Euflexxa	20	$106.71	2%	$ 2.13
J7320	Hylan G-F 20 injection	Synvisc	16	$198.74	60%	$ 119.24
J3490	High Molecular Weight Hyaluronan	ORTHOVISC©	30	$201.08	5%	$ 10.05
					ASP, +6%	$166.65

The impact of combining all of the sodium hyaluronate products into a single J Code creates an artificial ASP + 6% of $166.65, a $59.94 or 56% increase in payment for products currently assigned to J7317 and a decrease for products in J7320 and J3490 of $32.09 (16%) and $34.43 (17%) respectively. This is illustrated in Table IV.

Table IV
Impact of CMS Expenditure of Single Bundle J Code

HCPCS Code	Description	Brand name	Mg/ Dose	Maximum Allowable ASP +6%, Q4 2006	Maximum Allowable ASP +6%, Q1, 2007	Gain/(loss)
J7317	Sodium Hyaluronate injection	Hyalgan	20	$106.71	$166.65	$59.94
J7317	Sodium Hyaluronate injection	Supartz	25	$106.71	$166.65	$59.94
J7317	Sodium Hyaluronate injection	Euflexxa	20	$106.71	$166.65	$59.94
J7320	Hylan G-F 20 injection	Synvisc	16	$198.74	$166.65	$(32.09)
J3490	High Molecular Weight Hyaluronan	ORTHOVISC®	30	$201.08	$166.65	$(34.43)

Table V demonstrates the impact of increased costs a single J code would have on the course of treatment and the overall cost to the Medicare System. A single J code for the sodium hyaluronate category would create an artificial ASP. As a consequence, the prescribed treatment for a Medicare patient may not be clinically driven but impacted significantly by the margin between pricing and reimbursement.

Projections based on the single J code reimbursement suggest that there would be a shift in market share in Q2 2007 from 3-injection products to the two 5-injection products with 26 weeks of pain relief and to the 3-injection product with 12 weeks of pain relief product. These products currently have lowest ASP.

The projected average expenditure for course of treatment in Q4 2006 is $819.55 at a total cost to the Medicare program of $266,255,633. In Q2 2007, the result of assigning all sodium hyaluronates to one J code, causing a shift in market share allocation, increases the average course of treatment cost to $985.53 and total cost to the Medicare program of $320,267,250.

Table V
Projected Cost of Treatment
2006 Medicare Population Treated with Sodium Hyaluronate
325,000

Q4 2006	Mg / dose	ASP +6%	Injection fee	# of Inj	Course of Treatment Cost	Market Share	Contribution to ASP	Cost of Treatment for Medicare Population
Hyalgan	20	$106.71	$68.00	5	$ 873.55	22%	$ 192.18	
Supartz	25	$106.71	$68.00	5	$ 873.55	11%	$ 96.09	
Euflexxa	20	$106.71	$68.00	3	$ 524.13	2%	$ 10.48	
Synvisc	16	$198.74	$68.00	3	$ 800.22	60%	$ 480.13	
ORTHOVISC®	30	$201.08	$68.00	3	$ 807.24	5%	$ 40.36	
							$ 819.25	$ 266,255,633
Q1 2007								
Hyalgan	20	$166.65	$68.00	5	$ 1,173.25	22%	$ 258.12	
Supartz	25	$166.65	$68.00	5	$ 1,173.25	11%	$ 129.06	
Euflexxa	20	$166.65	$68.00	3	$ 703.95	2%	$ 14.08	
Synvisc	16	$166.65	$68.00	3	$ 703.95	60%	$ 422.37	
ORTHOVISC®	30	$166.65	$68.00	3	$ 703.95	5%	$ 35.20	
							$ 858.82	$ 279,116,175
Q2 2007								
Hyalgan	20	$166.65	$68.00	5	$ 1,173.25	35%	$ 410.64	
Supartz	25	$166.65	$68.00	5	$ 1,173.25	25%	$ 293.31	
Euflexxa	20	$166.65	$68.00	3	$ 703.95	15%	$ 105.59	
Synvisc	16	$166.65	$68.00	3	$ 703.95	20%	$ 140.79	
ORTHOVISC®	30	$166.65	$68.00	3	$ 703.95	5%	$ 35.20	
							$ 985.53	$ 320,297,250

II. Natural vs. Synthetic J Code Proposal

The assignment of J Codes based on natural vs. synthetic product also creates an artificial ASP and we believe an unsubstantiated differentiation in products. All sodium hyaluronate products come from natural sources; some are processed differently. The difference in processing should not be a factor of separation in classification.

Table VI demonstrates the impact that the Natural vs. Synthetic proposal would have on ASP. Gain or loss represents the difference between current maximum allowable payment and the estimated maximum allowable payment based on combining Hyalgan, Supartz, Euflexxa and ORTHOVISC®. Products with lower ASPs benefit from products with higher ASPs combined into one J code.

Table VI
Impact of Natural vs. Synthetic Proposal

HCPCS Code	Description	Brand name	mg/dose	Maximum $ Allowable ASP +6%, Q4 2006	Maximum $ Allowable ASP +6%, Q1, 2007	Gain/ (loss)
J7317	Sodium Hyaluronate injection	Hyalgan	20	$106.71	$118.50	$11.79
J7317	Sodium Hyaluronate injection	Supartz	25	$106.71	$118.50	$11.79
J7317	Sodium Hyaluronate injection	Euflexxa	20	$106.71	$118.50	$11.79
J3490	High Molecular Weight Hyaluronan	ORTHOVISC®	30	$201.08	$118.50	$(81.58)
J7320	Hylan G-F 20 injection	Synvisc	16	$198.74	$198.87	$0.127

Both the Single J Code and Natural vs. Synthetic proposals erodes the confidence level of the ASP program designed by CMS and inhibits innovative introduction into the market place of a 1- or 2- injection product for 26 weeks pain reduction product.

DePuy Mitek Recommendation

We strongly recommend permanent J codes assignment for ORTHOVISC®. We believe based on the clinical differences and the dosing, this would achieve the following:

- minimize the number of codes used in this category;
- address the dosage differences of the products,
- accommodate future product introduction in this category;
- supports CMS' decision to establish separate ASP rates under Medicare Part B; and
- eliminates the creation of an artificial ASP

Table VII outlines DePuy Mitek's recommendations for the descriptors and J Code classifications for current sodium hyaluronan products.

TABLE VII

Brand Name	Generic Name	Dose Per Injection	Current Description	Current Code	Recommended Description	Recommended Code
ORTHOVISC®	High Molecular Weight Hyaluronan	30 mg	Unclassified drugs	J3490	Hyaluronan (sodium hyaluronate) or derivative, **per 30 or more mg**, for intra-articular injection	**J XXXX**
Supartz	Sodium Hyaluronate	25 mg	Sodium hyaluronate, per 20 to 25 mg dose for intra-articular injection	J7317	Hyaluronan (sodium hyaluronate) or derivative, **per 20 to 29 mg**, for intra-articular injection	**J 7317**
Hyalgan	Sodium Hyaluronate	20 mg		J7317		**J 7317**
Euflexxa	Sodium Hyaluronate	20mg		J7317		**J 7317***
Synvisc	Hylan GF-20	16mg	Hylan G-F 20, 16 mg, for intra articular injection	J 7320	Hyaluronan (sodium hyaluronate) or derivative, **per 19 or less mg**, for intra-articular injection	**J 7320**

* Aligned with J7317 by manufacturer

Conclusion

We believe that without a unique J Code assigned to ORTHOVISC® in the upcoming assignment of codes there will be serious access to care issues for the Medicare population to ORTHOVISC®. We recommend that Hyaluronan (sodium hyaluronate) or derivative be assigned to J Codes based on the following dose ranges:

- Nineteen or less mg. per intra-articular injection - current J code 7320
- Twenty to 29 mg. per intra-articular injection - current J code 7317
- Thirty and above mg. per intra-articular injection - new J code JXXXX

We appreciate your consideration of the above comments.

Sincerely,

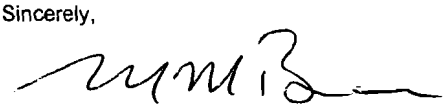

Michael McBreen
Vice President and General Manager - ORTHOVISC® Franchise
DePuy Mitek, a Johnson & Johnson company

160

ReedSmith

Reed Smith LLP
1301 K Street, N.W.
Suite 1100 - East Tower
Washington, D.C. 20005-3373
202.414.9200
Fax 202.414.9299

Joseph W. Metro
Direct Phone: 202.414.9284
Email: jmetro@reedsmith.com

October 10, 2006

Mark McClellan, M.D., Ph.D.
Administrator
Centers for Medicare & Medicaid Services
Department of Health and Human Services
Room 445-G, Hubert H. Humphrey Building
200 Independence Avenue, S.W.
Washington, DC 20201

Re: Medicare Program: Revisions to Payment Policies Under the Physician Fee Schedule for Calendar Year 2007 and Other Changes to Payment Under Part B (CMS-1321-P)

Dear Dr. McClellan:

Reed Smith LLP welcomes the opportunity to comment on behalf of one of our pharmaceutical manufacturer clients concerning CMS's proposed rule on Revisions to Payment Policies Under the Physician Fee Schedule for Calendar Year 2007 and Other Changes to Payment Under Part B (the "Proposed Rule"). The client is one of the country's leading research-based pharmaceutical companies and is devoted to making life-improving medicines available to patients, which include many Medicare beneficiaries.

Our client's comments on the Proposed Rule focus on CMS's provisions regarding ASP calculations (*i.e.*, the section of the Proposed Rule on "ASP Issues"). As detailed below, they address CMS's discussion and proposed definition of bona fide service fees and request for comments on bundling arrangements.

I. Fees Not Considered Price Concessions

In the Proposed Rule, CMS seeks to clarify what it considers to constitute a bona fide service fee and that bona fide service fees are not considered price concessions. To that end, CMS proposes to define bona fide service fees as fees paid by a manufacturer to an entity that represent fair market value for a bona fide, itemized service actually performed on behalf of the manufacturer that the manufacturer would otherwise perform (or contract for) in the absence of the service arrangement, and that is passed on, in whole or in part, to a client or customer of an entity, whether or not the entity takes title to the drug. CMS also proposes to clarify that administrative fees and other fees paid to group purchasing organizations or pharmacy benefit managers are not considered price concessions if they meet the general criteria for bona fide service fees.

Our client supports CMS's efforts to provide additional guidance concerning what constitutes a bona fide service fee. At the same time, our client believes it is imperative that the definition of such fees reflect real-world practices so that it provides a workable and realistic framework that can be used to further refine the calculation of ASP. Our client also requests that, to ensure consistency, CMS

specify in any guidance that its provisions on bona fide service fees apply to the calculation of ASP and Medicaid rebate calculations (e.g., AMP and Best Price).

In response to CMS's solicitation of comments on the specific types of services entities perform, our client does not believe that it is practicable to "itemize" or provide a "laundry list" of services in these comments. Our client recommends that CMS consider establishing a clear standard that, consistent with the personal services safe harbor to the anti-kickback statute, bona fide services be any that are reasonably intended to accomplish the commercially reasonable business purpose of the manufacturer and, as discussed below, consistent with fair market value. By establishing such a standard, the ultimate determination of whether a fee is being paid for a service (as opposed to being a price concession) will be made based on the specifics of the arrangement between the manufacturer and entity. Accordingly, arrangements for some of the services that CMS lists in its discussion of the Proposed Rule, such as inventory management, distribution, and other activities of distributors, would each need to be specifically assessed on their own merits against the standard.

Our client also recommends against the proposed standard that would require that the service be one the manufacturer would otherwise perform directly or contract for in the absence of the service arrangement. This standard is somewhat unclear, as it appears to define a bona fide service as only one that a manufacturer could perform for itself. Our client believes that such a test could be unduly restrictive of established, common business practices because there are many types of services that are unique to the service provider (e.g., refill reminders, certain inventory related services) that a manufacturer is not in a position to otherwise perform directly (or contract for outside of the particular service arrangement). These services are no less important to the manufacturer and no less desirable to its efficient operation. The use of the term "would otherwise perform" also may suggest that services be "absolutely" necessary to the manufacturer, as opposed to reasonably intended to accomplish a commercially reasonable business purpose. Clearly, manufacturers may engage third parties to perform services that are desirable, even if not absolutely "necessary." Applying the standard as written may place undue emphasis on the form rather than the substance of the service.

CMS also requests comments on fair market value determinations for bona fide services. We note that historically, CMS and the OIG have declined to make fair market value determinations. While the fair market value of many services may readily be ascertained, using external references, comparators, and the like, our client also recognizes the difficulty of determining fair market value due to the unique nature of some services. Accordingly, our client requests that CMS acknowledge that some service providers may be uniquely situated to provide services, such as when there is not otherwise an active market for the services (e.g., refill reminders to patients). In addition, CMS should recognize that services fees may be paid on a variety of bases. For example, certain service fees may be paid on a percentage basis, yet are objectively reasonable in amount with respect to the value of the service to the manufacturer, and still in fact constitute fair market value for the service. Our client also strongly urges CMS to revisit the proposed requirement that a fee may not be passed on in whole or in part in order to be considered a bona fide service fee. Our client does not believe this is an appropriate or useful test to determine whether something is an actual service fee. The nature of the services rendered should dictate the treatment of the fee being paid. In other words, the ultimate disposition of the fee does not take away from or otherwise change the characteristics of the services. Further, as a practical matter, it is difficult if not impossible for a manufacturer to determine whether a fee has, in fact, been passed on to an end user. Instead, our client recommends that CMS provide that a bona fide service fee is one paid for a bona fide service where the manufacturer has not contracted for the fee to be passed on by the middleman through to an end user with the intention of delivering to the end user a price concession from the manufacturer for its products.

Finally, with respect to administrative fees paid to group purchasing organizations and pharmacy benefit managers, our client recommends that CMS provide guidance to ensure consistency by

manufacturers in the treatment of such fees. To the extent that CMS determines these fees should be treated as services, our client does not believe that CMS should require that such arrangements also meet the general "bona fide service fee" standards. The standards for evaluating bona fide service fees and whether they are consistent with fair market value cannot be applied to administrative fees in any practical way. Such standards are not appropriate in light of the unique nature of these arrangements, as reflected in the GPO Administrative Fee safe harbor being separate from the discount safe harbor. Specifically, an itemization of services is not feasible with respect to these arrangements; nor is the "pass-through" standard manageable in light of the fact that some providers hold ownership interests in GPOs and PBMs. If CMS determines that GPO and PBM administrative fees should be considered service fees, then in connection with establishing a standard, it should consider providing guidance that GPO and PBM fees at or below an identified amount (e.g., 3%) are presumed to be for bona fide services. [1] Further, with respect to fair market value, the GPO safe harbor reflects an implicit presumption that fees that are 3% or less of the value of purchases may be considered fair market value, thus CMS should specify a similar presumption for GPO and PBM fees.

II. Other Price Concession Issues: Bundled Price Concessions

CMS solicits comments concerning various issues associated with bundled fee arrangements to ensure that ASP "is an accurate reflection of market prices for Part B drugs and that the treatment of bundled price concessions in the ASP calculation does not create inappropriate financial incentives." Specifically, CMS requests information concerning the frequency of bundled arrangements, different bundled arrangement structures, the bundling of Part B drugs with non-Part B products, and potential methodologies to apportion costs under bundled arrangements.

Our client believes that CMS should provide consistent guidance concerning bundling across various programs (i.e., Medicaid rebate, ASP calculation) and that such guidance should apply only prospectively. In our client's experience, there is not significant bundling with respect to Part B products because of their unique therapeutic nature. Accordingly, it may be more appropriate to address bundled arrangements in the impending AMP rulemaking required under the Deficit Reduction Act of 2005. In addition, CMS should proceed carefully in providing such guidance, because guidance that deems an arrangement to be a "bundle" may have different and unintended impacts on price reporting, depending on the programs involved. For example, if CMS guidance were to deem an arrangement a bundled sale that required allocation of discounts among the included products, it might serve to lower the Medicare ASP on one product in the bundle, but could simultaneously raise the Medicaid best price for a different product.

If CMS chooses to provide guidance on bundling in the ASP context, our client believes that such guidance should be through formal rulemaking with a comment period and that CMS should give particular attention to the way in which it defines what constitutes a bundled arrangement. Our client recommends that CMS identify a bundled arrangement as one in which a discount on one or more products or services is contingent on the actual purchase of one or more other products or services. Therefore, not all contracts involving multiple products will constitute bundled arrangements. For example, a contract that merely requires the placing of multiple products on a formulary should not be considered to trigger a bundled sale, because formulary status, in and of itself, does not impose a contractual requirement that the customer must make an actual purchase or utilize products in specific amounts. Given the many types of contracting arrangements that exist, however, we do not believe that it is practicable for CMS to attempt to define all of the types of arrangements that may qualify as

---

1 In adopting such a standard, however, CMS should be clear that such fees in excess of the 3% standard may be permissible.

ReedSmith

bundled sales, and CMS should continue to allow manufacturers to make "reasonable assumptions" in the absence of specific guidance.

Similarly, if CMS provides guidance on allocation methodologies for bundled arrangements, our client recommends that manufacturers be entitled to employ reasonable assumptions concerning the appropriate bases for proportionally allocating discounts among affected products that would allow manufacturers to take into account contract or market prices.

* * * *

We appreciate your consideration of these comments. Please do not hesitate to contact me if you have any questions or need additional information concerning the issues presented herein.

Very truly yours,

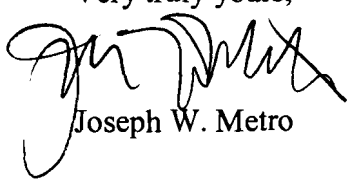

Joseph W. Metro

JWM:cr

161-C
7

Romeo A. Pavlic, MD
William S. Murphy, MD
Ralph M. Kunkel, MD
Donald B. Canaday, MD
Donald A. Chilson, MD
Joel R. Galloway, MD
Sanjeev Vaderah, MD

Inland Cardiology Associates, P.S.
Heart and Vascular Diseases
www.inlandcardiology.com

Timothy T.K. Chen, DO
Stephen N. Ewer, MD
Iyad Jamali, MD
Madar Abed, MD
David T. Jones, MD
Saad Tabbara, MD

October 6, 2006

Mark McClellan, MD, Ph.D
Administrator
Centers for Medicare and Medicaid Services
Department of Health and Human Services
Attention: CMS -1321 –P
Mail Stop: C4-26-05
7500 Security Boulevard
Baltimore, MD 21244-1850

RE: Proposed Rule; Revisions to Payment Policies under the Physician Fee Schedule for Calendar Year 2007 and Other Changes to Payment Under Part B (Federal Register, August 22, 2006)

Dear Dr. McClellan:

On behalf of Inland Cardiology Associates, PS, we appreciate the opportunity to submit these comments to the Centers for Medicare & Medicaid Services ("CMS") regarding the above proposed Revisions to Payment Policies under the Physician Fee Schedule for Calendar Year 2007 and Other Changes to Payment Under Part B; Proposed Rule ("Proposed Rule"). We are concerned about several provisions that will impact Medicare beneficiaries' access to services in outpatient cardiac centers, particularly those related to cardiac catheterizations. Specifically, we are concerned about the payment method proposed for cardiac catheterization related procedures. The Cardiovascular Outpatient Center Alliance ("COCA"), of which we are a member, will address the CMS proposal to require standards for Independent Diagnostic Testing Facilities ("IDTFs"). Our concerns related to the payment method are outlined below.

Payment Method

Under the proposed rule CMS states that the payment for Cardiac catheterization related procedures (e.g. CPT code 93510 TC, 93553 TC and 93555 TC) will be established by the Medicare carriers. The change in the payment method appears only in Addendum B, and CMS provides no explanation or justification in the body of the proposed rule for this change. We object to this approach because it is inconsistent with the overall policy of basing Medicare payment rates for physician services on a national fee schedule methodology. We are also concerned that if carrier pricing were to be implemented, the carriers would look to the values in the June 29, 2006 Notice that addressed the changes to the methodology for the development of practice expense (PE) relative value units (RVUs). Therefore, we request that CMS give serious consideration to addressing the flaws in the proposed changes to the bottom up "PE" methodology for procedures where the technical component (TC) can be billed separately. We know that developing an adequate solution will take time and, therefore, request that CMS set the 2007 relative value units for the three codes listed based on the 2006 values.

We urge CMS to use the current relative value units as the basis for determining reimbursement for these procedures rather than relying on the Medicare carriers to price these services. By doing so, CMS will be able to set a reimbursement rate that fairly reflects the costs of performing these procedures. This recommendation is supported by actual data from outpatient centers. COCA sponsored a study to estimate the costs of performing a cardiac catheterization (CPT Code 93510 TC) in an outpatient center. The study results demonstrated that the 2006 Part B physician fee schedule payment approximates the average cost of providing these services. As a result, we do not believe that a new pricing methodology is necessary.

The current relative value units result in a payment rate that is in relative parity with the payment amount hospitals receive under the hospital outpatient prospective payment system. In fact, the 2006 physician fee schedule payments for the three CPT codes included in the Ambulatory Procedure Classification ("APC") for cardiac catheterizations are 93 percent of the relevant APC rate.

In our response to CMS' Proposed Changes to the Practice Expense Methodology (Federal Register, June 29, 2006) we outlined our concerns with the proposed changes to the PE Methodology, I.e., use of a bottom-up methodology and the elimination of the non-physician work pool. The proposed payment rates resulting from the use of the practice expense RVU's for the left heart catheterization procedure alone (CPT code 93510 TC) reduce payment levels in 2007 by 16 percent, and by 2010 make overall reduction of 53 percent. The flaws in the methodology, particularly as they relate to the cardiac catheterization procedure codes were described in ICA/Dr. Murphy's previous letter of August, 2006, and more specifically in the August 22, 2006 comment letter submitted by COCA.

Cardiac catheterizations that are billed through the Medicare physician fee schedule are performed primarily in cardiology groups and freestanding centers which are grouped into a diverse group of diagnostic testing facilities known as IDTFs.

We believe that the development of unique standards for each type of diagnostic testing facilities will facilitate the development of a consistent Medicare policy for outpatient cardiac catheterization services. The standards will provide a solution to the issue that cardiac catheterization labs faced when the national coverage determination for outpatient catheterizations was rescinded because of the change of scope in the CMS contracts with the Peer Review Organizations in January 2006.

The need to develop unique standards for each type of diagnostic testing facility provider is consistent with the observation that CMS made in the Proposed Rule regarding the practice expense for different types of remote cardiac monitoring and anticoagulation monitoring. Similar to CMS's observation that these types of IDTFs are different, we believe that cardiac catheterization centers are unique and that their cost structure and quality standards are similar regardless of whether they are performed in a cardiology practice or an independent outpatient center. The COCA cost study shows that the cost profile of outpatient cardiac centers is quite different from the average profile of all IDTFs. We believe the COCA cost analysis will be helpful to CMS as it begins to develop standards, specifically for cardiac outpatient centers because the data can be used to estimate the impact that each standard has on practice expenses. The cost study will also be helpful as CMS works to develop a practice expense RVU for cardiac catheterization procedures that reflect the resources needed to perform the service.

In summary, we have grave concerns about the use of carrier-based pricing for procedures that are offered nationwide and historically have been paid according to the physician fee schedule methodology. The carrier based pricing approach is more often used for new services where there is insufficient data on which to determine a national rate. We have previously described our concerns with the proposed 2007 PE RVUs for the cardiac catheterization-related procedures, and, therefore, request that the 2006 rates be frozen so that payments reflect the costs of performing the procedure in the outpatient setting and are on par with the APC rate for a comparable family of cardiac catheterization-related procedures. In addition, we also note that carrier-based pricing has the potential to create disparities in beneficiary co-payment liability.

We thank you for the opportunity to describe our concerns about the proposed rule, specifically as it related to payment for cardiac catheterization-related procedures and the development of standards for centers that perform these procedures on an outpatient basis.

Sincerely,

William S. Murphy, MD, FACC, FCCP

RMG®

RADIATION MEDICAL GROUP, INC.

A PROFESSIONAL CORPORATION

RADIATION ONCOLOGY
Ronald T. Davis, M.D.
Sara G. Rosenthal, M.D.
Donald B. Fuller, M.D.
Damon E. Smith, M.D.
Gina J. Mansy, M.D.
Yonina Tova, M.D.
Tahir Ijaz, M.D.

PHYSICIST CONSULTANTS
Chief Physicist
Haoran Jin, Ph.D.
Chief Dosimetrist
Steven J. Hardy, C.M.D.

EXECUTIVE DIRECTOR/CFO
Douglas G. Myking, M.B.A.

ASSISTANT CFO
Victor Ho, M.B.A.

DIRECTOR OF CLINICAL OPERATIONS
Patricia Wilber, R.T.T.

RADIATION ONCOLOGY OFFICES
2466 First Avenue, Suite B
San Diego, CA 92101-1492
(619) 230-0400
FAX (619) 325-3688

701 E. Grand Avenue, Suite 200
Escondido, CA 92025-4404
(760) 839-7370
FAX (760) 738-7576

6699 Alvarado Rd., Suite 2109
San Diego, CA 92120-5253
(619) 229-3838
FAX (619) 229-3849

ADMINISTRATIVE OFFICE
P.O. Box 33865
San Diego, CA 92163-3865
(619) 220-4100
(800) 210-2400
FAX (619) 296-0526

WESTERN CANCER CENTER, INC.
Management Services Organization
www.rmgmed.com

Centers for Medicare and Medicaid Services
Department of Health and Human Services
Attention: CMS-1321-P
Mail Stop C4-26-05
7500 Security Boulevard
Baltimore, MD 21244-1850

RMG®

RADIATION MEDICAL GROUP, INC.

A PROFESSIONAL CORPORATION

RADIATION ONCOLOGY
Ronald T. Davis, M.D.
Sara G. Rosenthal, M.D.
Donald B. Fuller, M.D.
Damon E. Smith, M.D.
Gina J. Mansy, M.D.
Yonina Tova, M.D.
Sanjeev K. Aggarwal, M.D.
Tahir Ijaz, M.D.

PHYSICIST CONSULTANTS
John E. Steigerwalt, Ph.D.
Haorin Jin, Ph.D.
Richard E. Michaels, M.S.
Steven J. Hardy, C.M.D.
Marie Silverman, C.M.D.
Janet Carmichael, C.M.D.

ADMINISTRATOR/ C.F.O.
Douglas G. Myking, M.B.A.

DIRECTOR OF CLINICAL OPERATIONS
Patricia Wilber, R.T.T.

RADIATION ONCOLOGY OFFICES
2466 First Avenue, Suite B
San Diego, CA 92101-1492
(619) 230-0400
FAX (619) 234-2804

477 N. El Camino Real
Suite A-104
Encinitas, CA 92024-1329
(760) 634-4300
FAX (760) 632-9791

701 E. Grand Avenue, Suite 200
Escondido, CA 92025-4404
(760) 839-7370
FAX (760) 738-7576

6699 Alvarado Rd., Suite 2109
San Diego, CA 92120-5253
(619) 229-3838
FAX (619) 229-3849

ADMINISTRATIVE OFFICE
P.O. Box 33865
San Diego, CA 92163-3856
(619) 220-4100
(800) 210-2400
FAX (619) 296-0526

WESTERN CANCER CENTER, INC.
Management Service Organization

Accredited by

Accreditation Association
for Ambulatory Health Care, Inc.

October 9, 2006

Reference file code: CMS-1321-P

Submitted electronically via Word document attachment

http://www.cms.hhs.gov./eRulemaking

We appreciate the opportunity to submit comments on 42 CFR Parts 405, 410, 411, 414, 415, and 424 [CMS-1321-P] RIN 0938-AO24 Medicare Program; Revisions to Payment Policies Under the Physician Fee Schedule for Calendar Year 2007 and Other Changes to Payment Under Part B.

Image-guided robotic stereotactic radiosurgery (r-SRS) is both an alternative to surgery and an adjunct to radiotherapy involving a defined set of clinical resources to deliver effective treatment. Image-guided robotic stereotactic radiosurgery is not radiotherapy, as it is intended to ablate identifiable lesions, while preserving normal tissue adjacent to the target volume, rather than treat microscopic disease. The CyberKnife® is a complex image-guided robotic stereotactic radiosurgery system (r-SRS), delivering radiosurgical precision throughout the body, for as many treatments (fractions) as the clinician deems necessary for a given situation. CMS currently allows for up to five fractionated image-guided robotic stereotactic radiosurgery treatments and our data indicate that treatments average 3 fractions per course of treatment. Clinicians and patients have recognized the benefits of radiosurgery, which include no incisions, no anesthesia, lower risk of complications, and, therefore, improved patient quality of life.

Image-guided robotic stereotactic radiosurgery is substantially more resource-intensive than other forms of linac-based systems. It was for this reason that CMS created separate HCPCS codes to distinguish these technologies. Further, it is clear that the resources required for image-guided robotic stereotactic radiosurgery treatment are the same regardless of whether the treatment is performed in the first or a subsequent session.

Image-guided robotic stereotactic radiosurgery is a capital intensive technology, and, due to the relatively small number of patients for whom it is clinically appropriate (as compared with, for example, conventional external beam technology), it is not necessarily cost-efficient for a single hospital to provide these services by itself. Robotic stereotactic radiosurgery facilities that are associated with a particular hospital are typically available for use only by physicians on staff at that hospital, thus restricting their ability to serve the larger community and limiting access.

RADIATION MEDICAL GROUP, INC.
A PROFESSIONAL CORPORATION

RADIATION ONCOLOGY
Ronald T. Davis, M.D.
Sara G. Rosenthal, M.D.
Donald B. Fuller, M.D.
Damon E. Smith, M.D.
Gina J. Mansy, M.D.
Yonina Tova, M.D.
Sanjeev K. Aggarwal, M.D.
Tahir Ijaz, M.D.

PHYSICIST CONSULTANTS
John E. Steigerwalt, Ph.D.
Haorin Jin, Ph.D.
Richard E. Michaels, M.S.
Steven J. Hardy, C.M.D.
Marie Silverman, C.M.D.
Janet Carmichael, C.M.D.

ADMINISTRATOR/ C.F.O.
Douglas G. Myking, M.B.A.

DIRECTOR OF CLINICAL OPERATIONS
Patricia Wilber, R.T.T.

RADIATION ONCOLOGY OFFICES
2466 First Avenue, Suite B
San Diego, CA 92101-1492
(619) 230-0400
FAX (619) 234-2804

477 N. El Camino Real
Suite A-104
Encinitas, CA 92024-1329
(760) 634-4300
FAX (760) 632-9791

701 E. Grand Avenue, Suite 200
Escondido, CA 92025-4404
(760) 839-7370
FAX (760) 738-7576

6599 Alvarado Rd., Suite 2109
San Diego, CA 92120-5253
(619) 229-3838
FAX (619) 229-3849

ADMINISTRATIVE OFFICE
P.O. Box 33865
San Diego, CA 92163-3856
(619) 220-4100
(800) 210-2400
FAX (619) 296-0526

WESTERN CANCER CENTER, INC.
Management Service Organization

Accredited by

Accreditation Association
for Ambulatory Health Care, Inc.

Allowing carriers to pay for the technology when provided in freestanding centers would facilitate cost sharing among a number of hospitals (and others) to provide these services, improving device access to a more diverse population of patients in a given geographic region.

Comment:

A number of temporary codes have been established to enable hospitals to report the technical component costs of image-guided robotic stereotactic radiosurgery (r-SRS) treatment (HCPCS Codes G0339 and G0340). The proposed Rule regarding the Physician Fee Schedule for 2007 designates codes G0339 and G0340 as "C – Carriers price the code."

This is consistent with the technical component radiation oncology services of all kinds that are reimbursed under the Physician Fee Schedule, and have been since the inception of the Physician Fee Schedule methodology.

Recommendation:

The CyberKnife Coalition respectfully recommends and encourages CMS to:

- *Adopt the proposed change to include HCPCS Level II codes G0339 and G0340 on the CY 2007 PFS, classifying the codes with the modifier "C" to indicate that they may be carrier priced.*

We support this modification that would clearly establish carrier authority to cover image-guided robotic stereotactic radiosurgery in freestanding settings, subject to their establishment of appropriate quality assurance measures to ensure patient safety and regulatory compliance, to the satisfaction of the carrier.

We appreciate your consideration of our comment.

Sincerely,

Douglas G. Myking, M.B.A.
Executive Director and Chief Financial Officer
Radiation Medical Group, Inc.
2466 First Avenue, Suite B
San Diego, CA 92101
Phone: 619-220-4100
Email: dmyking@rmgmed.com

Virginia Tobiason

100 Abbott Park Rd.
0391, Bldg. AP6D-2
Abbott Park, IL 60064-6008

Phone: 847-937-8438
Fax: 847-935-8613

163

October 2, 2006

VIA OVERNIGHT MAIL

Mark B. McClellan, M.D., Ph.D., Administrator
Centers for Medicare & Medicaid Services
Department of Health and Human Services
Attention: CMS-1321-P
Mail Stop C4-26-05
7500 Security Boulevard
Baltimore, MD 21244-1850

RE: Medicare Program; Revisions to Payment Policies Under the Physician Fee Schedule for Calendar Year 2007 and Other Changes to Payment Under Part B (CMS-1321-P)

Dear Dr. McClellan:

Abbott welcomes the opportunity to comment on the Centers for Medicare & Medicaid Services' ("CMS") proposed rule on Revisions to Payment Policies Under the Physician Fee Schedule for Calendar Year 2007 and Other Changes to Payment Under Part B ("Proposed Rule").

Abbott is a global, broad-based health care company devoted to discovering new medicines, new technologies and new ways to manage health. Our products span the continuum of care, from nutritional products and laboratory diagnostics through medical devices and pharmaceutical therapies. The company employs 65,000 people and markets its products in more than 130 countries.

Our comments focus on two sections of the Proposed Rule: (1) CMS's proposed changes in average sales price ("ASP") reporting requirements, and (2) proposed provisions related to the establishment of payment amounts for new clinical laboratory tests.

I. Average Sales Price Issues

A. Fees Not Considered Concessions

CMS is proposing to clarify that bona fide service fees that are paid by a manufacturer to an entity, whether or not the entity takes title to the drug, are not considered price concessions for ASP reporting purposes. CMS proposes to define bona fide service fees as fees paid by a manufacturer to an entity that represent fair market value for a bona fide, itemized service actually performed on behalf of the manufacturer that the manufacturer would otherwise perform (or contract for) in the absence of the service arrangement, and that are not passed on, in whole or in part, to a client or customer of an entity, whether or not the entity takes title to the drug. We have several concerns about the proposal regarding bona fide service fees.

First, to the extent CMS intends the definition of "bona fide service fees" to be limited to payments for services that a manufacturer could otherwise physically perform (if it chose not to contract them out), we believe the definition is too narrow. Certain services, by their nature, can only be performed by a non-manufacturer, but that should not rule out a payment by a manufacturer for such a service from being viewed as a payment for a bona fide service.

Second, we are concerned that the proposed definition of "bona fide service fees" would exclude any payment passed on by the recipient to its clients or customers. We believe the relevant inquiry in determining whether a payment is a "bona fide service fee" is not whether the recipient passes any part of the payment to third parties, but rather, whether the manufacturer intends the payment as a fee for services rendered by the recipient, as opposed to a price concession to the recipient (or its customers). We also are concerned with the burden of having to track downstream distribution of our payments. Manufacturers are not routinely provided with information about such downstream transactions, and there are significant barriers to manufacturers obtaining this information (e.g., confidentiality issues, market competitiveness considerations, and customer liability concerns related to providing incorrect information). There is a significant risk that manufacturers would not be able to obtain downstream transaction information with the consistency and level of accuracy that would be necessary for ASP reporting purposes.

Finally, CMS indicates that it may give guidance on specific types of services and whether payments for those services should be viewed as bona fide services fees for purposes of the ASP calculation. We believe it would be more valuable for CMS to provide general guidance on the issue that can be used by manufacturers in making determinations with respect to any type of service. For example, we believe it is clear that payments for services which qualify for the personal services safe harbor should be viewed as bona fide service fees. On the other hand, the determination of whether payments made for non-safe harbored services would be more accurately viewed as payments for a bona fide service or as price concessions will often depend on individual price negotiations or company pricing policies. In general, we believe that a payment for a service should be viewed as a bona fide service fee only if it is (a) paid in connection with a service that meets the personal services safe harbor, or (b) is a payment for a service that meets a commercially reasonable business purpose of the manufacturer and is not intended as a price concession to the recipient.

B. Other ASP Calculation and Reporting Requirements

CMS has proposed a number of modifications to its ASP calculation and reporting requirements that we believe generally promote clarity in ASP requirements.

- **Estimation Methodology for Lagged Exempted Sales**. CMS is proposing to require that all manufacturers use a 12-month rolling average ratio methodology to estimate exempted sales known on a lagged basis. We agree that specific CMS guidance in this area promotes consistency and accuracy in ASP reporting, and that CMS's proposed methodology is appropriate.

- **Nominal Sales**. CMS proposes to continue the current methodology for identifying and excluding nominal sales (that is, sales that are exempt from the Medicaid best price calculation) from the manufacturer's calculation of the Medicare ASP. We agree with CMS that using a single method for identifying nominal sales for both ASP and Medicaid average manufacturer price ("AMP") promotes consistency and helps maintain continuity in the ASP calculation. We recommend that CMS adopt this proposal in the final rule.

- **Price Concessions for National Drug Codes ("NDCs") With Less Than 12 Months of Sales**. For circumstances in which a NDC with price concessions known on a lagged basis has not been sold for a full 12 months, CMS proposes to specify that the period used to estimate lagged price concessions is the total number of months the NDC has been sold. We believe this is a reasonable approach for reporting for products without a full year of sales, and we support this proposed clarification.

- **Redesignated NDCs.** The Proposed Rule addresses situations in which a manufacturer has changed the NDC assigned to a product and package size while continuing price concessions that span across sales of the product under its prior and redesignated NDCs. Specifically, CMS proposes that when an NDC is changed and lagged price concessions offered for the prior NDC remain in effect, the manufacturer generally must use 12 months (or the total number of months of sales of the prior and redesignated NDCs if the total number of months of sales is less than 12 months) of sales and price concession data from the prior and redesignated NDCs to estimate lagged price concessions applicable to the redesignated NDC. Again, we agree with CMS that this is an appropriate methodology for addressing continuing price concessions for redesignated NDCs, and we encourage CMS to adopt this provision in the final rule.

C. Widely Available Market Prices ("WAMP") and AMP Threshold

Section 1847A(d) of the Social Security Act requires the Secretary and the Office of the Inspector General ("OIG") to monitor market prices for drugs and biologicals to determine the WAMP, which is defined as the price that a prudent physician or supplier would pay for the drug or biological. If the OIG determines that the ASP for a drug or biological exceeds the WAMP or the applicable percentage of the AMP, the Secretary may disregard the ASP and base reimbursement on WAMP or AMP. Under the statute, the applicable threshold percentage was 5 percent in 2005 and the percentage designated by the Secretary in subsequent years. In CY 2006, CMS specified an applicable threshold percentage of 5 percent for both the WAMP and AMP, and CMS proposes to continue this 5 percent threshold in 2007. The OIG has issued two reports to date comparing the WAMP and the AMP for various drugs and biologicals, and the OIG's work continues in this area. However, CMS points out that "[t]here are a number of operational issues associated with" substituting a lower payment amount for a drug based on the OIG's findings that the ASP exceeds the WAMP or AMP by more than the established threshold. CMS invites comments on these operational issues.

We agree that CMS should proceed cautiously in adjusting Medicare reimbursement amounts for drugs and biologicals based on the OIG's reports comparing ASP and AMP. There are a number of differences between the AMP and ASP methodologies that could impact the price comparisons reported by OIG, and CMS should take these differences into account before imposing any price adjustments in response to the OIG's findings.

For instance, AMP and ASP use different methodologies to account for price concessions. ASP price concessions (e.g., rebates, chargebacks, prompt pay, wholesaler credits) are smoothed through the use of a 12-month rolling average for the quarterly calculation. In other words, the ASP for a quarter considers four quarters of price concession data. On the other hand, AMP price concessions are calculated using values for only one quarter (i.e.; they are not smoothed through the use of a 12-month rolling average). The following examples illustrate how these differences could impact the relationship between ASP and AMP.

Scenario 1: Price concessions are discontinued for a particular product. This would impact the AMP immediately for the first quarter without the price concession, creating a higher AMP. However, due to the use of a 12-month rolling average for price concessions under the ASP system, the ASP would not fully reflect the end of the price concessions for four quarters; in the interim, the ASP would be lower than the AMP.

Scenario 2: Price concessions are increased for a particular product as a percentage of sales. This would result in a higher ASP compared to the AMP, since the ASP smoothing mechanism would not reflect the full impact of these increased price concessions until the fourth quarter. On the other hand, the AMP would reflect the increased price concessions immediately, therefore lowering the AMP in comparison to ASP.

In addition to the price concession calculation issue, a number of other differences between AMP and ASP calculations could result in varied ASP and AMP values, including the following:

- ASP is based on all non-government direct sales, while AMP is based on the price realized for drugs distributed to the retail pharmacy class of trade.
- ASP is calculated at an NDC-11 level, while AMP is reported at an NDC-9 level.
- ASPs may not be restated, while AMPs can be restated retroactively.

CMS should ensure that any Medicare reimbursement policy based on comparisons between ASP and AMP recognizes the differences between the ASP and AMP methodologies.

Given that many market factors and methodological issues could temporarily impact the relationship between AMP and ASP, it is imperative that CMS not substitute a lower payment amount for a drug based on the OIG's findings related to pricing in a single quarter. There are too many factors that could influence pricing comparisons at one particular moment in time; such quarterly fluctuations should not form the basis for setting aside the regular statutory payment methodology for the product. Indeed, a premature payment adjustment based on a single quarter's data could result in skewed payment amounts and undermine reimbursement accuracy. Instead, CMS should examine pricing trends that point to a sustained, meaningful differential between AMP and ASP before disregarding the ASP for a drug.

II. Diagnostic Laboratory Tests

A. Procedures for Public Consultation for Payment for New Clinical Diagnostic Laboratory Test

In the Proposed Rule, CMS proposes to codify its current process for providing public consultation on the establishment of payment amounts for new clinical laboratory tests. We agree that the process for establishing laboratory test payment amounts should be transparent and consistent, and we thank CMS for addressing this issue in the Proposed Rule. Public input – and agency consideration of that input -- is critical to developing payment policy that adequately reflects the costs of new technology. We support adoption of this provision in the final rule with certain refinements and clarifications, as described below

B. Payment for New Clinical Diagnostic Laboratory Test: Crosswalking and Gapfilling

CMS also proposes to establish in regulation the procedures to set payment amounts for new clinical laboratory tests through either crosswalking or gapfilling.

1. Crosswalking

CMS proposes that when it establishes the payment amount for a new clinical laboratory test using the crosswalk methodology, it would use the existing local fee schedule amounts and national limitation amount for the new code. Payment for the new test code would be made at the lesser of the local fee schedule amount or the national limitation amount.

We are concerned, however, that the wide disparities in payments at the local level undermines CMS's attempts to approximate payment for a new test using existing codes. Although CMS guidance on this issue is limited, CMS presumably decides to crosswalk a technology to an existing code's payment level because of clinical similarities between the tests and/or CMS's determination regarding the appropriateness of the existing national payment limitation --- rather than because of a carrier-by-carrier payment analysis. We believe that using the national payment level for a crosswalked test would avoid wide geographic swings in payment and promote beneficiary access to new clinical laboratory tests nationwide. We therefore recommend that CMS crosswalk new codes to existing codes using the national limitation amount of the existing code rather than the local carrier amounts.

2. Gapfilling

With respect to gapfilling, CMS proposes to continue its current process of providing carriers with manual instructions outlining the sources of information carriers should examine in determining gapfill amounts. CMS notes that its current instructions direct carriers to consider the following sources information in setting amounts:

- Charges for the test and routine discounts to charges;
- Resources required to perform the test;
- Payment amounts determined by other payers;
- Charges, payment amounts, and resources required for other tests that may be comparable or otherwise relevant; and
- Other sources of information as appropriate, including clinical studies and information provided by clinicians practicing in the area, manufacturers, or other interested parties.

Under current policy and the proposed regulatory text, there is no CMS oversight or review process to ensure that carriers actually follow the instructions established by CMS, that carriers consider information provided by interested parties, or that carriers ultimately establish reasonable local payment amounts. Local carriers currently have wide discretion in setting payment rates, and as a result local payment rates are not always reasonable and consistent with charges and resources associated with new tests.

We believe that additional safeguards should be added to the gapfilling process to provide CMS oversight of the carrier payment determination process, since these local payment determinations form the basis of the national payment limitation in the second year of a new test. Specifically, CMS should assess the accuracy and appropriateness of carrier laboratory test payment determinations before calculating the national payment limit. This assessment should include validation that carriers have followed CMS instructions, and a solicitation and consideration of comments from physicians, laboratories, manufacturers, and other affected parties. CMS should be authorized to modify the proposed payment limit as necessary after its review of the carrier's process.

To that end, we recommend that the following regulatory language be added to proposed §414.408:

> Sec. 414.408 Payment for a new clinical diagnostic laboratory test.
>
> For a new clinical diagnostic laboratory test that is assigned a new or substantially revised code on or after January 1, 2005, CMS determines the payment amount based on either of the following:
>
> * * *
>
> (b) Gapfilling. Gapfilling is used when no comparable existing test is available.
>
> (1) Carrier-specific amounts are established for the new test code for the first year using the following sources of information to determine gapfill amounts, if available:

(i) Charges for the test and routine discounts to charges;

(ii) Resources required to perform the test;

(iii) Payment amounts determined by other payers; and

(iv) Charges, payment amounts, and resources required for other tests that may be comparable or otherwise relevant.

(2) In the second year, the test code is paid at the national limitation amount, which is the median of the carrier-specific amounts, **subject to CMS determination of the accuracy and appropriateness of such carrier-specific amounts using the following process:**

(i) CMS shall review each carrier payment amount to determine if it complies with CMS instructions.

(ii) CMS shall publish a notice announcing the proposed national limitation amount and summarizing the sources of information on which the proposed amount is based. The notice shall solicit input from physicians, laboratories, manufacturers, and other interested parties regarding payment for the test, including charges, other payer amounts, and resources required to perform the test (including direct and indirect costs of efficiently performing the test).

(iii) If CMS determines that a carrier payment amount does not reflect full compliance with CMS instructions, or that the carrier amount is inconsistent with data received from the public in response to the notice under clause (ii), CMS may adjust the national payment limitation accordingly to reflect the technological improvements or innovations of the new test.

* * * * *

We appreciate your consideration of our comments. Please feel free to contact me if you have any questions or if you need additional information.

Sincerely,

Virginia Tobiason
Senior Director,
Corporate Reimbursement

CENTER FOR
DIAGNOSTIC IMAGING

164

October 9, 2002

VIA UPS NEXT DAY MAIL

The Honorable Mark McClellan, M.D., Ph.D.
Centers for Medicare & Medicaid Services,
Department of Health and Human Services,
Attention: CMS-1512-PN,
Mail Stop C4-26-05,
7500 Security Boulevard,
Baltimore, MD 21244-1850

Re: CMS-1321-P

Dear Dr. McClellan:

Thank you for the opportunity to comment on the CMS proposed rule 1321-P. We will keep our comments brief because we have had the opportunity to contribute to the broader and more detailed response submitted by our industry association, National Coalition of Quality Diagnostic Imaging Services (NCQDIS). We request that you give additional attention to the following two areas, specifically as the concerns relate to imaging facilities.

1. **We appeal to CMS to pursue continuity in its regulations of all imaging facilities. Both the current and proposed payment and operating regulations are severely inconsistent and are a disincentive to provide high-quality imaging services for Medicare beneficiaries. Further, the inconsistencies in payment and operating regulations negate chances of success for the Administration's goal of more transparency of both cost and quality.**

   Center for Diagnostic Imaging, Inc. is a collection of hospital and physician partnerships in eight states with 12 distinct markets. Each imaging partnership is unique in that it has been developed to fit the local market it serves. Through our partnerships, CDI has facilities that are reimbursed as IDTFs, physician practices, and hospital outpatient facilities. We also have a free-standing ambulatory surgical center. At CDI, we strive to operate all of our facilities consistently and in a manner that maintains our stellar reputation for quality imaging and patient services. We require high and consistent requirements of technologists and other staff and our radiologists participate in a joint, sub-specialized, modality specific CQI program, including a robust peer review process.

   Currently CMS does not require the same operating standards for the various sources of imaging services, nor will you be reimbursing facilities

www.cdiradiology.com *or* www.heartct.com
5775 Wayzata Boulevard, Suite 400 Minneapolis, MN 55416 tel 952.543.6500 toll free 877.566.6500 fax 952.847.1152

such as CDI's at a generally consistent rate beginning in January, 2007 (See the AMIC Moran report of 9/06 - attached). Your proposed rule adds further variance and will, unfortunately, begin to influence our decisions on current and future partners and partnership structures. For example, many more operational regulations are imposed on IDTFs but for lesser pay than if we operate as a hospital outpatient facility. Making decisions based on inconsistent regulations is not in the best interest of the patients we serve nor our local hospital and physician partners. Nor will these decisions be in the best interest of CMS' budget. If CMS cannot enhance services to its Medicare beneficiaries, CMS should at least attempt to avoid eroding quality services already in place. The inconsistencies in how CMS regulates and reimburses imaging facilities will erode quality services for your beneficiaries.

Furthermore, the current Administration has endorsed an effort towards transparency in both quality and cost measures. CDI supports this movement and has and will continue to remain involved in the national effort to apply and report measurable indicators of quality. However, it is virtually impossible for any payer (including Medicare) or provider (including CDI) to be able to offer meaningful and measurable comparisons of imaging facilities because of the severe inconsistency in regulations and reimbursement.

2. **The proposed payment structure for diagnostic and therapeutic injection (DTI) procedures does not appear to be based on appropriate and comprehensive practice expense data.**

   We ask that you specifically re-address the differences in practice patterns in DTI services and differentiate your reimbursement based on practice expense data. As an experienced provider of DTI services, we are willing to share our practice expense data and to assist CMS in differentiating more thoroughly the components which make up the practice expense for various DTI procedures, with and without fluoroscopic guidance. Once CMS has proceeded with this clarification, CDI also commits to working to develop an industry collaborative for submitting reliable practice expense data to CMS.

Thank you for your attention to our concerns. We look forward to working with you to the benefit of our patients.

Sincerely yours,

Robert V. Baumgartner
Chief Executive Officer

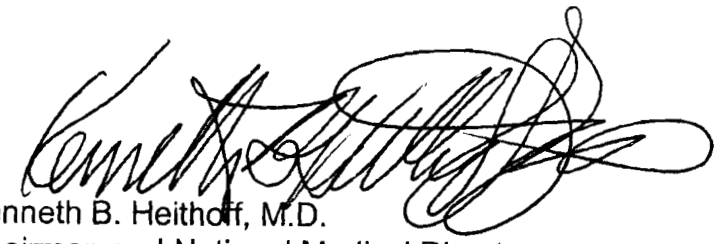

Kenneth B. Heithoff, M.D.
Chairman and National Medical Director

Assessing the Deficit Reduction Act Limits on Imaging Reimbursement: Cross-Site Comparisons of Cost and Reimbursement

August 2006

THE MORAN COMPANY

Assessing the Deficit Reduction Act Limits on Imaging Reimbursement: Cross-Site Comparisons of Cost and Reimbursement

Introduction

In §5102 of the Deficit Reduction Act of 2005 ("DRA"), Congress enacted special payment rules limiting reimbursements, beginning in 2007, for the technical component ("TC") of imaging services performed in the office setting[1]. Under the DRA policy, reimbursements for imaging services performed in the office would equal the lesser of the amount provided under the Medicare Physician Fee Schedule ("MPFS"), or the amount payable to hospitals under the Outpatient Prospective Payment System ("OPPS").

In the spring of 2006, a new organization, the Access to Medical Imaging Coalition ("AMIC"), formed to advocate elimination or mitigation of this policy. AMIC believed the policy would impose substantial payment reductions for a significant subset of imaging procedures performed in the office. It is our understanding that, in its communications with Congress regarding this policy, AMIC was asked to answer two questions:

- How will payments under the DRA policy compare to the cost of performing these imaging procedures in the office setting?

- In the aggregate, how do present payments for imaging services in the office setting compare to payments for similar services in the outpatient hospital setting?

AMIC engaged The Moran Company to help provide answers to these questions. This report presents the findings of our analysis, accompanied by a discussion of the data we used and the methodologies we employed in reaching these findings. Our findings can be summarized as follows:

1. We found that 126 of the 145 procedures (87%) whose payment would be affected by the DRA caps would be paid, under those caps, an amount less than the estimated cost of performing the procedure in the office setting. We used a cost estimation concept consistent with the Centers for Medicare and Medicaid ("CMS") Town Hall methodology to compute the practice expense component of the MPFS.

[1] The vast majority of imaging procedures permit separate reimbursement for the "technical component" associated with generating the image, as distinct from the "professional component" associated with having a trained physician read and interpret the images generated. When the same Medicare provider performs both services, that provider can bill a "global" fee. Under the DRA policy, payment limits on the TC component apply even if the global fee is billed.

2. We found that aggregate payments for imaging services across the office and hospital outpatient settings are very close to equal[2]. We compared 2006 payment rates in both settings (prior to application of the caps) using constant volumes for the procedures in 2004.

    a. When payments for imaging services are compared across sites of care, volume weighted payments in the office are slightly higher, by 0.6%, when weighting is done by the volume of procedures performed in the office.

    b. When volume is weighted by the volumes performed in the outpatient hospital setting, however, MPFS payments are 2.9% below OPPS payment levels prior to the implementation of the DRA.

3. We conclude from this that current payment policy, prior to the application of the DRA caps, does not exhibit a bias toward higher payments in one setting versus another.

4. Once the DRA caps are implemented, however, imaging reimbursement in the office would be materially lower, perhaps by 16-18%, than in the outpatient setting.

Our analysis was completed in June of 2006. On June 29, 2006 CMS published a Notice of Proposed Rulemaking regarding MPFS practice expense and five year review payment policies and methodology (i.e. CMS-1512-PN). On August 8, 2006, CMS published the MPFS proposed rule (CMS-1321-P) and the OPPS proposed rule (CMS-1506-P) for calendar year (CY) 2007. Each of these proposed rules contain payment policy changes and proposed methodological revisions which were not taken into consideration in this analysis. Additionally, with the release of the MPFS CY 2007 proposed rule (CMS-1321-P), CMS published a list of codes that will be subject to §5102 of the DRA (Addendum F of CMS-1321-P). This addendum was not available at the time of our analysis and accordingly, the list of codes used in this analysis (as discussed below) differ from those in Addendum F of the MPFS CY 2007 proposed rule. Finally, this analysis does not take into consideration any projected updates to the conversion factor (e.g., for CY 2007 the CF is currently estimated to decrease by 5.1%).

I. Estimated Cost of Procedures Affected by DRA Reimbursement Limits

Procedures Subject to the Policy

[2] The estimated cost of procedure analysis discussed in section I of this report did not take differences in payment policy into account, however the site of care analysis discussed in section II of this report does take differences in payment policy across settings (e.g., multiple procedure reductions and outlier payments) into account.

Our first task in developing these estimates was to determine which services might be subject to the policy. The statute applies the "lesser of MPFS or OPPS" test to "imaging services," which could be interpreted to include procedures other than diagnostic imaging services.[3] In the case of therapeutic services that involve imaging, such as treatment planning, certain nuclear medicine services and certain guidance procedures, it is possible that the Secretary, in implementing this policy, would conclude that the DRA limits apply to the technical component of such services if they have discrete billing codes under the AMA Current Procedure Terminology (CPT®)[4] and/or Healthcare Common Procedure Coding System (HCPCS). We, however, did not include most of these services in our analysis. After developing an initial list, we consulted with the American College of Radiology, which is a member of the Access to Medical Imaging Coalition, and employed a list of services modified by their comments and suggestions.

The full list of codes evaluated is presented in Appendix A and includes 524 CPT®/HCPCS codes which have associated technical component modifiers[5]. Certain imaging related services which also have associated technical component modifiers were excluded from our analysis as they fell into one of the following categories: a) carrier priced under the MPFS and therefore national reimbursement rates were unavailable, for example Positron Emission Tomography (PET)[6]; b) certain imaging guidance services; c) imaging services used intra-operatively; d) mammography services and computer-aided detection (CAD) services associated with mammography; e) radiation oncology services; f) services that are not covered by Medicare or are restricted by Medicare (i.e. N or R status indicator) under the physician fee schedule; g) certain nuclear medicine services; and h) services related to a pregnant uterus or fetus as these are not relevant to Medicare patients.

Payment Rates in 2006

To determine which procedures might be subject to the DRA payment rules, we used payment rates for both the MPFS and OPPS based on the respective Final Rule payment rates for these systems for calendar year 2006, the last year for which we had final payment rates for both systems. The MPFS rates were calculated using the total non-facility relative values, multiplied by the 2006 conversion factor.[7] The OPPS rates were based on the published rates for the APC to which each procedure maps under Appendix B of the final OPPS rule for 2006.[8]

---

[3] The statute explicitly excludes both screening and diagnostic mammography services from these caps.

[4] ***CPT®*** is a trademark of the American Medical Association.

[5] As stated in the introduction section of this report, the list of codes used in this analysis was developed in June 2006, prior to publication of CMS's proposed list of codes subject to the DRA (CMS-1321-P, Addendum F).

[6] Carrier priced codes were included in the site of service analysis as we were able to estimate price by average carrier payment rates extracted from the 2004 Part B Summary and OPPS files.

[7] The technical components of these procedures have no work values under the Resource-Based Relative Value Scale (RBRVS), hence the payment rates are the sum of the applicable practice expense and malpractice weights.

[8] For certain services, such as Magnetic Resonance Angiography (MRA), multiple C codes under OPPS correspond to one CPT code for that group of services under the physician fee schedule. When this

Estimated Cost

We developed our estimates of procedure-level, office-based cost using the most recent data available from CMS regarding procedure level cost of performing imaging services in the non-facility setting.[9] The methodology we used parallels the cost determination methodology CMS employs in establishing relative values under the practice expense component of the MPFS in several ways, but differs in that we are using these data to generate absolute estimates of cost as opposed to relative costs.

We start with the direct cost input values presented for clinical labor, medical supplies, and medical equipment, expressed as absolute dollars per procedure performed. We have published values for 494 of the 524 procedures on our list.[10] For the 30 procedures without published input values, we were unable to compute estimated cost. In some instances, our approximation of cost may be underestimated, as the CMS "Town Hall" data source was missing values for supplies (this occurred in 7 instances as noted on Appendix A) or was missing values for supplies and equipment (this occurred in 5 instances as noted in Appendix A).

To estimate indirect costs (that is, practice overhead costs unrelated to the performance of individual procedures), we employed the methodology CMS proposed to use in its Town Hall discussion. Under that methodology, CMS determined its indirect cost estimates on an indirect cost base including both the direct cost inputs, and the dollar value of the applicable physician work values. Using indirect cost data generated from survey data under the practice expense computation methodology, CMS generated procedure-level "Indirect Practice Costs Indices" (IPCIs) that reflect a blend of indirect cost information from the respective specialties performing each procedure, in proportion to each specialty's share of total procedure volume.[11] Under the CMS Town Hall methodology, these IPCIs were multiplied by the dollar value of the direct cost base to generate indirect cost weights, which were then added to the direct cost weights to calculate the practice expense RVUs. We followed this approach, but used the methodology to generate dollars per procedure values, rather than relative weights.

---

occurred, a single OPPS rate was not available and accordingly, an OPPS rate was not included in the comparison of cost to payment analysis, however these codes were included in the analysis across sites of care.

[9] Since this analysis was performed prior to release of the Notice of Proposed Rulemaking regarding MPFS practice expense and five year review payment policy (i.e. CMS-1512-PN) and prior to the MPFS proposed rule for 2007 (CMS-1321-P), we employed the data CMS published on its website in February 2006 in conjunction with its "Town Hall" presentation of alternative practice expense methodologies.

[10] In 37 cases no CPEP data was included in the published Town Hall database. Therefore we used the CPEP data published in the 2005 Final Rule database for these services.

[11] To maintain consistency with the CMS Town Hall methodology, we used the IPCIs published by CMS in February 2006. The American College of Radiology, however, pointed out to us that the "practice expense per hour" values CMS used for radiology were, while supposedly based on supplemental survey data submitted by ACR, materially lower than the actual survey values, apparently due to trimming and reweighting of survey records. Since we do not know the details of how CMS's methodology contractor re-weighted the survey data, we cannot determine what adjustments might be appropriate to the IPCI data used by CMS.

Said a different way, we are using the "official" cost inputs CMS published in its February 2006 Town Hall practice expense meeting. For direct costs, we are using the CPEP values, as they have been refined by the AMA RUC/PEAC process. For indirect costs, we are using the CMS Town Hall methodology of physician work (which for codes in this analysis is equal to zero) plus the direct cost, adjusted by a procedure-level IPCI.

Comparison of Costs to Payment

In Appendix A, we present our findings comparing our procedure-level cost estimates to the payment rates that would have been applicable had the DRA payment policy been implemented in 2006. We compared the MPFS rates to the corresponding OPPS rates at the procedure level, applying the "lesser of" policy to determine which procedures would have been capped, in that year, had this policy applied. We then compared the payment outcome to the cost estimate, and identified cases where cost exceeded payment.[12]

In summary, we found that 145 of the 494 codes for which we have complete data, were found to be affected by the DRA payment limits. Of these, 126 procedures, or 87% of the procedures, would be paid at a rate below the estimated cost of performing them in the office setting.

Procedure-level comparisons are shown in Appendix A.

II. Payments for Imaging Services Across Sites of Care

Data and Methodology Issues

To generate a consistent comparison of payments across sites of care, we used claims data from the 2004 Carrier and Outpatient Standard Analytical Files to calculate procedure-level scalars to adjust for payment policy differences across settings. On the office side, we used actual claims to determine what proportion of payment lines would have been reduced, in 2004, under the 25% reduction policy for multiple imaging procedures applicable to 2006. We then determined, for each procedure, the percentage change in payment that would have resulted.[13] On the outpatient hospital side, we looked at actual outlier payments for claims including imaging procedures in 2004, and

[12] Note that we are comparing 2006 payment rates to cost estimates generated using data on direct cost inputs (i.e. CPEP data) as published by CMS during the 02/15/06 Town Hall meeting or as published by CMS in the 2005 final rule database. This comparison is meaningful as the direct cost input dollar values are not linked to any particular year. The original CPEP direct cost input values were first generated in 1996-1997. After initial implementation of the resource-based practice expense methodology in 1999, these values were then "refined" via a five-year process involving the Practice Expense Advisory Committee (PEAC) of the AMA. The refined values for each procedure are not, in general, indexed to make them strictly comparable to payment rates across payment years. For this reason, we believe that the methodology we have employed produces what are likely to be conservative estimates of procedure-level cost.

[13] Under the MPFS, CMS has, by regulation, implemented a series of payment reductions for multiple procedures when two or more imaging studies are conducted of "contiguous body parts." Those regulations identify "families" of procedures, which, if reported on the same claim for the same date of service, invoke the 25% multiple procedure reduction policy.

calculated, for each procedure, the average percentage increase in payments that resulted from outlier payments.[14]

In performing our analyses, we had to set aside procedures for which data were not available under one system or another in either 2004 or 2006. We trimmed 21 codes for missing data. In several instances we had to crosswalk codes to make the payment values comparable across settings. Four MR angiography codes show up as CPT codes in the office setting, but are billed based on C-codes in the OPPS. Hence we clustered these procedures so that payments are based on the CPT volume when using the MPFS payment methodology, while payments under the OPPS policy are done at the APC level. For PET codes that are carrier-priced, and have no fee schedule values in 2006, we simulated MPFS payment rates based on actual carrier payments for the TC component in 2004.[15]

To account for case mix differences for imaging services in each setting, we calculated volume-weighted estimates of aggregate payment differences across settings. To do this we used the volume of cases observed in the office in 2004 and the volume observed to be paid under the OPPS.

Our findings are as follows:

Comparison of Payments for Imaging Services in Alternative Settings:
2006 Payment Policies & 2004 Volumes

Volumes Used:	MPFS		OPPS	
Rules & Rates:	MPFS	OPPS	MPFS	OPPS
Total Payments ($M)	$6,341	$6,302	$5,730	$5,900
MPFS Payments as a % of OPPS	100.6%		97.1%	

[14] In outlier claims that included non-imaging services, we pro-rated the outlier payment value based on charges. Our analysis did not include outlier payments for claims involving MRA or PET.

[15] We extracted the volume of services and payments from 2004 Part B Summary and OPPS files. We estimated a payment rate based on carrier payments in 2004 by taking an average payment per unit based on TC unit payments, and inflating that rate by .015% to account for the conversion factor increase in 2005 (0% increase in 2006). A number of PET codes dropped out of the analysis due to a lack of data. The 2004 service volume for the remaining PET codes (accounting for approximately 99% of PET payments in both systems) from the carrier file was priced using the 2006 OPPS rates, matching 2004 codes to 2006 equivalent codes. The 2004 service volume from the OPPS claims file was priced using the estimated average Carrier payment rate described above. PET codes excluded from the analysis were: 78608, G0030, G0032, G0033, G0034, G0036, G0039, G0040, G0041, G0042, G0043, G0233, due to no paid "TC" units in the 2004 Carrier File; 78459, 78810, G0031, G0044, G0046, G0231, G0232, due to only one or two paid "TC" units in the 2004 Carrier File which is too low a number to derive an average payment rate; G0038 due to no paid volume; and G0234 due to no OPPS payment rate.

As these data suggest, aggregate payments under both systems, when adjusted for comparability across disparate system features, are roughly comparable prior to application of the DRA policy. The data in the next table break out the effects of the adjustments for comparability.

Effects of Methodology Differences on Payment Comparison
2006 Payment Policies & 2004 Volumes
Excludes outlier payments for MRA and PET procedures

	Based on MPFS Procedure Volumes		
	MPFS Rates ($M)	MPFS % OPPS	OPPS Rates ($M)
Raw Rate Comparison	$6,402	104.8%	$6,108
Effects of Multiple Procedure Reduction	-$61		
Effects of Outlier Payments			$194
Adjusted Payments	$6,341	100.6%	$6,302

In this analysis, we are using the MPFS volumes in both settings to standardize the comparison. In the first line, we show how these volumes would weight up to total payments based solely on payment rate differences. We find that payments under the MPFS would be 4.8% higher than would be obtained by using the OPPS rates across the same volumes.

When the other major differences between systems are taken into consideration, however, the comparison approaches neutrality. Applying the multiple procedure reduction for contiguous body part studies lowers total MPFS payments by $61.3 M, or roughly 1%. Meanwhile, outlier payment adjustments increase payments under the OPPS methodology, for these same volumes, by $194 M, or by more than 3%. As a result, the "system to system" comparison shows the MPFS rates being, on average, 0.6% higher than the OPPS rates.

Procedure-Level Variation in Effects

When we look at procedure-level variations in this basic comparison, we find that the effects are heavily concentrated, both pro and con, in a limited number of procedures. The table below shows how concentrated these differentials are[16].

[16] This analysis excludes the MRA codes because the coding disparities across settings make direct comparisons unmeaningful.

Procedure-Level Variation in Cross-Site Payment Differentials

hcpcs2004	Description	MPFS Volume Under MPFS Payment Rules	MPFS Volume Under OPPS Payment Rules	MPFS-OPPS
			(millions of dollars)	
93307	Echo exam of heart	$455	$566	-$111
93320	Doppler echo exam, heart	$208	$309	-$100
71020	Chest x-ray	$114	$202	-$88
78478	Heart wall motion add-on	$110	$168	-$58
78480	Heart function add-on	$110	$167	-$57
76519	Echo exam of eye	$48	$91	-$42
93350	Echo transthoracic	$21	$59	-$38
73560	X-ray exam of knee, 1 or 2	$27	$58	-$31
71010	Chest x-ray	$19	$45	-$27
76514	Echo exam of eye, thickness	$2	$28	-$26
	Ten Largest Negative Comparisons	$1,113	$1,692	-$579
G0125	PET, regional imaging or whole body, single pulmon. nodule	$53	$32	$22
73721	Mri jnt of lwr extre w/o dye	$130	$105	$25
93925	Lower extremity study	$86	$51	$34
72158	Mri lumbar spine w/o & w/dye	$125	$67	$59
72148	Mri lumbar spine w/o dye	$252	$181	$70
93325	Doppler color flow add-on	$354	$277	$77
76075	Dxa bone density, axial	$214	$127	$87
93880	Extracranial study	$297	$208	$89
78465	Heart image (3d), multiple	$848	$744	$104
70553	Mri brain w/o & w/dye	$336	$178	$159
	Ten Largest Positive Comparisons	$2,695	$1,971	$725
	Other Procedures	$2,532	$2,640	-$108
	All Procedures	$6,341	$6,302	$38

As these data suggest, cross-site disparities are not uniform across procedures. While the MPFS rates produced weighted payments roughly $38 million higher than under the OPPS, this average masks large swings at the procedure level. The top ten procedures ranked by the dollar magnitude of the payment disparity had MPFS payments fall short of OPPS payments by $579 M, or by 34.2% on average. The top ten "winners," by contrast, show MPFS payments $725 million (36.8%) higher than would be paid under the OPPS methodology and rates.

The "lesser of MPFS or OPPS" payment policy under the DRA will, if implemented, have a highly concentrated effect on the limited number of procedures for which MPFS rates happen to be higher than the corresponding OPPS rates – while having no effect at all on the substantial number of procedures where MPFS payment is, at present, below the OPPS rates. As a result, our present finding of rough balance in payments for imaging services across sites of care would be materially altered toward lower aggregate payments in the office. While the exact comparison awaits final details on how CMS intends to implement the DRA policy, the manner in which CMS finalizes its proposal to revise the practice expense methodology for calculating RVUs, and any updates to the conversion factor, we anticipate that aggregate payments for the TC portion of imaging services would be 16-18% lower in the office setting than the aggregate amount of comparable APC payments in the hospital setting, holding volumes constant.

THE MORAN COMPANY

Analysis of Payment Versus Cost for Imaging Procedures Affected by DRA

Cost Based on CMS Values for Direct & Indirect Costs in Non-Facility Setting

** See Notes section at the end of this spreadsheet

HCPCS MOD	Description	$ MPFS Non-Fac RATE 06	OPPS[1] RATE 06	Est. CMS "Town Hall" Cost Data	DRA Capped Rate	Capped Payment as % of Est. Cost	Capped Rate Versus Est. CMS Cost
Totals							
70010TC	Contrast x-ray of brain	$ 172.81	$ 173.53	$ 165.99	$ -		$ -
70015TC	Contrast x-ray of brain	$ 54.19	$ 173.53	$ 167.80	$ -		$ -
70030TC	X-ray eye for foreign body	$ 16.67	$ 43.42	$ 37.33	$ -		$ -
70100TC	X-ray exam of jaw	$ 20.46	$ 43.42	$ 39.39	$ -		$ -
70110TC	X-ray exam of jaw	$ 25.01	$ 43.42	$ 48.77	$ -		$ -
70120TC	X-ray exam of mastoids	$ 25.01	$ 43.42	$ 43.15	$ -		$ -
70130TC	X-ray exam of mastoids	$ 31.45	$ 43.42	$ 71.65	$ -		$ -
70134TC	X-ray exam of middle ear	$ 29.56	$ 73.89	$ 55.39	$ -		$ -
70140TC	X-ray exam of facial bones	$ 25.01	$ 43.42	$ 32.25	$ -		$ -
70150TC	X-ray exam of facial bones	$ 31.45	$ 43.42	$ 52.66	$ -		$ -
70160TC	X-ray exam of nasal bones	$ 20.46	$ 43.42	$ 44.11	$ -		$ -
70170TC	X-ray exam of tear duct	$ 38.28	$ 205.56	$ -	$ -		$ -
70190TC	X-ray exam of eye sockets	$ 25.01	$ 43.42	$ 44.34	$ -		$ -
70200TC	X-ray exam of eye sockets	$ 31.45	$ 43.42	$ 53.48	$ -		$ -
70210TC	X-ray exam of sinuses	$ 25.01	$ 43.42	$ 33.12	$ -		$ -
70220TC	X-ray exam of sinuses	$ 31.45	$ 43.42	$ 43.43	$ -		$ -
70240TC	"X-ray exam, pituitary saddle"	$ 16.67	$ 43.42	$ 35.21	$ -		$ -
70250TC	X-ray exam of skull	$ 25.01	$ 43.42	$ 43.00	$ -		$ -
70260TC	X-ray exam of skull	$ 36.00	$ 73.89	$ 53.12	$ -		$ -
70300TC	X-ray exam of teeth	$ 10.61	$ 47.72	$ 12.45	$ -		$ -
70310TC	X-ray exam of teeth	$ 16.67	$ 47.72	$ 49.80	$ -		$ -
70320TC	Full mouth x-ray of teeth	$ 31.45	$ 47.72	$ 58.82	$ -		$ -
70328TC	X-ray exam of jaw joint	$ 19.33	$ 43.42	$ 37.33	$ -		$ -
70330TC	X-ray exam of jaw joints	$ 33.73	$ 43.42	$ 62.15	$ -		$ -
70332TC	X-ray exam of jaw joint	$ 84.51	$ 207.85	$ 88.57	$ -		$ -
70336TC	"Magnetic image, jaw joint"	$ 447.95	$ 303.49	$ 904.31	$ 303.49	34%	$ (600.82)
70350TC	X-ray head for orthodontia	$ 15.16	$ 43.42	$ 17.19	$ -		$ -
70355TC	Panoramic x-ray of jaws	$ 23.12	$ 43.42	$ 13.85	$ -		$ -
70360TC	X-ray exam of neck	$ 16.67	$ 43.42	$ 34.87	$ -		$ -
70370TC	Throat x-ray & fluoroscopy	$ 52.30	$ 79.10	$ 107.13	$ -		$ -
70371TC	"Speech evaluation, complex"	$ 84.51	$ 79.10	$ 86.60	$ 79.10	91%	$ (7.50)
70373TC	Contrast x-ray of larynx	$ 72.01	$ 101.04	$ 106.57	$ -		$ -
70380TC	X-ray exam of salivary gland	$ 26.91	$ 43.42	$ 49.12	$ -		$ -
70390TC	X-ray exam of salivary duct	$ 72.01	$ 101.04	$ 157.70	$ -		$ -
70450TC	Ct head/brain w/o dye	$ 188.73	$ 188.10	$ 335.77	$ 188.10	56%	$ (147.67)
70460TC	Ct head/brain w/dye	$ 226.63	$ 255.43	$ 447.14	$ -		$ -
70470TC	Ct head/brain w/o & w/dye	$ 282.72	$ 303.82	$ 548.45	$ -		$ -
70480TC	Ct orbit/ear/fossa w/o dye	$ 188.73	$ 188.10	$ 588.82	$ 188.10	32%	$ (400.72)
70481TC	Ct orbit/ear/fossa w/dye	$ 226.63	$ 255.43	$ 697.75	$ -		$ -
70482TC	Ct orbit/ear/fossa w/o&w/dye	$ 282.72	$ 303.82	$ 812.23	$ -		$ -
70486TC	Ct maxillofacial w/o dye	$ 188.73	$ 188.10	$ 469.27	$ 188.10	40%	$ (281.17)
70487TC	Ct maxillofacial w/dye	$ 226.63	$ 255.43	$ 579.51	$ -		$ -
70488TC	Ct maxillofacial w/o & w/dye	$ 282.72	$ 303.82	$ 733.38	$ -		$ -
70490TC	Ct soft tissue neck w/o dye	$ 188.73	$ 188.10	$ 447.74	$ 188.10	42%	$ (259.64)
70491TC	Ct soft tissue neck w/dye	$ 226.63	$ 255.43	$ 555.01	$ -		$ -
70492TC	Ct sft tsue nck w/o & w/dye	$ 282.72	$ 303.82	$ 713.16	$ -		$ -
70496TC	"Ct angiography, head"	$ 424.83	$ 297.22	$ 1,209.37	$ 297.22	25%	$ (912.15)
70498TC	"Ct angiography, neck"	$ 424.83	$ 297.22	$ 1,221.28	$ 297.22	24%	$ (924.06)
70540TC	Mri orbit/face/neck w/o dye	$ 440.37	$ 349.20	$ 1,054.25	$ 349.20	33%	$ (705.05)
70542TC	Mri orbit/face/neck w/dye	$ 528.67	$ 371.00	$ 1,108.59	$ 371.00	33%	$ (737.59)

HCPCS MOD	Description	MPFS Non-Fac RATE 06	OPPS RATE 06	Est CMS "Town Hall" Cost Data	DRA Capped Rate	Capped Payment as % of Est. Cost	$ Capped Rate Versus Est. CMS Cost
70543TC	Mri orbt/fac/nck w/o & w/dye	$ 977.38	$ 506.26	$ 1,382.10	$ 506.26	37%	$ (875.84)
70544TC	Mr angiography head w/o dye	$ 447.95	$ 349.20	$ 1,145.23	$ 349.20	30%	$ (796.03)
70545TC	Mr angiography head w/dye	$ 447.95	$ 371.00	$ 1,129.66	$ 371.00	33%	$ (758.66)
70546TC	Mr angiograph head w/o&w/dye	$ 873.92	$ 506.26	$ 1,753.28	$ 506.26	29%	$ (1,247.02)
70547TC	Mr angiography neck w/o dye	$ 447.95	$ 349.20	$ 1,150.90	$ 349.20	30%	$ (801.70)
70548TC	Mr angiography neck w/dye	$ 447.95	$ 371.00	$ 1,194.23	$ 371.00	31%	$ (823.23)
70549TC	Mr angiograph neck w/o&w/dye	$ 873.92	$ 506.26	$ 1,744.64	$ 506.26	29%	$ (1,238.38)
70551TC	Mri brain w/o dye	$ 447.95	$ 349.20	$ 1,038.82	$ 349.20	34%	$ (689.62)
70552TC	Mri brain w/dye	$ 537.39	$ 371.00	$ 1,097.67	$ 371.00	34%	$ (726.67)
70553TC	Mri brain w/o & w/dye	$ 995.19	$ 506.26	$ 1,288.39	$ 506.26	39%	$ (782.13)
71010TC	Chest x-ray	$ 18.57	$ 43.42	$ 25.13	$ -		$ -
71015TC	Chest x-ray	$ 20.46	$ 43.42	$ 33.77	$ -		$ -
71020TC	Chest x-ray	$ 25.01	$ 43.42	$ 33.43	$ -		$ -
71021TC	Chest x-ray	$ 29.56	$ 43.42	$ 42.34	$ -		$ -
71022TC	Chest x-ray	$ 29.56	$ 43.42	$ 53.56	$ -		$ -
71023TC	Chest x-ray and fluoroscopy	$ 31.45	$ 79.10	$ 103.85	$ -		$ -
71030TC	Chest x-ray	$ 31.45	$ 43.42	$ 54.69	$ -		$ -
71034TC	Chest x-ray and fluoroscopy	$ 57.60	$ 79.10	$ 141.46	$ -		$ -
71035TC	Chest x-ray	$ 20.46	$ 43.42	$ 50.02	$ -		$ -
71040TC	Contrast x-ray of bronchi	$ 58.36	$ 101.04	$ 119.89	$ -		$ -
71060TC	Contrast x-ray of bronchi	$ 88.68	$ 101.04	$ 196.84	$ -		$ -
71100TC	X-ray exam of ribs	$ 23.12	$ 43.42	$ 36.57	$ -		$ -
71101TC	X-ray exam of ribs/chest	$ 26.91	$ 43.42	$ 46.32	$ -		$ -
71110TC	X-ray exam of ribs	$ 31.45	$ 43.42	$ 47.77	$ -		$ -
71111TC	X-ray exam of ribs/chest	$ 36.00	$ 73.89	$ 65.87	$ -		$ -
71120TC	X-ray exam of breastbone	$ 26.15	$ 43.42	$ 37.52	$ -		$ -
71130TC	X-ray exam of breastbone	$ 28.42	$ 43.42	$ 46.16	$ -		$ -
71250TC	Ct thorax w/o dye	$ 236.48	$ 188.10	$ 443.33	$ 188.10	42%	$ (255.23)
71260TC	Ct thorax w/dye	$ 282.72	$ 255.43	$ 552.26	$ 255.43	46%	$ (296.83)
71270TC	Ct thorax w/o & w/dye	$ 353.96	$ 303.82	$ 710.41	$ 303.82	43%	$ (406.59)
71275TC	"Ct angiography, chest"	$ 485.47	$ 297.22	$ 803.94	$ 297.22	37%	$ (506.72)
71550TC	Mri chest w/o dye	$ 442.64	$ 349.20	$ 1,203.73	$ 349.20	29%	$ (854.53)
71551TC	Mri chest w/dye	$ 530.57	$ 371.00	$ 1,300.37	$ 371.00	29%	$ (929.37)
71552TC	Mri chest w/o & w/dye	$ 971.31	$ 506.26	$ 1,644.69	$ 506.26	31%	$ (1,138.43)
71555TC	Mri angio chest w or w/o dye	$ 447.95		$ 1,108.88	$ -		$ -
72010TC	X-ray exam of spine	$ 40.93	$ 43.42	$ 83.09	$ -		$ -
72020TC	X-ray exam of spine	$ 16.67	$ 43.42	$ 27.56	$ -		$ -
72040TC	X-ray exam of neck spine	$ 24.25	$ 43.42	$ 46.47	$ -		$ -
72050TC	X-ray exam of neck spine	$ 36.00	$ 73.89	$ 64.43	$ -		$ -
72052TC	X-ray exam of neck spine	$ 45.10	$ 73.89	$ 84.13	$ -		$ -
72069TC	X-ray exam of trunk spine	$ 19.33	$ 43.42	$ 45.36	$ -		$ -
72070TC	X-ray exam of thoracic spine	$ 26.15	$ 43.42	$ 37.52	$ -		$ -
72072TC	X-ray exam of thoracic spine	$ 29.56	$ 43.42	$ 48.27	$ -		$ -
72074TC	X-ray exam of thoracic spine	$ 36.76	$ 43.42	$ 59.58	$ -		$ -
72080TC	X-ray exam of trunk spine	$ 26.91	$ 43.42	$ 39.79	$ -		$ -
72090TC	X-ray exam of trunk spine	$ 26.91	$ 73.89	$ 61.35	$ -		$ -
72100TC	X-ray exam of lower spine	$ 26.91	$ 43.42	$ 49.24	$ -		$ -
72110TC	X-ray exam of lower spine	$ 36.76	$ 73.89	$ 69.32	$ -		$ -
72114TC	X-ray exam of lower spine	$ 47.37	$ 73.89	$ 93.80	$ -		$ -
72120TC	X-ray exam of lower spine	$ 36.00	$ 73.89	$ 63.47	$ -		$ -
72125TC	Ct neck spine w/o dye	$ 236.48	$ 188.10	$ 441.13	$ 188.10	43%	$ (253.03)
72126TC	Ct neck spine w/dye	$ 282.72	$ 255.43	$ 555.01	$ 255.43	46%	$ (299.58)
72127TC	Ct neck spine w/o & w/dye	$ 353.96	$ 303.82	$ 728.00	$ 303.82	42%	$ (424.18)
72128TC	Ct chest spine w/o dye	$ 236.48	$ 188.10	$ 443.33	$ 188.10	42%	$ (255.23)
72129TC	Ct chest spine w/dye	$ 282.72	$ 255.43	$ 552.26	$ 255.43	46%	$ (296.83)
72130TC	Ct chest spine w/o & w/dye	$ 353.96	$ 303.82	$ 728.00	$ 303.82	42%	$ (424.18)
72131TC	Ct lumbar spine w/o dye	$ 236.48	$ 188.10	$ 443.33	$ 188.10	42%	$ (255.23)
72132TC	Ct lumbar spine w/dye	$ 282.72	$ 255.43	$ 555.01	$ 255.43	46%	$ (299.58)

HCPCS MOD	Description	MPFS Non-Fac RATE 06	OPPS RATE 06	Est. CMS "Town Hall" Cost Data	DRA Capped Rate	Capped Payment as % of Est. Cost	Capped Rate Versus Est. CMS Cost
72133TC	Ct lumbar spine w/o & w/dye	$ 353.96	$ 303.82	$ 709.65	$ 303.82	43%	$ (405.83)
72141TC	Mri neck spine w/o dye	$ 447.95	$ 349.20	$ 904.31	$ 349.20	39%	$ (555.11)
72142TC	Mri neck spine w/dye	$ 537.39	$ 371.00	$ 1,108.59	$ 371.00	33%	$ (737.59)
72146TC	Mri chest spine w/o dye	$ 497.22	$ 349.20	$ 899.90	$ 349.20	39%	$ (550.70)
72147TC	Mri chest spine w/dye	$ 537.39	$ 371.00	$ 954.62	$ 371.00	39%	$ (583.62)
72148TC	Mri lumbar spine w/o dye	$ 497.22	$ 349.20	$ 908.72	$ 349.20	38%	$ (559.52)
72149TC	Mri lumbar spine w/dye	$ 537.39	$ 371.00	$ 1,114.05	$ 371.00	33%	$ (743.05)
72156TC	Mri neck spine w/o & w/dye	$ 995.19	$ 506.26	$ 1,264.76	$ 506.26	40%	$ (758.50)
72157TC	Mri chest spine w/o & w/dye	$ 995.19	$ 506.26	$ 1,145.52	$ 506.26	44%	$ (639.26)
72158TC	Mri lumbar spine w/o & w/dye	$ 995.19	$ 506.26	$ 1,270.99	$ 506.26	40%	$ (764.73)
72159TC	Mr angio spine w/o&w/dye	$ 489.26		$ 530.41	$ -		$ -
72170TC	X-ray exam of pelvis	$ 20.46	$ 43.42	$ 28.38	$ -		$ -
72190TC	X-ray exam of pelvis	$ 26.91	$ 43.42	$ 52.03	$ -		$ -
72191TC	Ct angiograph pelv w/o&w/dye	$ 471.82	$ 297.22	$ 783.11	$ 297.22	38%	$ (485.89)
72192TC	Ct pelvis w/o dye	$ 236.48	$ 188.10	$ 411.34	$ 188.10	46%	$ (223.24)
72193TC	Ct pelvis w/dye	$ 273.62	$ 255.43	$ 521.79	$ 255.43	49%	$ (266.36)
72194TC	Ct pelvis w/o & w/dye	$ 338.80	$ 303.82	$ 713.16	$ 303.82	43%	$ (409.34)
72195TC	Mri pelvis w/o dye	$ 442.64	$ 349.20	$ 1,054.25	$ 349.20	33%	$ (705.05)
72196TC	Mri pelvis w/dye	$ 530.57	$ 371.00	$ 1,108.59	$ 371.00	33%	$ (737.59)
72197TC	Mri pelvis w/o & w/dye	$ 980.41	$ 506.26	$ 1,368.62	$ 506.26	37%	$ (862.36)
72198TC	Mr angio pelvis w/o & w/dye	$ 447.95		$ 1,087.66	$ -		$ -
72200TC	X-ray exam sacroiliac joints	$ 20.46	$ 43.42	$ 35.62	$ -		$ -
72202TC	X-ray exam sacroiliac joints	$ 25.01	$ 43.42	$ 46.00	$ -		$ -
72220TC	X-ray exam of tailbone	$ 23.12	$ 43.42	$ 34.73	$ -		$ -
72240TC	Contrast x-ray of neck spine	$ 189.87	$ 173.53	$ 157.62	$ 173.53	110%	$ 15.91
72255TC	"Contrast x-ray, thorax spine"	$ 172.81	$ 173.53	$ 138.22	$ -		$ -
72265TC	"Contrast x-ray, lower spine"	$ 162.96	$ 173.53	$ 157.62	$ -		$ -
72270TC	"Contrast x-ray, spine"	$ 244.44	$ 173.53	$ 246.50	$ 173.53	70%	$ (72.97)
72275TC	Epidurography	$ 88.30	$ 173.53	$ 101.64	$ -		$ -
72285TC	X-ray c/t spine disk	$ 334.63	$ 724.32	$ 75.98	$ -		$ -
72295TC	X-ray of lower spine disk	$ 313.79	$ 724.32	$ 78.95	$ -		$ -
73000TC	X-ray exam of collar bone	$ 20.46	$ 43.42	$ 32.63	$ -		$ -
73010TC	X-ray exam of shoulder blade	$ 20.46	$ 43.42	$ 33.58	$ -		$ -
73020TC	X-ray exam of shoulder	$ 18.57	$ 43.42	$ 26.01	$ -		$ -
73030TC	X-ray exam of shoulder	$ 23.12	$ 43.42	$ 32.95	$ -		$ -
73040TC	Contrast x-ray of shoulder	$ 84.51	$ 207.85	$ 144.69	$ -		$ -
73050TC	X-ray exam of shoulders	$ 26.91	$ 43.42	$ 41.12	$ -		$ -
73060TC	X-ray exam of humerus	$ 23.12	$ 43.42	$ 34.28	$ -		$ -
73070TC	X-ray exam of elbow	$ 20.46	$ 43.42	$ 32.16	$ -		$ -
73080TC	X-ray exam of elbow	$ 23.12	$ 43.42	$ 47.23	$ -		$ -
73085TC	Contrast x-ray of elbow	$ 84.51	$ 207.85	$ 111.99	$ -		$ -
73090TC	X-ray exam of forearm	$ 20.46	$ 43.42	$ 33.43	$ -		$ -
73092TC	"X-ray exam of arm, infant"	$ 19.33	$ 43.42	$ 35.09	$ -		$ -
73100TC	X-ray exam of wrist	$ 19.33	$ 43.42	$ 33.87	$ -		$ -
73110TC	X-ray exam of wrist	$ 20.84	$ 43.42	$ 47.93	$ -		$ -
73115TC	Contrast x-ray of wrist	$ 63.67	$ 207.85	$ 147.32	$ -		$ -
73120TC	X-ray exam of hand	$ 19.33	$ 43.42	$ 32.15	$ -		$ -
73130TC	X-ray exam of hand	$ 20.84	$ 43.42	$ 39.41	$ -		$ -
73140TC	X-ray exam of finger(s)	$ 16.67	$ 43.42	$ 40.78	$ -		$ -
73200TC	Ct upper extremity w/o dye	$ 197.82	$ 188.10	$ 445.54	$ 188.10	42%	$ (257.44)
73201TC	Ct upper extremity w/dye	$ 236.48	$ 255.43	$ 555.01	$ -		$ -
73202TC	Ct uppr extremity w/o&w/dye	$ 296.74	$ 303.82	$ 757.11	$ -		$ -
73206TC	Ct angio upr extrm w/o&w/dye	$ 431.27	$ 297.22	$ 737.55	$ 297.22	40%	$ (440.33)
73218TC	Mri upper extremity w/o dye	$ 440.37	$ 349.20	$ 1,059.39	$ 349.20	33%	$ (710.19)
73219TC	Mri upper extremity w/dye	$ 528.67	$ 371.00	$ 1,114.05	$ 371.00	33%	$ (743.05)
73220TC	Mri uppr extremity w/o&w/dye	$ 977.38	$ 506.26	$ 1,368.62	$ 506.26	37%	$ (862.36)
73221TC	Mri joint upr extrem w/o dye	$ 440.37	$ 349.20	$ 993.22	$ 349.20	35%	$ (644.02)
73222TC	Mri joint upr extrem w/dye	$ 528.67	$ 371.00	$ 1,050.03	$ 371.00	35%	$ (679.03)

HCPCS MOD	Description	MPFS Non-Fac RATE 06	OPPS RATE 06	Est. CMS "Town Hall" Cost Data	DRA Capped Rate	Capped Payment as % of Est. Cost	% Capped Rate Versus Est. CMS Cost
73223TC	Mri joint upr extr w/o&w/dye	$ 977.38	$ 506.26	$ 1,270.99	$ 506.26	40%	$ (764.73)
73225TC	Mr angio upr extr w/o&w/dye	$ 440.75		$ 530.41	$ -		$ -
73500TC	X-ray exam of hip	$ 18.57	$ 43.42	$ 27.85	$ -		$ -
73510TC	X-ray exam of hip	$ 23.12	$ 43.42	$ 47.16	$ -		$ -
73520TC	X-ray exam of hips	$ 26.91	$ 73.89	$ 46.93	$ -		$ -
73525TC	Contrast x-ray of hip	$ 84.51	$ 207.85	$ 110.86	$ -		$ -
73540TC	X-ray exam of pelvis & hips	$ 23.12	$ 43.42	$ 46.16	$ -		$ -
73542TC	"X-ray exam, sacroiliac joint"	$ 84.51	$ 207.85	$ 66.32	$ -		$ -
73550TC	X-ray exam of thigh	$ 23.12	$ 43.42	$ 32.15	$ -		$ -
73560TC	"X-ray exam of knee, 1 or 2"	$ 20.46	$ 43.42	$ 33.43	$ -		$ -
73562TC	"X-ray exam of knee, 3"	$ 23.12	$ 43.42	$ 42.17	$ -		$ -
73564TC	"X-ray exam, knee, 4 or more"	$ 25.01	$ 43.42	$ 51.09	$ -		$ -
73565TC	X-ray exam of knees	$ 19.33	$ 43.42	$ 35.65	$ -		$ -
73580TC	Contrast x-ray of knee joint	$ 104.98	$ 207.85	$ 148.27	$ -		$ -
73590TC	X-ray exam of lower leg	$ 20.46	$ 43.42	$ 31.67	$ -		$ -
73592TC	"X-ray exam of leg, infant"	$ 19.33	$ 43.42	$ 34.55	$ -		$ -
73600TC	X-ray exam of ankle	$ 19.33	$ 43.42	$ 32.31	$ -		$ -
73610TC	X-ray exam of ankle	$ 20.84	$ 43.42	$ 40.00	$ -		$ -
73615TC	Contrast x-ray of ankle	$ 84.51	$ 207.85	$ 113.48	$ -		$ -
73620TC	X-ray exam of foot	$ 19.33	$ 43.42	$ 29.45	$ -		$ -
73630TC	X-ray exam of foot	$ 20.84	$ 43.42	$ 38.03	$ -		$ -
73650TC	X-ray exam of heel	$ 18.57	$ 43.42	$ 31.83	$ -		$ -
73660TC	X-ray exam of toe(s)	$ 16.67	$ 43.42	$ 38.63	$ -		$ -
73700TC	Ct lower extremity w/o dye	$ 197.82	$ 188.10	$ 443.33	$ 188.10	42%	$ (255.23)
73701TC	Ct lower extremity w/dye	$ 236.48	$ 255.43	$ 549.51	$ -		$ -
73702TC	Ct lwr extremity w/o&w/dye	$ 296.74	$ 303.82	$ 764.60	$ -		$ -
73706TC	Ct angio lwr extr w/o&w/dye	$ 431.27	$ 297.22	$ 858.72	$ 297.22	35%	$ (561.50)
73718TC	Mri lower extremity w/o dye	$ 440.37	$ 349.20	$ 1,059.39	$ 349.20	33%	$ (710.19)
73719TC	Mri lower extremity w/dye	$ 528.67	$ 371.00	$ 1,103.13	$ 371.00	34%	$ (732.13)
73720TC	Mri lwr extremity w/o&w/dye	$ 977.38	$ 506.26	$ 1,361.88	$ 506.26	37%	$ (855.62)
73721TC	Mri jnt of lwr extre w/o dye	$ 440.37	$ 349.20	$ 1,017.47	$ 349.20	34%	$ (668.27)
73722TC	Mri joint of lwr extr w/dye	$ 528.67	$ 371.00	$ 1,050.03	$ 371.00	35%	$ (679.03)
73723TC	Mri joint lwr extr w/o&w/dye	$ 977.38	$ 506.26	$ 1,264.76	$ 506.26	40%	$ (758.50)
73725TC	Mr ang lwr ext w or w/o dye	$ 447.95		$ 1,077.05	$ -		$ -
74000TC	X-ray exam of abdomen	$ 20.46	$ 43.42	$ 26.88	$ -		$ -
74010TC	X-ray exam of abdomen	$ 23.12	$ 43.42	$ 49.27	$ -		$ -
74020TC	X-ray exam of abdomen	$ 25.01	$ 43.42	$ 49.52	$ -		$ -
74022TC	"X-ray exam series, abdomen"	$ 29.56	$ 73.89	$ 59.58	$ -		$ -
74150TC	Ct abdomen w/o dye	$ 226.63	$ 188.10	$ 411.34	$ 188.10	46%	$ (223.24)
74160TC	Ct abdomen w/dye	$ 273.62	$ 255.43	$ 612.44	$ 255.43	42%	$ (357.01)
74170TC	Ct abdomen w/o & w/dye	$ 338.80	$ 303.82	$ 859.69	$ 303.82	35%	$ (555.87)
74175TC	Ct angio abdom w/o & w/dye	$ 471.82	$ 297.22	$ 849.93	$ 297.22	35%	$ (552.71)
74181TC	Mri abdomen w/o dye	$ 442.64	$ 349.20	$ 891.08	$ 349.20	39%	$ (541.88)
74182TC	Mri abdomen w/dye	$ 530.57	$ 371.00	$ 1,244.68	$ 371.00	30%	$ (873.68)
74183TC	Mri abdomen w/o & w/dye	$ 980.41	$ 506.26	$ 1,361.88	$ 506.26	37%	$ (855.62)
74185TC	"Mri angio, abdom w orw/o dye"	$ 447.95		$ 1,077.05	$ -		$ -
74190TC	X-ray exam of peritoneum	$ 52.30	$ 205.56	$ -	$ -		$ -
74210TC	Contrst x-ray exam of throat	$ 47.37	$ 87.44	$ 116.55	$ -		$ -
74220TC	"Contrast x-ray, esophagus"	$ 47.37	$ 87.44	$ 132.64	$ -		$ -
74230TC	"Cine/vid x-ray, throat/esoph"	$ 52.30	$ 87.44	$ 123.55	$ -		$ -
74240TC	"X-ray exam, upper gi tract"	$ 58.36	$ 87.44	$ 146.28	$ -		$ -
74241TC	"X-ray exam, upper gi tract"	$ 59.50	$ 87.44	$ 163.58	$ -		$ -
74245TC	"X-ray exam, upper gi tract"	$ 95.50	$ 136.58	$ 258.46	$ -		$ -
74246TC	Contrst x-ray uppr gi tract	$ 65.94	$ 87.44	$ 182.06	$ -		$ -
74247TC	Contrst x-ray uppr gi tract	$ 67.84	$ 87.44	$ 212.98	$ -		$ -
74249TC	Contrst x-ray uppr gi tract	$ 103.08	$ 136.58	$ 285.75	$ -		$ -
74250TC	X-ray exam of small bowel	$ 52.30	$ 87.44	$ 165.23	$ -		$ -
74251TC	X-ray exam of small bowel	$ 52.30	$ 136.58	$ 710.48	$ -		$ -

HCPCS MOD	Description	MPFS Non-Fac RATE 09	OPPS RATE 06	Est. CMS "Town Hall" Cost Data	DRA Capped Rate	Capped Payment as % of Est. Cost	Capped Rate Versus Est. CMS Cost
74260TC	X-ray exam of small bowel	$ 59.50	$ 136.58	$ 592.02	$ -		$ -
74270TC	Contrast x-ray exam of colon	$ 68.59	$ 87.44	$ 238.00	$ -		$ -
74280TC	Contrast x-ray exam of colon	$ 89.82	$ 136.58	$ 330.47	$ -		$ -
74283TC	Contrast x-ray exam of colon	$ 102.70	$ 87.44	$ 197.84	$ 87.44	44%	$ (110.40)
74290TC	"Contrast x-ray, gallbladder"	$ 29.56	$ 87.44	$ 102.28	$ -		$ -
74291TC	"Contrast x-rays, gallbladder"	$ 16.67	$ 87.44	$ 105.16	$ -		$ -
74320TC	Contrast x-ray of bile ducts	$ 126.20	$ 205.56	$ 139.93	$ -		$ -
74327TC	X-ray bile stone removal	$ 71.25	$ 134.99	$ 190.18	$ -		$ -
74328TC	X-ray bile duct endoscopy	$ 126.20		$ -	$ -		$ -
74329TC	X-ray for pancreas endoscopy	$ -		$ -	$ -		$ -
74330TC	X-ray bile/panc endoscopy	$ 126.20		$ -	$ -		$ -
74340TC	X-ray guide for GI tube	$104.98	$ 79.10	$ -	$ 79.10		$ 79.10
74350TC	"X-ray guide, stomach tube"	$126.20	$ 101.04	$ 140.02	$ 101.04	72%	$ (38.98)
74355TC	"X-ray guide, intestinal tube"	$104.98	$ 101.04	$ -	$ 101.04		$ 101.04
74360TC	"X-ray guide, GI dilation"	$126.20	$ 134.99	$ -	$ -		$ -
74400TC	"Contrst x-ray, urinary tract"	$ 67.84	$ 152.10	$ 169.25	$ -		$ -
74410TC	"Contrst x-ray, urinary tract"	$ 78.45	$ 152.10	$ 175.09	$ -		$ -
74415TC	"Contrst x-ray, urinary tract"	$ 85.27	$ 152.10	$ 219.56	$ -		$ -
74420TC	"Contrst x-ray, urinary tract"	$ 104.98	$ 152.10	$ -	$ -		$ -
74425TC	"Contrst x-ray, urinary tract"	$ 52.30	$ 152.10	$ -	$ -		$ -
74430TC	"Contrast x-ray, bladder"	$ 42.07	$ 152.10	$ 130.06	$ -		$ -
74440TC	"X-ray, male genital tract"	$ 45.10	$ 152.10	$ 135.25	$ -		$ -
74445TC	X-ray exam of penis	$ 45.10	$ 152.10	$ -	$ -		$ -
74450TC	"X-ray, urethra/bladder"	$ 58.36	$ 152.10	$ -	$ -		$ -
74455TC	"X-ray, urethra/bladder"	$ 63.67	$ 152.10	$ 139.98	$ -		$ -
74470TC	X-ray exam of kidney lesion	$ 50.02	$ 101.04	$ -	$ -		$ -
74475TC	"X-ray control, cath insert"	$ 162.96	$ 303.37	$ 140.01	$ -		$ -
74480TC	"X-ray control, cath insert"	$ 162.96	$ 134.99	$ 139.16	$ 134.99	97%	$ (4.17)
74485TC	"X-ray guide, GU dilation"	$ 126.20	$ 134.99	$ 147.60	$ -		$ -
74710TC	X-ray measurement of pelvis	$ 42.07	$ 73.89	$ 36.48	$ -		$ -
74740TC	"X-ray, female genital tract"	$ 52.30	$ 205.56	$ 116.89	$ -		$ -
74775TC	X-ray exam of perineum	$ 58.36	$ 152.10	$ -	$ -		$ -
75552TC	Heart mri for morph w/o dye	$ 447.95	$ 349.20	$ 1,407.79	$ 349.20	25%	$ (1,058.59)
75553TC	Heart mri for morph w/dye	$ 447.95	$ 371.00	$ 1,922.43	$ 371.00	19%	$ (1,551.43)
75554TC	Cardiac MRI/function	$ 447.95	$ 349.20	$ 2,104.96	$ 349.20	17%	$ (1,755.76)
75555TC	Cardiac MRI/limited study	$ 447.95	$ 349.20	$ 2,209.16	$ 349.20	16%	$ (1,859.96)
75600TC	Contrast x-ray exam of aorta	$ 503.66	$ 1,215.14	$ 458.23	$ -		$ -
75605TC	Contrast x-ray exam of aorta	$ 503.66	$ 1,215.14	$ 232.84	$ -		$ -
75625TC	Contrast x-ray exam of aorta	$ 503.66	$ 1,215.14	$ 207.62	$ -		$ -
75630TC	"X-ray aorta, leg arteries"	$ 525.26	$ 1,215.14	$ 218.29	$ -		$ -
75635TC	Ct angio abdominal arteries	$ 619.62	$ 297.22	$ 875.22	$ 297.22	34%	$ (578.00)
75650TC	"Artery x-rays, head & neck"	$ 503.66	$ 1,215.14	$ 210.53	$ -		$ -
75658TC	"Artery x-rays, arm"	$ 503.66	$ 517.67	$ 231.66	$ -		$ -
75660TC	"Artery x-rays, head & neck"	$ 503.66	$ 375.54	$ 233.80	$ 375.54	161%	$ 141.74
75662TC	"Artery x-rays, head & neck"	$ 503.66	$ 1,215.14	$ 308.97	$ -		$ -
75665TC	"Artery x-rays, head & neck"	$ 503.66	$ 1,215.14	$ 237.16	$ -		$ -
75671TC	"Artery x-rays, head & neck"	$ 503.66	$ 1,215.14	$ 300.42	$ -		$ -
75676TC	"Artery x-rays, neck"	$ 503.66	$ 1,215.14	$ 226.30	$ -		$ -
75680TC	"Artery x-rays, neck"	$ 503.66	$ 1,215.14	$ 273.04	$ -		$ -
75685TC	"Artery x-rays, spine"	$ 503.66	$ 1,215.14	$ 233.80	$ -		$ -
75705TC	"Artery x-rays, spine"	$ 503.66	$ 375.54	$ 218.79	$ 375.54	172%	$ 156.75
75710TC	"Artery x-rays, arm/leg"	$ 503.66	$ 1,215.14	$ 241.48	$ -		$ -
75716TC	"Artery x-rays, arms/legs"	$ 503.66	$ 1,215.14	$ 302.63	$ -		$ -
75722TC	"Artery x-rays, kidney"	$ 503.66	$ 1,215.14	$ 243.37	$ -		$ -
75724TC	"Artery x-rays, kidneys"	$ 503.66	$ 1,215.14	$ 331.36	$ -		$ -
75726TC	"Artery x-rays, abdomen"	$ 503.66	$ 1,215.14	$ 229.52	$ -		$ -
75731TC	"Artery x-rays, adrenal gland"	$ 503.66	$ 1,215.14	$ 242.60	$ -		$ -
75733TC	"Artery x-rays, adrenals"	$ 503.66	$ 375.54	$ 337.50	$ 375.54	111%	$ 38.04

HCPCS MOD	Description	MPFS Non-Fac RATE 06	OPPS RATE 06	Est CMS "Town-Hall" Cost Data	DRA Capped Rate	Capped Payment as % of Est. Cost %	Capped Rate Versus Est. CMS Cost
75736TC	"Artery x-rays, pelvis"	$ 503.66	$ 1,215.14	$ 236.21	$ -		$ -
75741TC	"Artery x-rays, lung"	$ 503.66	$ 517.67	$ 189.05	$ -		$ -
75743TC	"Artery x-rays, lungs"	$ 503.66	$ 1,215.14	$ 208.10	$ -		$ -
75746TC	"Artery x-rays, lung"	$ 503.66	$ 517.67	$ 213.30	$ -		$ -
75756TC	"Artery x-rays, chest"	$ 503.66	$ 517.67	$ 300.74	$ -		$ -
75774TC	"Artery x-ray, each vessel"	$ 503.66	$ 517.67	$ 169.48	$ -		$ -
75790TC	Visualize A-V shunt	$ 54.19	$ 517.67	$ 169.97	$ -		$ -
75801TC	"Lymph vessel x-ray, arm/leg"	$ 216.77	$ 205.56	$ -	$ 205.56		$ 205.56
75803TC	"Lymph vessel x-ray,arms/legs"	$ 216.77	$ 205.56	$ -	$ 205.56		$ 205.56
75805TC	"Lymph vessel x-ray, trunk"	$ 244.44	$ 205.56	$ -	$ 205.56		$ 205.56
75809TC	"Nonvascular shunt, x-ray"	$ 31.45	$ 101.04	$ 142.49	$ -		$ -
75810TC	"Vein x-ray, spleen/liver"	$ 503.66	$ 517.67	$ -	$ -		$ -
75820TC	"Vein x-ray, arm/leg"	$ 38.28	$ 375.54	$ 199.56	$ -		$ -
75822TC	"Vein x-ray, arms/legs"	$ 59.12	$ 375.54	$ 196.18	$ -		$ -
75825TC	"Vein x-ray, trunk"	$ 503.66	$ 517.67	$ 175.72	$ -		$ -
75827TC	"Vein x-ray, chest"	$ 503.66	$ 517.67	$ 174.84	$ -		$ -
75831TC	"Vein x-ray, kidney"	$ 503.66	$ 517.67	$ 184.18	$ -		$ -
75833TC	"Vein x-ray, kidneys"	$ 503.66	$ 517.67	$ 214.18	$ -		$ -
75840TC	"Vein x-ray, adrenal gland"	$ 503.66	$ 1,215.14	$ 92.09	$ -		$ -
75842TC	"Vein x-ray, adrenal glands"	$ 503.66	$ 1,215.14	$ 107.12	$ -		$ -
75860TC	"Vein x-ray, neck"	$ 503.66	$ 375.54	$ 220.10	$ 375.54	171%	$ 155.44
75870TC	"Vein x-ray, skull"	$ 503.66	$ 375.54	$ 194.31	$ 375.54	193%	$ 181.23
75872TC	"Vein x-ray, skull"	$ 503.66	$ 517.67	$ 201.68	$ -		$ -
75880TC	"Vein x-ray, eye socket"	$ 38.28	$ 375.54	$ 185.42	$ -		$ -
75885TC	"Vein x-ray, liver"	$ 503.66	$ 1,215.14	$ 90.89	$ -		$ -
75887TC	"Vein x-ray, liver"	$ 503.66	$ 517.67	$ 189.96	$ -		$ -
75889TC	"Vein x-ray, liver"	$ 503.66	$ 1,215.14	$ 90.89	$ -		$ -
75891TC	"Vein x-ray, liver"	$ 503.66	$ 517.67	$ 184.51	$ -		$ -
75893TC	Venous sampling by catheter	$ 503.66		$ 186.02	$ -		$ -
75894TC	"X-rays, transcath therapy"	$ 965.25	$ 303.37	$ -	$ 303.37		$ 303.37
75896TC	"X-rays, transcath therapy"	$ 839.43	$ 303.37	$ -	$ 303.37		$ 303.37
75898TC	Follow-up angiography	$ 42.07	$ 101.04	$ -	$ -		$ -
75901TC	Remove cva device obstruct	$ 81.10	$ 101.04	$ 282.52	$ -		$ -
75902TC	Remove cva lumen obstruct	$ 81.10	$ 101.04	$ 106.64	$ -		$ -
75940TC	"X-ray placement, vein filter"	$ 503.66	$ 303.37	$ -	$ 303.37		$ 303.37
75945TC	Intravascular us	$ 182.29	$ 152.01	$ -	$ 152.01		$ 152.01
75960TC	Transcath iv stent rs&i	$ 595.37	$ 375.54	$ -	$ 375.54		$ 375.54
75961TC	"Retrieval, broken catheter"	$ 419.90	$ 375.54	$ 212.05	$ 375.54	177%	$ 163.49
75962TC	Repair arterial blockage	$ 629.86	$ 375.54	$ 224.65	$ 375.54	167%	$ 150.89
75964TC	"Repair artery blockage, each"	$ 335.01	$ 375.54	$ 155.93	$ -		$ -
75966TC	Repair arterial blockage	$ 629.86	$ 375.54	$ 258.67	$ 375.54	145%	$ 116.87
75968TC	"Repair artery blockage, each"	$ 335.01	$ 375.54	$ 171.37	$ -		$ -
75970TC	Vascular biopsy	$ 461.21	$ 375.54	$ -	$ 375.54		$ 375.54
75978TC	Repair venous blockage	$ 629.86	$ 375.54	$ 200.27	$ 375.54	188%	$ 175.27
75980TC	Contrast xray exam bile duct	$ 216.77	$ 303.37	$ -	$ -		$ -
75984TC	Xray control catheter change	$ 78.45	$ 101.04	$ 147.66	$ -		$ -
75989TC	Abscess drainage under x-ray	$ 126.20		$ 130.26	$ -		$ -
75992TC	"Atherectomy, x-ray exam"	$ 629.86	$ 517.67	$ -	$ 517.67		$ 517.67
76000TC	Fluoroscope examination	$ 52.30	$ 79.10	$ 181.90	$ -		$ -
76001TC	"Fluoroscope exam, extensive"	$ 104.98		$ -	$ -		$ -
76010TC	"X-ray, nose to rectum"	$ 20.46	$ 43.42	$ 31.67	$ -		$ -
76020TC	X-rays for bone age	$ 20.46	$ 43.42	$ 24.76	$ -		$ -
76040TC	"X-rays, bone evaluation"	$ 31.45	$ 73.89	$ 35.53	$ -		$ -
76061TC	"X-rays, bone survey"	$ 40.17	$ 73.89	$ 87.60	$ -		$ -
76062TC	"X-rays, bone survey"	$ 57.60	$ 73.89	$ 144.73	$ -		$ -
76065TC	"X-rays, bone evaluation"	$ 29.56	$ 73.89	$ 121.83	$ -		$ -
76066TC	"Joint survey, single view"	$ 44.34	$ 43.42	$ 33.58	$ 43.42	129%	$ 9.84
76070TC	"Ct bone density, axial"	$ 118.24	$ 72.70	$ 342.39	$ 72.70	21%	$ (269.69)

HCPCS MOD	Description	MPFS Non-Fac RATE 06	OPPS RATE 06	Est. CMS "Town Hall" Cost Data	DRA Capped Rate	Capped Payment as % of Est. Cost	Capped Rate Versus Est. CMS Cost
76071TC	"Ct bone density, peripheral"	$ 114.07	$ 94.82	$ 45.08	$ 94.82	210%	$ 49.74
76075TC	"Dxa bone density, axial"	$ 123.92	$ 72.70	$ 36.57	$ 72.70	199%	$ 36.13
76076TC	Dxa bone density/peripheral	$ 30.32	$ 37.97	$ 29.76	$ -		$ -
76077TC	Dxa bone density/v-fracture	$ 30.32	$ 43.42	$ 21.83	$ -		$ -
76078TC	Radiographic absorptiometry	$ 30.32	$ 43.42	$ 19.78	$ -		$ -
76080TC	X-ray exam of fistula	$ 42.07	$ 101.04	$ 62.01	$ -		$ -
76086TC	X-ray of mammary duct	$ 104.98	$ 101.04	$ 75.80	$ 101.04	133%	$ 25.25
76088TC	X-ray of mammary ducts	$ 146.28	$ 101.04	$ 103.84	$ 101.04	97%	$ (2.80)
76093TC	"Magnetic image, breast"	$ 704.51		$ 1,583.12	$ -		$ -
76094TC	"Magnetic image, both breasts"	$ 955.77		$ 1,590.95	$ -		$ -
76098TC	"X-ray exam, breast specimen"	$ 16.67	$ 43.42	$ 17.26	$ -		$ -
76100TC	X-ray exam of body section	$ 50.02	$ 73.89	$ 227.33	$ -		$ -
76101TC	Complex body section x-ray	$ 56.85	$ 101.04	$ 348.58	$ -		$ -
76102TC	Complex body section x-rays	$ 70.11	$ 205.56	$ 497.70	$ -		$ -
76120TC	Cine/video x-rays	$ 42.07	$ 79.10	$ 137.04	$ -		$ -
76125TC	Cine/video x-rays add-on	$ 31.45	$ 43.42	$ -	$ -		$ -
76376TC	3d render w/o postprocess	$ 133.02	$ 36.52	$ 94.93	$ 36.52	38%	$ (58.41)
76377TC	3d rendering w/postprocess	$ 141.74	$ 94.82	$ 75.79	$ 94.82	125%	$ 19.03
76380TC	CAT scan follow-up study	$ 139.84	$ 94.82	$ 319.85	$ 94.82	30%	$ (225.03)
76400TC	"Magnetic image, bone marrow"	$ 447.95	$ 303.49	$ 1,074.82	$ 303.49	28%	$ (771.33)
76506TC	Echo exam of head	$ 56.85	$ 59.09	$ 165.92	$ -		$ -
76510TC	"Ophth us, b & quant a"	$ 85.65	$ 94.52	$ 116.10	$ -		$ -
76511TC	"Ophth us, quant a only"	$ 79.96	$ 94.52	$ 68.68	$ -		$ -
76512TC	"Ophth us, b w/non-quant a"	$ 72.76	$ 94.52	$ 55.86	$ -		$ -
76513TC	"Echo exam of eye, water bath"	$ 61.39	$ 94.52	$ 86.66	$ -		$ -
76514TC	"Echo exam of eye, thickness"	$ 2.27	$ 36.52	$ 4.06	$ -		$ -
76516TC	Echo exam of eye	$ 48.89	$ 59.09	$ 64.97	$ -		$ -
76519TC	Echo exam of eye	$ 52.30	$ 94.52	$ 73.20	$ -		$ -
76529TC	Echo exam of eye	$ 45.86	$ 59.09	$ 64.26	$ -		$ -
76536TC	Us exam of head and neck	$ 56.85	$ 94.52	$ 172.33	$ -		$ -
76604TC	"Us exam, chest, b-scan"	$ 52.30	$ 94.52	$ 113.69	$ -		$ -
76645TC	"Us exam, breast(s)"	$ 42.07	$ 59.09	$ 134.24	$ -		$ -
76700TC	"Us exam, abdom, complete"	$ 79.21	$ 94.52	$ 194.04	$ -		$ -
76705TC	Echo exam of abdomen	$ 56.85	$ 94.52	$ 150.06	$ -		$ -
76770TC	"Us exam abdo back wall, comp"	$ 79.21	$ 94.52	$ 187.87	$ -		$ -
76775TC	"Us exam abdo back wall, lim"	$ 56.85	$ 94.52	$ 153.80	$ -		$ -
76778TC	Us exam kidney transplant	$ 79.21	$ 94.52	$ 208.44	$ -		$ -
76800TC	"Us exam, spinal canal"	$ 56.85	$ 94.52	$ 134.38	$ -		$ -
76830TC	"Transvaginal us, non-ob"	$ 61.39	$ 94.52	$ 174.70	$ -		$ -
76831TC	"Echo exam, uterus"	$ 61.39	$ 152.01	$ 163.59	$ -		$ -
76856TC	"Us exam, pelvic, complete"	$ 61.39	$ 94.52	$ 179.36	$ -		$ -
76857TC	"Us exam, pelvic, limited"	$ 67.08	$ 59.09	$ 157.46	$ 59.09	38%	$ (98.37)
76870TC	"Us exam, scrotum"	$ 61.39	$ 94.52	$ 182.57	$ -		$ -
76872TC	"Us, transrectal"	$ 80.72	$ 94.52	$ 203.08	$ -		$ -
76880TC	"Us exam, extremity"	$ 56.85	$ 94.52	$ 200.10	$ -		$ -
76885TC	"Us exam infant hips, dynamic"	$ 61.39	$ 59.09	$ 208.10	$ 59.09	28%	$ (149.01)
76886TC	"Us exam infant hips, static"	$ 56.85	$ 94.52	$ 135.37	$ -		$ -
76970TC	Ultrasound exam follow-up	$ 42.07	$ 59.09	$ 117.90	$ -		$ -
76975TC	GI endoscopic ultrasound	$ 61.39	$ 94.52	$ 259.77	$ -		$ -
76977TC	Us bone density measure	$ 32.97	$ 36.52	$ 5.40	$ -		$ -
78006TC	Thyroid imaging with uptake	$ 95.50	$ 146.77	$ 333.29	$ -		$ -
78007TC	"Thyroid image, mult uptakes"	$ 103.08	$ 165.46	$ 149.98	$ -		$ -
78010TC	Thyroid imaging	$ 73.52	$ 146.77	$ 225.93	$ -		$ -
78011TC	Thyroid imaging with flow	$ 96.64	$ 146.77	$ 242.79	$ -		$ -
78015TC	Thyroid met imaging	$ 103.08	$ 246.36	$ 294.86	$ -		$ -
78016TC	Thyroid met imaging/studies	$ 139.08	$ 246.36	$ 480.43	$ -		$ -
78018TC	"Thyroid met imaging, body"	$ 217.15	$ 246.36	$ 438.32	$ -		$ -

HCPCS MOD	Description	MPFS Non-Fac RATE 06	OPPS RATE 06	Est. CMS "Town Hall" Cost Data	DRA Capped Rate	Capped Payment as % of Est. Cost	Capped Rate Versus Est. CMS Cost
78020TC	Thyroid met uptake	$ 54.95	$ 89.50	$ 95.88	$ -		$ -
78070TC	Parathyroid nuclear imaging	$ 166.37	$ 165.46	$ 167.09	$ 165.46	99%	$ (1.63)
78075TC	Adrenal nuclear imaging	$ 217.15	$ 165.46	$ 652.97	$ 165.46	25%	$ (487.51)
78102TC	"Bone marrow imaging, ltd"	$ 82.24	$ 233.05	$ 225.22	$ -		$ -
78103TC	"Bone marrow imaging, mult"	$ 126.96	$ 233.05	$ 303.20	$ -		$ -
78104TC	"Bone marrow imaging, body"	$ 162.96	$ 233.05	$ 345.90	$ -		$ -
78185TC	Spleen imaging	$ 94.74	$ 233.05	$ 291.41	$ -		$ -
78195TC	Lymph system imaging	$ 162.96	$ 233.05	$ 456.57	$ -		$ -
78201TC	Liver imaging	$ 94.74	$ 256.53	$ 248.61	$ -		$ -
78202TC	Liver imaging with flow	$ 114.83	$ 256.53	$ 283.98	$ -		$ -
78205TC	Liver imaging (3D)	$ 236.48	$ 256.53	$ 281.18	$ -		$ -
78206TC	Liver image (3d) with flow	$ 228.90	$ 256.53	$ 795.36	$ -		$ -
78215TC	Liver and spleen imaging	$ 117.10	$ 256.53	$ 256.07	$ -		$ -
78216TC	Liver & spleen image/flow	$ 139.08	$ 256.53	$ 143.14	$ -		$ -
78220TC	Liver function study	$148.56	$ 256.53	$ 151.50	$ -		$ -
78223TC	Hepatobiliary imaging	$ 146.28	$ 256.53	$ 447.74	$ -		$ -
78230TC	Salivary gland imaging	$ 87.92	$ 224.33	$ 218.98	$ -		$ -
78231TC	Serial salivary imaging	$ 126.96	$ 224.33	$ 147.06	$ -		$ -
78232TC	Salivary gland function exam	$ 141.36	$ 224.33	$ 155.79	$ -		$ -
78258TC	Esophageal motility study	$ 114.83	$ 224.33	$ 302.69	$ -		$ -
78261TC	Gastric mucosa imaging	$ 164.10	$ 224.33	$ 325.12	$ -		$ -
78262TC	Gastroesophageal reflux exam	$ 169.78	$ 224.33	$ 308.47	$ -		$ -
78264TC	Gastric emptying study	$ 165.23	$ 224.33	$ 375.51	$ -		$ -
78278TC	Acute GI blood loss imaging	$ 194.41	$ 224.33	$ 452.27	$ -		$ -
78290TC	Meckel fs divert exam	$ 122.03	$ 224.33	$ 451.59	$ -		$ -
78291TC	Leveen/shunt patency exam	$ 122.41	$ 224.33	$ 327.12	$ -		$ -
78300TC	"Bone imaging, limited area"	$ 99.67	$ 237.57	$ 216.64	$ -		$ -
78305TC	"Bone imaging, multiple areas"	$ 146.28	$ 237.57	$ 282.34	$ -		$ -
78306TC	"Bone imaging, whole body"	$ 170.54	$ 237.57	$ 316.20	$ -		$ -
78315TC	"Bone imaging, 3 phase"	$ 191.00	$ 237.57	$ 460.49	$ -		$ -
78320TC	Bone imaging (3D)	$ 236.48	$ 237.57	$ 285.22	$ -		$ -
78350TC	"Bone mineral, single photon"	$ 30.32	$ 43.42	$ 90.48	$ -		$ -
78428TC	Cardiac shunt imaging	$ 90.58	$ 250.17	$ 301.85	$ -		$ -
78445TC	Vascular flow imaging	$ 75.04	$ 123.96	$ 257.22	$ -		$ -
78456TC	Acute venous thrombus image	$ 162.20	$ 123.96	$ 580.62	$ 123.96	21%	$ (456.66)
78457TC	Venous thrombosis imaging	$ 106.49	$ 123.96	$ 228.64	$ -		$ -
78458TC	"Ven thrombosis images, bilat"	$ 160.69	$ 123.96	$ 258.37	$ 123.96	48%	$ (134.41)
78460TC	"Heart muscle blood, single"	$ 94.74	$ 250.17	$ 235.24	$ -		$ -
78461TC	"Heart muscle blood, multiple"	$ 188.73	$ 397.11	$ 188.71	$ -		$ -
78464TC	"Heart image (3d), single"	$ 282.72	$ 250.17	$ 315.79	$ 250.17	79%	$ (65.62)
78465TC	"Heart image (3d), multiple"	$ 471.44	$ 397.11	$ 639.90	$ 397.11	62%	$ (242.79)
78466TC	Heart infarct image	$ 104.98	$ 250.17	$ 232.73	$ -		$ -
78468TC	Heart infarct image (ef)	$ 146.28	$ 250.17	$ 343.29	$ -		$ -
78469TC	Heart infarct image (3D)	$ 209.19	$ 250.17	$ 334.99	$ -		$ -
78472TC	"Gated heart, planar, single"	$ 220.94	$ 250.17	$ 268.55	$ -		$ -
78473TC	"Gated heart, multiple"	$ 329.71	$ 299.43	$ 172.27	$ 299.43	174%	$ 127.16
78478TC	Heart wall motion add-on	$ 62.91	$ 89.50	$ 29.22	$ -		$ -
78480TC	Heart function add-on	$ 62.91	$ 89.50	$ 29.22	$ -		$ -
78481TC	"Heart first pass, single"	$ 209.19	$ 250.17	$ 29.79	$ -		$ -
78483TC	"Heart first pass, multiple"	$ 314.55	$ 299.43	$ 40.05	$ 299.43	748%	$ 259.38
78494TC	"Heart image, spect"	$ 280.06	$ 250.17	$ 334.18	$ 250.17	75%	$ (84.01)
78496TC	Heart first pass add-on	$280.06	$ 89.50	$ 38.58	$ 89.50	232%	$ 50.92
78580TC	Lung perfusion imaging	$ 137.19	$ 197.37	$ 270.09	$ -		$ -
78584TC	Lung V/Q image single breath	$ 128.09	$ 321.74	$ 136.35	$ -		$ -
78585TC	Lung V/Q imaging	$ 225.87	$ 321.74	$ 453.71	$ -		$ -
78586TC	"Aerosol lung image, single"	$ 103.84	$ 197.37	$ 216.86	$ -		$ -
78587TC	"Aerosol lung image, multiple"	$ 111.80	$ 197.37	$ 290.87	$ -		$ -
78588TC	Perfusion lung image	$ 128.47	$ 321.74	$ 456.82	$ -		$ -

HCPCS MOD	Description	MPFS Non-Fac RATE 06	OPPS RATE 06	Est. CMS "Town Hall" Cost Data	DRA Capped Rate	Capped Payment as % of Est. Cost	Capped Rate Versus Est. CMS Cost
78591TC	"Vent image, 1 breath, 1 proj"	$ 113.69	$ 197.37	$ 215.57	$ -		$ -
78593TC	"Vent image, 1 proj, gas"	$ 137.95	$ 197.37	$ 253.58	$ -		$ -
78594TC	"Vent image, mult proj, gas"	$ 198.58	$ 197.37	$ 287.07	$ 197.37	69%	$ (89.70)
78600TC	"Brain imaging, ltd static"	$ 114.83	$ 307.73	$ 419.51	$ -		$ -
78601TC	"Brain imaging, ltd w/flow"	$ 136.05	$ 307.73	$ 288.06	$ -		$ -
78605TC	"Brain imaging, complete"	$ 136.05	$ 307.73	$ 248.94	$ -		$ -
78606TC	"Brain imaging, compl w/flow"	$ 155.00	$ 307.73	$ 450.96	$ -		$ -
78607TC	Brain imaging (3D)	$ 262.25	$ 307.73	$ 849.83	$ -		$ -
78610TC	Brain flow imaging only	$ 63.67	$ 307.73	$ 238.06	$ -		$ -
78615TC	Cerebral vascular flow image	$ 154.24	$ 307.73	$ 289.29	$ -		$ -
78630TC	Cerebrospinal fluid scan	$ 201.61	$ 208.38	$ 459.92	$ -		$ -
78635TC	CSF ventriculography	$ 101.94	$ 208.38	$ 462.21	$ -		$ -
78645TC	CSF shunt evaluation	$ 137.19	$ 208.38	$ 466.37	$ -		$ -
78647TC	Cerebrospinal fluid scan	$ 236.48	$ 208.38	$ 794.14	$ 208.38	26%	$ (585.76)
78650TC	CSF leakage imaging	$ 185.32	$ 208.38	$ 461.15	$ -		$ -
78660TC	Nuclear exam of tear flow	$ 85.27	$ 208.38	$ 228.44	$ -		$ -
78700TC	"Kidney imaging, static"	$ 122.03	$ 217.56	$ 229.51	$ -		$ -
78701TC	Kidney imaging with flow	$ 142.12	$ 217.56	$ 286.51	$ -		$ -
78704TC	Imaging renogram	$ 158.03	$ 217.56	$ 283.73	$ -		$ -
78707TC	Kidney flow/function image	$ 178.50	$ 217.56	$ 288.89	$ -		$ -
78708TC	Kidney flow/function image	$ 178.50	$ 246.93	$ 162.35	$ -		$ -
78709TC	Kidney flow/function image	$ 178.50	$ 246.93	$ 467.44	$ -		$ -
78710TC	Kidney imaging (3D)	$ 236.48	$ 217.56	$ 275.80	$ 217.56	79%	$ (58.24)
78715TC	Renal vascular flow exam	$ 63.67	$ 217.56	$ 267.81	$ -		$ -
78730TC	Urinary bladder retention	$ 58.36	$36.52	$263.24	$ 36.52	14%	$ (226.72)
78740TC	Ureteral reflux study	$ 85.27	$ 217.56	$ 318.50	$ -		$ -
78760TC	Testicular imaging	$ 107.25	$ 217.56	$ 222.01	$ -		$ -
78761TC	Testicular imaging/flow	$ 128.09	$ 217.56	$ 263.88	$ -		$ -
78800TC	"Tumor imaging, limited area"	$ 136.05	$ 246.36	$ 212.35	$ -		$ -
78801TC	"Tumor imaging, mult areas"	$ 168.64	$ 246.36	$ 313.11	$ -		$ -
78802TC	"Tumor imaging, whole body"	$ 221.70	$ 246.36	$ 444.43	$ -		$ -
78803TC	Tumor imaging (3D)	$ 262.25	$ 246.36	$ 861.69	$ 246.36	29%	$ (615.33)
78804TC	"Tumor imaging, whole body"	$ 431.65	$ 650.00	$ 819.63	$ -		$ -
78805TC	"Abscess imaging, ltd area"	$ 136.05	$ 246.36	$ 220.93	$ -		$ -
78806TC	"Abscess imaging, whole body"	$ 257.70	$ 246.36	$ 449.10	$ 246.36	55%	$ (202.74)
78807TC	Nuclear localization/abscess	$ 262.25	$ 246.36	$ 830.00	$ 246.36	30%	$ (583.64)
93303TC	Echo transthoracic	$ 155.38	$ 189.01	$ 303.43	$ -		$ -
93304TC	Echo transthoracic	$ 78.83	$ 89.99	$ 209.25	$ -		$ -
93307TC	Echo exam of heart	$ 155.38	$ 189.01	$ 254.22	$ -		$ -
93308TC	Echo exam of heart	$ 78.83	$ 89.99	$ 183.78	$ -		$ -
93312TC	Echo transesophageal	$ 154.62	$ 353.31	$ 498.92	$ -		$ -
93314TC	Echo transesophageal	$ 154.62		$ 490.84	$ -		$ -
93320TC	"Doppler echo exam, heart"	$ 69.35	$ 99.76	$ 111.34	$ -		$ -
93321TC	"Doppler echo exam, heart"	$ 45.10	$ 89.99	$ 42.02	$ -		$ -
93325TC	Doppler color flow add-on	$ 118.24	$ 89.99	$ 49.46	$ 89.99	182%	$ 40.53
93350TC	Echo transthoracic	$ 72.01	$ 189.01	$ 343.02	$ -		$ -
93880TC	Extracranial study	$216.79	$152.01	$ 413.49	$ 152.01	37%	$ (261.48)
93890TC	"Tcd, vasoreactivity study"	$ 185.70	$ 94.52	$ 403.99	$ 94.52	23%	$ (309.47)
93892TC	"Tcd, emboli detect w/o inj"	$ 193.28	$ 94.52	$ 431.59	$ 94.52	22%	$ (337.07)
93893TC	"Tcd, emboli detect w/inj"	$ 188.35	$ 94.52	$ 409.28	$ 94.52	23%	$ (314.76)
93922TC	Extremity study	$ 103.84	$ 95.34	$ 202.32	$ 95.34	47%	$ (106.98)
93923TC	Extremity study	$ 155.76	$ 95.34	$ 308.34	$ 95.34	31%	$ (213.00)
93924TC	Extremity study	$ 184.94	$ 95.34	$ 401.27	$ 95.34	24%	$ (305.93)
93925TC	Lower extremity study	$ 263.39	$ 152.01	$ 558.97	$ 152.01	27%	$ (406.96)
93926TC	Lower extremity study	$ 157.65	$ 94.52	$ 339.08	$ 94.52	28%	$ (244.56)
93930TC	Upper extremity study	$ 211.47	$ 152.01	$ 417.80	$ 152.01	36%	$ (265.79)
93931TC	Upper extremity study	$ 137.57	$ 94.52	$ 287.26	$ 94.52	33%	$ (192.74)
93965TC	Extremity study	$ 106.11	$ 95.34	$ 209.48	$ 95.34	46%	$ (114.14)

HCPCS MOD	Description	MPFS Non-Fac RATE 06 *	OPPS RATE 06 *	Est. CMS "Town Hall" Cost Data **	DRA Capped Rate	Capped Payment as % of Est. Cost	Capped Rate Versus Est. CMS Cost
93970TC	Extremity study	$ 205.78	$ 152.01	$ 414.35	$ 152.01	37%	$ (262.34)
93971TC	Extremity study	$ 140.98	$ 94.52	$ 271.01	$ 94.52	35%	$ (176.49)
93975TC	Vascular study	$ 283.47	$ 152.01	$ 554.15	$ 152.01	27%	$ (402.14)
93976TC	Vascular study	$ 160.69	$ 152.01	$ 292.43	$ 152.01	52%	$ (140.42)
93978TC	Vascular study	$ 176.98	$ 94.52	$ 411.42	$ 94.52	23%	$ (316.90)
93979TC	Vascular study	$ 125.44	$ 94.52	$ 298.22	$ 94.52	32%	$ (203.70)
93980TC	Penile vascular study	$ 105.73	$ 152.01	$ 207.72	$ -		$ -
93981TC	Penile vascular study	$ 115.59	$ 94.52	$ 183.42	$ 94.52	52%	$ (88.90)
93990TC	Doppler flow testing	$ 156.90	$ 94.52	$ 328.80	$ 94.52	29%	$ (234.28)
G0130TC	Single energy x-ray study	$ 32.21	$ 43.42	$ -	$ -		$ -
G0365TC	Vessel mapping hemo access	$ 156.90	$ 152.01	$ 223.75	$ 152.01	68%	$ (71.74)

* Source: MPFS rates were calculated using the most current version of 2006 Relative Value Units (RVUs) as published in the RVU files on the CM
OPPS rates were calculated using the most current version of the applicable Ambulatory Payment Classification (APC) as published in Addendum I
** Source: CMS "Town Hall" Cost Data was calculated using Clinical Practice Expert Panel (CPEP) inputs as published by CMS during the 2/15/06
CMS sponsored Town Hall meeting. In the 37 instances where CPEP inputs were missing from this town hall data source, CPEP inputs from the 2
database were utilized. In certain instances we could not identify a value from either source and could not calculate cost data,
while we left these on the list so it could be noted that they may potentially be affected by the DRA policy, they were not included in our analysis of I
In 7 instances, CPEP inputs were missing for supplies and/or were missing for supplies
and equipment (5 instances). When CPEP inputs are missing, the Est. CMS "Town Hall" Cost Data may be underestimated.

165

Centers for Medicare & Medicaid Services
Department of Health and Human Services
Attention: CMS-1321-P
Mail Stop C4-26-05
7500 Security Blvd
Baltimore, MD 21244-1850

Sept. 4, 2006

RE: BONE MASS MEASUREMENT TESTS
Fed. Reg. Vol. 71, No. 162/Tuesday, August 22, 2006

We wish to comment on the Proposed Rules referenced in the above document. In general, we believe this writing fails to accurately describe and consider CT Bone Densitometry as an important modality in managing this important disease state. As background to our comments, it is helpful to recognize that "some" Primary Care Physicians who place DXA devices in their offices and Radiologists who control CT scanners have somewhat of a turf dispute. Due to the large potential market to primary physicians for DXA devices as compared to the number of CT facilities, larger device companies with greater promotional abilities market DXA much more widely. Having said this, however, "all" of the big CT manufacturers offer CT Bone Densitometry, many using our device. Primary care physicians with DXA devices in their offices have an incentive to perpetrate the belief that DXA is superior to QCT. Many of these same physicians have joined efforts in the International Society of Bone Densitometry, which is essentially void of QCT users and researchers. Radiologists are trained in equipment technology and imaging physics. As they have access to CT scanners, it is not surprising they can readily understand the imaging properties and measurement performances of QCT and DXA. Most radiologists will likely recognize the several diagnostic advantages of QCT over DXA. The exceptions include the requirement to use a sophisticated CT instrument, which is not usually available in offices, and although a very low dose procedure, the radiation dose can be higher with QCT. However, the dose from modern DXA devices with vertebral fracture analysis [VFA] is comparable to QCT.

Not only the overly favorable reporting of DXA but the restriction of follow-up monitoring to only DXA would be extremely unfair to QCT and especially those patients being served by this technique. The implementation of such a restriction would essentially grant a monopoly to DXA companies and users and seriously harm the medical care of those thousands of patients being so ably served today by QCT. This proposal is suspect especially in light of the fact that QCT has distinct advantages in monitoring patients under therapy. Such a restrictive decision would have no cost savings

Image Analysis, Inc.
1380 Burkesville Street ● Columbia, KY 42728 ● USA ● Phone 270/384-6400 ● Fax 270/384-6405

to CMMS, as both are reimbursed at the same rate. DXA is often not, but QCT is, available in smaller communities making such a decision unfair to those patients. DXA and QCT cannot be used to follow-up the other device in monitoring since they measure different bone volumes and are not interchangeable. We are developing methods using the 3-D data of QCT, which may allow follow-up of DXA but DXA certainly cannot follow-up QCT. We ask for removal of the recommendation for restrictions on reimbursements for monitoring and a more accurate description of CT bone densitometry.

We want to make the following specific comments:

1. CT Bone Densitometry is widely available.

We estimate that approximately 10,000 QCT devices have been placed in operation and most CT facilities in the U.S. currently have BMD capabilities. CT BMD should not be grouped with the "other" category, which includes appendicular devices, SXA, RA, ultrasound, etc. QCT is highly regarded as an advantageous technique and widely used.

2. Definition of a "Bone Mass Measurement"

The definition given could be redefined to reflect it is a "density" measurement preferably over a "mass" measurement. Also quoting from the Register, the use of terminology such as "bone densitometer" (other than a single photon or dual-photon absorptiometry) or with a bone sonometer system that has been cleared for marketing for this use by the FDA" This definition and the use of the exclusions almost completely excludes QCT. Further, the statement that "by the newer techniques of DXA, which are believed to be superior in accuracy and precisions" give an inaccurate impression of the known science. Many of the leading bone densitometry researchers report that QCT has superior diagnostic accuracy and significantly greater sensitivity than DXA to detect and monitor osteoporosis. This superior performance of QCT should exclude it from in the category of the "other" devices and place it at least on level with DXA.

We propose a definition, which includes all the currently used techniques and clearly includes such a major technique as QCT. We see no need to specifically exclude isotope source absorptiometers. They are at least as accurate and sensitive as the appendicular devices or RA and superior to ultrasound devices, which as a side comment do not measure 'bone mineral density'. We propose a definition such as "bone density measurements may be 3-D volumetric bone density measurements in g/cc (QCT) or 2-D projection measurements of areal density in g/cm^2 (DXA, SXA,RA) all being x-ray based and carried out in the axial or appendicular skeleton. Other projection techniques include ultrasound measurements of bone quality end points. BMD may be performed with any FDA cleared device under 21 CFR part 807/814.

3. Monitoring of BMD changes.

The current writing states "the monitoring would have to be performed by the use of a dual energy x-ray absorptiometry system (axial system). DXA is precise, safe, and

Image Analysis, Inc.
1380 Burkesville Street ● Columbia, KY 42728 ● USA ● Phone 270/384-6400 ● Fax 270/384-6405

low in radiation exposure and permits more accurate and reliable monitoring of individuals over time". Although such statements have great commercial value, they are in part inaccurate. It is widely known that QCT measurements of the lumbar spine are the most sensitive and most reliable technique to monitor individuals over time. Most any research scientist working in the bone density field who is not biased by his/her use of only a DXA device will readily agree with this statement. QCT of the lumbar spine provides the earliest detection of osteoporosis over all other techniques. QCT is increasingly being used in multi-center drug studies because of its superior sensitivity to monitor changes in bone density. Instead of the usually DXA recommended 2 years for follow-up with therapy, investigators have shown a therapeutic response with QCT after 3 months. This greatly hastens the detection of non-responders while allowing a more reliable measurement of bone density changes over time. The DXA companies are currently working on methods to rotate their devices to attempt to acquire 3-D data like QCT. This alone speaks loudly of what they think of 3-D bone density measurements.

The referenced publications listed below and excerpted statements support our conclusions and are enclosed for review:

Genant et al, Review – Noninvasive Assessment of Bone Mineral and Structure: State of the Art. J Bone and Mineral Research, Vol. 11, No. 6, 1996

"QCT's ability to selectively assess the metabolically active and structurally important trabecular bone in the vertebral centrum [57,99-102] results in the excellent ability to discriminate vertebral fracture and to measure bone loss, generally with better sensitivity than projectional methods such as DXA or DPA."

Lang et al, Bone, 1997 Jul;21(1):101-8

" For trebecular BMD the precision was 1.1% and 1.6% for the femoral neck and trochanteric subregions compared to 3.3% and 1.6% for the corresponding integral envelopes. Trabecular BMD measurements were reproducible and highly correlated to biomechanical strength measurements".

Bolotin et al, Journal of Bone and Mineral Research, Vol. 16, No. 5, 2001

"The growing number of investigations that have shown DXA-derived in vivo BMD to be subject to sizable inherent systemic inaccuracies that may adversely influence measurement outcomes [32-39]. Such BMD inaccuracies could seriously compromise the integrity of measurements undertaken to diagnose, monitor, and evaluate the osteopenic/osteoporotic condition and predictive bone fragility of any individual patient."

Black et al, The Effects of Parathyroid Hormone and Alendronate Alone or in Combination in Postmenopausal Osteoporosis. N Eng J Med 2003:349:1207-15

Figures 1 and 2 show, but don't provide graphically comparison, the therapeutic response of PaTH as measured by QCT and DXA. DXA shows about 6% increase in BMD while QCT shows about 25% increases for the spinal results. This is consistent with other publications. The results show approximately a 400% larger measurement response with QCT. This allows for earlier detection of response and for more reliable monitoring of change over time. { My comments, please see p.1211}

Bolotin et al, Patient-Specific DXA Bone Mineral Density Inaccuracies: Quantitative Effects of Nonuniform Extraosseous Fat Distributions. Journal of Bone and Mineral Research, Vol. 18, No. 6, 2003

"Nonuniform extra osseous fat is shown to raise the magnitude of inaccuracies in DXA in vivo BMD measurements into the range of 20-50% in clinically relevant cases. Hence, DXA-based bone fragility diagnoses/prognoses and evaluations of bone responsiveness to treatment can be unreliable."

Banks et al, Effect of Degenerative Spinal and Aortic Calcification on Bone Density Measurements in Post-Menopausal Women: Links Between Osteoporosis and Cardiovascular Disease? European Journal of Clinical Investigation (1994) 24, 813-817

"Women with spinal degenerative calcification had higher spine bone density when measured by dual photon absorptiometry compared to those without calcification (P<0-01), but this was not reflected by the quantitative computer tomography or the proximal femur bone densities, suggesting that spinal calcification artificially increases spinal bone density when measured by dual photon techniques."

Weigert et al, DXA in Obese Patients: Are normal values really normal? Imaging Center of West Hartford, CT and University of California, San Francisco, CA

"The results of this study suggest that DXA of both the spine and hip overestimate BMD in obese women and the results should be interpreted with caution".

Yu W et al, Calcif Tissue Int. 1995 Sep;57(3):169-74

"For all women, BMD by PA- and L-DXA was affected more by DJD than by fracture status. We conclude that QCT and mL-DXA are superior to PA-DXA and L-DXA in detecting bone loss in patients with DJD."

Guglielmi et al, Acta Radiologica, rad57868.3d

"There is no evidence supporting that trabecular BMD measurements by QCT are influenced by OA. Instead, degenerative changes have an effect on both cortical and integral QCT, and on DXA at the lumbar spine and the hip. For subjects with established OA, assessment of BMD by volumetric QCT may be suggested."

Griswold et al, Diagnostic Imaging Nov. 2001

"Quantitative CT is almost always done by radiologists. Patients who cannot be studied well by DXA: obese patients and degenerative hypertrophic bone, a history of spinal surgery, excessive vascular calcifications, and severe scoliosis (Figures 4 and 5). In addition, QCT is more sensitive to the trabecular bone loss of early menopause as well as to the response to therapy, which is frequently first seen in trabecular bone."

4. Diagnostic Accuracy

QCT and DXA measure largely different bone components. QCT by isolating and measuring a purely trabecular bone region in the axial skeleton allows the early detection of low BMD well before any other technique. The much higher metabolic activity of trabecular bone results in larger measurement changes of BMD, which provides greater reliability due to this much higher sensitivity. For monitoring therapy or for early detection of osteoporosis, QCT is clearly superior. DXA measurements of the Hip predict hip fractures better than any other technique but the recent availability of CT DXAView of the hip can reproduce this result with comparable performance. Please see the following supporting publications:

Guglielmi et al, Quantitative Computed Tomography at the Axial and Peripheral Skeleton. Eur. Radiology, 7 (Suppl.2), S32-S42

"QCT has been shown to discriminate better between healthy women and those with osteoporosis than posteroanterior DXA [5]. In summary, the great advantage of QCT over other densitometry methods is its ability to measure exclusively the high turnover trabecular bone. This accounts for the high sensitivity of the technique. Therefore, several authors have considered QCT as the method of choice in predicting fracture risk in the spine."

P. von der Recke et al, The Impact of Degenerative Conditions in the Spine on Bone Mineral Density and Fracture Risk Prediction. Osteoporosis Int. (1996) 6:43-49

"In conclusion, osteophytes and endplate sclerosis have a considerable influence on spinal bone mass measurements in elderly postmenopausal women and affect the diagnostic ability of spinal scans to discriminate osteoporotic women."

Guglielmi et al, Osteoporosis: Diagnosis with Lateral and Posteroanterior Dual X-ray Absorptiometry Compared with Quantitative CT[1]. Radiology 1994; 192:845-850, Vol. 192, No. 3

"Although both L-DXA and PA-DXA correlated well with quantitative CT (r = .73 and .72, respectively; P <.0001), L-DXA correlated better than PA-DXA with age (r = -.69 and -.50, respectively; P<.0001). Women with osteoporosis showed higher bone loss with quantitative CT (1.33% per year) and L-DXA (0.3% per year) than with PA-DXA (0.07% per year). Logistic regression analysis indicated that quantitative CT and L-DXA but not PA-DXA are significant predictors of osteoporotic fractures."

Hologic's commercial brochure

"30% of patients who need therapy are missed [by DXA] without IVA"

Black et al, One year of Alendronate after one year of Parathyroid Hormone (1-84) for Osteoporosis. The New England Journal of Medicine, Vol. 349, No. 13

"There is a difference particularly evident for bone mineral density in trabecular bone at the spine on quantitative CT".

Lang et al, Radiology, 1998 Nov; 209(2):525-30

"Spinal trabecular BMD is strongly associated with both trochanteric and vertebral factures".

Gramp et al, J Bone Mineral Res. 1997 May;12(5):697-711

"Diagnostic agreement among these measurements in classifying women as osteopenic or osteoporotic was poor, with kappa scores averaging about 0.4 (exceptions were QCT TRAB/INTG BMD, DXA LAT BMD, and RA PHAL BMD, with kappa scores ranging from 0.63 to 0.89".

Rehman et al, Arthritis Rheum. 2002 May; 46(5):1292-7

"QCT was a significant predictor of vertebral fractures. CART analysis showed that a BMD value < 0.065 g/cc was associated with a 7-fold higher risk of fracture. BMD of the lumbar spine as measured by QCT, but not DXA, is an independent predictor of vertebral fractures."

Maricic, J Clinical Densitometry, Vol. 1, No. 3, 251-257, Fall 1998

"These studies suggested that lateral DXA is comparable to QCT and more sensitive than PA for the detection of low bone mass, and is more highly associated with fractures than PA BMD (*3*)".

Conclusions:

CT Bone Densitometry is widely available, is the most sensitive method to detect and monitor bone density changes and provides the highest diagnostic accuracy for predicting patients with fractures. It is increasing becoming the method of choice for highly accurate monitoring of bone density changes in drug studies.

The restriction of monitoring to only DXA devices should be removed. We respectively request a modification in the writings for the Proposed Rules, which accurately reflect the widespread and respected use of CT Bone Densitometry.

Cc: enclosures

Sincerely,

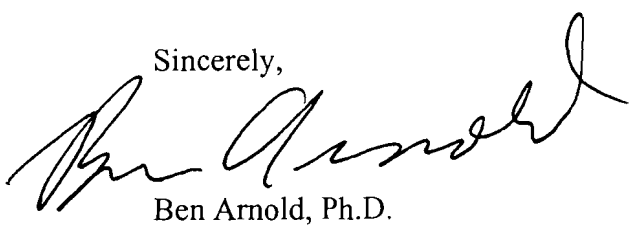

Ben Arnold, Ph.D.
President

Image Analysis, Inc.
1380 Burkesville Street ● Columbia, KY 42728 ● USA ● Phone 270/384-6400 ● Fax 270/384-6405

JOURNAL OF BONE AND MINERAL RESEARCH
Volume 11, Number 6, 1996
Blackwell Science, Inc.

Review

Noninvasive Assessment of Bone Mineral and Structure: State of the Art

HARRY K. GENANT, KLAUS ENGELKE, THOMAS FUERST, CLAUS-C. GLÜER, STEPHAN GRAMPP, STEVEN T. HARRIS, MICHAEL JERGAS, THOMAS LANG, YING LU, SHARMILA MAJUMDAR, ASHWINI MATHUR, and MASA TAKADA

INTRODUCTION

In the past decade, considerable progress has been made in the development of methods for assessing the skeleton noninvasively so that osteoporosis can be detected early, its progression and response to therapy carefully monitored, or the risk of fracture effectively ascertained. Clinicians can now evaluate the peripheral, central, or entire skeleton as well as the trabecular or cortical bone envelopes with a high degree of accuracy and precision, and they have the capacity to estimate bone strength and propensity to fracture. The purposes of this commentary are to assess the current capabilities of bone densitometry methods as well as recent technical advances in these methods; to review the statistical approaches applied in studies of bone densitometry; to examine methods of expressing longitudinal sensitivity in densitometry; to address the issues of fracture risk prediction with bone densitometry using either single or multisite measurements; and to delineate the criteria for appropriate use of bone densitometry.

PRINCIPAL BONE MEASUREMENT TECHNIQUES

There are a variety of techniques for noninvasive assessment of the skeleton: radiographic absorptiometry (RA), single-photon and single X-ray absorptiometry (SPA/SXA), dual-photon and dual X-ray absorptiometry (DPA/DXA), spinal and peripheral quantitative computed tomography (QCT/pQCT), quantitative ultrasound (QUS), and quantitative magnetic resonance (QMR), and magnetic resonance microscopy (μMR). These techniques vary in precision, accuracy, and discrimination and differ substantially in fundamental methodology, clinical and research utility, and general availability (Table 1).

Radiographic absorptiometry

Radiographic absorptiometry (RA), also known as photodensitometry, was one of the first quantitative techniques to assess integral bone (trabecular and cortical) mass.[1] In RA, hand radiographs are taken with aluminum wedges placed on the films and analyzed using an optical densitometer. The bone mineral density (BMD) is calibrated relative to that of the aluminum wedge and is expressed in arbitrary units.[2–10] Typically, investigators have used the middle phalanges or metacarpals for RA measurements. Although RA is an inexpensive and readily accessible technique, its implementation was initially characterized by high precision errors of about 9–10%.[1] Recently developed computer-assisted methods have reduced operator errors and improved precision.[1–10] There are several RA techniques. One technique uses centralized analysis of hand radiographs and averages the BMD of the second to fourth middle phalanges.[7] Another technique developed in Japan uses the diaphysis of the second metacarpal to determine BMD.[2,5] A third technique developed in Europe measures the diaphysis and proximal metaphysis of the second middle phalanx.[3,4]

Published short-term precision errors for computer-assisted RA range between 0.6 and 1.7% for in vitro measurements and between 0.3 and 2.4% for in vivo measurements.[2–6,8] The comparison of RA results with ash weights of cadaveric phalanges gave an accuracy error of 4.8%,[6]

which is comparable to that obtained with other densitometry techniques.[11,12] Thus, RA appears to be suitable for the measurements of the BMD of phalanges and metacarpals, and is used in about 500 centers worldwide.

RA measurements of age-related bone loss were reported by Trouerbach et al. who measured the diaphysis of the second middle phalanx. The annual bone loss was 3.5% for recently postmenopausal women (age 50–57) and 0.8% for older postmenopausal women (age 58–73).[3,4] Matsumoto et al. reported bone loss of 1.6% per year at the diaphysis of the second metacarpals in normal women (age 50–59). They also showed that BMD of the second metacarpals peaks in normal women at age 30–39. Afterward, BMD decreases gradually until the age of 50 and more rapidly thereafter.[2] A preliminary study from San Francisco showed that bone loss of the second to fourth middle phalanges was 0.41% per year for normal women (age 22–79). This loss was comparable to that observed by spinal and radial DXA in the same population.[13]

Very few studies have addressed the ability of RA to discriminate spinal fractures. Analyzing incident fractures in serial spinal X-ray films, Ross et al. reported an odds ratio of 1.65 for RA and 1.50 for radial DXA.[14] Preliminary data from a study in San Francisco also suggested that phalangeal RA (odds ratio = 1.93, $p = 0.08$) discriminates osteoporotic spinal fractures better than radial DXA (odds ratio = 1.55, $p = 0.25$) but not as well as spinal DXA (odds ratio = 2.16, $p = 0.02$).[13]

Table 1. Comparison of Approximate Worldwide Distribution and of Precision Error, Accuracy Error, and Radiation Dose of Techniques for Bone Numeral Measurement

Technique (world distribution)	*Precision error (%)*	*Accuracy error (%)*	*Effective dose equivalent* (μSv)*
RA (500)			
phalanx/metacarpal	1–2	5	~5
SXA/DXA (3000)			
radius/calcaneus	1–2	4–6	<1
DXA (6000)			
PA spine	1–1.5	4–10	~1
Lat spine	2–3	5–15	~3
proximal femur	1.5–3	6	~1
forearm	~1	5	<1
whole body	~1	3	~3
QCT (4000)			
spine trabecular	2–4	5–15	~50
spine integral	2–4	4–8	~50
pQCT (1000)			
radius trabecular	1–2	?	~1
radius total	1–2	2–8	~1
QUS (2000)			
SOS calcaneus/tibia	0.3–1.2	?	0
BUA calcaneus	1.3–3.8	?	0

*Dose for annual background ~2000 μSv, for abdominal radiograph ~500 μSv, and for abdominal CT ~4000 μSv.[273]

The numbers given for precision errors and accuracy errors are from various publications. Since these numbers were obtained using different methods and sometimes distinct statistical approaches, they have to be perceived as a guideline for clinical practice.

Single photon and X-ray absorptiometry

Single photon absorptiometry (SPA) was introduced in the 1960s[15] and was widely used until recently when it was superseded by single X-ray absorptiometry (SXA). Both methods make possible a quantitative assessment of the bone mineral content (BMC) at peripheral sites of the skeleton (e.g., distal or ultradistal radius, calcaneus). A highly collimated photon beam from a radionuclide source (usually ^{125}I), or a small X-ray tube is used to measure radiation attenuation at the measurement site. The replacement of the radionuclide source by an X-ray tube using SXA, a feature of most of the recently developed densitometers, has imparted better precision and improved spatial resolution to these systems and has reduced examination time.[14,16,17] Because SXA is an area projectional technique, separate measurement of trabecular and cortical bone is not possible. For example, a measurement of the radial shaft (often referred to as the one-third radius or proximal radius) includes mainly cortical bone. While the relatively uniform structure at this site, which is 95% cortical bone, ensures a good range of precision, the metabolically more responsive trabecular bone is barely included.[18] Measurements of the ultradistal radius include more trabecular bone (up to 40%), but difficulty in precisely targeting the region of interest and inhomogeneity of the trabecular bone content may result in poorer precision at this site, particularly if older devices are used.[19,20] The rectilinear scanning devices now in use show improved precision at this site.[21] The value of bone mineral measurements at the calcaneus was initially controversial because of the uncertain relationship between BMD at this site and body weight or exercise.[22,23] However, excellent results in recent studies document the value of calcaneus (as well as radius) measurements in predicting osteoporotic fractures.[24–28] SPA/SXA has proven to be a valuable method in the diagnosis of osteoporosis, providing reasonable precision and low radiation exposure. Worldwide there are over 2000 systems in use.

Dual photon and X-ray absorptiometry

Single energy measurements are not possible at sites with variable soft tissue thickness and composition (i.e., the axial skeleton, hip, or whole body). For these purposes dual-photon absorptiometry (DPA) techniques were introduced to correct for unknown path length in the body. This approach uses a radionuclide source, typically ^{153}Gd at two effective energy levels.[29]

Dual X-ray absorptiometry (DXA), based on the method of X-ray spectrophotometry that was developed in the 1970s, was introduced commercially as the direct successor to DPA in 1987.[30–33] While DXA uses the same principles as DPA, in DXA the radionuclide source is replaced by an

X-ray tube. Depending on the manufacturer, beams of two distinct energy levels are either produced by the X-ray generator or selectively filtered from an X-ray spectrum. The main advantages of an X-ray system over a DPA radionuclide system are shortened examination time due to an increased photon flux of the X-ray tube and greater accuracy and precision caused by higher resolution and removal of errors due to source decay correction.[34] The preferred anatomic sites for DXA measurement of bone mineral include the lumbar spine, the proximal femur, and the whole body, but peripheral sites can also be scanned. The digital image resulting from the measurement allows a gross survey of the region examined. With the initial DXA devices, the examination procedure took 6–15 minutes, newly developed devices using enhanced generators or a fan beam instead of a pencil beam X-ray source have shortened the examination time to 2 minutes or less.[35] The in vivo precision of the posteroanterior DXA examination of the lumbar spine is 0.5–1.5% with an accuracy error of 5–10%.[36–41] The worldwide distribution of DXA systems is over 6000.

Because of the presence of osteophytes, aortic calcifications, degenerative facet hypertrophy, and intervertebral disc space narrowing in degenerative disc disease, the BMD may be increased artificially in the posteroanterior measurement of the lumbar spine. This is an important drawback of this method especially in elderly patients. Furthermore, the area projectional measurement includes substantial portions of compact bone, thereby reducing the ability to discriminate between osteoporotic and nonosteoporotic subjects.[42–45] A lateral examination of the lumbar spine makes possible an evaluation of the vertebral body—with almost exclusive measurement of the trabecular bone. Therefore, the correlation between lateral DXA and quantitative computed tomography (QCT), both measures of the vertebral body, has been found to be stronger than that between posteroanterior DXA and QCT.[46,47] This lateral method can reduce the errors intrinsic in the posteroanterior examination of the lumbar spine. However, overlap of the iliac crest may substantially increase the measured bone density primarily at the level L4, and L2 is overlapped by ribs in almost all patients. Nevertheless, the inclusion of L2–L4 usually yields the best precision and diagnostic sensitivity.[48,49] Beyond that, the reproducibility of the lateral DXA measurement is poorer because of the greater thickness and nonuniformity of the soft tissue in the lateral projection.[48,50–54] The adverse effect on reproducibility of measurements of the spine in the lateral decubitus position has been addressed with newer densitometers which have a tube-detector system that can be rotated. This "C" arm allows for lateral spine scanning with the patient in the supine position, thereby reducing obliquity and resulting overlap of the pelvis and rib and improving the in vivo reproducibility to about 2%.[49,55] Several studies indicate that age-related bone loss is more pronounced in the lateral measurement of BMD. Furthermore, because the lateral approach is more strongly associated with prevalent vertebral fractures than is standard posteroanterior BMD, it has a potentially superior diagnostic sensitivity.[49,56–58]

DXA is also employed for measurements of the appendicular skeleton. Most standard DXA densitometers allow for highly precise measurement of the radius or calcaneus using regions of interest like those derived from SPA and SXA measurements and also user-defined subregions.[59–63] Recently introduced DXA densitometers specially designed for the forearm may provide these measurements at a lower cost.

Low radiation dose, availability, and ease of use have made DXA the most widely used technique for measuring bone density in clinical trials and epidemiological studies.[64,65] Different DXA densitometers from one manufacturer usually yield comparable results. Depending on the scan mode and region scanned, these results are often within the precision error of the densitometer.[66–70] The results may display substantial variation, however, if they are obtained using a variety of densitometers from different manufacturers. This variation arises from differences in bone standards, edge detection algorithms, and regions of interest that are incorporated into the different devices. A group at San Francisco under the auspices of the International DXA Standardization Committee, which includes all leading manufacturers of DXA equipment and representatives of several scientific organizations, has proposed a standardized BMD (sBMD, given in mg/cm^2) for measurements of the lumbar spine, based on the excellent correlation of in vivo data for the lumbar spine among all densitometers.[71] The standardized BMD provides compatibility of results obtained at the lumbar spine on different scanners. To provide similar standardization at other sites, such as the femoral neck, changes of the analysis software may be required because of substantial differences in the regions of interest that the different manufacturers have incorporated into the design of their devices.

Because DXA is a projectional technique, the measured bone density does not reflect a true volumetric density but rather an area density, calculated as the quotient of the BMC and the area. This normalization by the projected area partially reduces the effect of body size. However, it does not take the true volume, for example of a vertebra, into account. For a constant volumetric bone density, a larger vertebra would typically yield higher areal BMD results than a smaller one. Several volumetric estimates of bone density derived from either posteranterior DXA or both posteroanterior and lateral DXA of the lumbar spine have been proposed to enhance vertebral fracture discrimination.[56,72–75] In the context of a large epidemiological study, a volumetric estimate of femoral neck bone density, the bone mineral apparent density (BMAD) did not improve the predictive value of standard BMD measurements for future hip fractures.[76] Further studies are required to confirm these early results and to establish the role of volumetric estimates of projectional bone density.

As a result of the high resolution of DXA scanners, anatomic details of the examined region are depicted clearly. Using DXA to obtain lateral images of the lumbar spine offers the advantage that the scanning beam—in contrast to conventional cone beam radiography—is generally parallel to the vertebral endplates. This allows a better definition of vertebral dimensions for a morphometric analysis. In reference to the DXA approach, this method has been called morphometric X-ray absorptiometry, or MXA.[77]

Overlying structures such as ribs or iliac crest may have an adverse effect on the morphometric analysis. To enhance the accuracy of MXA, technical modifications of the X-ray tube and the detector system may provide images with higher resolution and thus enhance the analysis of vertebral deformities. These techniques are still in the developmental and early clinical evaluation stages.

Architectural properties derived from conventional pelvic radiographs, such as the thickness of the femoral cortex or the width of the trochanteric region, have been found to be associated with future hip fractures.[78] Researchers have examined geometric properties of the femur on DXA scans and found that the hip axis length was significantly associated with future hip fractures independently of age and BMD.[79] Measurement of the hip axis length has been automated, allowing for an uncomplicated and reproducible assessment of an individual's hip axis length.[80] Similarly, geometric variables derived from DXA scans of the radius predicted the fracture load in vitro.[81] These studies primarily document the importance of architectural bone properties for the biomechanics of fracture and may potentially account for differences in the fracture risk between ethnic groups.[82,83] Further studies in this field are required, and the assessment of simple geometric variables may be an interesting asset to DXA.

Quantitative computed tomography

Quantitative computed tomography (QCT) can determine in three dimensions the true volumetric density (mg/cm^3) of trabecular or cortical bone at any skeletal site. However, because of the high responsiveness of spinal trabecular bone, and its importance for vertebral strength, QCT has been principally employed to determine trabecular bone density in the vertebral centrum.[84] In this application, QCT has been used for assessment of vertebral fracture risk,[85–87] measurement of age-related bone loss,[57,88,89] and follow-up of osteoporosis and other metabolic bone diseases.[90] The validity of this technique for measurement of vertebral cancellous bone is widely accepted, and it is used at over 4000 centers worldwide. Generally, spinal QCT is performed on standard clinical CT scanners. It employs an external bone mineral reference phantom to calibrate the CT number measurements to bone-equivalent values as well as special software to place regions of interest inside the vertebral bodies typically of L1–L3.

To improve precision and reduce acquisition and analysis time, the sagittal location of midvertebral slices and the axial placement of regions of interest can be highly automated.[91,92] The software automatically locates the vertebral body, maps its outer edges, and employs anatomic landmarks such as the spinous process and spinal canal to calculate sizes and locations of the region of interest. The systems can place trabecular, cortical, or integral regions of interest. The typical automatic analysis time for a vertebral body is about 5 s, and the total scanning time is several minutes.

QCT can be performed in single-energy (SEQCT) or dual-energy (DEQCT) modes, which differ in accuracy, precision, and radiation.[93] The accuracy of SEQCT for spinal bone mineral determination depends on variable marrow fat composition in the vertebrae, the accuracy of the calibration standard, and beam hardening errors and scatter, among other factors.[93–95] The principal source of marrow is fat, which causes SEQCT measurements to underestimate BMD and overestimate BMD loss. However, the vertebral marrow-fat content increases with age, and a simple correction procedure that takes this into account can reduce the BMD accuracy errors to levels that are small compared with the biological variation.[96] Additionally, marrow-fat errors can be further reduced by using a kVp setting that minimizes the fat sensitivity for the given scanner. Although it is possible to improve accuracy by employing DEQCT, this approach incurs reduced in vivo precision and higher dose and thus is recommended only for research studies that require higher accuracy.[97,98]

The in vivo precision errors of 2–4% and the accuracy errors of 5–15% reported for spinal QCT are generally higher than those observed for posteroanterior DXA of the spine and comparable with those of lateral DXA. However, QCT's ability to selectively assess the metabolically active and structurally important trabecular bone in the vertebral centrum[57,99–102] results in the excellent ability to discriminate vertebral fracture and to measure bone loss, generally with better sensitivity than projectional methods such as DXA or DPA. Ross et al. employed prospective data to assess the predictive power of various BMD measurements for vertebral fracture and found that a spinal QCT measurement two standard deviations (2 SD) below the normative value was 40% more predictive of future vertebral fracture than was the corresponding spinal DPA measurement. Interestingly, they also found that both spinal DPA and QCT had statistically significant associations with fracture even when they were combined in the fracture prediction model, indicating that these two techniques may provide independent information about vertebral fracture risk.[102]

Other studies have examined BMD decrements between normal subjects and those with vertebral fractures. These studies reported that the decrement as measured by spinal QCT is significantly higher than that observed by posteroanterior DXA and that vertebral fracture discrimination is generally superior with QCT.[47,57,63,86,100] Because the metabolic rate in the vertebral trabecular bone is substantially greater than that of the surrounding cortical bone, the ability of QCT to selectively measure trabecular bone gives it comparitively good sensitivity for measurement of age-related bone loss following the menopause.[84] In a cross-sectional study of 108 postmenopausal women, Gulgielmi et al.[57] measured overall bone loss rates of 1.96%/year with QCT compared with 0.97%/year and 0.45%/year, respectively, for lateral DXA and posteroanterior DXA. Generally, it has been found that the cross-sectional bone loss rate in females is typically 1.2%/year when measured with QCT and a little over one-half that value when measured with DXA or DPA.[90] Block et al. carried out a comprehensive QCT study of the patterns of age-related bone loss rate and found that bone loss in women was best described by a two-phase (linear-exponential) regression, with a linear bone loss of 0.45 mg/cc/year up to the menopause, followed by a 25 mg/cc decrement during the early

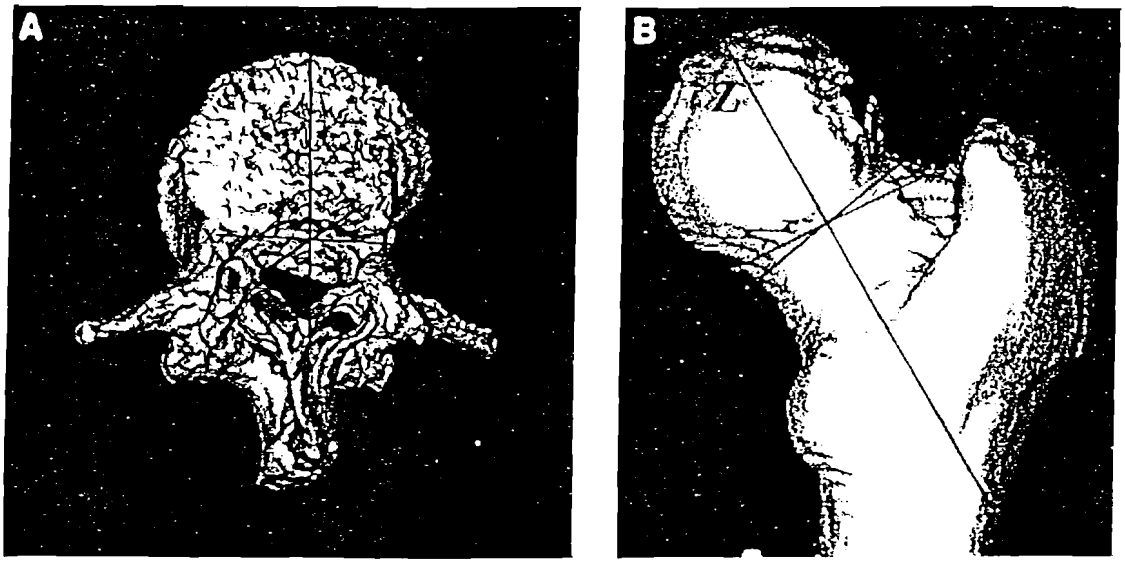

FIG. 1. (a) Three-dimensional representation of excised lumbar vertebral body. The vertebral body, mounted in a water-filled cylinder, was encompassed with 3-mm contiguous slices, segmentation was obtained by mapping the bone surface using a contour tracking algorithm. (b) Three-dimensional representation of proximal femur of patient with osteoporosis secondary to paraplegia. Proximal femur was encompassed with 3-mm contiguous slices, and segmentation was obtained by mapping the bone surface using a contour-tracking algorithm

menopause and an exponential pattern of bone loss of 1.99 mg/cc/year following the menopause.[88]

While use of QCT has centered on two-dimensional characterization of vertebral trabecular bone, there is interest in developing three-dimensional, or volumetric computed tomography (vQCT), techniques both to improve spinal measurements as well as to extend QCT assessments to the proximal femur (Figs. 1a and 1b). These three-dimensional techniques encompass the entire object of interest either with stacked-slice or spiral CT scans and can employ anatomic landmarks to automatically define coordinate systems for reformatting of the CT data into anatomically relevant projections.

In the spine, three-dimensional methods have been investigated both to improve longitudinal performance and discriminatory capability. Volumetric methods would be expected to improve the in vivo precision of QCT, first by employing image alignment techniques to reproducibly quantify the same volume of tissue in longitudinal studies,[103,104] and second, by assessing the trabecular bone from the entire vertebral centrum, a volume roughly 9–10 times larger than the standard elliptical region of interest. However, assessment of a larger volume of interest covering the trabecular bone in the centrum does not necessarily improve the identification of vertebral fracture over standard two-dimensional QCT methods. Thus volumetric studies of regional BMD, which examine subregions of the centrum that may vary in their contribution to vertebral strength[105,106] and studies of the cortical shell,[107–110] the condition of which may be important for vertebral strength in osteoporotic individuals,[111] are of interest for future investigation.

Because of the proximal femur's complex architecture and dramatic three-dimensional variation in its density, the two-dimensional QCT methods widely used in the spine cannot be used to assess the proximal femur. Thus, there is no clinically accepted QCT technique for the hip and virtually all densitometric assessment of the proximal femur is performed with DXA, which provides an integral measurement of trabecular and cortical bone. Early attempts to apply vQCT methods to the proximal femur measured purely trabecular bone[112,113] because trabecular bone shows the earliest loss and will most effectively identify individuals at risk for fracture. However, the contributions of trabecular and cortical bone to proximal femur strength vary with the proximal femur site.[114] Thus, well defined volumes of interest selectively measuring trabecular and cortical bone, as provided by QCT, may be important for the assessment of bone strength at various sites in the proximal femur. Additionally, the crucial role of geometry in determining proximal femur strength has been well documented.[78,80,115–117] QCT, with the inherent ability to resample data along any axis of interest, yields geometric information not obtainable with projectional techniques. For example, Lotz et al. resampled CT data along an axis defined by the peaks of the greater and lesser trochanters and found that the product of average intertrochanteric CT number and intertrochanteric area correlated extremely well ($r^2 = 0.90$) with in vitro fracture load in a configuration simulating a fall to the side.[118] In addition to the assessment of proximal femur strength, vQCT could play a useful role in monitoring differential trabecular or cortical bone response to pharmacological interventions.

There are additional research initiatives in the areas of high resolution and microcomputed tomography (HRCT, μCT). While the average BMD measured within a relatively large region of interest is a valuable tool for the assessment of osteoporosis, an improved assessment of bone strength

and fracture risk prediction may also require microstructural analysis. Apart from trabecular BMD, two main factors that affect bone strength are the architecture of the trabecular network and the thickness of the cortical shell. While the spatial resolution of clinical CT scanners (typically > 0.5 mm) is inadequate for highly accurate cortical measurements and for an analysis of discrete trabecular morphological parameters, newer CT developments try to address these issues. Two main approaches can be distinguished: (1) the development of new image acquisition and analysis protocols using existing clinical CT scanners; and (2) the development of new HRCT scanners for in vivo investigations of peripheral bones or for in vitro two- or three-dimensional μCT for structural analysis of very small bone samples (typically < 1 cm^3).

These efforts to develop new imaging and analysis protocols for existing scanners with limited spatial resolution have often focused on a regional analysis of BMD. In studies on the spine, Sandor et al.[107,119] divided the trabecular area into several regions of interest in the form of a spider net. The BMD was distributed in a W-shaped pattern with maximum BMD in the lateral and anterior portions of the vertebral body. Regions with highest BMD showed the highest loss with age. Hangartner and Gilsanz[120] and Sumner et al.[121] addressed techniques to determine the peak appendicular cortical density and vertebral cortical thickness, respectively. Flynn et al.[122] used CT to determine regional bone density in 18 small cylindrical regions of interest in the lower lumbar spine. Pattern classification methods identified vertebral architectural density patterns that potentially provide enhanced fracture discrimination.

Instead of the usual trabecular BMD analysis, Braillon and colleagues[123] suggested the standard deviation of the BMD values as a parameter that partially reflects structural variations in the cross-sections of the lumbar vertebrae. A high BMD standard deviation indicates a high degree of grey-level variations in the image and thus a highly networked bone architecture. Engelke et al., using a very low-dose technique, applied this idea to a dataset of 214 women.[124] However, this study did not confirm a significant potential of the BMD standard deviation as measured in trabecular spinal QCT to improve the capability of BMD to separate osteoporotic from nonosteoporotic subjects.[124] However, this technique could possibly be useful at higher radiation which provides better depiction of the structure.

Another direction is the development of in vivo high resolution, thin slice computed tomography (slice thickness 1–1.5 mm). A high resolution image of a vertebral body that clearly displays structural information in a higher dose CT image is shown in Fig. 2. However, the quantitative extraction of this information is difficult, and the results often vary substantially according to which image processing technique is used. Some investigational work using thin slice tomography has been published recently by Chevalier et al.[125] They measured a feature termed the trabecular fragmentation index (length of the trabecular network divided by the number of discontinuities) to separate osteoporotic subjects from normals subjects. However, this index did not readily separate postmenopausal osteoporotic women with vertebral fractures from normal or osteopenic subjects.[125] A similar trabecular texture analysis approach was also reported by Ito.[126]

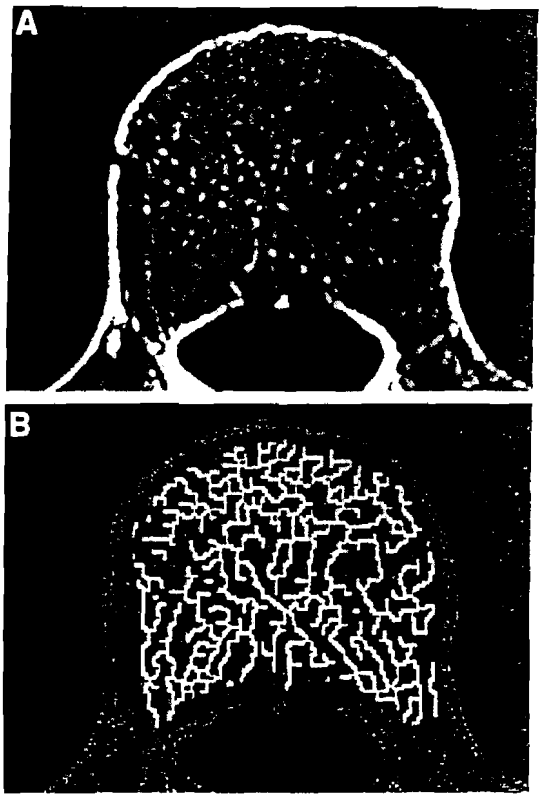

FIG. 2. High resolution (500 × 500 μm) CT image of a 1.0 mm slice of a vertebral body imaged in vivo. Trabecular structure is well delineated in grayscale (A) and skeletonized (B) images.

Ultra-high resolution CT scanners for peripheral skeletal in vivo measurements have been developed by Ruegsegger et al.[127–130] The images, with a spatial resolution of 100–200 μm, show trabecular structure in the radius and the tibia. These state-of-the-art scanners probably approach the limits of spatial resolution achievable in vivo when administering acceptable exposure rates. The images can be used for quantitative trabecular structural analysis and also for a separate assessment of cortical BMD.

Feldkamp et al.[131,132] constructed a μCT system for in vitro three-dimensional analysis of small bone samples. The spatial resolution of 60–100 μm clearly separates individual trabeculae and thus allows for a three-dimensional analysis of a trabecular network. Based on data sets from this CT scanner, Engelke et al.[133,134] developed a three-dimensional digital model of trabecular bone (Figs. 3a and 3b) that can be used to compare two- and three-dimensional structural analysis methods and to investigate the effect of decreasing spatial resolution and image processing technique on the extraction of structural parameters. Three-dimensional data sets can be used not only for calculating classic histomorphometric parameters like trabecular thickness and separation[135,136] but also for determining topological measurements like the Euler number which is a measure of three-dimensional connectivity.[137] Another in

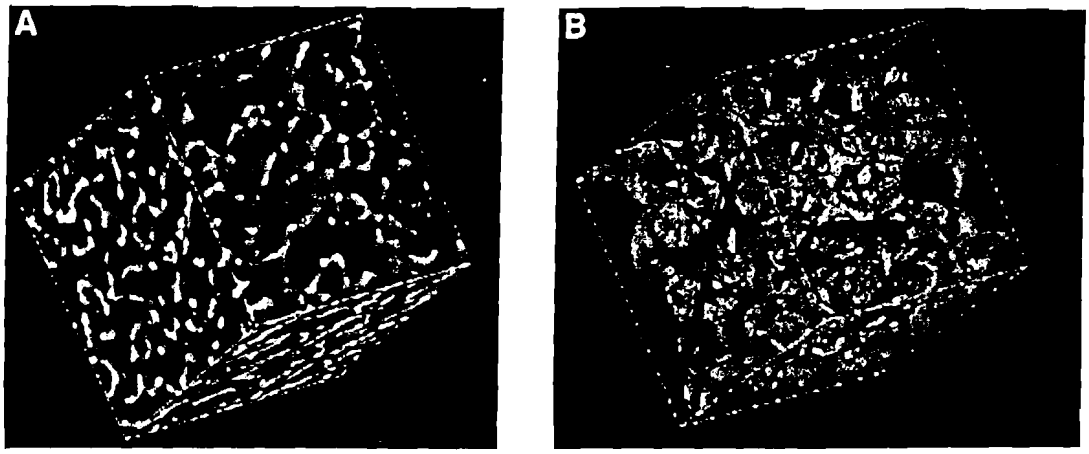

FIG. 3. Micro CT volumetric image (voxel size, 80 μm^3) of bovine bone (a) and resulting three-dimensional digital model of trabecular bone (b).

vitro CT scanner with a spatial resolution of 20 μm has recently been developed by Rüeggsegger et al.[138,139]

Whereas the CT scanners described above use an X-ray tube as a radiation source, other investigators[140–142] have explored the potential of high intensity, tight collimation synchrotron radiation, which allows for either faster scanning or higher spatial resolution for imaging bone specimens.

Peripheral quantitative computed tomography

Special purpose peripheral QCT (pQCT) scanners have been employed for the measurement of BMC and BMD of the peripheral skeleton. Initially, a radionuclide source (usually ^{125}I) was used; however, state-of-the-art scanners employ X-ray sources.[130,143–147] pQCT allows for a true volumetric density measurement of appendicular bone without superimposition of other tissues and provides exact three-dimensional localization of the target volume. Ease of use and the ability to assess separately cortical and trabecular bone, and to measure BMD, BMC, and the axial cross-sectional area, make the method an interesting alternative to SPA or SXA.

There are about 1000 pQCT systems in use, mostly in Europe. The great majority of these systems represent a clinical pQCT scanner, with a smaller number (about 20) representing ultra-high resolution, high-precision pQCT systems for research applications. With the commonly used clinical pQCT scanner, measurements in the distal radius are performed at only one site with a single axial slice of 2.5 mm thickness located at the level that represents 4% of the ulnar length from the distal radial cortical endplate (Figs. 4a and 4b).

The short-term in vivo precision of the clinical pQCT has been measured using groups of healthy young volunteers. Butz et al.[148] found relative precision errors (CV) of 1.7% for trabecular, 0.8% for total, and 0.9% for cortical BMD measurements. Lehmann et al.[149] (pQCT with an X-ray source) and Schneider et al.[143] (pQCT with a radionuclide source) calculated absolute precision errors for trabecular regions of interest between 2.6 and 3.1 mg/cm^3, which resulted in CVs of under 1%. In a study by Grampp et

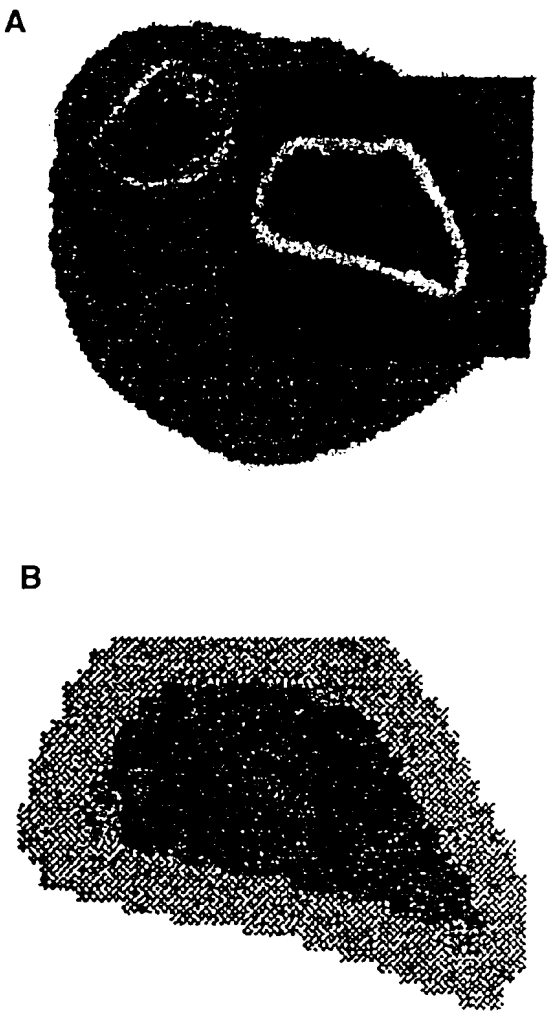

FIG. 4. pQCT cross-sectional image of forearm showing delineation of cortical bone (a) and central trabecular bone (b).

al.,[150] of pre- and postmenopausal women, the average absolute precision errors for the trabecular and total region were of the same order as in the previous studies (1.8–3.4 and 3.8–8.5 mg/cm^3, respectively), but the resulting CVs of the postmenopausal population were higher (0.9–2.1 and 1.1–2.6%, respectively), because of lower average BMD in their groups. Long-term in vitro precision with phantom measurements was calculated by Wapniarz et al. to be about 0.9%.[151]

In vitro, the accuracy of the method was calculated to be about 2%.[127] In a cadaver study in which radii were measured with pQCT and then ashed, Takada et al. found high correlations between total pQCT BMC and ash weight (r = 0.90) and between pQCT total BMD and ash weight (r = 0.82).[152]

The relationship between pQCT parameters and aging in healthy subjects was evaluated in several studies. Using a high resolution scanner, Rüegsegger et al. found that in contrast to trabecular BMD which declined with age, cortical density (but not cortical BMC or area) remained constant between the ages of 20 and 70 years.[145] Similar observations with a clinical pQCT scanner were made by Grampp et al.,[153] who found only relatively small annual BMD changes in healthy volunteers of −0.30% in total, −0.25% in trabecular, and −0.19% in cortical BMD. In this study, the highest age-related changes in pQCT parameters measured at the radius occurred in the cortical thickness measures with an average annual decrease of −0.69% in cortical BMC and −0.52% in cortical area indicating principally a thinning of the cortex by endosteal resorption.[153] Other studies found higher annual changes in BMD but did not consider BMC or cortical area. Schneider et al.[143] found annual decreases of 0.5% in the trabecular BMD of healthy women and 1.9% in osteoporotic women, and Butz et al.,[148] found changes of 0.9% in the trabecular and 1.1% in the total BMD. The differences between the studies are not entirely clear but may be related to different criteria in the definition of the study subjects.

The influence of BMD in trabecular and in cortical bone on the total BMD measured by pQCT was evaluated in a study by Rico et al. with healthy young male and female volunteers.[154] Here, the cortical BMD proved to be more closely related to the total BMD than was trabecular BMD. This was indicated by the higher correlation coefficients for comparisons of pQCT total versus cortical BMD (r = 0.95), as compared with total versus trabecular (r = 0.62), and of trabecular versus cortical BMD (r = 0.43).

In some studies, pQCT measurements of BMD at the radius were found to be successful in distinguishing between osteoporotic and nonosteoporotic patients and in monitoring subjects during clinical studies.[130,145] However, other authors have reported conflicting results, especially for peripheral trabecular BMD.[155,156]

The importance of the measurement of cortical bone per se was suggested by Sparado et al. who found in a biomechanical study that the cortical shell contributes substantially to the mechanical strength of the distal radius.[157] The thinning of the cortical rim at the radius was a potential mechanism contributing to osteoporotic changes,[130,145] and it identified this compartment as a promising location for BMC and thickness measurements. These findings were supported in a study by Grampp et al.[153] that examined the ability of BMD, BMC, and cross-sectional area to detect osteoporotic changes. Only the cortical area and BMC significantly distinguished between women with nontraumatic vertebral fractures and healthy postmenopausal women; these two parameters also showed the highest age-adjusted odds ratio for fracture risk. These data suggest that pQCT measurement of cortical rather than trabecular bone at the radius may have greater diagnostic sensitivity in terms of appendicular measurements.

Modern pQCT scanners also incorporate a multislice data acquisition capability covering a larger volume of bone as compared with the commonly used single slice technique.[158,159] The measurement of several slices is potentially more representative of changes in the distal radius and may therefore reflect the bone status of an individual more accurately. If studies employing this multislice pQCT technique are successful, they may contribute to more extensive use of this already promising technique.

Quantitative ultrasound

The use of quantitative ultrasound (QUS) for the assessement of skeletal status has seen continued interest in recent years. The attractiveness of QUS lies in its low cost, portability, ease of use, and freedom from ionizing radiation. These benefits combined with preliminary clinical results showing good diagnostic sensitivity for fracture discrimination have encouraged further basic investigation and commercial development. Currently there are more than one half dozen commercially available QUS devices, although none has been approved for clinical use by the FDA. For this reason, QUS devices for bone assessment are found primarily at research centers in the United States whereas they have a much wider distribution in Europe and Asia (there may be up to 2000 systems in use worldwide).

Ultrasound properties can be measured by reflection or transmission.[160] Current commercial systems rely on sonic transmission using two ultrasound transducers (a transmitter and receiver) positioned on each side of the tissue to be measured (Fig. 5). These devices measure ultrasound parameters primarily in trabecular bone at the calcaneus and patella, cortical bone at the tibia, and integral bone at the phalanges. The parameters measured include ultrasound transmission velocity (UTV) and/or the frequency dependency of the attenuation of ultrasound signal, called broadband ultrasound attenuation (BUA).

UTV is commonly measured at the calcaneus, tibia, patella, and phalanges. Ultrasound velocity is determined as the quotient of transit time and body part width or length and is quoted in meters per second (m/s). At the calcaneus, the width is either the overall heel width (bone and soft tissue) or the width of bone alone.[161] The first gives a measure of UTV called the speed of sound (SOS) while the second is referred to as ultrasound velocity through bone (UVB). Values of UTV measured at the calcaneus range from 1400 to 1900 m/s.[162–165] There is considerable overlap of SOS and UVB in this range with UVB generally being higher than SOS. Moreover, SOS measured on dif-

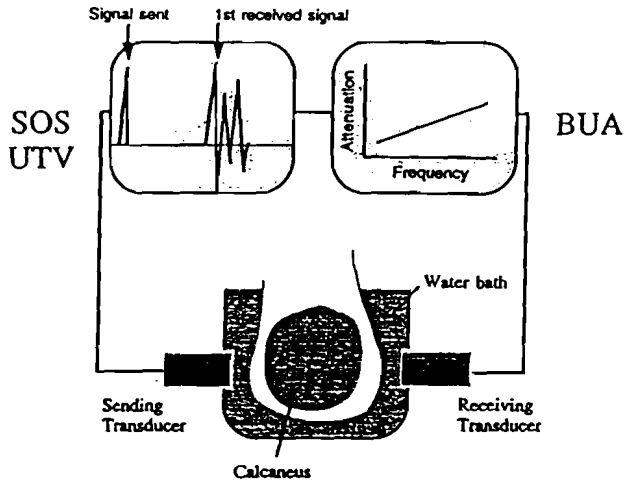

FIG. 5. A schematic diagram showing the measurement of ultrasound attenuation (BUA) and velocity (UTV) at the calcaneus. This is a transmission measurement which uses a water bath to provide acoustic coupling between the transducers and the heel.

ferent instruments differs because disparate algorithyms are employed. Patellar velocity is typically 1600–2200 m/s.[166] Velocity measured in the cortical bone at the midtibia is higher and ranges from 3300–4300 m/s. The accuracy of these measurements is difficult to assess because the complex structure of bone and its inhomogeneity result in variable conduction paths and transit times and make determination of true velocity ambiguous. However, estimates of the accuracy of patellar velocity suggest that the measured value underestimates true ultrasound velocity by approximately 100 m/s.[167] The precision error of UTV measurements is about of 0.3–1.5%.[161,165,167–170] Cross-sectional investigations of age-related changes in calcaneal SOS in healthy women have shown reductions in velocity at annual rates of 1.3–4.9 m/s (0.1–0.3%) per year.[162,163] One study that included data from young normal women showed a steady decline in calcaneal SOS from 20 to 90 years of age.[162] Studies of ultrasound velocity in the tibia have found similar reductions in velocity of approximately 1.2 m/s per year while in the patella velocity decreases by 3 m/s per year.[167]

The other QUS parameter commonly measured is attenuation. Attenuation of the ultrasound signal occurs as energy is removed from the wave by absorption and scattering in the bone, marrow, and soft tissue. The attenuation parameter BUA, introduced above, was first proposed by Langton et al.[171] It is determined at the calcaneus and is a measure of the frequency dependence of the attenuation of ultrasound. This dependence is approximately linear over the range 200–600 kHz. BUA is defined as the slope of attenuation versus frequency in this range and is reported in units of decibels per megahurtz.

Another attenuation parameter that has been investigated is ultrasound attenuation in bone (UAB).[172,173] It is computed as the mean attenuation of ultrasound signal at a select number of frequencies between 200 and 600 kHz. Precision of the BUA measurement (0.9–6.3%) is not as high as that of UTV.[163,170,174–179] The annual rate of change in BUA has been reported to range from 0.4–0.8 dB/MHz (0.4–1.0%) per year.[162,163,175] Large changes in BUA have been observed immediately after menopause (2.5% per year between 0 and 5 years after menopause) followed by a period of slower change (0.5% per year).[175]

Before being used for biomechanical investigations, ultrasound was used to assess mechanical properties in engineering and industrial applications. The mechanical properties of a material or tissue are determined by its material and structural properties. Material properties are independent of geometry and architecture while structural properties are determined by these factors. The parameters measured with ultrasound, BUA and UTV, are influenced not only by bone density but also bone structure and composition. It is generally believed that both BUA and UTV are determined by bone density and bone microarchitecture (trabecular number, connectivity, and orientation). McCarthy et al. have recently investigated the relationship between velocity and specimen orientation, density, porosity, and temperature.[180] They demonstrated significant correlations between ultrasound velocity and bone specific gravity and porosity. In a study with bovine bone cubes, Glüer et al. examined the relationship between ultrasound velocity and trabecular bone structure determined by analysis of μCT images.[173] They found that the velocity was largely influenced by trabecular separation. In this same investigation, the attenuation parameters BUA and UAB were shown to be influenced by connectivity and trabecular separation. Moreover, these associations with bone structure were independent of the associations between the QUS parameters and BMD. Other work by Glüer et al. has shown that BUA is dependent on trabecular orientation, with BUA being as much as 50% higher along the axis parallel to the principal orientation of the trabeculae.[181] UAB has also been shown to have a negative linear correlation ($r = 0.90$) with trabecular plate separation as determined by histomorphometry.[182] Other work has shown that a combination of BUA and velocity can be used to estimate Young's modulus in trabecular bone.[183] The promise of QUS may lie in this apparent dependence of the ultrasound parameters on bone structure. It has been shown that osteoporosis involves a change in bone architecture as well as BMD.[136] These architectural changes can significantly influence the mechanical competence of bone. If ultrasound is shown to reflect structural characteristics of bone, it may provide important information to augment that obtained by current X-ray–based measures (DXA and QCT) of bone density.

Many in vitro and in vivo studies have been undertaken to elucidate the nature of the information derived from ultrasound measurement. UTV is directly related to the elasticity as well as the density of bone. Ultrasound velocity has been used to study the elastic properties of human and bovine cortical bone.[184,185] Both investigations showed high correlations between mechanically and ultrasonically determined elastic moduli. In other studies with trabecular bone samples velocity correlated well with ultimate strength ($r = 0.71–0.75$).[186,187] These results strongly suggest a

relationship between QUS and bone structure and strength beyond that which can be explained by BMD.

In vivo studies investigating the relationship between QUS parameters and bone density seem to confirm these findings. Numerous studies have compared BUA at the calcaneus with bone density measured by various techniques. Correlation coefficients have ranged from 0.33 to 0.83 for lumbar spine BMD and 0.30 to 0.87 for the femoral neck.[170,176,177,188,189] Site-matched comparisons of BUA and BMD at the calcaneus yielded correlations in the range 0.56–0.75.[174–178] While these correlations are significant, 50% of the variability of BUA remains unexplained by BMD. Whether this unexplained 50% is related to bone strength or structure or to some parameter unrelated to osteoporosis has yet to be determined. Given the significant correlations between BUA and BMD, the question arises as to whether BMD can be accurately predicted by ultrasound measurement. Accurate prediction would allow the use of low-cost, radiation-free QUS devices for the assessment of BMD. However, the correlations are at best moderate and the errors in predicting lumbar spine or femoral neck BMD are too high to allow QUS to be a used for estimation of BMD per se.[170,178,190,191]

Clinical investigations of the ability of QUS to discriminate between populations with fractures and those without have shown promising results. Several studies have demonstrated that velocity measurements at the patella, tibia, or phalanges can identify patients with prevalent vertebral fractures with the same effectiveness as conventional bone mass measurements at the spine, hip, or forearm.[165,167,168,192–194] A recent report also showed that patellar ultrasound velocity could predict incident vertebral fracture.[195] Measurements of QUS parameters at the calcaneus have also shown strong association with fracture risk. Several small case-control studies have established that BUA is significantly lower in patients who have suffered previous hip fracture compared with age-matched controls.[196,197] One report showed that BUA was as powerful as DXA of the proximal femur in identifying the fracture group as measured by Z-scores and ROC analysis.[197] Two cohort studies have shown that BUA at the calcaneus is associated with incident hip fracture.[198,199] Other investigations have shown the association of calcaneal QUS with vertebral fracture. These studies have found the diagnostic sensitivity of either BUA and SOS to be equal to or greater than that of spine and hip DXA.[14,116,199,200] Using models that combine DXA and QUS measurements, these studies have also been able to show BUA and SOS maintain their ability to identify patients with vertebral fractures even after adjusting for the effect of BMD. This provides additional evidence that QUS measures characteristics of bone strength that are potentially independent of density.

Quantitative magnetic resonance and magnetic resonance microscopy

Magnetic resonance (MR) is a complex technology that has evolved rapidly since its introduction to medical science in the early 1970s. Based upon the application of high magnetic fields, transmission of radiofrequency (RF) waves and detection of RF signals from excited hydrogen protons, this technique has revolutionized medical imaging in general. Recently, the ability of quantitative magnetic resonance (QMR) and magnetic resonance microscopy (μMR) to assess osteoporosis has been explored.

To date, most MR imaging techniques have been limited to the study of soft tissue or of gross skeletal structure because compact bone does not generate any detectable MR signal. However, newly developed QMR techniques have been used to study trabecular bone, specifically. The presence of the trabecular bone matrix affects the signal intensity of bone marrow, an effect that is particularly enhanced in specific imaging sequences. The magnetic properties of trabecular bone and bone marrow are significantly different. These differences produce distortions of the magnetic lines of force, which make the local magnetic field within the tissue inhomogeneous and alter the relaxation properties of tissue, such as the apparent transverse relaxation time T2*, in gradient-echo images. From theoretical considerations, such changes in T2* should directly relate to the density of the surrounding trabecular network and its spatial geometry. The resultant shortening of relaxation time becomes greater with an increase in the concentration of trabecular bone in the surrounding homogeneous marrow tissue. Thus, in a normal dense trabecular network, T2* shortening should be more pronounced than in rarefied osteoporotic trabeculae.

Experimental studies have confirmed the theoretical predictions, suggesting QMR as a promising tool for studying trabecular bone architecture and assessing osteoporosis. Davis, Genant, and Dunham[201] have shown a reduction in the in vitro T_2^* of both water and cottonseed oil in the presence of bone powder at a magnetic field strength of 5.9 tesla. Rosenthal et al.[202] have measured a reduction in the T_2^* of water present in the trabecular spaces compared with extratrabecular water, using specimens of excised human vertebrae at 0.6 tesla. Majumdar et al.,[203] using specimens of dried human vertebral bodies' various bone densities, have examined susceptibility mediated relaxation effects. The mean trabecular bone density for each specimen, measured by QCT, was significantly related to the overall relaxation rate ($1/T_2^*$) of intertrabecular saline. Similar relations in vivo have also been established in the forearm, distal femur, and proximal tibia sites at which the trabecular bone network shows significant variations as a function of the distance from the joint line, with the bone density and relaxation rate, 1/T2*, being greatest in the epiphysis and progressively decreasing toward the metaphysis and diaphysis.[204] In studies on the distal radius, precision errors in measured T2* times were found to range from 1.3 to 2.9 ms, corresponding to 3.8–9.5% CV.[205] In a similar fashion, Ford and Wehrli[206] have used a method called MR interferometry to assess variations in T_2^* between osteoporotics and normal subjects and found reasonable discriminatory capability.

Theoretically and from computer simulations[203,207] and phantom studies,[208] the relaxation time T_2^* of bone marrow is affected not only by the density of the trabecular matrix but also by its spatial architecture. In early experiments with specimens, Majumdar et al.[209] have shown a correlation between T_2^* and the elastic modulus which re-

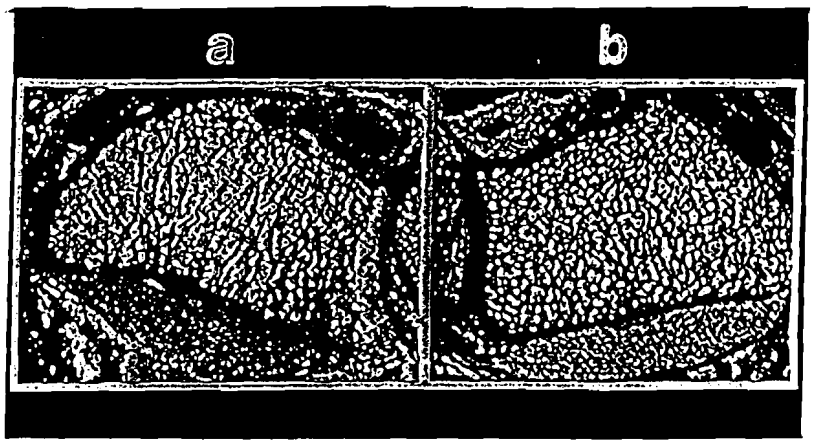

FIG. 6. High-resolution magnetic resonance images of the distal radius in the axial plane. The image resolution is 156 μm in plane and 700 μm in slice thickness. The echo time is minimized to 8.4 ms, and the total scan time is 19 minutes. In these images, the marrow is bright and the trabeculae appear as dark striations (a) osteoporotic subject (b) normal subject. Note the dense network in the normal subject and the sparse trabecular network in the osteoporotic subject.

flects the biomechanical properties of trabecular bone. Chung et al.[210] found a strong correlation (r = 0.91) between the Young's modulus of elasticity and 1/T2' in trabecular bone specimens from human lumbar spine, while Jergas et al.[211] have shown similar relationships using specimens of tibial bone.

Thus, this measured QMR parameter T_2^* may enhance the capability for fracture discrimination and fracture risk prediction. This technique has the advantage that it can be performed at medium-to-low resolution, resulting in decreased acquisition times, and permitting the use of scanners at fields of 1.5 tesla or less.

MR microscopy (μMR) may prove to be an additional, valuable MR-based technique for the quantitative study of trabecular microarchitecture both in vitro and in vivo. In vitro, using small RF surface coils in high-field scanners, MR microscopy can be performed at resolutions sufficient to discriminate individual bone trabeculae.[212,213] In vitro images have been obtained at in-plane resolutions as low as 33 μm, while in vivo images range from resolutions of 78 × 78 × 300 μm through the phalanges[214] to images at a resolution of 156 × 156 × 700 μm in the distal radius[215] and 200 × 234 × 1000 μm in the calcaneus.[216] Typically, the image is first segmented into bone and marrow phases, and histomorphometric analysis is then performed on the resulting binary image. Stereological parameters such as the trabecular bone area and volume fraction, mean intercept length, mean trabecular width, and mean trabecular spacing and trabecular number can thus be calculated. Wehrli et al. have compared the standard measures with stereological measures of bone volume fraction derived from MR images obtained at 9.4 tesla and found good correlations,[213] while Antich et al. have conducted similar experiments and found changes in accordance with histomorphometry measures.[212] Kapadia et al. have extended the in vitro techniques to obtain images in an overiectomized rat model and have shown the ability to measure changes in trabecular structure following overiectomy.[217]

Because of limitations of the signal to noise and total imaging time, smaller individual trabeculae usually cannot be resolved with the resolution achievable in vivo at clinical field strengths, but the images show the larger trabeculae and the texture of the trabecular network. However, using standard techniques of stereology as well as texture analysis tools such as fractal analysis, the trabecular structure can still be quantified. In an early study establishing the feasibility of using such images to quantify trabecular structure, MR images of the distal radius have been obtained using a modified gradient echo sequence on a 1.5 tesla imager, at a spatial resolution of 156 mm, and slice thickness of 0.7 mm.[215] It is well known that the amount of trabecular bone is greatest at distal sites of the radius and decreases proximally, and this is readily seen in the MR images. In Figs. 6a and 6b, a representative axial section from a normal subject and an osteoporotic subject clearly depict the loss of the integrity of the trabecular network with the development of osteoporosis. Similar images obtained in the calcaneus of a normal subject are shown in Fig. 7. The orientation of the trabeculae is significantly different in the subtalar region as compared, for example, with the posterior region. The ellipses, representing the mean intercept length, show a preferred orientation and hence map the anisotropy of trabecular structure. In preliminary in vivo studies in the calcaneus, gray-scale reference values from fat, muscle, and tendon were used to calculate a reproducible threshold value. This approach gave a midterm in vivo precision of ~3–5% CV for trabecular width and spacing.[218]

In MR, the appearance of the image depends on several factors other than image resolution. The pulse sequence used to obtain the image, whether it is a spin-echo or gradient echo, the echo time, and the magnetic field strength are all important factors that may modify the trabecular dimensions depicted in an MR image.[219] Furthermore, when the image resolution is comparable to the trabecular dimensions a small error is manifested as a large relative error, and hence the stereological measures from MR images are likely to be subject to these effects. In the analysis of such images, the threshold is also shown to have

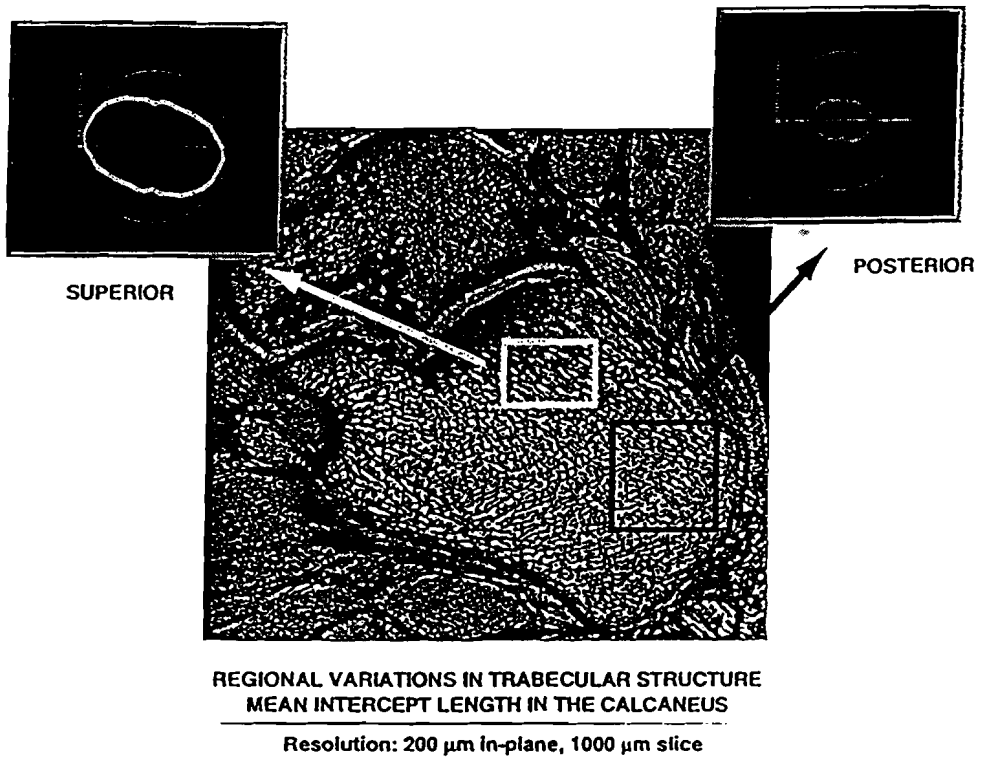

FIG. 7. High-resolution magnetic resonance image through the sagittal plane in the calcaneus. The anisotrophy of trabeculae (dark striations in bright marrow) is clearly seen. The mean intercept length, a measure of the mean trabecular width as a function of angle is shown. The major axis of the ellipse defines the preferred trabecular orientation. The anisotrophy of trabeculae is most pronounced in the subtalar region as is also demonstrated by the elliptical plot of the mean intercept length. The ellipses are scaled identically, thus it can also be seen that the thickest trabeculae are found in the subtalar region.

a significant effect on the estimated parameters.[215] Technical challenges brought about by the standardization of image acquisition and analysis and improved understanding of those processes underlying image formation could allow MR to become a potential tool for assessment of trabecular bone structure in vivo. As a noninvasive, nonionizing technique, MR can provide three-dimensional images in arbitrary orientations and can also depict trabecular structure. Although it is a relatively expensive, time-consuming technique to use for primary screening for osteoporosis, it provides a potential platform for identifying particularly high-risk patients after initial bone densitometry and perhaps for assigning these patients to more aggressive therapies.

STATISTICAL APPROACHES IN STUDIES OF BONE DENSITOMETRY

Because of the availability of various densitometric techniques to measure BMD and the importance of determining the high-risk patient (in a clinical setting) or a high-risk group (in an epidemiological setting) for osteoporotic fracture, it is important to assess and compare the ability of these techniques to accurately discriminate the high-risk patient or group from a general population at risk. Statistical methods used for this include summary descriptive statistics for the high-risk group like the Z-score and the T-score, univariate *t*-test for the comparison of mean BMD measured by a particular technique in two groups (patient group and controls), logistic regression for measuring the risk of osteoporotic fractures through the odds ratio, and discriminant analysis for developing a discrimination rule that minimizes the chances of misclassifying a member of the patient group into normal group and vice versa. Even though all these statistical models broadly address the issue of comparison and assessment of the discriminatory ability of different techniques for two groups, they are based on different mathematical models and assumptions and thus should be used carefully depending upon the study design and the research questions.

The most commonly used descriptive statistics in the field of bone densitometry have been the Z-score and the T-score. The Z-score for a patient result measured by a particular technique is defined as the deviation from the mean result for the age-matched controls divided by the standard deviation of these measurements for the age-matched controls. The T-score is defined similarly but using young controls as the reference group. In addition, the Z-scores (T-scores) of two different techniques can be compared with each other directly regardless of the differences in the units. Since these scores are easy to calculate and interpret, they are used diagnostically to represent an indi-

vidual patient's BMD status in comparison with the appropriate control group. In order to assess and compare the discriminative ability of two techniques, the mean Z-score and mean T-score for that group with respect to the appropriate control group can be calculated. The magnitude of these scores gives some estimate of which technique discriminates the high-risk group from the controls more efficiently (a bigger mean Z-score is an indication of better discrimination). However, the conclusions based on these scores are limited because the probability of misclassification depends on the characteristics of the BMD measurements other than those used in the composition of these scores. In fact the statistical tests based on these measures are valid only under certain assumptions regarding the distribution of the BMD values. These assumptions are violated by having unequal variances for one or both sets of BMD measurements in the two groups. The effects of unequal variances can be seen through misleading mean Z-scores and T-scores. For example, keeping the parameters of the control group the same but changing the population variance of the patient group will result in different probabilities of misclassifications for the same mean Z-score (or T-score). These scores in addition do not use the sample size information of the control group and are thus not comparable across studies with small sample sizes in the control group (at least 50 subjects are needed to nullify the sample size effect).

As an alternative to these scores, the *t*-statistic takes into account the variances and sample size of the two groups. This again results in two *t*-statistics (corresponding to two mean Z- or T-scores for the two techniques) with a bigger *t*-statistic indicating better discrimination. Since the *t*-test is designed for detecting mean differences only, conclusions about assessing and comparing discriminative ability should not be drawn on the basis of the *t*-statistic. For a comparison between the means of two groups, on the other hand, the *t*-statistic is more appropriate compared with the Z-score (or T-score).[220-223] However, all three methods are less efficient for assessing and comparing the discriminative ability of two techniques and should not be used for this purpose. In addition to the problems stated above, incorporating statistical analysis for comparing more than two techniques is not easy.

In contrast to the Z-score, T-score, and the *t*-test, which compare the means of two groups, logistic regression and discriminant analysis are statistical techniques that model the probability of osteoporotic fracture as a function of the covariates such as BMD. The coefficients from the logistic regression analysis are then used to measure the risk (odds ratio) for a specific BMD technique and thus can be used to decide which of the several techniques is associated with uncovering a higher risk compared with the controls. These measures of risk are important in selecting the group whose members are at a high risk of fracture. As pointed out above, the model can be adjusted for other covariates including BMD measured by different techniques, and other continuous variables like age, height, and weight or categorical variables like sex and race. The logistic regression model, given an individual's covariate values, can provide an estimate of the probability of developing fractures. This can then be used for classifying that patient into a high-risk or control group by comparing this predicted probability with a cutoff point, for example 0.5. This method of classification is called logistic discrimination and can be used in a clinical setting. ROC curve analysis of these predicted probabilities can be used to compare different techniques, and the areas under the ROC curve can be tested for differences to assess the best discriminative technique.[224-226]

Discriminant analysis is a technique designed to create a classification rule that minimizes the probability of misclassification between two or more groups. The explanatory variables such as BMD and age are combined in an optimum fashion (similar to the right side of the logistic regression model), which is called the discriminant function, such that the difference between the two groups with respect to this linear combination is maximized. Discriminant scores are then obtained for each individual based on the person's BMD and age, for example, which are then used to calculate the probability of developing fractures. These probabilities are then used to classify the individual into the high risk or control group. The coefficients of the discriminant function measure the relative importance of a particular explanatory variable in the overall discrimination. Two different discriminant analysis models can be compared statistically to determine whether one model is better. Thus, discriminant analysis can be used to compare different BMD techniques.[227,228] The discriminant analysis rule can also be used in a clinical setting in the same manner as defined above for logistic regression.

The logistic regression and discriminant analysis are very similar. When the explanatory variables are normally distributed in both the groups with equal variances and equal between-variable correlations (this also implies that none of the covariates is discrete), discriminant analysis is more efficient and has a greater statistical power than logistic regression. In the presence of discrete covariates and departures from assumptions of normality, logistic regression is more efficient.[229-231]

As a summarizing technique, the ROC curve analysis should be used. It can be used as a summary of the discriminative ability for any statistical model that results in scores. Thus, raw measurements, logistic regression, and discriminant analysis as well as any technique that results in summary scores for each individual can be summarized using the ROC curve. The areas under these curves can be tested for significance and thus can help in identifying not only the best technique but also the best statistical model.[232,233]

If, instead of fracture, the primary endpoint is, for example, time to fracture since menopause, survival analysis models need to be used. These models are appropriate for situations in which some patients are lost to follow-up or do not sustain a fracture before the end of the study. Logistic regression and discriminant analysis models treat all fracture cases the same while the survival analysis models take into account the time until fracture. In addition, logistic regression and discriminant analysis models ignore controls who are lost to follow-up while survival analysis incorporates the information contained in the data for these individuals. Therefore, for studies with data on the time until

fracture, survival analysis models are more efficient than logistic regression models.[234]

Most studies of osteoporosis are either prospective or case control studies. Prospective studies are expensive to conduct especially for rare outcomes. In contrast, case-control studies, which select all the available cases along with appropriate controls, are relatively inexpensive and more manageable to conduct for rare outcomes. All of the statistical methods discussed above can be applied to both the prospective and the case-control study designs. Ideally, a prospective study in which there is a random selection of patients for the covariate of interest is more desirable than a case-control study. More often, prospective cohort studies are conducted, and even though they are not based on a random sample, they are still valid for studying a causal relationship between the covariates and the outcome of interest. By design, these studies incorporate the time effect into the analysis. Case-control studies on the other hand can suffer because of selection bias, which can be caused by the difficulty of obtaining an appropriate control group. In addition, the BMD values obtained for the patient group might have changed as a result of fracture and thus might be inappropriate. These problems are reflected in the meta-analysis conducted by Ross et al.[235] in which they report more homogeneity of results among prospective studies compared with other studies. All of these considerations point toward the need to conduct more prospective studies along with appropriate statistical analysis.

ASSESSING LONGITUDINAL SENSITIVITY IN BONE DENSITOMETRY

A comparison of techniques with respect to their ability to monitor changes in skeletal status (here referred to as longitudinal sensitivity) is typically based on an assessment of their precision, i.e., reproducibility. Thus, as a first step, the precision of a technique has to be calculated in the correct fashion (i.e., as a root mean square average and not as arithmetic mean as is commonly done.[236] However, longitudinal sensitivity does not depend solely on precision but rather on the ratio of precision and responsiveness.[90] A technique that shows poorer precision but demonstrates larger changes over time (e.g., as a result of disease progression or treatment response) may be more sensitive than a competing "high precision" approach.[90,237,238] Responsiveness depends on many factors, including the measurement site (generally lower turnover at peripheral measurement sites), the type of bone assessed (trabecular bone has a higher turnover rate compared with cortical bone), and the skeletal characteristic measured (currently there is still only limited information about the respective responsiveness of e.g., ultrasound versus density parameters).

Another issue complicating the comparison of precision is the difference in the measurement units of skeletal characteristics (e.g., how to compare dB/MHz with g/cm^2). But even if results are expressed in the same units, precision errors still may not be comparable. If two techniques are calibrated differently (i.e., a regression of one versus the other yields a slope different from unity) their measured precision errors are not comparable.

Expressing precision errors on a percentage basis does not generally solve these problems and in some cases makes the comparison even more difficult. First of all, the level of precision depends on the level of the measurement itself. Linear absolute changes over time appear nonlinear. Parfitt has addressed these purely mathematical problems as well as other caveats in greater detail.[239] Second, even absolute precision errors are not constant across subject groups but generally increase in the elderly, osteoporotic population. However, when expressed on a percentage basis this problem is amplified further because the standard deviation is divided by a smaller mean.[240] Specification of the subject group thus is even more important if precision errors are expressed on a percentage basis. Finally, techniques that feature a range of measurement results with a large offset from zero (e.g., SOS) typically will have smaller precision errors if those expressed on a percentage basis.

Recognizing these difficulties, several investigators have expressed the need for standardizing precision measurements in a different way. Standardization could for example be performed by dividing precision errors by one of the following factors: (1) the difference between healthy and osteoporotic individuals, (2) rates of changes due to disease or treatment, (3) the natural variability of healthy individuals, and (4) normal annual rates of skeletal changes. Other more sophisticated approaches for expressing diagnostic sensitivity have been suggested. Miller based his approach to standardized precision errors on the ratio of percent precision and percent range of results (5th to 95th percentile).[161] Davis et al. have proposed the use of the time interval it takes for two-point measurements to determine the rate of change within ±1% accuracy.[241] Glüer proposed the concept of the "Characteristic Follow-up Time." It is based on the normal annual rates of skeletal changes and represents the follow-up time between two exams required to measure bone loss in an individual at statistically reasonable significance levels[242] quantified by the time it takes to observe statistically significant changes in fracture risk.[243] Finally, Blumsoh et al. proposed an "index of individuality" based on the ratio of the intra- versus inter-subject variability of response.[244] Many other researchers have expressed a need to standardize precision, and other concepts may well be found in the literature.

There is a consensus that the methods of assessing longitudinal sensitivity require standardization, but there is disagreement about the preferred approach. However, some general requirements for acceptable concepts can be put forward. The standardization should not substantially depend on the degree of osteoporosis. Otherwise results may be difficult to compare across different studies using different populations and different criteria for osteoporosis, and results obtained at different institutions would hardly be regarded as truly comparable. Also, the new measure should be easily interpretable and have practical clinical relevance. Probably, if amplified within the same subject group, most approaches will in practice yield similar ranking of the longitudinal sensitivity of competing techniques. Comparibility across subject groups is more difficult to

achieve. As long as no consensus on the standard method, employing one of the simpler approaches for standardization may be indicated: dividing the precision error by the age-related change typical for that subject group. If this statistic is not available one could obtain a crude estimate by dividing the precision error by the standard deviation of the subjects of the study. The smaller the resulting ratios the better the longitudinal sensitivity.

PREDICTING FRACTURE RISK WITH BONE DENSITOMETRY

Many cross-sectional and prospective studies have documented that low bone density at different anatomic sites is significantly associated with the risk of osteoporotic fractures, including fractures of hip and spine.[245–250] These studies also suggested that the risk of fracture is not only significantly associated with the bone mass and density at the anatomical site of the fractures but also other remote body sites. For example, the risk of spine or hip fracture increases as bone density decreases at the lumbar spine, hip, forearm, calcaneus, and hand. Since osteoporosis is a generalized, if not homogeneous process, and since BMD shows at least modest correlations across sites, it is understandable that BMD at one site is predictive of fracture at another site in a population but not necessarily in the individual patient. This raises questions about the relationship among bone densities at various sites and the effectiveness of using BMD from one anatomical site or combining the information from several sites to assess the risks of fractures.

Many studies have reported significant correlations between measurements made at one site and those made at another.[251,252] In a study of 7659 postmenopausal women aged 65 years and older, Steiger and colleagues[65] reported correlations ranging from 0.5 to 0.8 for values measured at the spine, femoral neck, Ward's triangle, trochanteric, intertrochanteric region, distal radius, proximal radius, and calcaneus. Because the rates of bone loss differ at different sites as the bone loss progresses, the correlations between bone density decrease with increasing age; for example, the correlation between BMD of the femoral neck and spine was 0.65 for 65 to 69 year olds but only 0.49 for those age 85 or older.[65] Therefore, the correlations, though statistically significant, are not strong enough to permit the prediction of BMD values for one site from measurements of another.[251,252] This is evident by the fact that such predictions always have large root mean squared (RMS) errors despite strong statistical significance of the regression coefficients.

In a recent prospective study, Pouilles and colleagues[253] examined 85 healthy Caucasian women aged 45–60 years and followed them for 6 months to 3 years. BMD of the lumbar spine (L2–L4), right hip (femoral neck, Ward's triangle, and greater trochanter) were measured both at baseline and the follow-up visit. The correlation coefficients between vertebral and hip BMD at baseline ranged from 0.46 to 0.52, and the correlation coefficients among hip measurements ranged from 0.44 to 0.61. Defining a patient at risk if her BMD Z-score was less than −1, Pouilles found that 39–48% of women at risk according to spine BMD were normal according to their hip BMD measurements. However, among 25 women classified as at risk according to femoral neck BMD, 32% were normal by spine BMD. Twenty-six percent of women had a different risk status according to the femoral neck versus spine BMD. The annual percentage of bone loss was also only modestly correlated, ranging from 0.34 to 0.69 between vertebral and hip BMD and from 0.44 to 0.61 among hip measurements. Similarly, discordance was also found in classifying individuals as fast or slow bone losers according to the annual percentage bone loss at the different sites.

In a report of 744 women from the Hawaii Osteoporosis Study, Davis and colleagues[254,255] noticed a similar discordance of bone mass measured at the spine, calcaneus, distal radius, and proximal radius after adjusting for age. Only 13.6% of women were consistently in the lower tertiles of all four sites. The 42.7% of women who had at least one of the bone mass measures in the lower tertile were in the middle or higher tertile groups according to other measured sites. About 15% of women had bone mass in both lower and higher tertile groups. Less than one third (31.3%) of the women were consistently in the same tertile group for all four sites.

If clinical management of osteoporosis were based on bone mass or density from only one site, a substantial number of patients could potentially be misdiagnosed or mistreated. Therefore, both studies support the concept that measurements of bone density at several different sites may be helpful at least for assigning risks related to osteopenia in a clinical setting. Although many studies have measured BMD at multiple anatomic sites and evaluated their individual association with risk of fracture, only a few of them have assessed the independent contributions of these bone mass measurements.

The largest prospective study of osteoporotic fracture is the Study of Osteoporotic Fracture, which has nearly 10,000 non-black women 65 or more years of age from four centers. Cummings and colleagues[256] compared the effectiveness of DXA measured BMD at the proximal femur (including total, neck, intertrochanteric region, trochanteric, Ward's triangle), lumbar spine, distal radius, midradius, and calcaneus in predicting hip fractures in 8314 women with an average follow-up time of 1.8 years. After adjusting for the effect of age, the relative risk of hip fracture with a 1 SD decrease in proximal femur measurements was about 70% greater than the relative risk using BMD of the spine or forearm, while the relative risk related to decreasing calcaneus BMD was between that of the hip and spine. The authors concluded that low hip bone density is a stronger predictor of hip fracture than bone density at other sites, which is consistent with other studies.[257,258] In a more recent analysis of data from the same study, Black and colleagues[259] examined the effectiveness of combining hip and spine BMD to identify a high-risk group for hip fracture. They found that after adjusting for age and femoral neck BMD, the spine BMD was no longer significantly associated with the risk of hip fractures. Individuals with a femoral neck BMD less than a given cutoff value had a higher chance of getting a hip fracture than those individ-

uals with either a femur or spine BMD lower than the same cutoff value. Therefore, they concluded that using a combination of femoral neck and spine BMD to identify elderly women at high risk of hip fracture is no better than using the femoral neck BMD alone, and an additional scan of lumbar spine may not be justified. Nevertheless, other studies suggest that additional measurements may reduce misclassification for individual patients.

In the Hawaii Osteoporosis Study of American women whose average age at entry into the study was 63.3 years, Wasnich, Davis, and colleagues[254,255] compared the association of BMC at the calcaneus, distal radius, proximal radius, and lumbar spine with incident vertebral fractures. The relative risk of incident vertebral fracture associated with a 1 SD decrease in BMC was lowest for the lumbar spine and highest for the calcaneus. Multivariate analysis suggested that BMC values at the calcaneus and distal radius were independently associated with the probability of spine fracture. When −2 SD was used as a cutoff point for the two sites, the probability of vertebral fracture by combining the two tests was 25% compared with 20% using only one test. When these women were classified according to their tertiles of age-adjusted Z-scores of bone mass at the above-mentioned four sites, Davis and colleagues found that the number of low bone mass sites predicted the risk of new spine fractures with an odds ratio of 1.3 per increase in one low bone mass site after adjusting for age and the number of spine and nonspine prevalent fractures. Other reported results from this study[14,102] consistently suggest that measurement of BMD at multiple anatomic sites and a combination of the information might be helpful in predicting the risk of spine fractures for the individual patient.[254,255]

Hip and spine fractures are important clinical outcomes for osteoporosis. However, there are nearly 750,000 nonhip, nonspine fractures each year in the United States alone, suggesting that predicting fractures of all types has clinical importance.[245,260] In a prospective study of 304 Rochester women with 8.3 years of median follow-up time, Melton and colleagues[247] found that after adjusting for age, 1 SD decreases in BMD of the lumbar spine, trochanteric region, and femoral neck were significantly related to the incidence rate of all fractures (relative hazards of 1.4, 1.2, and 1.3, respectively) and that BMD values at the hip and spine were better individual predictors for risk of fractures of all types in comparison to BMD at the forearm. A preliminary observation of data from a large prospective cohort study further suggests that combining BMD at the calcaneus, femoral neck, and spine may improve the prediction of all fractures.[261]

The effectiveness of combining BMD at various sites, however, has still not been conclusively demonstrated. The results in the above-mentioned studies depend on the variables used in the statistical analyses and can change when other risk variables (prevalent fractures, vertebral dimensions, etc.) and measurements using other modalities (ultrasound and QCT, etc.) are included.[14,262] The sample size also affects the conclusion of the study.[263] In addition, different statistical methods such as logistic regression, discriminant analysis, Cox proportional hazard model, and classification and regression tree (CART) analysis[264] may produce different classification algorithms. Furthermore, studies of vertebral fractures frequently use different definitions of fracture, and therefore are not directly comparable. Beside these technical limitations, the clinical benefit of combining multiple site measurements of BMD has not been carefully studied. While clinicians are concerned with the best diagnostic and treatment strategies for an individual, epidemiological studies help to select preventive strategies for the entire population, such as how to do mass screening to determine the prevalence of particular diseases. The additional cost of scanning both the hip and the spine for an individual patient, after scanning one of the sites, may be small compared with the cost of therapeutic decisions derived from these measurements. However, the cost can be substantial in screening large groups of postmenopausal women. More studies, especially cost effectiveness studies to compare diagnostic and treatment strategies based on information of bone denisty from a single or multiple sites should be carried out.

APPROPRIATE APPLICATIONS OF BONE DENSITOMETRY

The greater efficiency provided by the recent innovations in bone densitometry, aside from improving technical performance, has allowed reductions in the cost of examinations. Given the current impetus to disseminate information about osteoporosis, to make new instrumentation more readily available, and to limit its costs, these methods of bone densitometry are becoming widely used in routine medical practice. A consensus is forming about the clinical indications for the appropriate use of densitometry, and four indications have emerged.[235,265]

Evaluation of perimenopausal women for initiation of estrogen therapy

Decisions about the initiation of estrogen therapy may be contingent on a number of factors, including the current level of bone density, the severity of menopausal symptoms, patient or physician preferences, laboratory evidence of rapid bone loss, and the long-term risk of cardiovascular disease.[266] The absolute level of bone density at the menopause and the magnitude of subsequent bone loss are important considerations in assessing the risk for fracture. The decision to begin prophylaxis against osteoporosis, therefore, can be facilitated by knowledge of a woman's bone density. Furthermore, compliance with estrogen therapy may be enhanced by quantitative information concerning fracture risk and efficacy of treatment.

Detection of osteoporosis and assessment of its severity

Quantitative evaluation of the skeleton may be indicated in individuals in whom osteoporosis is suspected or in whom atraumatic fracture is suspected based on radiographic findings. Recent evidence, as reviewed here, supports the concept that the absolute level of bone density is predictive of fracture risk, e.g., most of the variance in bone strength can be attributed to bone density, and a gradient of increasing

fracture risk is associated with declining levels of bone density.[256,267,268] Thus, bone density per se provides the primary standard of osteoporosis risk and provides an important basis for therapeutic decisions.

Evaluation of patients with metabolic diseases that affect the skeleton

Many metabolic disorders, such as hyperparathyroidism, Cushing's syndrome, and chronic corticosteroid therapy have profound influences on calcium metabolism and may adversely affect the skeleton. Additional relatively common disorders known to influence bone include testerone deficiency, amenorrhea, eating disorders, treatment with supressive doses of thyroid hormone, alcoholism, disuse, treatment with multiple anticonvulgants, treatment with heparin, and renal osteodystrophy. In these secondary forms of osteoporosis, bone density measurements may be important because they carry prognostic as well as therapeutic implications.

Monitoring of treatment and evaluation of disease course

The importance of bone density measurements would be diminished were there no clinically useful treatments capable of affecting bone mass and the consequent risk of fracture. There is an extensive literature surrounding the effect of various treatments upon bone mass but a much smaller literature surrounding fracture risk. Prospective, randomized, controlled trials have demonstrated both a beneficial effect upon bone density and a decrease in spinal fracture rate for etidronate,[269,270] alendronate,[271] and transdermal estrogen treatment.[272]

In the past, bone density measurements were associated with large precision errors relative to estimated rates of change and could not reliably monitor changes in bone density in individual patients. Given the recent improvements in measurement precision and speed of performance and the large skeletal effects observed in certain metabolic disorders and with certain medical regimens, monitoring of individual patients may be considered when important therapeutic decisions are to be made. In general, such serial measurements are usually obtained at the spine using DXA or QCT because of their favorable longitudinal sensitivity. However, specific guidelines regarding the appropriate techniques, site, and frequency of measurement are yet to be established.

REFERENCES

1. Morgan DB, Spiers FW, Pulvertaft CN, Fourman P 1967 The amount of bone in the metacarpal and phalanx according to age and sex. Clin Radiol 18:101–108.
2. Matsumoto C, Kushida K, Yamazaki K, Imose K, Inoue T 1994 Metacarpal bone mass in normal and osteoporotic Japanese women using computed x-ray densitometry. Calcif Tissue Int 54:324–329.
3. Trouerbach WT, Birkenhäger JC, Collette BJA, Drogendijk AC, Schmitz PIM, Zwamborn AW 1987 A study on the phalanx bone mineral content in 273 normal pre- and postmenopausal females (transverse study of age-dependent bone loss). Bone Miner 3:53–62.
4. Trouerbach WT, Birkenhäger JC, Schmitz PIM, vanHemert AM, vanSaase JLCM, Collette HJA, Zwamborn AW 1987 A cross-sectional study of age-related loss of mineral content of phalangeal bone in men and women. Skel Radiol 17:338–343.
5. Hayashi Y, Yamamoto K, Fukunaga M, Ishibashi T, Takahashi K, Nishii Y 1990 Assessment of bone mass by image analysis of metacarpal bone roentgenograms: A quantitative digital image processing (DIP) method. Radiation Med 8:173–178.
6. Yang S-O, Hagiwara S, Engelke K, Dhillon MS, Guglielmi G, Bendavid EJ, Socjima O, Nelson D, Genant HK 1994 Radiographic absorptiometry for bone mineral measurement of the phalanges: Precision and accuracy study. Radiology 192:857–859.
7. Cosman F, Herrington B, Himmelstein S, Lindsay R 1991 Radiographic absorptiometry: A simple method for determination of bone mass. Osteoporosis Int 2:34–38.
8. Colbert C, Bachtell RS 1981 Noninvasive measurements of bone mass and their clinical application. In: Cohn SH (ed.) Radiographic absorptiometry. CRC Press, Boca Raton, Florida, U.S.A., pp. 52–84.
9. Kälebo P, Strid KG 1988 Bone Mass Determination from Microradiographs by computer-assisted videodensitrmetry II. Aluminum as a reference substance. Acta Radiologica 29: 611–617.
10. Strid KG, Kälebo P 1988 Bone mass determination from microradiographs by computer-assisted videodensitometry. I. Methodology. Acta Radiologica 29:465–472.
11. Grampp S, Jergas M, Glüer CC, Lang P, Brastow P, Genant HK 1993 Radiological diagnosis of osteoporosis: current methods and perspectives. Radiol Clin N Am 31:1133–1145.
12. Jergas M, Genant HK 1993 Current methods and recent advances in the diagnosis of osteoporosis. Arthritis Rheum 36:1649–1662.
13. Takada M, Engelke K, Hagiwara S, Grampp S, Jergas M, Glüer C, Genant HK 1995 Radiographic absorptiometry of phalanges: In vivo study. J Bone Miner Res 10(Suppl 1)S374.
14. Ross P, Huang C, Davis J, Imose K, Yates J, Vogel J, Wasnich R 1995 Predicting vertebral deformity using bone densitometry at various skeletal sites and calcaneus ultrasound. Bone 16:325–332.
15. Cameron JR, Sorenson JA 1963 Measurement of bone mineral in vivo: An improved method. Science 142:230–232.
16. Kelly TL, Crane G, Baran DT 1994 Single x-ray absorptiometry of the forearm: Precision, correlation, and reference data. Calcif Tissue Int 54:212–218.
17. Bjarnason K, Nilas L, Hassager C, Christiansen C 1995 Dual energy x-ray absorptiometry of the spine—decubitus lateral versus anteroposterior projection in osteoporotic women: Comparison to single energy x-ray absorptiometry of the forearm. Bone 16:255–260.
18. Schlenker RA, Von Seggen WW 1976 The distribution of cortical and trabecular bone mass along the lengths of the radius and ulna and the implications for in vivo bone mass measurements. Calcif Tissue Res 20:41–52.
19. Wahner HW, Eastell R, Riggs BL 1985 Bone mineral density of the radius: Where do we stand? J Nucl Med 26:1339–1341.
20. Vogel JM 1987 Application principles and technical considerations in SPA. In: Genant HK (ed.) Osteoporosis Update 1987. Radiology Research and Education Foundation, San Francisco, California, U.S.A., pp. 219–231.
21. Vogel JM, Anderson JT 1972 Rectilinear transmission scanning of irregular bones for quantification of mineral content. J Nucl Med 13:13–18.

22. Williams JA, Wagner J, Wasnich R, Heilbrun L 1984 The effect of long-distance running upon appendicular bone mineral content. Med Sci Sports Exerc 16:223–227.
23. Suominen H, Heikkinen E, Vaino P, Lahtinen T 1984 Mineral density of calcaneus in men at different ages: A population study with special reference to life-style factors. Age Ageing 13:273–281.
24. Yano K, Wasnich RD, Vogel JM, Heilbrun LK 1984 Bone mineral measurements among middle-aged and elderly Japanese Residents in Hawaii. Am J Epidemiol 119:751–764.
25. Wasnich R 1987 Fracture prediction with bone mass measurements. In: Genant HK (ed.) Osteoporosis Update 1987. Radiology Research and Education Foundation, San Francisco, California, U.S.A., pp. 95–101.
26. Vogel JM, Wasnich RD, Ross PD 1988 The clinical relevance of calcaneus bone mineral measurements: A review. Bone Miner 5:35–58.
27. Black D, Cummings SR, Melton LJ 1992 Appendicular bone mineral and a woman's lifetime risk of hip fracture. J Bone Miner Res 7:639–646.
28. Cheng S, Suominen H, Era P, Heikkinen E 1994 Bone density of the calcaneus and fractures in 75- and 80-year-old men and women. Osteoporosis Int 4:48–54.
29. Mazess RB, Barden HS 1987 Single- and dual photon absorptiometry for bone measurement in osteoporosis. In: Genant HK (ed.) Osteoporosis Update. Radiology Research and Education Foundation, San Francisco, California, U.S.A., pp. 73–80.
30. Jacobson B 1964 X-ray spectrophotometry in vivo. Am J Roentgenol 91:202–210.
31. Gustavson L, Jacobson B, Kusoffsky L 1974 X-ray spectrophotometry for bone mineral determinations. Med Biol Eng Comput 12:113–118.
32. Reiss KH, Killig K, Schuster W 1973 Dual photon x-ray beam applications. In: Mazess RB (ed.) International Conference on Bone Mineral Measurement. US Department of Health, Education, and Welfare, Chicago, Illinois, U.S.A., pp. 80–87.
33. Stein JA, Lazewatsky JL, Hochberg AM 1987 Dual energy x-ray bone densitometer incorporating an internal reference system. Radiology 165(P):313.
34. Kelly T, Slovick D, Schoenfield D, Neer R 1988 Quantitative digital radiography versus dual photon absorptiometry of the lumbar spine. J Clin Endocr Metab 67:839–844.
35. Mazess R, Chesnut III CH, McClung M, Genant HK 1992 Enhanced precision with dual-energy x-ray absorptiometry. Calcif Tissue Int 51:14–17.
36. Wahner HW, Dunn WL, Brown ML, Morin RL, Riggs BL 1988 Comparison of dual-energy x-ray absorptiometry and dual photon absorptiometry for bone mineral measurements of the lumbar spine. Mayo Clin Proc 63:1075–1084.
37. Glüer CC, Steiger P, Selvidge R, Ellicsen-Kliefoth K, Hayashi C, Genant HK 1990 Comparative assessment of dual-photon-absorptiometry and dual-energy-radiography. Radiology 174: 233–228.
38. Cullum ID, Ell PJ, Ryder JP 1989 X-ray dual photon absorptiometry: A new method for the measurement of bone density. Br J Radiol 62:587–592.
39. Lilley J, Walters BG, Heath DA, Drole Z 1991 In vivo and in vitro precision of bone density measured by dual-energy x-ray absorption. Osteoporosis Int 1:141–146.
40. Orwoll ES, Oviatt SK 1991 Longitudinal precision of dual-energy x-ray absorptiometry in a multicenter study. J Bone Miner Res 6:191–197.
41. Ho CP, Kim RW, Schaffler MB, Sartoris DJ 1990 Accuracy of dual-energy radiographic absorptiometry of the lumbar spine: Cadaver study. Radiology 176:171–173.
42. Drinka PJ, DeSmet AA, Bauwens SF, Rogot A 1992 The effect of overlying calcification on lumbar bone densitometry. Calcif Tissue Int 50:507–510.
43. Frye MA, Melton III LJ, Bryant SC, Fitzpatrick LA, Wahner HW, Schwartz RS, Riggs BL 1992 Osteoporosis and calcification of the aorta. Bone Miner 19:185–194.
44. Whitehouse RW, Karantanas A, Adams JE 1992 Discrepancies in spinal bone mass measured by QCT and DXA. In: Ring EFG (ed.) Current research in osteoporosis and bone mineral measurement II: 1992. British Institute of Radiology, London, U.K. pp. 26.
45. Ryan PJ, Evans P, Blake GM, Fogelman I 1992 The effect of vertebral collapse on spinal bone mineral density measurements in osteoporosis. Bone Miner 18:267–272.
46. Finkelstein J, Cleary RL, Butler J, Antonelli R, Mitlak B, Debraska D, Zamora-Quezada JC, Neer R 1994 A comparison of lateral versus anterior-posterior spine dual x-ray absorptiometry for the diagnosis of osteopenia. J Clin Endocrinol Metab 78:724–730.
47. Yu W, Glüer C-C, Grampp S, Jergas M, Fuerst T, Wu CY, Lu Y, Fan B, Genant HK i1995 Spinal bone mineral assessment in postmenopausal women: A comparison between dual x-ray absorptiometry and quantitative computed tomography. Osteoporosis Int 5:433–439.
48. Rupich RC, Griffin MG, Pacifici R, Avioli LV, Susman N 1992 Lateral dual-energy radiography: Artifact error from rib and pelvic bone. J Bone Miner Res 7:97–101.
49. Jergas M, Breitenseher M, Glüer CC, Black D, Lang P, Grampp S, Engelke K, Genant HK 1995 Which vertebrae should be assessed using lateral dual-energy x-ray absorptiometry of the lumbar spine? Osteoporosis Int 5:196–204.
50. Hangartner TN, Johnston CC 1990 Influence of fat on bone measurements with dual-energy absorptiometry. Bone Miner 9:71–81.
51. Tothill P, Pye DW 1992 Errors due to non-uniform distribution of fat in dual x-ray absorptiometry of the lumbar spine. Br J Radiol 65:807–813.
52. Larnach TA, Boyd SJ, Smart RC, Butler SP, Rohl PG, Diamond TH 1992 Reproducibility of lateral spine scans using dual energy x-ray absorptiometry. Calcif Tissue Int 51:255–258.
53. Reid IR, Evans MC, Stapleton J 1992 Lateral spine densitometry is a more sensitive indicator of glucocorticoid-induced bone loss. J Bone Miner Res 7:1221–1225.
54. Engelke K, Glüer CC, Genant HK 1995 Factors influencing short-term precision of dual x-ray bone absorptiometry (DXA) of spine and femur. Calcif Tissue Int 56:19–25.
55. Blake GM, Jagathesan T, Herd RJM, Fogelman I 1994 Dual x-ray absorptiometry of the lumbar spine: The precision of paired anteroposterior/lateral studies. Br J Radiol 67:624–630.
56. Duboeuf F, Pommet R, Meunier PJ, Delmas PD 1994 Dual-energy x-ray absorptiometry of the spine in anteroposterior and lateral projections. Osteoporosis International 4:110–116.
57. Guglielmi G, Grimston SK, Fischer KC, Pacifici R 1994 Osteoporosis: Diagnosis with lateral and posteroanterior dual X-ray absorptiometry compared with quantitative CT. Radiology 192:845–850.
58. Mazess RB, Barden HS, Eberle RW, Drue Denton M 1995 Age changes of spine density in posterior-anterior and lateral projections in normal women. Calcif Tissue Int 56:201–205.
59. Hagiwara S, Engelke K, Yang S-O, Dhillon MS, Guglielmi G, Nelson DS, Genant HK 1994 Dual x-ray absorptiometry forearm software: Accuracy and intermachine relationship. J Bone Miner Res 9:1425–1427.

60. Faulkner KG, McClung MR, Schmeer MS, Roberts LA, Gaither KW 1994 Densitometry of the radius using single and dual energy absorptiometry. Calcif Tissue Int 54:208–211.
61. Yamada M, Ito M, Hayashi K, Nakamura T 1993 Calcaneus as a site for assessment of bone mineral density: Evaluation in cadavers and healthy volunteers. Am J Roentgenol 161:621–627.
62. Yamada M, Ito M, Hayashi K, Ohki M, Nakamura T 1994 Dual energy x-ray absorptiometry of the calcaneus: Comparison with other techniques to assess bone density and value in predicting risk of spine fracture. Am J Roentgenol 163:1435–1440.
63. Laval-Jeantet A-M, Bergot C, Williams M, Davidson K, Laval-Jeantet M 1995 Dual-energy x-ray absorptiometry of the calcaneus: Comparison with vertebral dual-energy x-ray absorptiometry and quantitative computed tomography. Calcif Tissue Int 56:14–18.
64. Black DM, Reiss TF, Nevitt MC, Cauley J, Karpf D, Cummings SR 1993 Design of the Fracture Intervention Trial. Osteoporosis Int 3(Suppl 3):S29–S39.
65. Steiger P, Cummings SR, Black DM, Spencer NE, Genant HK 1992 Age-related decrements in bone mineral density in women over 65. J Bone Miner Res 7:625–632.
66. Blake GM, Parker JC, Buxton FMA, Fogelman I 1993 Dual x-ray absorptiometry: A comparison between fan beam and pencil beam scans. Br J Radiol 66:902–906.
67. Faulkner K, Glüer C, Estilo M, Genant H 1993 Cross-Calibration of DXA Equipment: Upgrading from a Hologic QDR 1000/W to a QDR 2000. Calcif Tissue Int 52:79–84.
68. Eiken P, Bärenholdt O, Jensen BL, Gram J, Nielsen SP 1994 Switching from DXA pencil-beam to fan-beam. I: Studies in vitro at four centers. Bone 15:667–670.
69. Eiken P, Kolthoff N, Bärenholdt O, Hermansen F, Nielsen SP 1994 Switching from DXA pencil-beam to fan-beam. II: Studies in vivo. Bone 15:671–676.
70. Abrahamsen B, Gram J, Hansen TB, Beck-Nielsen H 1995 Cross calibration of QDR-2000 and QDR-1000 dual-energy x-ray densitometers for bone mineral and soft-tissue measurements. Bone 16:385–390.
71. Genant HK, Grampp S, Glüer CC, Faulkner KG, Jergas M, Engelke K, Hagiwara S, van Kuijk C 1994 Universal standardization for dual x-ray absorptiometry: Patient and phantom cross-calibration results. J Bone Miner Res 9:1503–1514.
72. Carter DR, Bouxsein ML, Marcus R 1992 New approaches for interpreting projected bone densitometry data. J Bone Miner Res 7:137–145.
73. Peel NFA, Eastell R 1994 Diagnostic value of estimated volumetric bone mineral density of the lumbar spine in osteoporosis. J Bone Miner Res 9:317–320.
74. Matkovic V, Jelic T, Wardlaw G, Ilich JZ, Goel PK, Wright JK, Andon MB, Smith KT, Heaney RP 1994 Timing of peak bonemass in Caucasian females and its implications for the prevention of osteoporosis. J Clin Invest 93:799–808.
75. Jergas M, Breitenseher M, Glüer CC, Yu W, Genant HK 1995 Estimates of volumetric bone density from projectional measurements improve the discriminatory capability of dual x-ray absorptiometry. J Bone Miner Res 10:1101–1110.
76. Cummings SR, Marcus R, Palermo L, Ensrud KE, Genant HK 1994 Does estimating volumetric bone density of the femoral neck improve the prediction of hip fracture? A prospective study. J Bone Miner Res 9:1429–1432.
77. Steiger P, Cummings SR, Genant HK, Weiss H 1994 Morphometric x-ray absorptiometry of the spine: Correlation in vivo with morphometric radiography. Osteoporosis Int 4:238–244.
78. Glüer CC, Cummings SR, Pressman A, Li J, Glüer K, Faulkner KG, Grampp S, Genant HK 1994 Prediction of hip fractures from pelvic radiographs: The study of osteoporotic fractures. J Bone Miner Res 9:671–677.
79. Faulkner KG, Cummings SR, Glüer CC, Palermo L, Black D, Genant HK 1993 Simple measurement of femoral geometry predicts hip fracture: The study of osteopotic fractures. J Bone Miner Res 8:1211–1217.
80. Faulkner KG, McClung M, Cummings SR 1994 Automated evaluation of hip axis length for predicting hip fracture. J Bone Miner Res 9:1065–1070.
81. Myers ER, Hecker AT, Rooks DS, Hipp JA, Hayes WC 1993 Geometric variables from DXA of the radius predict forearm fracture load. Calcif Tissue Int 52:199–204.
82. Nakamura T, Turner CH, Yoshikawa T, Slemenda CW, Peacock M, Burr DB, Mizuno Y, Orimo H, Ouchi Y, Johnston CC 1994 Do variations of hip geometry explain differences in hip fracture risk between Japanese and white Americans. J Bone Miner Res 9:1071–1076.
83. Cummings SR, Cauley JA, Palermo L, Ross PD, Wasnich RD, Black D, Faulkner KG 1994 Racial differences in hip axis lengths might explain racial differences in rates of hip fractures. Osteoporosis Int 4:226–229.
84. Genant HK, Cann CE, Ettinger B, Gordan GS 1982 Quantitative computed tomography of vertebral spongiosa: A sensitive method for detecting early bone loss after oophorectomy. Ann Intern Med 97:699–705.
85. Cann CE, Genant HK 1980 Precise measurement of vertebral mineral content using computed tomography. J Comput Assist Tomogr 4:493–500.
86. Pacifici R, Rupich R, Griffin M, Chines A, Susman N, Avioli LV 1990 Dual energy radiography versus quantitative computer tomography for the diagnosis of osteoporosis. J Clin Endocrinol Metab 70:705–710.
87. Yu W, Glüer CC, Grampp S, Jergas M, Wu CY, Genant HK 1994 Spinal bone mineral assessment in postmenopausal women: A comparison between dual x-ray absorptiometry and quantitative computed tomography. J Bone Miner Res 9 (Suppl):S406.
88. Block J, Smith R, Glüer CC, Steiger P, Ettinger B, Genant HK 1989 Models of spinal trabecular bone loss as determined by quantitative computed tomography. J Bone Miner Res 4:249–257.
89. Kalender WA, Klotz E, Süss C 1987 Vertebral bone mineral analysis: an integrated approach. Radiology 164:419–423.
90. Genant HK, Steiger P, Block JE, Glüer CC, et al., 1987 Quantitative computed tomography: Update 1987. Calcif Tiss Int 41:179–186.
91. Kalender WA, Brestowsky H, Felsenberg D 1988 Bone mineral measurements: Automated determination of the midvertebral CT section. Radiology 168:219–221.
92. Steiger P, Steiger S, Ruegsegger P, Genant HK 1987 Two- and three-dimensional quantitative image evaluation techniques for densitometry and volumetrics in longitudinal studies. In: Genant HK (ed.) Osteoporosis Update 1987. University of California Printing Services, San Francisco, California, U.S.A., pp. 171–180.
93. Genant HK, Boyd DP 1977 Quantitative bone mineral analysis using dual energy computed tomography. Invest Radiology 12(6):545–551.
94. Glüer CC, Reiser UJ, Davis CA, Rutt BK, Genant HK 1988 Vertebral mineral determination by quantitative computed tomography (QCT): Accuracy of single and dual energy measurements. J Comput Assist Tomogr 12:242–258.
95. Cann CE 1987 Quantitative computed tomography for bone mineral analysis: Technical considerations. In: Genant HK (ed.) Osteoporosis Update 1987. University of California

Printing Services, San Francisco, California, U.S.A., pp. 131–145.
96. Glüer CC, Genant HK 1989 Impact of marrow fat on accuracy of quantitative CT. J Comput Assist Tomogr 13:1023–1035.
97. Goodsitt MM, Rosenthal DI, Reinus WR, Coumas J 1987 Two postprocessing CT techniques for determining the composition of trabecular bone. Invest Radiol 22:209–215.
98. van Kuijk C, Grashuis JL, Steenbeek JCM, Schütte HE, Trouerbach WT 1990 Evaluation of postprocessing dual-energy methods in quantitative computed tomography. Part 2. Practical Aspects. Invest Radiol 25:882–889.
99. Cann CE, Genant HK, Kolb FO, Ettinger B 1985 Quantitative computed tomography for prediction of vertebral fracture risk. Bone 6:1–7.
100. Heuck A, Block J, Glüer CC, Steiger P, Genant HK 1989 Mild versus definite osteoporosis: Comparison of bone densitometry techniques using different statistical models. J Bone Miner Res 4:891–899.
101. Sambrook P, Barlett C, Evans R, Hesp R, Katz D, Reeve J 1985 Measurements of lumbar spine bone mineral: A comparison of dual photon absortiometry and computed tomography. Br J Radiol 58:621–624.
102. Ross PD, Genant HK, Davis JW, Wasnich RD 1993 Predicting vertebral fracture incidence from prevalent fractures and bone density among non-black, osteoporotic women. Osteoporosis Int 3:120–126.
103. Steiger P, Glüer CC, Steiger S, Genant HK 1988 Determination of an object coordinate system for the longitudinal three-dimensional assessment of vertebral bone mineral content. Presented at the 74th RSNA Scientific Assembly and Annual Meeting, Chicago, Illinois, U.S.A.
104. Lang T, Song S, Genant HK 1995 Performance of a Surface-Matching Algorithm for 3-D Alignment of Volumetric QCT Studies Perth International Bone Meeting, Fremantle, Australia, pp. 41.
105. Cody DD 1991 Correlations between vertebral regional bone mineral density (rBMD) and Whole Bone Fracture Load. Spine 16:146–154.
106. Flynn MJ, Cody DD 1993 The assessment of vertebral bone macroarchitecture with X-ray computed tomography. Calcif Tissue Int 53:S170–S175.
107. Sandor T, Felsenberg D, Kalender WA, Clain A, Broen E 1992 Compact and trabecular components of the spine using quantitative computed tomography. Calcif Tissue Int 50:502–506.
108. Sandor T, Felsenberg D, Kalender W, Brown E 1992 Heterogeneity of the loss of BMD from spinal cortical bone. 9th Int Workshop on Bone Densitometry, Traverse City, Michigan, U.S.A.
109. Rockoff SD, Sweet E, Bluestein J 1969 The relative contribution of trabecular and cortical bone to the strength of human lumbar vertebrae. Calcif Tissue Res 3:163–175.
110. McBroom RJ, Hayes WC, Edwards WT, Goldberg RP, White AA 1985 Prediction of vertebral body compressive fracture using quantitative computed tomography. J Bone Joint Surg (Am) 67:1206–1214.
111. Faulkner KG, Cann CE, Hasegawa BH 1990 CT-derived finite element models to determine vertebral cortex strength. In: Loew MH (ed.) Medical Imaging IV: Image Processing, Vol 1233. SPIE, Newport Beach, California, U.S.A., pp. 194–202.
112. Reiser U, Genant HK 1984 Determination of bone mineral content in the femoral neck by quantitative computed tomography. Radiological Society of North America, Washington, D.C., U.S.A.
113. Sartoris DJ, Andre M, Resnick C, Resnick D 1986 Trabecular bone density in the proximal femur: Quantitative CT assessment. Radiology 160:707–712.
114. Esses SI, Lotz JC, Hayes WC 1989 Biomechanical properties of the proximal femur determined in vitro by single-energy quantitative computed tomography. J Bone Miner Res 4:715–722.
115. Beck TJ, Christopher BR, Warden KE, Scott WW, Rao GU 1990 Predicting femoral neck strength from bone mineral data: A structural approach. Invest Radiol 25:6–18.
116. Yoshikawa T, Turner CH, Peacock M, Slemenda CW, Weaver CM, Teegarden D, Markwardt B, Burr DB 1994 Geometric structure of the femoral neck measured using dual-energy x-ray absorptiometry. J Bone Miner Res 9:1053–1064.
117. Phillips JR, Williams JF, Melick RA 1975 Prediction of the strength of the neck of femur from its radiological appearance. Biomed Eng 10:367–372.
118. Lotz JC, Hayes WC 1990 Estimates of hip fracture risk from falls using quantitative computed tomography. J Bone Joint Surg (Am) 72:689–700.
119. Sandor T, Felsenberg D, Kalender W, Brown E 1991 Global and regional variations in the spinal trabecular bone: Single and dual energy examinations. J Clin Endocrinol Metab 72: 1157–1168.
120. Hangartner TN, Gilsanz V 1993 Measurement of cortical bone by computed tomography. Calcif Tissue Int 52:160.
121. Sumner DR, Olson CL, Freeman PM, Lobick JJ, Andriacchi TP 1989 Computed tomography assessment of cortical bone geometry. J Biomech 22:649–653.
122. Flynn MJ, Cody DD, Peterson E, Wang DC, Kleerekoper M 1992 Recognition of lower lumbar vertebral architecture patterns in osteoporosis. Radiology 185(P):126.
123. Braillon PM, Bochu M, Meunier PJ 1993 Quantitative computed tomography (QCT): A new analysis of bone quality in osteoporosis and osteomalacia. 9th International Workshop on Bone Densitometry, Vol 52. Calcif Tissue Int, Traverse City, Michigan, U.S.A., pp. 166.
124. Engelke K, Grampp S, Glüer C-C, Jergas M, Yang S-O, Genant HK 1995 Significance of QCT Bone Mineral Density and its Standard Deviation as Parameters to Evaluate Osteoporosis. J Comp Assist Tomogr 19:111–116.
125. Chevalier F, Laval-Jeantet AM, Laval-Jeantet M, Bergot C 1992 CT image analysis of the vertebral trabecular network in vivo. Calcif Tissue Int 51:8–13.
126. Ito M, Ohki M, Hayashi K, Yamada M, Uetani M, Nakamura T 1995 Trabecular texture analysis of CT images in the relationship with spinal fracture. Radiology 194:55–59.
127. Durand EP, Rüegsegger P 1991 Cancellous bone structure: Analysis of high-resolution CT images with the run-length method. J Comp Assist Tomogr 15:133–139.
128. Durand EP, Rüegsegger P 1992 High-contrast resolution of CT images for bone structure analysis. Med Phys 19:569–573.
129. Rüegsegger P, Elsasser U, Anliker M, Gnehm H, Kind H, Prader A 1976 Quantification of bone mineralization using computed tomography. Radiology 121:93–97.
130. Rüegsegger P, Durand E, Dambacher MA 1991 Localization of regional forearm bone loss from high resolution computed tomographic images. Osteoporosis Int 1:76–80.
131. Feldkamp LA, Goldstein SA, Parfitt AM, Jesion G, Kleerekoper M 1989 The direct examination of three-dimensional bone architecture in vitro by computed tomography. J. Bone Miner Res 4:3–11.
132. Kuhn JL, Goldstein SA, Feldkamp LA, Jesion G 1990 Evaluation of a microcomputed tomography system to study trabecular bone structure. J Orthop Res 8:833–842.
133. Engelke K, Klifa C, Munch B, Glüer C, Genant H 1994

Morphological analysis of the trabecular network: The influence of image processing technique on structural parameters. 10th International Bone Densitometry Workshop, Vol 25, Suppl 2. Bone and Mineral, Venice, Italy, pp. S8.
134. Engelke K, Klifa C, Song S, Glüer CC, Genant HK 1994 A digital model of trabecular bone. In: Research ASfBaM (ed.) 16th Annual Meeting of the American Society for Bone and Mineral Research, Vol 9, Suppl. 1. J Bone Miner Res, Kansas City, U.S.A., pp. S275.
135. Parfitt AM 1983 The stereologic basis of bone histomorphometry: Theory of quantitative microscopy and reconstruction of the third dimension. In: Recker R (ed.) Bone Histomorphometry: Techniques and Interpretations. CRC Press, Boca Raton, Florida, U.S.A., pp. 53–87.
136. Parfitt AM, Matthews C, Villanueva A 1983 Relationships between surface, volume, and thickness of iliac trabecular bone in aging and in osteoporosis. J Clin Invest 72:1396–1409.
137. Odgaard A, Gundersen HJG 1993 Quantification of connectivity in cancellous bone, with special emphasis on 3-D reconstructions. Bone 14:173–182.
138. Rüeggsegger P, Koller B 1994 A micro-ct system for the non-destructive analysis of bone samples. 10th. International Bone Densitometry Workshop, Vol 25 (Suppl 2). Bomiet, Venice, Italy, pp. S4.
139. Rüeggsegger P, Müller R 1995 3D-Microtomography of Human Bones Perth Int. Bone Meeting, Reth, Australia, pp. 42.
140. Engelke K, Dix W, Graeff W, Lohmann M, Meiss L, Reumann R, Glüer C-C, Faulkner K, Genant H 1991 Quantitative Microtomography and Microradiography of Bones Using Synchrotron Radiation 8th Int Workshop on Bone Densitometry, Vol 1. Osteoporosis International Bad Reichenhall, Germany, pp. 193.
141. Graeff W, Engelke K 1991 Microradiography and Microtomography. In: Ebashi S, Koch M, Rubenstein E (eds.) Handbook on Synchrotron Radiation, Vol 4. North-Holland, Amsterdam, The Netherlands, pp. 361–405.
142. Bonse U, Busch F, Günnewig O, Beckman F, Delling G, Hahn M, Graeff W 1994 3D computed x-ray tomography of human cancellous bone at 8 μm spatial and 10^{-4} energy resolution. Bone Miner 25:25–38.
143. Schneider P, Börner W 1991 Periphere quantitative Computertomographie zur Knochenmineralmessung mit einem neuen speziellen QCT-Scanner. Fortschr Röntgenstr 154:292–299.
144. Rüegsegger P, Dambacher MA, Rüegsegger MS, Fischer JA 1984 Bone loss in perimenopausal and postmenopausal women. J Bone Joint Surg 66A:1015–1023.
145. Rüegsegger P, Durand EP, Dambacher MA 1991 Differential effects of aging and disease on trabecular and compact bone density of the radius. Bone 12:99–105.
146. Hangartner TN, Overton TR 1982 Quantitative assessment of bone denisty with a special purpose computed tomography scanner. J Comp Assist Tomogr 6:1156–1162.
147. Hosie CJ, Smith DA 1986 Precision of measurement of bone density with a special purpose computed tomography scanner. Br J Radiol 59:345–350.
148. Butz S, Wüster C, Scheidt-Nave C, Götz M, Ziegler R 1994 Forearm BMD as measured by peripheral quantitative computed tomography (pQCT) in a German reference population. Osteoporosis Int 4:179–184.
149. Lehmann R, Wapniarz M, Kvasnicka HM, Baedeker S, Klein K, Allolio B 1992 Reproduzierbarkeit von Knochendichtemessungen am distalen Radius mit einem hochauflösenden Spezialscanner für periphere quantitative Computertomographie (Singel Energy PQCT). Radiologe 32:177–181.
150. Grampp S, Lang P, Jergas M, Glüer CC, Takada M, Engelke K, Genant HK 1994 Peripheral quantitative computed tomography: Short-term in-vivo precision and comparison to forearm DXA. J Bone Miner Res 9:A368.
151. Wapniarz M, Lehmann R, Randerath O, Baedeker S, John W, Klein K, Allolio B 1994 Precision of dual x-ray absorptiometry and peripheral computed tomography using mobile densitometry units. Calcif Tissue Int 54:219–223.
152. Takada M, Engelke K, Hagiwara S, Genant HK 1994 Precision and accuracy of peripheral quantitative computed tomography in vitro. J Bone Miner Res 9:279.
153. Grampp S, Lang P, Jergas M, Glüer CC, Engelke K, Genant HK 1995 Comparison of total and trabecular bone density measurements at peripheral and axial sites. Eur Radiol 5:169.
154. Rico H, Ganzalez-Riola J, Revilla M, Villa LF, Gomez-Castresana F, Escribano J 1994 Cortical versus trabecular bone mass: Influence of activity on both bone components. Calcif: Tissue Int 54:470–472.
155. Schneider P, Börner W, Mazess RB, Barden H 1988 The relationship of peripheral to axial bone density. Bone Miner 4:279–287.
156. Smith DAS, Hosie CJ, Deacon AD, Hamblen DL 1990 Quantitative g-ray computed tomography of the radius in normal subjects and osteoporotic patients. Br J Radiol 63:776–782.
157. Spadaro JA, Werner FW, Brenner RA, Fortino MD, Fay LA, Edwards WT 1994 Cortical and trabecular bone contribute strength to the osteopenic distal radius. J Orthop Res 12:211–218.
158. Kaisel W, Rüegsegger P 1991 3D-QCT at peripheral measuring sites. Osteoporosis Int 1:193.
159. McClean BA, Overton TR, Hangartner TN, Rathee S 1990 A special purpose x-ray fan beam CT scanner for trabecular bone density measurement in the appendicular skeleton. Phys Med Biol 35:11–19.
160. Antich PP, Anderson JA, Ashman RB, Dowdey JE, Gonzales J, Murry RC, Zerwekh JE, Pak CY 1991 Measurement of mechanical properties of bone material in vitro by ultrasound reflection: Methodology and comparison with ultrasound transmission. J Bone Miner Res 6:417–426.
161. Miller CG, Herd RJM, Ramalingam T, Fogelman I, Blake GM 1993 Ultrasonic velocity measurements through the calcaneus: Which velocity should be measured? Osteoporosis Int 3:31–35.
162. Schott AM, Hans D, Sornay-Rendu E, Delmas PD, Meunier PJ 1993 Ultrasound measurements on os calcis: Precision and age-related changes in a normal female population. Osteoporosis Int 3:249–254.
163. Waud C, Lew R, DT. B 1992 The relationship between ultrasound and densitometric measurements of bone mass at the calcaneus in women. Calcif Tissue Int 51:415–418.
164. Jergas M, Uffmann M, Wittenberg R, Müller P, Köster O 1992 Ultraschallgeschwindigkeitsmessungen an belastungstragenden und nicht- belastungstragenden Stellen des peripheren Skeletts. Der Einfluß körperlicher Aktivität bei Fußballspielern. Fortschr Röntgenstr 157:420–424.
165. Jergas M, Uffmann M, Müller P, Köster O 1993 Ultraschallgeschwindig-keitsmessungen zur Diagnose der postmenopausalen Osteoporose. Fortschr Röntgenstr 158:207–213.
166. Stegman MR, Heaney RP, Recker RR, Travers-Gustafson D, Leist J 1994 Velocity of ultrasound and its association with fracture history in a rural population. Am J Epidemiol 139: 1027–1034.
167. Heaney RP, Avioli LV, Chestnut CH, Lappe J, Recker RR, Brandburger GH 1989 Osteoporotic bone fragility: Detection by ultrasound transmission velocity. JAMA 261:2986–2990.
168. Orgee J, McCloskey EV, Foster H, Coombes G, Khan S, Kanis JA 1994 Tibial ultrasound velocity—a useful clinical measure of skeletal status. J Bone Min Res 9:S156.

169. Foldes J, Rimon A, Popovitzer M 1994 Ultrasonic measurement of the tibia: Initial evaluation of a novel approach. In: Ring E, Elvins D, Bhalla A (eds.) Bath Conference on Osteoporosis and Bone Mineral Measurement. The British Institute of Radiology, Bath, U.K., pp. 58.
170. Faulkner KG, McClung MR, Coleman LJ, Kingston-Sandahl E 1994 Quantitative ultrasound of the heel: Correlation with densitometric measurements at different skeletal sites. Osteoporosis Int 4:42–47.
171. Langton CM, Palmer SB, Porter RW 1984 The measurement of broadband ultrasound attenuation in cancellous bone. Eng Med 13:89–91.
172. Evans JA, Tavakoli MB 1990 Ultrasonic attenuation and velocity in bone. Phys Med Biol 35:1387–1396.
173. Glüer CC, Wu CY, Jergas M, Goldstein SA, Genant HK 1994 Three quantitative ultrasound parameters reflect bone structure. Calcif Tissue Int 55:46–52.
174. Glüer CC, Vahlensieck M, Faulkner KG, Engelke K, Black D, Genant HK 1992 Site-matched calcaneal measurements of broadband ultrasound attenuation and single x-ray absorptiometry: Do they measure different skeletal properties? J Bone Miner Res 7:1071–1079.
175. Herd RJM, Ramalingham T, Ryan PJ, Fogelman I, Blake GM 1992 Measurements of Broadband Ultrasound Attenuation in the calcaneus in premenopausal and postmenopausal women. Osteoporosis Int 2:247–251.
176. Agren M, Karellas A, Leahey D, Marks S, Baran D 1991 Ultrasound attenuation of the calcaneus: A sensitive and specific discriminator of osteopenia in postmenopausal women. Calcif Tissue Int 48:240–244.
177. Baran DT, McCarthy CK, Leahey D, Lew R 1991 Broadband ultrasound attenuation of the calcaneus predicts lumbar and femoral neck density in caucasian women: A preliminary study. Osteoporosis Int 1:110–113.
178. Salamone LM, Krall EA, Harris S, Dawson-Hughes B 1994 Comparison of broadband ultrasound attenuation to single x-ray absorptiometry measurements at the calcaneus in postmenopausal women. Calcif Tissue Int 54:87–90.
179. Herd RJ, Blake GM, Ramalinham T, Miller CG, Ryan PJ, Fogelman I 1993 Measurements of postmenopausal bone loss with a new contact ultrasound system. Calcif Tiss Int 53:153–157.
180. McCarthy RN, JeffCott LB, McCartney RN 1990 Ultrasound speed in equine cortical bone: Effects of orientation, density, porosity, and temperature. J Biomech 23:1139–1143.
181. Glüer CC, Wu CY, Genant HK 1992 Broadband Ultrasound Attenuation signals depend on trabecular orientation: An in-vitro study. 9th International Workshop on Bone Densitometry, abstract to be published in Calcif Tissue Int, Traverse City, Michigan, U.S.A.
182. Grimm MJ, Chung H-W, Wehrli FW, Williams JL 1994 Assessment of mechanical and structural properties on trabecular bone using ultrasound velocity and attenuation. Univ Penn Orthopaedic J (in press).
183. Grimm MJ, Williams JL 1993 Use of ultrasound attenuation and velocity to estimate Young's modulus in trabecular bone. In: Li JKL, Reisman SS (eds.) Nineteeth IEEE Annula Northeast Bioengineering Conference. IEEE, Newark, New Jersey, U.S.A., pp. 62–63.
184. Abendschein W, Hyatt GW 1970 Ultrasonics and selected physical properties of bone. Clin Orthop Rel Res 69:294–301.
185. Ashman RB, Cowin SC, van Buskirk WC, Rice JC 1984 A continuous wave technique for the measurement of the elastic properties of cortical bone. J Biomech 17:349–361.
186. Ashman RB, Rho JY 1988 Elastic modulus of trabecular bone material. J Biomech 21:177–181.
187. Turner CH, Eich M 1991 Ultrasonic velocity as a predictor of strength in bovine cancellous bone. Calcif Tissue Int 49:116–119.
188. Zagzebski JA, Rossmann PJ, Mesina C, Mazess RB, Madsen EL 1991 Ultrasound transmission measurements through the os calcis. Calcif Tissue Int 49:107–111.
189. Massie A, Reid DM, Porter RW 1993 Screening for osteoporosis: Comparison between dual energy x-ray absorptiometry and broadband ultrasound attenuation in 1000 perimenopausal women. Osteoporosis Int 3:107–110.
190. Herd RJ, Blake GM, Miller CG, Parker JC, Fogelman I 1994 The ultrasonic assessment of osteopenia as defined by dual x-ray absorptiometry. Br J Radiol 67:631–635.
191. Young H, Howey S, Purdie DW 1993 Broadband ultrasound attenuation compared with dual-energy x-ray absorptiometry in screening for postmenopausal low bone density. Osteoporosis Int 3:160–164.
192. Stegman MR, Heaney RP, Recker RR 1995 Comparison of speed of sound ultrasound with single photon absorptiometry for determining fracture odds ratios. J Bone Miner Res 10: 346–352.
193. Foldes AJ, Popovtzer MM 1995 Ultrasonic measurement of the tibia: Clinical evaluation. Perth International Bone Meeting, Fremantle, Australia, pp. 52.
194. Alenfeld F, Wüster C, Beck C, Ziegler R 1995 Validity of ultrasound measurements of bone mineral density on the phalanges of the hand. Perth International Bone Meeting, Fremantle, Australia, pp. 54.
195. Heaney RP, Avioli LV, Chesnut III CH, Lappe J, Recker RR, Brandenburger GH 1995 Ultrasound velocity through bone predicts incident vertebral deformity. J Bone Miner Res 10: 341–345.
196. Baran DT, Kelly AM, Karellas A, Gionet M, Price M, Leahy D, Steuterman S, McSherry B, Roche J 1988 Ultrasound attenuation of the os calcis in women with osteoporosis and hip fractures. Calcif Tissue Int 43:138–142.
197. Stewart A, Reid DM, Porter RW 1994 Broadband ultrasound attenuation and dual energy x-ray absorptiometry in patients with hip fractures: which technique discriminates fracture risk. Calcif Tissue Int 54:466–469.
198. Porter R, Miller C, Grainger D, Palmer S 1990 Prediction of hip fracture in elderly women: A prospective study. Br Med J 301:638–641.
199. Glüer CC, Cummings SR, Bauer DC, Stone K, Pressman A, Genant HK 1994 Associations between quantitative ultrasound and recent fractures. J Bone Miner Res 9:S153.
200. Turner CH, Peacock M, Schaefer CA, Timmerman L, Johnston CC 1994 Ultrasonic measurements discriminate hip fractures independently of bone mass. J Bone Miner Res 9:S157.
201. Davis CA, Genant HK, Dunham JS 1986 The effects of bone on proton NMR relaxation times of surrounding liquids. Invest Radiol 21:472–477.
202. Rosenthal H, Thulborn KR, Rosenthal DI, Rosen BR 1990 Magnetic susceptibility effects of trabecular bone on magnetic resonance bone marrow imaging. Invest Radiol 25:173–178.
203. Majumdar S 1991 Magnetic field inhomogeneity effects induced by inherent tissue susceptibility differences in gradient echo magnetic resonance imaging: Computer simulations. Mag Res Med 22:101–110.
204. Majumdar S, Genant HK 1992 In vivo relationship between marrow relaxation time T_2^* and trabecular bone density using a chemical shift selective asymmetric spin-echo sequence. J Mag Res Imaging 2:209–219.
205. Grampp S, Majumdar S, Jergas M, Lang P, Gies A, Genant HK 1995 MRI of bone marrow in the distal radius: In vivo

precision of effective transverse relaxation times. Eur Radiol 5:43–48.
206. Ford JC, Wehrli FW 1991 In vivo quantitative characterization of trabecular bone by NMR interferometry and localized proton spectroscopy. Mag Res Med 17:543–551.
207. Ford JC, Wehrli FW, Chung H 1993 Magnetic field distribution in models of trabecular bone. Mag Res Med 30:373–379.
208. Engelke K, Majumdar S, Genant HK 1994 Impact of trabecular structure on marrow relaxation time, T2*: Phantom studies. Mag Res Med 31:380–387.
209. Majumdar S, Keyak J, Lee I, Genant H, Skinner H 1992 Relationship between marrow relaxation time T2* and elastic modulus. Society of Magnetic Resonance in Medicine, Berlin, Germany.
210. Chung H, Wehrli FW, Williams JL, Kugelmass SD 1993 Relationship between NMR transverse relaxation, trabecular bone architecture, and strength. Proc Natl Acad Sci USA 90:10250–10254.
211. Jergas M, Majumdar S, Keyak JH, Lee IY, Newitt DC, Grampp S, Skinner HB, Genant HK 1995 Relationships between Young's modulus of elasticity, ash density and magnetic resonance imaging (MRI derived effective transverse relaxation time T2* in human tibial specimens. J Comput Assist Tomogr 19:472–479.
212. Antich P, Mason R, McColl R, Zerwech J, Pak C 1994 Trabecular architecture studies by 3D MRI microscopy in bone biopsies. J Bone Miner Res 9S1:327.
213. Chung H, Wehrli F, Williams J, Kugelmass S, Wehrli S 1995 Quantitative analysis of trabecular microstructure by 400 MHz nuclear magnetic resonance imaging. J Bone Miner Res 10:803–811.
214. Jara H, Wehrli FW, Chung H, Ford JC 1993 High-resolution variable flip angle 3D MR imaging of trabecular microstructure in vivo. Mag Res Med 29:528–539.
215. Majumdar S, Genant H, Grampp S, Jergas M, Newitt D, Gies A 1994 Analysis of trabecular bone structure in the distal radius using high resolution MRI. Eur Radiol 4:517–524.
216. Majumdar S, Genant H, Gies A, Guglielimi G 1993 Regional variations in trabecular structure in the calcaneus assessed using high resolution magnetic resonance images and quantitative image analysis. J Bone Miner Res 8S:351.
217. Kapadia RD, High W, Bertolini D, Sarkar SK 1993 MR microscopy: A novel diagnostic tool in osteoporosis research. In: Christiansen C (ed.) 4th International Symposium on Osteoporosis & Consensus Development Conference, Hong Kong, pp. 38.
218. Ouyang X, Lang P, Selby K, Zucconi F, Gindele A, Klifa C, Engelke K, Majumdar S, Genant HK 1995 Analysis of high resolution MRI images of calcaneus: Gray-level thresholding and trabecular quantification. Society of Magnetic Resonance Third Scientific Meeting, Nice, France.
219. Majumdar S, Newitt DC, Jergas M, Gies AA, Chiu EC, Osman D, Keltner J, Keyak J, Genant HK 1995 Evaluation of technical factors affecting the quantification of trabecular bone structure using magnetic resonance imaging. Bone 17: 417–430.
220. Brownie C, Habicht J, Cogill B 1986 Comparing indicators of health and nutritional status. Am J Epidemiol 124:1031–1044.
221. Rosner B 1990 Fundamentals of biostatistics. PWS-KENT Publishing Company, 3rd Ed., Boston, Massachusetts, U.S.A.
222. Daniel W 1991 A Foundation for Analysis in the Health Sciences. John Wiley and Sons, 5th Ed., New York, U.S.A.
223. Kleinbaum D, Kupper L, Muller K 1988 Applied Regression Analysis and Other Multivariate Methods. PWS-KENT Publishing Company, Boston, Massachusetts, U.S.A.
224. Hosmer DW, Lemeshow S 1989 Applied logistic regression. John Wiley & Sons, New York, New York, U.S.A.
225. Schlesselman JJ 1982 Case-control Studies Design, Conduct, Analysis. Oxford University Press, New York, New York, U.S.A.
226. Kleinbaum D, Kupper L, Morgenstern H 1982 Epidemiologic Research—Principles and Quantitative Methods. Van Nostrand Reinhold, New York, U.S.A.
227. Lachenbruch P 1975 Discriminant Analysis. Hafner Press, New York, New York, U.S.A.
228. Johnson R, Wichern D 1988 Applied Multivariate Statistical Analysis. Prentice-Hall Inc., Englewood Cliffs, New Jersey, U.S.A.
229. Efron B 1975 The efficiency of logistic regression compared to normal discriminant analysis. J Am Stat Assoc 70:892–898.
230. Baron A 1991 Misclassification among methods used for multiple group discrimination—the effects of distributional properties. Stat Med 10:757–766.
231. Feinstein A, Wells C, Walter S 1990 A comparison of multivariable mathematical methods for predicting survival—I. Introduction, rationale and general strategy. J Clin Epidemiol 43:339–347.
232. Metz CE 1978 Basic principles of ROC analysis. Semin Nuc Med 8:283–298.
233. Hanley JA, McNeil BJ 1983 A method of comparing the areas under receiver operation characteristic curves derived from the same cases. Radiology 148:839–843.
234. Cox D, Oakes D 1984 Analysis of Survival Data. Chapman and Hall, London, New York, U.S.A.
235. Ross PD, Davis JW, Vogel JM, Wasnich RD 1990 A critical review of bone mass and the risk of fractures in osteoporosis. Calcif Tissue Int 46:149–161.
236. Glüer CC, Blake G, Blunt BA, Jergas M, Genant HK 1995 Accurate assessment of precision errors: How to measure the reproducibility of bone densitometry techniques. Osteoporosis Int 5:262–270.
237. Genant HK, Block JE, Steiger P, Glüer CC, Ettinger B, Harris ST 1989 Appropriate use of bone densitometry. Radiology 170:817–822.
238. Genant HK, Cann C 1981 Vertebral mineral determination using quantitative computed tomography. In: DeLuca HAF, Frost HM, Jee WSS, Johnston CC, Parfitt AM (eds.) Tenth Steenbock Symposium, University Park Press, Madison, Wisconsin, U.S.A., pp. 37–47.
239. Parfitt AM 1995 Is the rate of bone loss influenced by the initial value? Biostatistical and statistical issues. Perth International Bone Meeting, Freemantle, West Australia, pp. 69.
240. Ryan PJ, Blake GM, Herd R, Parker J, Fogelman I 1993 Spine and femur BMD by DXA in patients with varying severity spinal osteoporosis. Calcif Tissue Int 52:263–268.
241. Davis JW, Ross PD, Wasnich RD, MacLean CJ, Vogel JM 1991 Long-term precision of bone loss rate measurements among postmenopausal women. Calcif Tissue Int 48:311–318.
242. Glüer CC, Blunt B, Engelke K, Jergas M, Grampp S, Genant HK 1994 "Characteristic follow-up time"—A new concept for standardized characterization of a technique's ability to monitor longitudinal changes. Bone Miner 25(Suppl 2):S40.
243. He Y-F, Ross PD, Davis JW, Epstein RS, Vogel JM, Wasnich RD 1994 When should bone density measurements be repeated? Calcif Tissue Int 55:243–248.
244. Blumsohn A, Hannon RA, Al-Dehaimi AW, Eastell R 1994 Short-term intraindividual variability of markers of bone turnover in healthy adults. J Bone Miner Res 9(Suppl 1):S153.
245. Seeley D, Browner W, Nevitt M, Genant H, Scott J, Cummings S, Group. TSoOF 1991 Which fractures are associated

with low appendicular bone mass in elderly women? Ann Intern Med 115:837–842.
246. Cummings S, Black D, Nevitt M, Browner W, Cauley J, Genant H, Mascioli S, Scott J, Seeley D, Steiger P, Vogt T, Group SoOFR 1990 Appendicular bone density and age predict hip fracture in women. JAMA 263:665–668.
247. Melton L, Atkinson E, O'Fallon W, Wahner H, Riggs B 1993 Long-term fracture prediction by bone mineral assessed at different sites. J Bone Miner Res 8:1227–1233.
248. Hui SL, Slemenda CW, Johnston CC 1990 The contribution of bone loss to postmenopausal osteoporosis. Osteoporosis Int 1:30–34.
249. Black D, Cummings SR, Genant HK, Nevitt MC, Palermo L, Browner W 1992 Axial and appendicular bone density predict fractures in older women. J Bone Miner Res 7:633–638.
250. Smith DM, Khairi MRA, Johnston CC Jr. 1975 The loss of bone mineral with aging and its relationship to risk of fracture. J Clin Invest 56:311–318.
251. Mazess R, Barden H 1990 Interrelationships among bone densitometry sites in normal young women. Bone Miner 11: 347–356.
252. WHO. 1994 Assessment of fracture risk and its application to screening for postmenopausal osteoporosis: A report of a WHO study group World Health Organization. Geneva, Switzerland.
253. Pouilles JM, Tremollieres F, Ribot C 1993 Spine and femur densitometry at the menopause: Are both sites necessary in the assessment of the risk of osteoporosis. Calcif Tiss Int 52:344–347.
254. Davis JW, Ross PD, Wasnich RD 1994 Evidence for both generalized and regional low bone mass among elderly women. J Bone Miner Res 9:305–309.
255. Wasnich R 1993 Bone mass measurement: Prediction of risk. Am J Med. 95(5A):65–105.
256. Cummings SR, Black DM, Nevitt MC, Browner W, Cauley J, Ensrud K, Genant HK, Hulley SB, Palermo L, Scott J, Vogt TM 1993 Bone density at various sites for prediction of hip fractures: The study of osteoporotic fractures. Lancet 341:72–75.
257. Riggs BL, Wahner HW, Seeman E, et al. 1982 Changes in bone mineral density of the proximal femur and spine with aging: Differences between the postmenopausal and senile osteoporosis syndromes. J Clin Invest 70:716–723.
258. Mazess RB, Barden H, Ettinger M, Schultz E 1988 Bone density of the radius, spine, and proximal femur in osteoporosis. J Bone Miner Res 3:13–18.
259. Black D, Bauer D, Lu Y, Tabor H, Genant H, Cummings S 1995 Should BMD be measured at multiple sites to predict fracture risk in elderly women? J Bone Miner Res 10:S7.
260. Johnston C, Slemenda C 1993 Risk assessment: theoretical considerations. Am J Med. 95(5A):25–55.
261. Lu Y, Mathur A, Black D, Fuerst T, Genant HK, Study of Osteoporotic Fractures Research Group 1996 Survival tree analysis for fracture risk. Presented at the World Congress on Osteoporosis, Amsterdam, The Netherlands, May 18–23, 1996 (Abst).
262. Ross PD, Huang C, Davis JW, Wasnich RD 1995 Vertebral dimension measurements improve prediction of vertebral fracture incidence. Bone 16:257S–262S.
263. Cooper C, Atkinson E, Jacobsen S, O'Fallon W, Melton L 1993 Population-based study of survival after osteoporotic fractures. Am J Epidemiol 137:1001–1005.
264. Brieman L, Friedman J, Olshen R 1984 Classification and Regression Trees. Wadsworth, Belmont, California, U.S.A.
265. Johnston Jr CC, Slemenda CW, Melton III LJ 1991 Clinical use of bone densitometry. New Engl J Med 324:1105–1109.
266. Rubin SM, Cummings SR 1992 Results of bone densitometry affect women's decisions about taking measures to prevent fractures. Ann Int Med 116:990–995.
267. Ross PD, Heilbrun LK, Wasnich RD, Davis JW, Vogel JM 1989 Perspectives: Methodologic issues in evaluating risk factors for osteoporotic fractures. J Bone Miner Res 4:649–656.
268. Seeley DG, Browner WS, Cummings SR, Genant HK 1990 Which fractures are predicted with measurement of bone mineral density? Radiology 177(P):128.
269. Storm T, Thamsborg G, Steiniche T, Genant HK, Sørenson OH 1990 Effect of intermittent cyclical etidronate therapy on bone mass and fracture rate in women with postmenopausal osteoporosis. New Engl J Med 322:1265–1271.
270. Watts NB, Harris ST, Genant HK, Wasnich RD, Miller PD, Jackson RD, Licata AA, Ross P, Woodson GCI, Yanover MJ, Mysiw J, Kohse L, Rao MB, Steiger P, Richmond B, Chesnut CHI 1990 Intermittent cyclical etidronate treatment of postmenopausal osteoporosis. New Engl J Med 323:73–79.
271. Liberman UA, Weiss SR, Bröll J, Minne HW, Quan H, Bell NH, Rodriguez-Portales J, Downs RW, Jr., Dequeker J, Favus M, et al. 1995 Effect of oral alondronate on bone mineral density and the incidence of fractures in postmenopausal osteoporosis. New Engl J Med 333:1437–1443.
272. Lufkin EG, Wahner HW, O'Fallon WM 1992 Treatment of postmenopausal osteoporosis with transdermal estrogen. Ann Intern Med 117:1–9.
273. Kalender WA 1992 Effective dose values in bone mineral measurements by photon absorptiometry and computed tomography. Osteoporosis Int 2:82–87.

Address reprint requests to:
Harry K. Genant, M.D.
Professor of Radiology, Medicine
and Orthopaedic Surgery
Chief, Musculoskeletal Radiology
Director, Osteoporosis Research Group
Department of Radiology
University of California
San Francisco, CA 94143 U.S.A.

The NEW ENGLAND JOURNAL of MEDICINE

ESTABLISHED IN 1812 SEPTEMBER 25, 2003 VOL. 349 NO. 13

The Effects of Parathyroid Hormone and Alendronate Alone or in Combination in Postmenopausal Osteoporosis

Dennis M. Black, Ph.D., Susan L. Greenspan, M.D., Kristine E. Ensrud, M.D., M.P.H., Lisa Palermo, M.A., Joan A. McGowan, Ph.D., Thomas F. Lang, Ph.D., Patrick Garnero, Ph.D., Mary L. Bouxsein, Ph.D., John P. Bilezikian, M.D., and Clifford J. Rosen, M.D., for the PaTH Study Investigators*

ABSTRACT

BACKGROUND

Parathyroid hormone increases bone strength primarily by stimulating bone formation, whereas antiresorptive drugs reduce bone resorption. We conducted a randomized, double-blind clinical study of parathyroid hormone and alendronate to test the hypothesis that the concurrent administration of the two agents would increase bone density more than the use of either one alone.

METHODS

A total of 238 postmenopausal women (who were not using bisphosphonates) with low bone mineral density at the hip or spine (a T score of less than −2.5, or a T score of less than −2.0 with an additional risk factor for osteoporosis) were randomly assigned to daily treatment with parathyroid hormone (1–84) (100 μg; 119 women), alendronate (10 mg; 60 women), or both (59 women) and were followed for 12 months. Bone mineral density at the spine and hip was assessed by dual-energy x-ray absorptiometry and quantitative computed tomography. Markers of bone turnover were measured in fasting blood samples.

RESULTS

The bone mineral density at the spine increased in all the treatment groups, and there was no significant difference in the increase between the parathyroid hormone group and the combination-therapy group. The volumetric density of the trabecular bone at the spine increased substantially in all groups, but the increase in the parathyroid hormone group was about twice that found in either of the other groups. Bone formation increased markedly in the parathyroid hormone group but not in the combination-therapy group. Bone resorption decreased in the combination-therapy group and the alendronate group.

CONCLUSIONS

There was no evidence of synergy between parathyroid hormone and alendronate. Changes in the volumetric density of trabecular bone, the cortical volume at the hip, and levels of markers of bone turnover suggest that the concurrent use of alendronate may reduce the anabolic effects of parathyroid hormone. Longer-term studies of fractures are needed to determine whether and how antiresorptive drugs can be optimally used in conjunction with parathyroid hormone therapy.

From the Departments of Epidemiology and Biostatistics (D.M.B., L.P.) and Radiology (T.F.L.), University of California, San Francisco, San Francisco; the University of Pittsburgh Medical Center, Pittsburgh (S.L.G.); the Departments of Medicine and Epidemiology, Minneapolis Veterans Affairs Medical Center and University of Minnesota, Minneapolis (K.E.E.); the National Institute of Arthritis and Musculoskeletal and Skin Diseases, National Institutes of Health, Bethesda, Md. (J.A.M.); Synarc, Lyons, France (P.G.); the Department of Orthopedic Surgery, Beth Israel Deaconess Medical Center, Boston (M.L.B.); the Department of Medicine, College of Physicians and Surgeons, Columbia University, New York (J.P.B.); the Maine Center for Osteoporosis Research, St. Joseph Hospital, Bangor (C.J.R.); and the Jackson Laboratory, Bar Harbor, Me. (C.J.R.). Address reprint requests to Dr. Black at the University of California, San Francisco, Coordinating Center, 74 New Montgomery St., Suite 600, San Francisco, CA 94105, or at dblack@psg.ucsf.edu.

*The PaTH (Parathyroid Hormone and Alendronate) Study investigators are listed in the Appendix.

N Engl J Med 2003;349:1207-15.

THE PREVENTION OF OSTEOPOROTIC fractures with the use of antiresorptive drugs represents an established therapeutic approach for patients with osteoporosis.[1-3] The results of double-blind, randomized, placebo-controlled trials have indicated that nitrogen-containing bisphosphonates such as alendronate and risedronate, which work principally by suppressing bone resorption, reduce the risk of fracture and increase bone mineral density.[4-8]

Unlike bisphosphonates, parathyroid hormone is anabolic when it is administered intermittently for osteoporosis. Both parathyroid hormone (1–34) and parathyroid hormone (1–84) increase bone density by stimulating bone formation rather than by reducing bone resorption.[9-12] Recently, the 34-amino-acid fragment, parathyroid hormone (1–34), was shown to reduce the risk of fracture[9] and is now available for the treatment of persons with established osteoporosis and a high risk of fracture.

Whether the use of a bisphosphonate and parathyroid hormone together would provide a therapeutic advantage by combining different mechanisms for the reduction of the risk of fracture is unknown. Parathyroid hormone (1–34) has been studied as an addition to ongoing therapy with estrogen (an antiresorptive agent),[13,14] but no similar trials have been conducted using bisphosphonates. Furthermore, no antiresorptive agent (including estrogen or a bisphosphonate) has been studied together with parathyroid hormone from the start of therapy in previously untreated patients. We conducted a multicenter, randomized, double-blind trial comparing monotherapy with parathyroid hormone (1–84) or alendronate with combination therapy consisting of both agents in postmenopausal women with osteoporosis. Here we report the results at 12 months.

METHODS

STUDY PARTICIPANTS

We recruited postmenopausal women 55 to 85 years of age from four clinical centers in the United States (Bangor, Me.; Minneapolis; New York; and Pittsburgh). Women were enrolled if they had a T score of less than −2.5 for bone mineral density at the femoral neck, total hip, or spine, or if they had a T score of less than −2.0 at one of these sites and at least one of the following risk factors: an age of 65 years or more, a history of postmenopausal fracture (vertebral or nonvertebral), and a maternal history of hip fracture. We excluded women who had been treated with bisphosphonates for a total of more than 12 months or for more than 4 weeks during the previous 12 months or who had diseases or took medications that are known to affect bone metabolism. The institutional review board at each clinical center approved the study protocol, and all women provided written informed consent before enrollment.

TREATMENTS

The study treatments were full-length parathyroid hormone (1–84) (100 μg daily [NPS Pharmaceuticals]), alendronate (10 mg daily [Fosamax, Merck]), calcium carbonate (500 mg of elemental calcium [Tums, SmithKlineBeecham]), and a multivitamin containing 400 IU of vitamin D (Rugby Laboratories). The women injected parathyroid hormone (1–84) or matching placebo in the morning using a cartridge-loaded pen. Cartridges were changed every two weeks. Alendronate or matching placebo was taken each morning with a full glass of water after an overnight fast.

STUDY DESIGN

After a two-week run-in phase, 238 women were randomly assigned to one of three treatment regimens to be followed for one year. A total of 119 women were assigned to take parathyroid hormone plus placebo that matched the alendronate, 59 women were assigned to take parathyroid hormone plus alendronate, and 60 women were assigned to take alendronate plus placebo that matched the parathyroid hormone. All participants received daily doses of calcium and vitamin D. In the second year of the study, which is ongoing, women in the original parathyroid hormone group were randomly assigned to receive either alendronate or matching placebo, and women in the other two original groups received alendronate. Because the original parathyroid hormone group was to be split into two groups during the second year of the study, it was twice as large as each of the other original groups. This report covers the first 12 months of the study, the only period during which parathyroid hormone was administered. Participants, clinicians, and investigators remained unaware of the treatment-group assignments, except for a clinician at the coordinating center who was responsible for reports to the data and safety monitoring board. Although support for drug products and quantitative computed tomography (CT) was provided by various pharmaceuti-

cal companies, they had no role in the design or interpretation of the study.

EFFICACY OUTCOME VARIABLES

Areal bone mineral density (in grams per square centimeter) was assessed with the use of dual-energy x-ray absorptiometry (Hologic QDR-4500A or Delphi densitometers). Bone mineral density was measured at the hip (femoral neck and total hip regions), the posteroanterior lumbar spine (L1 to L4), and the radius (the distal one third of the radial shaft) at base line and at 12 months. The coefficient of variation for the areal density is 1 to 2 percent.[15]

Volumetric bone mineral density (in grams per cubic centimeter) and the bone geometry in trabecular and cortical compartments were assessed with the use of quantitative CT at the spine (L1 and L2) and the hip (femoral neck and total hip regions). Findings on quantitative CT, performed at three clinical centers at base line and at 12 months, were evaluated by a central imaging facility (University of California, San Francisco) according to methods that have been described previously.[16,17] The coefficient of variation is 2 to 4 percent for volumetric density[15] and 5 to 6 percent for cortical volume.

Serum drawn after an overnight fast was stored (at −70°C) until it was assayed in a central laboratory (Synarc, Lyons, France). Serum C-terminal telopeptide of type I collagen (a marker of bone resorption) and N-propeptide of type I collagen (a marker of bone formation) were measured with two-site immunoassays on an automatic analyzer (Eleccys, Roche Diagnostics). Intraassay and interassay coefficients of variation for serum N-propeptide and serum C-terminal telopeptide are approximately 4 percent and 6 percent, respectively. Bone-specific alkaline phosphatase was measured with the use of the Ostase assay (Beckman).

ADHERENCE, SAFETY ASSESSMENT, AND ADVERSE EVENTS

Adherence to treatment was assessed by means of the return of unused cartridges (parathyroid hormone) and tablets (alendronate). Full adherence to treatment was defined as the use of at least 80 percent of the injections or tablets for at least 11 months.

Fasting serum calcium concentrations were measured at base line and at 1, 3, and 12 months. Participants were instructed not to take the injection the day of these clinic visits. Twenty-four-hour urinary excretion of calcium and creatinine was measured at base line and at three months. Specific ordered algorithms for use in women in whom the serum or urinary calcium level became elevated (repeated assessment, discontinuation of calcium supplementation, reduction of the dose of parathyroid hormone, and then discontinuation of parathyroid hormone treatment) were followed if the serum calcium concentration was more than 10.5 mg per deciliter (2.62 mmol per liter), if the urinary calcium excretion was more than 400 mg per 24 hours (9.98 mmol per day), or if the ratio of the urinary calcium concentration to the urinary creatinine concentration was more than 0.4.

Patients were questioned at each visit about adverse events, which were coded with the use of preferred terms from the Medical Dictionary for Regulatory Activities (MedDRA)[18] and classified by a clinician at the University of California, San Francisco, who was unaware of the treatment-group assignments. The preferred terms were categorized according to anticipated types of adverse events whose rates had been increased in previous trials of parathyroid hormone[9] and alendronate,[4,5] as well as according to organ systems; the treatment groups were then compared in terms of the rates of adverse events in previous trials as well as those affecting each organ system.

STATISTICAL ANALYSIS

We attempted to follow all the women who underwent randomization for all study visits and procedures, regardless of their level of adherence to the assigned treatment regimen. Analyses were performed according to the intention-to-treat principle unless otherwise indicated. Group means and 95 percent confidence intervals are given for the percent changes from base line in variables measured by dual-energy x-ray absorptiometry and quantitative CT; these values were used to assess the significance of changes within each group. Medians and interquartile ranges are reported for changes in the levels of markers of bone turnover; t-tests were used to compare the combination-therapy group with each of the other two groups in terms of the mean percent change, and Wilcoxon tests were used to compare the groups in terms of markers of bone turnover. No adjustments were made for multiple comparisons. The statistical significance of differences among the treatment groups in the frequency of base-line risk factors and the rates of adverse events was assessed with the use of one-way analysis of variance for continuous variables and

two-by-three chi-square tests for dichotomous variables. Given the standard deviations in this trial, with a power of 90 percent, we could detect a difference in the areal bone mineral density of about 2.8 percent for the spine and 2.2 percent for the hip.

RESULTS

CHARACTERISTICS OF THE WOMEN AND ADHERENCE TO TREATMENT

Table 1 summarizes the base-line characteristics of the women. The mean (±SD) T score for the bone mineral density of the femoral neck was −2.2±0.7. A total of 165 women (69 percent) had at least one T score below −2.5, and 112 (47 percent) reported a fracture after menopause. There were no significant differences among the treatment groups in base-line characteristics, except for the areal bone mineral density of the spine (which was about 6 percent higher in the combination-therapy group than in either of the other groups; P=0.03 for the three-way comparison). No similar trend was evident with regard to the volumetric density of the spine.

A total of 227 women (95 percent) completed the 12-month visit. For the first 12 months of the study, 75 percent of the women had full adherence to treatment involving injections, and 81 percent had full adherence to treatment involving tablets. There were no differences in adherence according to treatment group.

AREAL AND VOLUMETRIC BONE MINERAL DENSITY

The areal bone mineral density of the lumbar spine (as measured by dual-energy x-ray absorptiometry) increased significantly within each treatment group (Fig. 1). Changes were similar in the parathyroid hormone group and the combination-therapy group (increases of 6.3 percent and 6.1 percent, respectively) and were somewhat smaller in the alendronate group (4.6 percent; difference between the combination-therapy group and the alendronate group, 1.5 percentage points; 95 percent confidence interval, −0.5 to 3.6). At the total hip and the femoral neck, the bone mineral density remained essentially unchanged in the parathyroid hormone group but increased in the combination-therapy group and

Table 1. Base-Line Characteristics of the Women.*

Characteristic	Parathyroid Hormone Group (N=119)	Combination-Therapy Group (N=59)	Alendronate Group (N=60)	P Value
Age — yr	69.4±7.3	70.2±6.8	70.7±6.8	0.47
Age at menopause — yr	46.7±6.5	47.2±7.2	48.3±5.2	0.27
Race — no. (%)				0.50
White	111 (93.3)	57 (96.6)	58 (96.7)	
Other	8 (6.7)	2 (3.4)	2 (3.3)	
Height loss since 25 yr of age — mm	40.3±27.8	40.8±27.2	34.5±25.3	0.35
Body-mass index	25.6±4.6	27.1±5.6	25.1±4.5	0.07
Clinical fracture since 45 yr of age — no. (%)	57 (47.9)	30 (50.8)	25 (41.7)	0.64
Any previous alendronate use — no. (%)	13 (10.9)	4 (6.8)	10 (16.7)	0.23
Areal bone mineral density on dual-energy x-ray absorptiometry — g/cm²				
Lumbar spine	0.771±0.104	0.819±0.120	0.778±0.125	0.03
Total hip	0.710±0.098	0.738±0.077	0.712±0.092	0.13
Femoral neck	0.599±0.084	0.612±0.067	0.596±0.072	0.50
Distal one third of radius	0.556±0.076	0.566±0.071	0.551±0.073	0.49
Volumetric density on quantitative CT — g/cm³†				
Integral spine	0.174±0.023	0.178±0.026	0.178±0.028	0.56
Trabecular spine	0.083±0.022	0.087±0.025	0.085±0.024	0.68
Integral total hip	0.211±0.028	0.220±0.031	0.217±0.025	0.14
Trabecular total hip	0.073±0.022	0.074±0.025	0.076±0.019	0.71

* Plus–minus values are means ±SD. The body-mass index is the weight in kilograms divided by the square of the height in meters.

† Data on quantitative CT measurements were available for 178 women.

the alendronate group. The increase at the total hip in the combination-therapy group was significantly greater than that in the parathyroid hormone group (1.9 percent vs. 0.3 percent; difference, 1.6 percentage points; 95 percent confidence interval, 0.3 to 2.9). The bone mineral density at the distal radius decreased significantly in the parathyroid hormone group (a 3.4 percent reduction), but the reduction appeared to be mitigated by the presence of alendronate in the combination-therapy group (a 1.1 percent reduction; difference, 2.3 percentage points; 95 percent confidence interval, 1.2 to 3.5). The loss in the alendronate group was similar to that in the combination-therapy group.

Quantitative CT was used to measure volumetric bone mineral density of trabecular bone at the spine and the hip (Fig. 2) and volumetric bone mineral density and geometric variables in cortical bone at the hip (Fig. 3). The integral volumetric density (cortical plus trabecular bone) at the spine showed a pattern similar to that seen in the areal density of the spine. The volumetric density of the trabecular bone at the spine increased markedly in all groups. However, the increase in the parathyroid hormone group was approximately twice as great as that found in the combination-therapy group (25.5 percent vs. 12.9 percent; difference, 12.6 percentage points; 95 percent confidence interval, 2.8 to 22.4). The change in the alendronate group (10.5 percent) was similar to that in the combination-therapy group. The volumetric density of the trabecular bone at the hip increased in all treatment groups. Although the pattern of differences among the groups was similar to that observed in the volumetric density of trabecular bone at the spine, these differences did not reach statistical significance.

The pattern of changes in cortical-bone variables (Fig. 3) was different from that observed with trabecular bone. The volumetric density of cortical bone at the total hip decreased significantly in the parathyroid hormone group, whereas there was no significant change in the combination-therapy group (a reduction of 1.7 percent vs. an increase of 0.1 percent; difference, 1.8 percentage points; 95 percent confidence interval, 0.7 to 3.0), and there was an increase in the alendronate group (1.2 percent; alendronate group minus combination-therapy group, 1.1 percentage points; 95 percent confidence interval, −0.3 to 2.4). Patterns were similar for the volumetric density of cortical bone at the femoral neck. In the parathyroid hormone group, the cortical bone volume increased significantly at the total hip (3.5 percent) and femoral neck (3.4 percent), but there were no significant increases in the other treatment groups. There was a significant difference between the parathyroid hormone group and the combination-therapy group in the change in cortical volume at the femoral neck (a 3.4 percent

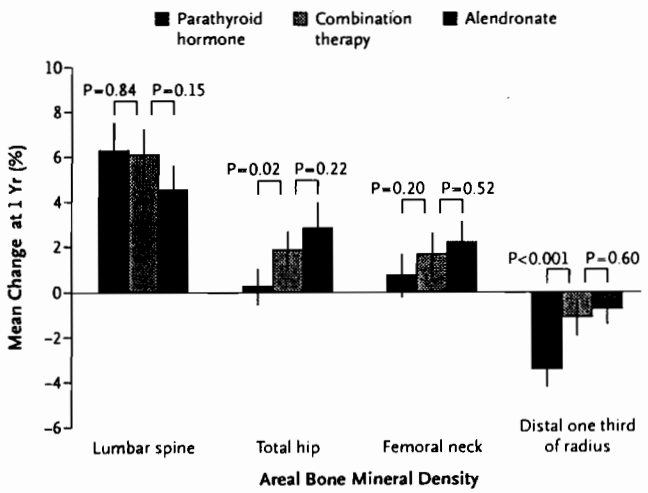

Figure 1. Mean Percent Changes in Areal Bone Mineral Density on Dual-Energy X-Ray Absorptiometry.

The vertical lines represent the 95 percent confidence intervals. Negative changes represent decreases.

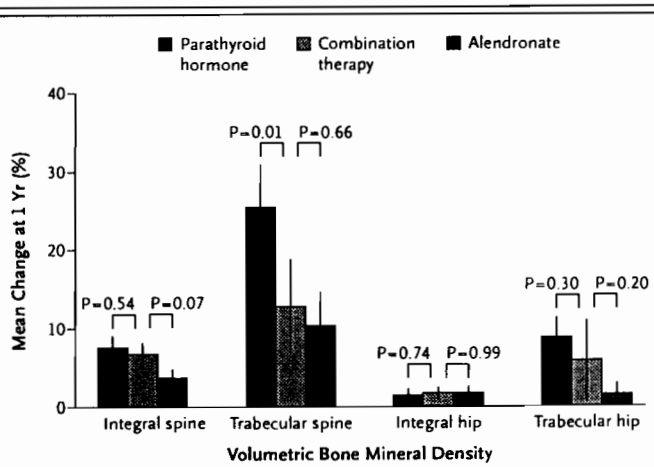

Figure 2. Mean Percent Changes in Volumetric Bone Mineral Density for Integral (Cortical plus Trabecular) and Trabecular Bone on Quantitative CT.

The vertical lines represent the 95 percent confidence intervals.

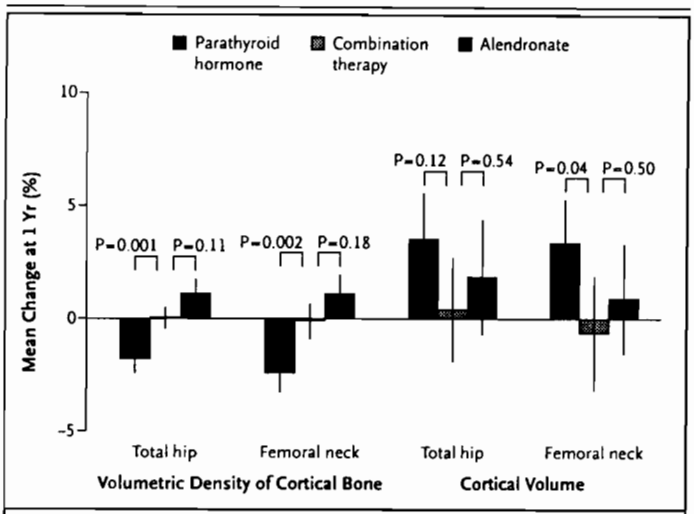

Figure 3. Mean Percent Changes in Volumetric Density of Cortical Bone and Cortical Volume at the Hip on Quantitative CT.

The vertical lines represent the 95 percent confidence intervals. Negative changes represent decreases.

increase vs. a 0.6 percent decrease; difference, 4.0 percentage points; 95 percent confidence interval, 0.1 to 7.9), but not in the change in cortical volume at the total hip (increases of 3.5 percent vs. 0.4 percent; difference, 3.1 percentage points; 95 percent confidence interval, −0.8 to 7.1). The cortical bone mineral content did not change in any of the treatment groups.

BIOCHEMICAL MARKERS OF BONE TURNOVER

The parathyroid hormone group had a rapid, large increase in the level of N-propeptide of type I collagen, a marker of bone formation; the increase was sustained over the 12-month period (an increase of 150 percent at 12 months) (Fig. 4). Treatment with parathyroid hormone was associated with an increase in the concentration of serum C-terminal telopeptide of type I collagen, a marker of bone resorption, although this increase was somewhat delayed in comparison with the change in the N-propeptide concentration. The combination-therapy group had an increase in the concentration of N-propeptide at 1 month, but the concentration had decreased to slightly below the base-line value by 3 months (and was 15.7 percent below base line at 12 months). In the combination-therapy group, the C-terminal telopeptide concentration had decreased by 50 percent at one month and remained at that level. In the alendronate group, there was a rapid decrease in the C-terminal telopeptide level (a 58 percent decrease at one month), followed by a similar decrease (59 percent at three months) in the N-propeptide level. Changes in the concentrations of bone-specific alkaline phosphatase were similar to the changes in the N-propeptide concentrations (data not shown).

FRACTURES

Eight clinical fractures occurred during the trial. The incidence was similar in all three treatment groups (approximately 3 percent).

SAFETY AND ADVERSE EVENTS

There was a small but significant increase in the mean serum calcium concentration in the parathyroid hormone group at 1 and 3 months, but the concentration had returned to the base-line value by 12 months (9.5 mg per deciliter [2.38 mmol per liter] at base line; 9.7 mg per deciliter [2.42 mmol per liter] at 1 month; 9.8 mg per deciliter [2.45 mmol per liter] at 3 months; and 9.5 mg per deciliter at 12 months). The combination-therapy group had a small increase at one month, but the concentration had returned to the base-line value by three months ($P=0.004$ for the comparison with the parathyroid hormone group at three months). As expected, there was a decrease in the serum calcium concentration among the women in the alendronate group.

Twenty-two women (12 percent in the parathyroid hormone group, 14 percent in the combination-therapy group, and none in the alendronate group) met the criteria for an elevated serum calcium concentration on at least one occasion, but only five had values above 11.2 mg per deciliter (2.80 mmol per liter). Fifteen women (8 percent in the parathyroid hormone group, 10 percent in the combination-therapy group, and none in the alendronate group) met the criteria for elevated urinary calcium excretion. Both serum and urinary levels returned to normal in almost all women either after a confirmatory measurement (step 1 in the algorithm) or after the discontinuation of calcium supplementation (step 2). Only two women required a reduction in the dose of parathyroid hormone because of increased calcium levels. One additional woman who was receiving parathyroid hormone had a normal serum calcium concentration at all study visits but had transient hypercalcemia associated with an intercurrent illness; the hypercalcemia resolved within 24 hours with intravenous hydration.

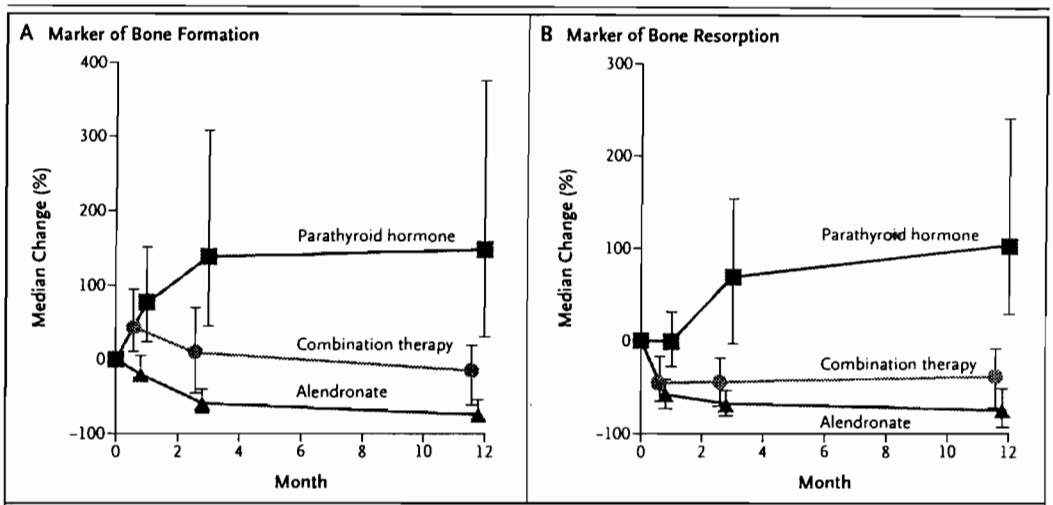

Figure 4. Median Percent Changes in Serum Concentrations of Biochemical Markers of Bone Formation (N-Propeptide of Type I Collagen, Panel A) and Bone Resorption (C-Terminal Telopeptide of Type I Collagen, Panel B).

The differences between the combination-therapy group and the parathyroid hormone group at 12 months and between the combination-therapy group and the alendronate group at 12 months were significant ($P<0.001$). I bars represent the interquartile ranges. Negative changes represent decreases.

A total of 226 women reported at least one adverse event, and 20 reported at least one serious adverse event. The proportions did not differ according to treatment group, nor did the rates of adverse events that were previously found to be associated with parathyroid hormone treatment (injection-site complications, nausea, fatigue, headache, dizziness, or limb pain).

Two deaths occurred during the trial, both due to rapidly progressing dementia and both in women in the parathyroid hormone group. One of these women had taken only one dose of parathyroid hormone. The data and safety monitoring board judged that the two deaths were unrelated to the study medication.

There was a significant increase in the mean serum uric acid concentration in both the parathyroid hormone group (1.03 mg per deciliter [61 μmol per liter]) and the combination-therapy group (0.85 mg per deciliter [51 μmol per liter]; $P<0.001$ for both increases), whereas there was no change in the alendronate group. Three women had gout — one in the parathyroid hormone group and two in the combination-therapy group.

DISCUSSION

Our randomized clinical trial was designed to assess whether combination therapy with parathyroid hormone and a bisphosphonate is superior to monotherapy with parathyroid hormone or a bisphosphonate. Daily injections of parathyroid hormone (1–34) and parathyroid hormone (1–84) have been shown to increase bone mineral density,[9,12,13] and parathyroid hormone (1–34) has been shown to reduce the risk of vertebral and nonvertebral fractures.[9] Although parathyroid hormone therapy increases both bone formation and bone resorption, bone formation is increased preferentially over resorption, at least initially. The bisphosphonate alendronate has also been shown to increase bone mineral density and reduce the risk of fracture, but its mechanism of action differs from that of parathyroid hormone; it preferentially suppresses bone resorption over bone formation.[4,5]

By stimulating bone formation and inhibiting bone resorption simultaneously, combination therapy might be more effective than therapy with parathyroid hormone or alendronate alone. We hypothesized that, as compared with parathyroid hormone therapy alone, combination therapy with parathyroid hormone and alendronate would induce larger increases in bone mineral density, preserve the increase in bone formation, and minimize increases in bone resorption. However, taken together, the changes in areal and volumetric bone mineral density, cortical volume, and the levels of biochemical markers of bone turnover found in our study pro-

vide little evidence that this combination is better than either drug alone.

The use of quantitative CT allowed us to evaluate trabecular bone separately from cortical bone. The volumetric density of trabecular bone at the spine increased more with parathyroid hormone alone than with combination therapy or alendronate alone. In the parathyroid hormone group, the cortical volume at the hip increased, the volumetric density decreased, and the bone mineral content was unchanged — observations that are consistent with the findings of other studies[19-21] and with the previously demonstrated actions of parathyroid hormone, including the induction of new bone that is not fully mineralized, as well as the increasing cortical porosity.[19,22,23] In studies in nonhuman primates,[19] these changes were not associated with decreases in bone strength. However, in humans, it is not known whether the changes we observed in cortical bone with parathyroid hormone therapy have a positive, negative, or neutral effect on bone strength and the risk of fracture. Overall, the changes that were induced by parathyroid hormone therapy in cortical and trabecular bone were not seen with combination therapy or with alendronate monotherapy, which suggests that combination therapy alters the distinct effects of parathyroid hormone on bone. Ultimately, further study is needed to determine the effect of parathyroid hormone–based combination therapy on the risk of fracture.

The parathyroid hormone group had a clear and early increase in the levels of the marker of bone formation, with a somewhat delayed but substantial increase in the levels of the marker of resorption. These observations are consistent with the findings of previous studies.[10-13] The expectation that combination therapy would maintain the increased bone formation seen with parathyroid hormone alone while dampening increases in resorption was not substantiated by the data. Although the levels of the marker of bone resorption did decrease substantially with combination therapy and the levels of the marker of bone formation remained relatively constant over the 12-month period, the expected large and sustained increases in bone formation were negated after 1 month. If increases in bone formation are indicative of the effects of parathyroid hormone on bone, these results suggest that the anabolic actions of parathyroid hormone might not be optimally realized with combination therapy.

We examined the concurrent administration of antiresorptive therapy and parathyroid hormone therapy only in women who were not already taking medication for osteoporosis; therefore, we cannot address questions regarding antiresorptive therapy initiated before or after the initiation of parathyroid hormone therapy. Little is known about the use of parathyroid hormone therapy after antiresorptive therapy. However, the addition of parathyroid hormone to ongoing estrogen therapy apparently did not reduce the ability of parathyroid hormone to increase bone turnover.[13,14] Increases in bone mineral density achieved with combined estrogen and parathyroid hormone were similar to those observed with parathyroid hormone monotherapy. A recent study of combination alendronate and parathyroid hormone (1–34) (40 μg) therapy in men, initiated after 6 months of alendronate monotherapy, showed that the increases in bone mineral density over 24 months of combination therapy were less than those observed over 24 months of parathyroid hormone monotherapy.[24] However, there have been no studies of parathyroid hormone monotherapy initiated after the discontinuation of any type of antiresorptive therapy. Our report cannot provide insight about whether antiresorptive therapy administered after a course of parathyroid hormone therapy is of clinical benefit. Although one small, nonrandomized study of alendronate therapy given after therapy with parathyroid hormone (1–84) showed an additional increase in bone mineral density,[12] it is unclear whether antiresorptive drugs should be used after parathyroid hormone therapy.

We used the full-length 84-amino-acid parathyroid hormone molecule. The effects of parathyroid hormone (1–84) on the bone mineral density at the spine and the hip in our study are similar to those that have been found with 20 μg (the approved dose) of parathyroid hormone (1–34) in other 1-year studies[10,11] and are somewhat smaller than those found in one longer (21-month) study.[9] However, the generalizability of our results with the concurrent initiation of parathyroid hormone (1–84) and alendronate combination therapy to therapy with parathyroid hormone (1–34) is uncertain. Whether our results with the concurrent initiation of alendronate therapy and parathyroid hormone therapy apply to other bisphosphonates or other antiresorptive drugs is unknown. Taken together, these results do not support the concurrent initiation of alendronate with parathyroid hormone treatment.

Supported by a contract (NIAMS-045, N01-AR-9-2245) with the National Institute of Arthritis and Musculoskeletal and Skin Disorders. Study medications were provided by NPS Pharmaceuticals (parathyroid hormone and matching placebo), Merck (alendronate and matching placebo), and SmithKlineBeecham (calcium). Supplementary funds for quantitative CT were provided by Merck.

APPENDIX

The following persons participated in the PaTH Study: *Columbia University* — J.P. Bilezikian (principal investigator), K. Lee, J. Sliney (study coordinators); *Minneapolis Veterans Affairs Medical Center* — K.E. Ensrud (principal investigator), V. Wyum, N. Michaels; *University of Pittsburgh Medical Center* — S.L. Greenspan (principal investigator), J.L. Ryan (study coordinator), J.M. Wagner; *Maine Center for Osteoporosis Research–St. Joseph's Hospital* — C.J. Rosen (principal investigator), L. Fowler, D. Storm (study coordinators); *University of California, San Francisco* — D.M. Black (principal investigator), T. Hue (project director), L. Palermo (statistician), D. Sellmeyer and D.C. Bauer (study physicians); *Data and Safety Monitoring Board* — L. Raisz (chair), S. Hui, R. Recker, D. Kiel, D. Hanley.

REFERENCES

1. National Osteoporosis Foundation. Physician's guide to prevention and treatment of osteoporosis. Belle Mead, N.J.: Excerpta Mediea, 1999.
2. Cranney A, Guyatt G, Griffith L, Wells G, Tugwell P, Rosen C. Meta-analyses of therapies for postmenopausal osteoporosis. IX. Summary of meta-analyses of therapies for postmenopausal osteoporosis. Endocr Rev 2002;23:570-8.
3. Genant HK, Cooper C, Poor G, et al. Interim report and recommendations of the World Health Organization Task-Force for Osteoporosis. Osteoporos Int 1999;10:259-64.
4. Black DM, Cummings SR, Karpf DB, et al. Randomised trial of effect of alendronate on risk of fracture in women with existing vertebral fractures. Lancet 1996;348:1535-41.
5. Cummings SR, Black DM, Thompson DE, et al. Effect of alendronate on risk of fracture in women with low bone density but without vertebral fractures: results from the Fracture Intervention Trial. JAMA 1998;280:2077-82.
6. Harris ST, Watts NB, Genant HK, et al. Effects of risedronate treatment on vertebral and nonvertebral fractures in women with postmenopausal osteoporosis: a randomized controlled trial. JAMA 1999;282:1344-52.
7. Cranney A, Wells G, Willan A, et al. Meta-analyses of therapies for postmenopausal osteoporosis. II. Meta-analysis of alendronate for the treatment of postmenopausal women. Endocr Rev 2002;23:508-16.
8. Cranney A, Tugwell P, Adachi J, et al. Meta-analyses of therapies for postmenopausal osteoporosis. III. Meta-analysis of risedronate for the treatment of postmenopausal osteoporosis. Endocr Rev 2002;23:517-23.
9. Neer RM, Arnaud CD, Zanchetta JR, et al. Effect of parathyroid hormone (1-34) on fractures and bone mineral density in postmenopausal women with osteoporosis. N Engl J Med 2001;344:1434-41.
10. Orwoll ES, Scheele WH, Paul S, et al. The effect of teriparatide [human parathyroid hormone (1-34)] therapy on bone density in men with osteoporosis. J Bone Miner Res 2003;18:9-17.
11. Kurland ES, Cosman F, McMahon DJ, Rosen CJ, Lindsay R, Bilezikian JP. Parathyroid hormone as a therapy for idiopathic osteoporosis in men: effects on bone mineral density and bone markers. J Clin Endocrinol Metab 2000;85:3069-76.
12. Rittmaster RS, Bolognese M, Ettinger MP, et al. Enhancement of bone mass in osteoporotic women with parathyroid hormone followed by alendronate. J Clin Endocrinol Metab 2000;85:2129-34.
13. Lindsay R, Nieves J, Formica C, et al. Randomised controlled study of effect of parathyroid hormone on vertebral-bone mass and fracture incidence among postmenopausal women on oestrogen with osteoporosis. Lancet 1997;350:550-5.
14. Lane NE, Sanchez S, Modin GW, Genant HK, Pierini E, Arnaud CD. Parathyroid hormone treatment can reverse corticosteroid-induced osteoporosis: results of a randomized controlled clinical trial. J Clin Invest 1998;102:1627-33.
15. Cummings SR, Bates D, Black DM. Clinical use of bone densitometry: scientific review. JAMA 2002;288:1889-97. [Erratum, JAMA 2002;288:2825.]
16. Lang TF, Li J, Harris ST, Genant HK. Assessment of vertebral bone mineral density using volumetric quantitative CT. J Comput Assist Tomogr 1999;23:130-7.
17. Lang TF, Keyak JH, Heitz MW, et al. Volumetric quantitative computed tomography of the proximal femur: precision and relation to bone strength. Bone 1997;21:101-8.
18. MedDRA (medical dictionary for regulatory activities). Reston, Va.: MedDRA Maintenance and Support Services Organization (MSSO). (Accessed September 2, 2003, at http://www.meddramsso.com/newwebaug2001/meddramsso/meddra/index.htm.)
19. Burr DB, Hirano T, Turner CH, Hotchkiss C, Brommage R, Hock JM. Intermittently administered human parathyroid hormone (1-34) treatment increases intracortical bone turnover and porosity without reducing bone strength in the humerus of ovariectomized cynomolgus monkeys. J Bone Miner Res 2001;16:157-65.
20. Rehman Q, Lang TF, Arnaud CD, Modin GW, Lane NE. Daily treatment with parathyroid hormone is associated with an increase in vertebral cross-sectional area in postmenopausal women with glucocorticoid-induced osteoporosis. Osteoporos Int 2003;14:77-81.
21. Zanchetta JR, Bogado CE, Ferretti JL, et al. Effects of teriparatide [recombinant human parathyroid hormone (1-34)] on cortical bone in postmenopausal women with osteoporosis. J Bone Miner Res 2003;18:539-43.
22. Misof BM, Roschger P, Cosman F, et al. Effects of intermittent parathyroid hormone administration on bone mineralization density in iliac crest biopsies from patients with osteoporosis: a paired study before and after treatment. J Clin Endocrinol Metab 2003;88:1150-6.
23. Dempster DW, Cosman F, Kurland ES, et al. Effects of daily treatment with parathyroid hormone on bone microarchitecture and turnover in patients with osteoporosis: a paired biopsy study. J Bone Miner Res 2001;16:1846-53.
24. Finkelstein JS, Hayes A, Hunzelman JL, Wyland JJ, Lee H, Neer RM. The effects of parathyroid hormone, alendronate, or both in men with osteoporosis. N Eng J Med 2003;349:1216-26

JOURNAL OF BONE AND MINERAL RESEARCH
Volume 18, Number 6, 2003

Patient-Specific DXA Bone Mineral Density Inaccuracies: Quantitative Effects of Nonuniform Extraosseous Fat Distributions

HH BOLOTIN,[1] H SIEVÄNEN,[2,3] and JL GRASHUIS[4]

ABSTRACT

Nonuniform extraosseous fat is shown to raise the magnitude of inaccuracies in DXA in vivo BMD measurements into the range of 20–50% in clinically relevant cases. Hence, DXA-based bone fragility diagnoses/prognoses and evaluations of bone responsiveness to treatment can be unreliable.

Patient-specific DXA in vivo bone mineral areal density (BMD) measurements have been demonstrated to be inherently inaccurate even when extraosseous fat (*F*) and lean muscle tissue (*L*) are uniformly distributed throughout the scan region of interest (ROI). The present work extends these investigations to quantitative evaluation of the extent to which clinically realistic soft tissue inhomogeneities external to the bone within the DXA scan ROI affect patient-specific in vivo BMD measurement inaccuracies. The results are particularly relevant to patient-specific lumbar vertebral and proximal femoral sites. Norland, Hologic, and Lunar DXA scans and corresponding DXA simulation studies of the same set of 225 different phantom arrays were carried out. The phantoms were specially fabricated absorptiometric replications of bone mineral material (*B*), red marrow (*RM*), and yellow marrow (*YM*) mixtures, and extraosseous *F* and *L* combinations spanning the anthropometric ranges encountered clinically. The three different DXA scanners yielded BMD results that effectively coincided, were in excellent agreement with the findings of the present corresponding DXA-simulation studies in each case, and confirmed the validity of the DXA BMD inaccuracy analysis formalism. It was found that only relatively small extraosseous soft tissue inhomogeneities within the ROI of DXA BMD scans can increase substantially the already sizable BMD inaccuracies shown earlier to pertain for uniformly distributed extraosseous soft tissues. The extent of these in vivo BMD inaccuracies (%) are shown to depend on the mean extraosseous *F*-to-*L* areal density ratio and its degree of nonuniformity within the local bone scan ROI, the marrow thickness and specific composition, and the actual BMD in any given case. It was found that patient-specific DXA-measured in vivo BMD inaccuracies can, in many clinically encountered cases, be as large as 20–50%, particularly so for osteopenic, osteoporotic, and elderly patients. It is concluded that, because these DXA in vivo BMD inaccuracies are unavoidable and clinically unpredictable, diagnoses/prognoses of bone fragility and evaluations of bone responsiveness to treatment of *individual* patients based mainly on DXA in vivo BMD measurements can be unreliable. (J Bone Miner Res 2003;18:1020–1027)

Key words: DXA, bone mineral density inaccuracies, nonuniform extraosseous fat distributions, marrow, anthropometrics

INTRODUCTION

THE INCREASING INCIDENCE of osteoporosis in the vulnerable population groups [1–3] has intensified the need for effective and reliable means of diagnosis and assessment of the condition and for the evaluation of the patient-specific therapeutic efficacy of its treatments. For more than a decade, the appraisal of skeletal bone mineral status in clinical practice and research has been based mainly on noninvasive planar DXA measurements of in vivo bone mineral areal density (BMD, g/cm^2).[4] However, notwithstanding the widespread clinical use of, and extensive reliance on, DXA

The authors have no conflict of interest.

[1]School of Medical Sciences, RMIT University, Bundoora, Victoria, Australia.
[2]The Bone Research Group, UKK Institute, Tampere, Finland.
[3]Research Department, Tampere University Hospital, Tampere, Finland.
[4]Department of Medical Informatics and Radiology, Erasmus University Rotterdam, Rotterdam, The Netherlands.

for clinical research, diagnostics of osteoporosis, and prognostics of the risk of osteoporotic fractures,[4-13] it is particularly disquieting that there is mounting evidence and serious concern that these measurements are subject to sizable inherent patient-specific inaccuracies.

These inaccuracies derive from the known inapplicability of planar DXA methodology to bone sites comprised of more than two absortiometrically distinguishable components within the scan region of interest (ROI)—the *two-component DXA limitation*.[14-26] The extent of these inaccuracies is sufficient to call into question a number of aspects of osteopenic and osteoporotic diagnoses/prognoses, bone fragility, remedial bone therapy effectiveness, and other related systematic features gleaned primarily from DXA in vivo BMD measurements. Faulkner[13] has reviewed the relevant evidence and explored the prospect that measured in vivo BMD, in and of itself, may not be homologous with bone strength. Marshall et al.[10] concluded that in vivo DXA measurement of BMD is not sufficiently definitive to be relied on to identify those specific individuals who will develop a future bone fracture. The likelihood that these inherent DXA in vivo BMD inaccuracies and unsettling clinical observations[10,13,18,19,24-29] are linked[20-24,30]—the former effectively manifest in the latter—looms as a fundamental issue relevant to the intrinsic viability and reliability of patient-specific planar DXA in vivo bone densitometry and bone fragility studies in clinical practice and research.

The principal objective of the present work was to extend the scope of these previous quantitative studies of inherent DXA in vivo BMD measurement inaccuracies by systematic investigation of the extent to which *nonuniform* distributions of extraosseous fat within the scan ROI further contribute to and affect these BMD measurement inaccuracies. It is noted that such a systematic and comprehensive study would not be feasible or practical using actual patients or in situ cadavers, because in neither could the *true* BMD and/or the requisite details of soft tissue composition and distribution within the scan ROI be ascertained[20] [the "true" value of BMD, $(BMD)_{true}$, being that BMD value that would be obtained from a DXA in vivo measurement free of attendant inaccuracies]. Furthermore, in neither case could the investigator determine or preselect for interrogation any of these pertinent anthropometric and X-ray absorptiometric particulars to an extent sufficient to elucidate the underlying causative relationships fully. Thus, the use of realistic phantom arrays that closely replicate these soft tissue anthropometrics becomes essential in any thorough quantitative endeavor to establish and understand the fundamental causes of these inaccuracies and the extent to which they can affect patient-specific DXA in vivo BMD measurements. The present work differs from earlier, ostensibly similar, efforts[6,14-19,25,26,31-33] in that it develops directly from the underlying source of these inaccuracies and does so across the entire practical clinical range of BMD and soft tissue anthropometrics.

MATERIALS AND METHODS

Phantom and DXA scans

Phantom materials formulated[23] as X-ray absorptiometric equivalents of bone material (B), red and yellow marrows (RM and YM, respectively), lean muscle tissue (L), and fat (F) were assembled into 225 different "anthropometric" arrays, as schematically represented in Fig. 1. These arrays spanned the full range of soft tissue anthropometrics encountered clinically, and as well, a broad range of nonuniform distributions of extraosseous fat and lean muscle tissue. The fabrication of these phantom tissues was based on the essentials of the loaded-epoxy resin method of White et al.[34] All phantom materials were identical in composition and overall dimensions to those used in our earlier publication.[23]

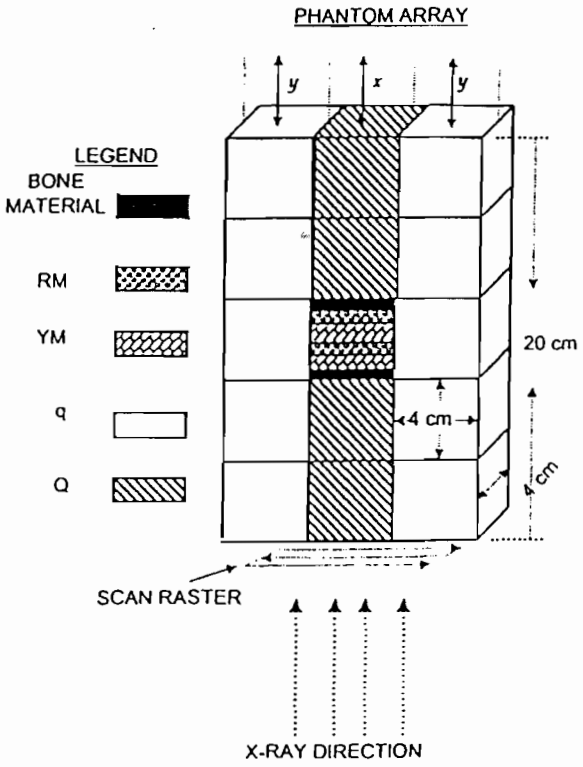

FIG. 1. Schematic representation typical of the 225 different phantom assemblies used in the present work, indicating the bone position, marrow composition, direction of incident DXA scan X-rays (simulated and actual), and scan raster. Each extraosseous phantom block was a 4-cm cube; the overall A/P thickness of the represented "torso" was 20 cm. The F-to-L areal density ratio, q, designates the composition of the extraosseous soft tissue lateral to the "bone," Q, that in the scan region in which bone material intercepts the X-ray flux, and y and x denote linear dimensional measures along X-ray paths in these regions, respectively. Bone material, yellow marrow (YM) and red marrow (RM) were 4 × 4-cm slabs of requisite thicknesses.

In each such phantom assembly, the extraosseous "soft tissue" material lateral to the "bone" was the absorptiometric equivalent of a specific preselected homogeneous F-to-L areal density ratio $q = (\rho_F y_F/\rho_L y_L)$; y is the linear anterior-posterior (A/P) dimension (cm) of the given extraosseous "tissue" along X-ray paths lateral to bone, and q is the lateral extraosseous soft tissue descriptor relevant to the extraction of BMD from DXA scans.[20-23] Along X-ray paths traversing "bone material" in the phantom array, the linear extent of the extraosseous soft tissue and its F-to-L areal density ratio are denoted by x and Q, respectively, so

that $Q = (\rho_f x_f/\rho_L x_L)$. However, in this study, q and Q were generally not the same, and y was not equal to x.[23] The various separate values of q and Q used (0.0, 0.1, 0.3, 0.6, and 1.0) spanned the full range encountered clinically,[35] ranging from 0% to 50% F by weight in the scan ROI.

The thicknesses of phantom bone material inserted into the "bone site" of each phantom array were selected to be $(BMD)_{true}$ values of 0.6, 0.8, and 1.4 g/cm^2, ranging[9,36] from that typical of the osteoporotic, through osteopenic, to high BMD values, respectively. The remaining bone-site space was completely filled with various combinations of *RM* and *YM* phantom slabs. The fraction of the marrow volume that was yellow in each case, $g = (YM)/(YM + RM)$ = 0.6, 0.8, and 1.0 (40% *RM*, 20% *RM*, and wholly *YM*, respectively), spanned the marrow constitutions typical of mature and elderly patients.[37,38] In this way, phantom arrays replicating 225 different combinations of BMD and intra-/extraosseous soft tissue anthropometrics and absorptiometrics were assembled and DXA scanned.

As in our earlier work,[23] Norland XR-26 (Norland, Fort Atkinson, WI, USA), Hologic QDR-1000 (Hologic, Waltham, MA, USA), and Lunar DPX-α (Lunar, Madison, WI, USA) densitometers were used. All particulars of these DXA scans were as detailed earlier.[23]

DXA simulation studies of phantom arrays

As dual poly-energetic DXA simulated BMD values (after beam-hardening corrections were made) were in excellent quantitative agreement (< ~0.2%) with actual DXA poly-energetic BMD measurement results and with dual mono-energetic DXA BMD simulation findings (intrinsically free of beam-hardening) for similar 20-cm-thick phantom arrays,[23] dual *mono-energetic* DXA BMD simulations of each of the phantom arrays were carried out.[20–22]

The BMD values of all simulated scans, $(BMD)_{sim}$, were evaluated (as are the BMD values obtained in standard clinical DXA scans) using the analytic DXA equation,[20]

$$(BMD)_{meas,sim} = \frac{[\ln(J_1/J_{01})\ln(J_2/J_{02}) - \ln(J_2/J_{02})\ln(J_1/J_{01})]}{[\lambda_{1B}\ln(J_2/J_{02}) - \lambda_{2B}\ln(J_1/J_{01})]}. \quad (1)$$

where $\ln(J_1/J_{01})$ and $\ln(J_1/I_{01})$ represent the natural logarithms of the fraction of incident low-energy X-ray photon spectral region transmitted through the specimen lateral to and through the "bone," respectively, and $\ln(J_2/J_{02})$ and $\ln(I_2/I_{02})$ are the corresponding values for the high-energy X-ray region, with λ_{1B} and λ_{2B} being, respectively, the low- and high-energy X-ray mass attenuation coefficients (cm^2/g) of bone material at the two energies.

However, the DXA equation (Eq. 1) will yield the true value of BMD if, and only if, proper account can be taken of the presence of marrow (and its composition) and any differences that pertain between the makeup of the extraosseous fat/lean tissue in the X-ray "shadow" of the bone and lateral to it (q,Q differences).[20] As DXA cannot, $(BMD)_{meas}$ may differ markedly from $(BMD)_{true}$, with DXA methodology unable to estimate the extent of these BMD inaccuracies. However, these inaccuracies can be quantitatively assessed in the present study, because in both the actual DXA scans and the corresponding simulation studies of each phantom array, all anthropometric and X-ray absorptiometric particulars, no matter how disparate, are known a priori.

BMD calibration

Fifteen additional similar phantom arrays were also assembled with the same standard intra- and extraosseous dimensions, each constituted with $q = Q$, and all marrow slabs replaced by material identical in composition to that of the extraosseous phantom tissue, q, of the same array. Because these assemblies were comprised of only two absortiometrically distinct materials (bone material plus a single intra-/extraosseous soft tissue equivalent), the two-component DXA limitation was satisfied fully, allowing DXA-measured BMD to be determined correctly (i.e., without inaccuracy). These 15 phantom assemblies were DXA scanned using all five $q = Q$ values for each of the three selected phantom BMD values. Scans of these $q = Q = g$ arrays established (calibrated) the three true (actual) BMD values, $(BMD)_{true}$, of phantom bone material used in the other 225 phantom arrays. In this way, the corresponding overall percentage inaccuracies in both DXA-measured and normalized DXA-simulated BMD [$(BMD)_{meas}$ and $(BMD)_{sim}$, respectively] were obtained for each of the 225 phantom array cases:

$$(\%BMD\ Inaccuracy)_{meas,sim} = \frac{[(BMD)_{true} - (BMD)_{meas,sim}]}{(BMD)_{true}} \times 100\% \quad (2)$$

Estimates of q,Q differences in DXA in vivo vertebral and proximal femoral scans

To obtain reasonable estimates of the extent to which the extraosseous soft tissue areal density ratios along X-ray paths passing lateral to (q) and those intersecting bone (Q) in planar DXA in vivo BMD scans actually differ within the scan ROI of lumbar vertebral and proximal femoral bone sites for most patients encountered clinically, a number of anatomical atlases were consulted. These depicted actual cross-sectional anatomical cadaveric slices,[39] computerized tomographic,[40–41] and magnetic resonance imaging[41] sections in which extraosseous adipose tissues (both subcutaneous and intraperitoneal) are distinguishable from lean muscle tissue and internal organs.

Careful measurements were made of the separate overall extraosseous fat and lean tissue dimensions along a large number of individual notional A/P X-ray paths passing lateral to and through the bone in each depicted contiguous transverse anatomical section image through the lumbar spinal and proximal femoral bone sites, as exemplified in Norland, Hologic, and Lunar DXA manuals and various texts.[42] In addition, the selected soft tissue ROI boundaries laterally adjacent to the bone were varied in breadth, and the new soft tissue anthropometrics encompassed were again evaluated. In each case, the separate average fat and lean tissue A/P dimensions were weighted by their respective

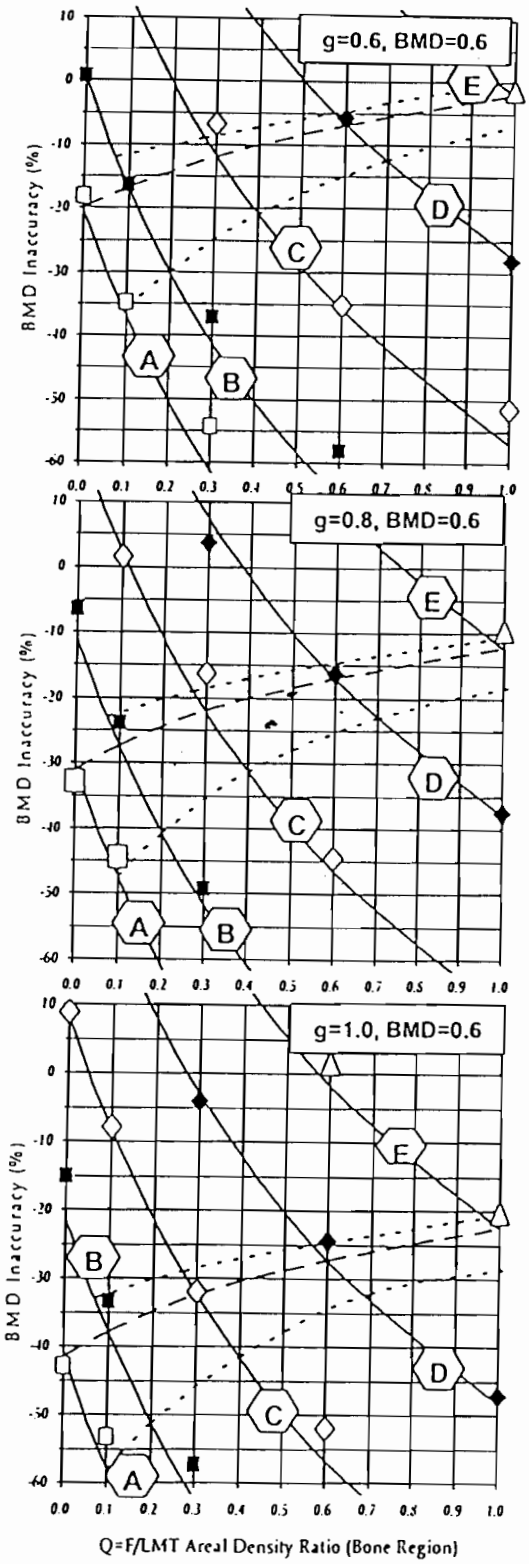

FIG. 2. Results of the present series of quantitative simulation studies (solid lines) and actual Norland DXA scans (individual data point symbols) of a set of 75 different phantom arrays of the type depicted in Fig. 1 for a *true* BMD value of 0.6 g/cm^2 displayed over the clinically relevant range of intra- and extraosseous soft tissues of adult patients. The upper segment of this figure relates to bone marrow with 60% yellow marrow, the middle section to marrow with 80% yellow marrow, and the lower section is the case of fully yellow marrow. The fractional BMD inaccuracies (%) inherent in DXA measured in vivo BMD are plotted as a function of Q, the extraosseous F-to-L areal density ratio within that section of the scan ROI section in which bone material is present. These are shown for representative extraosseous F-to-L areal density ratio values lateral to the bone. (A) $q = 0$, (B) $q = 0.1$, (C) $q = 0.3$, (D) $q = 0.6$, and (E) $q = 1.0$, with the actual measured DXA scan BMD inaccuracies designated by open squares, solid squares, open diamond shapes, solid diamond shapes, and open triangles, respectively. Demarcations of the limits $-0.10 \leq Q \leq +0.03$ found in the present work to represent the effective range of extraosseous soft tissue areal density ratio differences $(q - Q)$ encountered in most A/P DXA lumbar spine and proximal femoral BMD scans of typical patients are delineated by the upper and lower dotted curves, while the central dashed curve denotes the DXA BMD inaccuracies pertaining for the case of uniformly composed extraosseous tissue $(q - Q) = 0$ within the scan ROI. Positive % inaccuracies overestimate the true BMD; negative BMD % inaccuracies are underestimates.

volumetric densities,[23] ρ_f and ρ_L, to obtain the mean F-to-L areal density ratios, q and Q, and the $(q - Q)$ difference (positive and/or negative). In doing so, all nonfat tissues (internal organs, muscle tissue, etc.) present in the scan ROI were assigned the same volumetric density and linear X-ray attenuation coefficients of lean muscle tissue.[23] In this way, the difference between the average extraosseous F-to-L areal density ratio lateral to the bone and that along each notional X-ray path intersecting bone mineral material in the ROI $(q - Q)$ was obtained.

Because no transverse sections of particularly obese or exceedingly slender persons were depicted in the above noted anatomical atlases, the *overall* A/P torso and hip thicknesses of the full range of patients presenting for DXA BMD scans were not represented. To obtain the $(q - Q)$ value for any given q value that might reasonably be anticipated clinically, various A/P uniform fat layers were notionally added or removed from the depicted "normal" cross-sectional anatomical atlas slices, and new overall resultant q, Q, and $(q - Q)$ values were simply derived from them in each case. Because adult weight gain (loss) largely results from the accretion (loss) of subcutaneous (and/or visceral) fat, the thickness of the fat added (lost) seems to be spread relatively uniformly across the local scan ROI when viewed in A/P projection DXA BMD measurements of supine patients. On this basis, extrapolations from the "normal" 20-cm-thick cross-sectional atlas slices were transformed into reasonably realistic representations of A/P torso thicknesses ranging from 16 to 28 cm, effectively covering the full range of F-to-L areal density ratios and A/P torso thicknesses encountered clinically. These estimates of inhomogeneous fat distributions in the lateral and bone-shadow segments of DXA scans of these bone sites were found to be contained within the limits $-0.10 \leq (q - Q) \leq +0.03$ in most cases, for all q values pertaining to A/P lumbar spinal and proximal femoral DXA scan regions of most patients presenting for BMD measurement.

RESULTS

The percentage inaccuracies found in the present DXA-measured BMD scans using Norland XR-26, Hologic QDR-1000, and Lunar DPX-α densitometers were effectively

indistinguishable for each of the "anthropometrically" different 225 phantom arrays, as was also the case in our earlier phantom studies.[23] The results of the present investigation need therefore be displayed for any single densitometer (arbitrarily selected here for our Norland data only). Because the full span of the $(q - Q)$ differences DXA scanned and simulated in the present study may not be encountered clinically, the percentage BMD inaccuracies (Eq. 2) displayed in Figs. 2–4 are largely restricted to those data and results corresponding to anthropometric factors [q, Q, $(q - Q)$, g, and $(BMD)_{true}$] anticipated to be clinically relevant for adult patients (some results outside these ranges are also included to elucidate the trends and extent of inherent DXA BMD percentage inaccuracies that could result from whatever inhomogeneities in extraosseous soft tissue values, $(q - Q)$, might pertain, or be introduced, in some research or clinical studies). These data also make clear the sensitivity of the percentage BMD inaccuracies to inhomogeneous anthropometric and X-ray absorptiometric aspects of the various intra- and extraosseous soft tissues.

Also displayed in Figs. 2–4 are those demarcations of the limits $[-0.10 \leq (q - Q) \leq +0.03]$ found in the present investigation to reasonably represent the range of extraosseous soft tissue areal density ratio differences $(q - Q)$ encountered in actual A/P DXA lumbar spine and proximal femoral BMD scans of typical patients. For example, in the particular case of an osteopenic individual [$(BMD)_{true} = 0.8$ g/cm^2] with a marrow composition 80% yellow ($g = 0.8$) and a lateral F-to-L areal density ratio $q = 0.3$, a DXA-measured BMD value may well underestimate the true BMD by between ~14% [$(BMD)_{meas} \approx 0.69$ g/cm^2] and ~23% [$(BMD)_{meas} \approx 0.62$ g/cm^2], leading to possible misdiagnosis of this patient as osteoporotic. For an osteoporotic individual, $(BMD)_{true} = 0.6$ g/cm^2, with the same soft tissue compositions (Fig. 2), the underestimates of the true BMD value range between ~19% [$(BMD)_{meas} \approx 0.49$ g/cm^2] and ~31% [$(BMD)_{meas} \approx 0.41$ g/cm^2].

It is also seen (Figs. 2–4) that the red/yellow marrow compositional effect (g-dependence) on DXA-measured BMD inaccuracies still pertains, no matter the value of q, Q, $(q - Q)$, or $(BMD)_{true}$.

DISCUSSION

The extent of these inaccuracies have been quantitatively delineated on a foundation of anatomically realistic phantom representation of in vivo soft tissue and bone anthropometrics and X-ray absorptiometrics relevant to the broad range of patients presenting for clinical DXA BMD scan procedures. Of particular importance, the present study has extended the earlier quantitative expositions[20–24] of DXA in vivo BMD inaccuracies to those more anatomically realistic cases in which the extraosseous fat and lean soft tissue mix is not uniform throughout the scan ROI. In particular, it has been shown here that the values of the extraosseous fat-to-lean soft tissue areal density ratios lateral to and in the bone-shadow regions, and their differences, $(q - Q)$, in the *local* bone site DXA scan ROI are anthropometric parameters directly relevant to and affecting the extent of BMD inaccuracies manifest in DXA-derived in

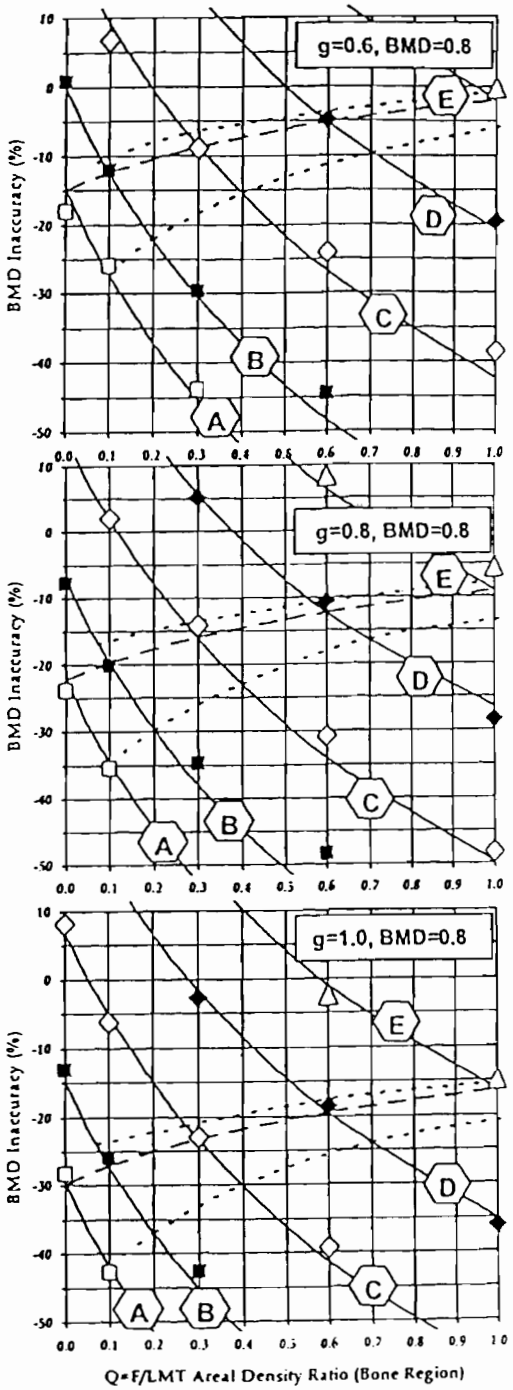

FIG. 3. DXA BMD inaccuracy results (%) obtained for a set of 75 different phantom arrays similar to those of Fig. 2, but for the case of *true* BMD = 0.8 g/cm^2. (Other relevant descriptive details given in caption of Fig. 2.)

vivo measurements. This is of some clinical importance, because it is clear that fat and lean tissues are not distributed uniformly throughout the body, and that the general distribution of soft tissues and accretion/loss of extraosseous fat is significantly different for children and adults, men and women, and pre and postmenopausal women.[43] Further-

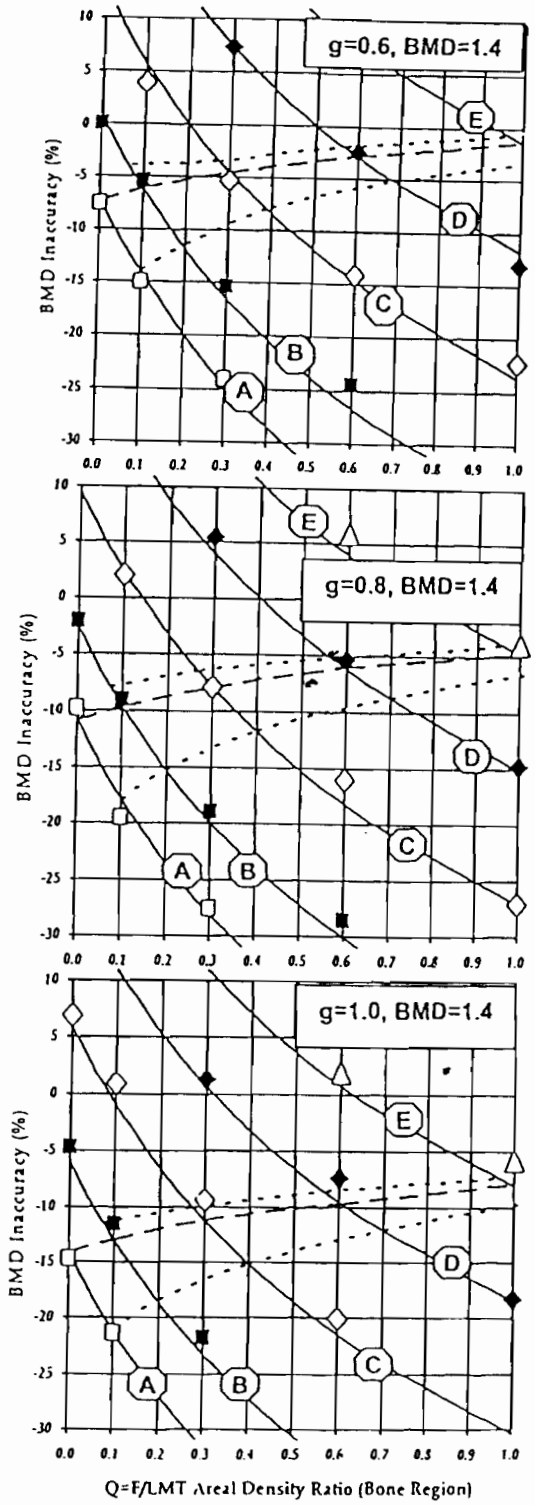

FIG. 4. DXA BMD inaccuracy results (%) obtained for a set of 75 different phantom arrays similar to those of Figs. 2 and 3, but for the case of *true* BMD = 1.4 g/cm^2. (Other relevant descriptive details given in caption of Fig. 2.)

more, the specific local bone-site F-to-L areal density ratio in the scan ROI may vary, sometimes considerably, as a function of age, physical condition, bone site, and other external factors such as the specific boundaries selected for the scan ROI. If the lateral segments of the ROI defining the extraosseous soft tissue areal density, q, can be varied by the DXA operator (or are DXA instrument dependent), somewhat different values for q and $(q - Q)$ could pertain for scans of a given bone site, thereby altering the effective BMD inaccuracy and the measured value of BMD. As such, measures of patient whole body fat-mass/total body-mass/body mass index, although indicative, may not necessarily be reliable or dependable descriptors of particular *local* bone site F-to-L areal density ratios within the scan ROI. Just as q is bone-site dependent, so too can be the quantity $(q - Q)$. In addition to other scan particulars, the relevant q and $(q - Q)$ values can also differ in A/P, lateral, and other DXA scan projections of the same bone site, leading to different BMD inaccuracies and, therefore, different measured BMD values. (It is noted here that the present study, by design, was unaffected by bone-edge detection concerns or uncertainties related to bone alignment relative to incident X-ray paths.)

It is also seen that within reasonable limits of extraosseous soft tissue disparity and composition (Figs. 2–4), the inherent $(BMD)_{meas}$ inaccuracies in patient-specific DXA in vivo measurements can readily be expected to exceed 20% in clinically realistic cases. Particularly for osteoporotic patients (low true BMD), for postmenopausal and elderly individuals (marrow tending to higher yellow content in the lumbar vertebrae and proximal femoral regions),[37,38] and for nonobese and lean patients (moderate and low relative fat content within and surrounding the lean tissues within the DXA scan ROI), the inaccuracies in DXA-derived BMD measurements can be quite large (30–50%). As a result, patient-specific DXA-measured in vivo BMD values can be seriously in error, more often than not considerably underestimating the true BMD of the very patients whose BMD it is most important for DXA to assess accurately. Given the reported 2-fold increase in population-based fracture risk per each SD decrement in BMD,[44] these sizable inaccuracies can be seen to insinuate confounding aspects into the clinical assessments of patient-specific fracture risk and diagnoses of osteoporosis based on the simple T-score criterion (T-score < -2.5).

As a consequence of the inability of planar DXA methodology to assess the absorptiometrics of both the extraosseous F-to-L areal density ratio in the bone-shadow region, Q, and the bone marrow, g, (one of the most labile of body tissues),[36–38,45–47] the inaccuracies in DXA-measured in vivo BMD values may be both large and unpredictable in any given patient case. This is as expected, because the presence of marrow, irrespective of its specific red/yellow mix, g, effectively modifies the overall soft tissue areal density ratio (combined intra- and extraosseous tissues) along all X-ray paths traversing marrow within any given scanned bone. The marrow composition (largely affected through hematopoietic activity) can vary with patient age, disease, drug therapy, immobilization, physical activity regimen, bed confinement, infection, etc. This is the case particularly in the vertebrae and proximal extremities of appendicular bones where hematopoietic activity can be quite variable.[18,37,38,45,46] Similarly, the extraosseous fat-

to-lean muscle tissue areal density ratio in the ROI of DXA BMD scans of patients can separately alter as a result of dietary regimens, hormonal changes, drug therapy, exercise programs, illness, etc. Consequently, changes in the soft tissue parameters, with or without accompanying true changes in bone mineral material, can be reflected in changes in DXA-measured BMD that may mislead interpretations of prospective BMD measurements of individual patients. Indeed, all DXA-measured in vivo BMD values will reflect this variability to some unknown extent, and as a result, may lead to interpretations and evaluations of diagnostic, prognostic, longitudinal, or cross-sectional BMD measurements that are seriously flawed.

In this context, it is important to stress that it is not the overall thickness or the difference in the linear thicknesses of fat alone or of lean tissues alone (or the linear extent of the body section alone) in either or both segments of the scan ROI (lateral to the bone and in the bone-shadow) that are relevant to the magnitude of inherent inaccuracies in DXA in vivo BMD measurements. Rather, it is the overall F-to-L areal density ratio, q, and the effective difference between the F-to-L areal density ratios (q and Q) along X-ray paths through the scan ROI that is of consequence. Thus, the local bone-site ratio of the F-to-L masses along the X-ray paths, and not the overall patient fat mass or lean mass or body mass singly, is the relevant soft tissue anthropometric parameter affecting DXA-measured in vivo BMD values. It is on these grounds that previous conflicting reports[48–61] specifying patient fat mass rather than body lean mass (and vice versa) to be the soft tissue parameter correlated strongly with DXA-measured BMD may be resolved, because neither one of these anthropometric quantities alone underpins the inherent DXA in vivo BMD inaccuracies from which these ostensible BMD correlations arise.

It is clear that when *true* BMD decreases, the bone must be more fragile to some extent (effectively the definition of "osteoporosis"). However, the present results have shown equally clearly that because of the sizable inherent, patient-specific DXA in vivo BMD measurement inaccuracies demonstrated here and in earlier works,[14–24,30] a decrease (increase) in measured BMD may not necessarily signal any change in the bone fragility for a given *individual*. As a consequence of demonstrated large inherent systematic patient-specific DXA in vivo BMD inaccuracies, it is of utmost importance that it be recognized that DXA-*measured* BMD and *true* BMD are not necessarily synonymous. It is also difficult not to conclude from this and past investigations that introspective review and critical assessment of those aspects of present consensual knowledge of in vivo bone fragility and bone responsiveness to treatment based primarily on DXA BMD measurements are very much warranted.

ACKNOWLEDGMENTS

This research was supported in part by Grant 202011 of the National Health and Medical Research Council (Australia) and the Research Fund of Tampere University Hospital (Finland).

REFERENCES

1. Cooper C, Campion C, Melton LJ III 1992 Hip fractures in the elderly: A worldwide projection. Osteoporos Int 2:285–289.
2. Poulsen LW, Qvesel D, Brixsen K, Verterby A, Boldsen JL 2001 Low bone mineral density in the femoral neck of medieval women: A result of multiparity? Bone 28:454–458.
3. Kannus P, Niemi S, Parkkari J, Palvanen M, Vuori I, Järvinen M 1999 Hip fractures in Finland between 1970 and 1997 and predictions for the future. Lancet 353:802–805.
4. Genant HK, Engelke K, Fuerst T, Glueer C-C, Grampp S, Harris S, Jergas M, Lang T, Lu Y, Majundar S, Mathur A, Takada M 1992 Noninvasive assessment of bone mineral and structure: State of the art. J Bone Miner Res 11:707–730.
5. Dunn L, Wahner HW 1994 Commercial instruments available for bone mineral measurements. In: Wahner HW, Fogelman I (eds.) The Evaluation of Osteoporosis: Dual Energy X-ray Absorptiometry in Clinical Practice. Martin Dunitz, Ltd., London, UK, pp. 35–48.
6. Wahner HW, Dunn WL, Brown ML, Morin RL, Riggs BL 1988 Comparison of dual-energy X-ray absorptiometry for bone mineral measurements of the lumbar spine. Mayo Clin Proc 63:1075–1084.
7. Jergas M, Breitneseher M, Gluer C-C, Yu W, Genant HK 1995 Estimates of volumetric bone density from projectional measurements improve the discriminatory capability of dual X-ray absorptiometry. J Bone Miner Res 10:1101–1110.
8. Hansen MA, Overgaard K, Riis BJ, Christiansen C 1991 Role of peak bone mass and bone loss in postmenopausal osteoporosis: 12 year study. BMJ 30:961–964.
9. Hui SL, Slemenda CW, Johnston CC 1989 Baseline measurement of bone mass predicts fracture in white women. Ann Intern Med 114:355–361.
10. Marshall D, Johnell O, Wedel H 1996 Meta-analysis of how well measures of bone mineral density predict occurrence of osteoporotic fracture. BMJ 312:1254–1259.
11. Cummings SR, Black DM, Nevitt MC, Browner W, Cauley J, Ensrud K, Genant HK, Palermo L, Scott J, Vogt TM for the Study of Osteoporotic Fractures Research Group 1993 Bone density at various sites for prediction of hip fracture. Lancet 341:72–75.
12. Hui SL, Gao S, Zhou X-H, Johnston CC, Lu Y, Gluer C-C, Grampp S, Genant HK 1997 Universal standardization of bone density measurements: A method with optimal properties for calibration among several instruments. J Bone Miner Res 12:1463–1470.
13. Faulkner KG 2000 Bone matters: Are density increases necessary to reduce fracture risk? J Bone Miner Res 15:183–187.
14. Webber CE 1987 The effect of fat on bone mineral measurements in normal subjects with recommended values of bone, muscle, and fat attenuation coefficients. Clin Phys Physiol Meas 8:143–148.
15. Sorenson JA 1990 Effects of nonmineral tissues on measurements of bone mineral content by dual-photon absorptiometry. Med Phys 17:905–912.
16. Tothill P, Pye DW 1992 Errors due to non-uniform distribution of fat in dual X-ray absorptiometry of the lumbar spine. Br J Radiol 65:807–813.
17. Tothill P, Avenell A, Reid RM 1994 Precision and accuracy of measurements of whole-body bone mineral: Comparisons between Hologic, Lunar and Norland dual energy absorptiometers. Br J Radiol 67:1210–1217.
18. Kuiper JW, Van Kuijk C, Grashuis JL, Ederveen AGH, Schutte HE 1996 Accuracy and influence of marrow fat on quantitative CT and dual-energy X-ray absorptiometry measurements of the femoral neck in vitro. Osteoporos Int 6:25–30.
19. Antonacci MD, Hanson DS, Hegeness MH 1996 Pitfalls in the measurement of bone mineral density by dual energy X-ray absorptiometry. Spine 21:87–91.
20. Bolotin HH 1998 Analytic and quantitative exposition of patient-specific systematic inaccuracies inherent in planar DXA-derived in vivo BMD measurements. Med Phys 25:139–151.
21. Bolotin HH 1998 A new perspective on the causal influence of soft tissue composition on DXA-measured in vivo bone mineral density. J Bone Miner Res 13:1739–1746.
22. Bolotin HH 1998 A new perspective on the effects of body weight and body fat mass on DXA-measured in vivo bone-mineral density. Osteoporos Int 8:514.
23. Bolotin HH, Sievänen H, Grashuis JL, Kuiper JW, Järvinen 2001 Inaccuracies inherent in patient-specific dual-energy X-ray absorp-

tiometry bone mineral density measurements: Comprehensive phantom-based evaluation. J Bone Miner Res 16:417–426.
24. Bolotin HH, Sievänen 2001 Inaccuracies inherent in dual-energy X-ray absorptiometry in vivo bone mineral density can seriously mislead diagnostic/prognostic interpretation of patient-specific bone fragility. J Bone Miner Res 16:799–805.
25. Formica C, Loro M-L, Gilsanz V, Seeman E 1995 Inhomogeneity in body fat distribution may result in inaccuracy in the measurement of vertebral bone mass. J Bone Miner Res 10:1504–1511.
26. Farrell TJ, Webber CE 1989 The error due to fat inhomogeneity in lumbar spine bone mineral measurements. Clin Phys Physiol Meas 10:57–64.
27. Lochmüller E-M, Eckstein F, Kaiser D, Zeller JB, Landgraf J, Puts R, Steldinger R 1998 Prediction of vertebral failure loads from spinal and femoral dual-energy X-ray absorptiometry and calcaneal ultrasound: An in situ analysis with intact soft tissue. Bone 23:417–424.
28. Svendsen OL, Hassager C, Skodt V, Christiansen C 1995 Impact of soft tissue on in vivo accuracy of bone mineral measurements in the spine, hip, and forearm: A human cadaver study. J Bone Miner Res 10:868–873.
29. Bjarnason K, Hassager C, Svendsen OL, Stang H, Christiansen C 1996 Anteroposterior and lateral spinal DXA for the assessment of vertebral body strength: Comparison with hip and forearm measurement. Osteoporos Int 6:37–42.
30. Bolotin HH 2001 Inaccuracies inherent in dual-energy X-ray absorptiometry in vivo bone mineral densitometry may flaw osteopenic/osteoporotic interpretations and mislead assessment of antiresorptive therapy effectiveness. Bone 28:548–555.
31. Hangartner TN, Johnston CC 1990 Influence of fat on bone measurements with dual-energy absorptiometry. Bone Miner 9:71–81.
32. Cullum ID, Ell PJ, Ryder JP 1989 X-ray dual-photon absorptiometry: A new method for measurement of bone density. Br J Radiol 62:587–592.
33. Hassager C, Jensen SB, Gotfredsen A, Christiansen C 1991 The impact of measurement errors on the diagnostic value of bone mass measurements: Theoretical consideration. Osteoporos Int 1:250–256.
34. White DR, Martin RJ, Darlison R 1977 Epoxy resin tissue substitutes. Br J Radiol 50:814–421.
35. Wang J, Heymsfield SB, Aulet M, Thornton JC, Pierson RN Jr 1989 Body fat from body density: Underwater weighing vs. dual-photon absorptiometry. Am J Physiol 256:E829–E834.
36. Dunnill MS, Anderson JA, Whitehead R 1967 Quantitative histological studies on age change in bone. J Pathol Bacteriol 94:275–291.
37. Custer 1974 An Atlas of the Blood and Bone Marrow. Saunders, Philadelphia, PA, USA, pp. 33–42.
38. Glowacki J 1995 Influence of age on human marrow. Calcif Tissue Int 35(Suppl 1):S50–S51.
39. Spitzer VM, Whitlock DG 1998 National Library of Medicine Atlas of the Visible Human Male: Reverse Engineering of the Human Body. Jones and Bartlett Publishers, Sudbury, MA, USA.
40. Ellis H, Logan B, Dixon A 1991 Human Cross-Sectional Anatomy: Atlas of Body Sections and CT Images. Butterworth-Heinemann Ltd., Oxford, UK.
41. Cahill DR, Orland MJ, Miller GM, Bland JM, Altman DG 1995 Atlas of Human Cross-Sectional Anatomy with CT and MR Images. 3rd ed. Wiley-Liss, New York, NY, USA.
42. Wahner HW, Steiger P, von Setten E 1994 Instruments and measurements techniques. In: Wahner HW, Fogelman I (eds.) The Evaluation of Osteoporosis: Dual Energy X-Ray Absorptiometry in Clinical Practice. Martin Dunitz, Ltd., London, UK, pp. 14–34.
43. Ley CJ, Lees B, Stevenson JC 1992 Sex- and menopause-associated changes in body-fat distribution. Am J Clin Nutr 55: 950–954.
44. Riggs BL, Melton LJ III 1992 The prevention and treatment of osteoporosis. N Engl J Med 327:620–627.
45. Ricci C, Cova M, Kang YS, Yang A, Rahmouni A, Scot WW, Zerhouni EA 1990 Normal age-related pattern of cellular and fatty bone marrow distribution in the axial skeleton MR Imaging study. Radiology 177:83–88.
46. Mazess RB 1983 Errors in measuring trabecular bone by computed tomography due to marrow and bone composition. Calcif Tissue Int 35:148–152.
47. Minaire P, Edouard C, Arlot M, Meunier PJ 1984 Marrow changes in paraplegic patient. Calcif Tissue Int 36:338–340.
48. Compston JE, Laskey MA, Croucher PL, Coxon A, Kreitzman S 1992 Effect of diet-induced weight loss on total body bone mass. Clin Sci (Lond) 82:429–432.
49. Harris SS, Dawson-Hughes B 1996 Weight, body composition, and bone density in postmenopausal women. Calcif Tissue Int 59:428–432.
50. Hystup L, Andersen T, McNair P, Breum L, Trasbol I 1993 Bone metabolism in obesity: Changes to severe overweight and dietary weight reduction. Acta Endocrinol 129:393–398.
51. Ravn P, Cizza G, Bjarnason H, Thompson F, Daley M, Wasnich RD, McClung M, Hosking D, Yates AJ, Christiansen C for the Early Postmenopausal Intervention Cohort (EPIC) Study Group 1999 Low body mass index is an important risk factor for low bone mass and increased bone loss in early postmenopausal women. J Bone Miner Res 14:1622–1627.
52. Jensen LB, Quaade F, Sorensen OH 1994 Bone loss accompanying voluntary weight loss in obese humans. J Bone Miner Res 9:459–461.
53. Reid IR, Evans MC, Ames RW 1994 Volumetric bone density of the lumbar spine is related to fat mass but not lean mass in normal postmenopausal women. Osteoporos Int 4:362–367.
54. Bevier WC, Wiswell RA, Pyka G, Kozak KC, Newhall KM, Marcus R 1989 Muscle strength, physical fitness and weight, but not age predict femoral neck bone mass. J Bone Miner Res 4:441–448.
55. Chen Z, Lohman TG, Stini WA, Ritenbaugh C, Aickin M 1997 Fat or lean tissue mass: Which is the major determinant of bone mineral mass in healthy postmenopausal women? J Bone Miner Res 12:144–152.
56. Glauber HS, Vollmer WM, Nevitt MC, Ensrud KE, Orwoll ES 1995 Body weight versus body fat distribution, adiposity, and frame size as predictors of bone density. J Clin Endocrinol Metab 80:1118–1123.
57. Liel Y, Edwards J, Shary J, Spicer KM, Gordon L, Bell NH 1988 The effects of race and body habitus on bone mineral density of the radius, hip and spine in premenopausal women. J Clin Endocrinol Metab 66:1247–1250.
58. Pritchard JE, Nowson CA, Wark JD 1996 Bone loss accompanying dietary induced or exercise induced weight loss: A randomized controlled study. Int J Obes Relat Metab Disord 20:513–523.
59. Reid IR, Plank LD, Evans MC 1992 Fat mass is an important determinant of whole body bone density in premenopausal women but not in men. J Clin Endocrinol Metab 75:779–782.
60. Slemenda CW 1995 Body composition and skeletal density: Mechanical loading or something more? J Clin Endocrinol Metab 80:1761–1763.
61. Revilla M, Vill LF, Sanchez-Atrios A, Hernandez ER, Rico H 1997 Influences of body mass index on the age-related slope of total regional bone mineral content. Calcif Tissue Int 61:1345–1348.

Address reprint requests to:
HH Bolotin, PhD, DSc, FRSV, FAIP
School of Medical Sciences
RMIT University
Bundoora, Victoria 3083, Australia
E-mail: herb.bolotin@rmit.edu.au

Received in original form July 31, 2002, in revised form December 12, 2002; accepted December 16, 2002

Eur. Radiol. 7 (Suppl. 2), S32–S42 (1997)

European Radiology

Quantitative computed tomography at the axial and peripheral skeleton

G. Guglielmi[1], P. Schneider[2], T.F. Lang[3], G.M. Giannatempo[1], M. Cammisa[1], H.K. Genant[3]

[1]Department of Radiology, Scientific Institute, Hospital "CSS", I-71013 San Giovanni Rotondo (FG), Italy
[2]Clinic for Nuclear Medicine, University of Würzburg, Germany
[3]Department of Radiology, University of California, San Francisco, California, USA

Introduction

Quantitative computed tomography (QCT) is an established technique for measuring BMD in the axial spine and appendicular (forearm, tibia) skeleton [1–3]. Because it provides cross-sectional images, QCT is unique amongst methods of measurement in providing separate estimates of trabecular and cortical bone BMD as a true volumetric mineral density in g/cm^3. In this application, QCT has been used for assessment of vertebral fracture risk [4, 5], measurement of age-related bone loss [6–8], and follow-up of osteoporosis and other metabolic bone diseases [9]. The goals of this commentary are to assess the current capabilities of QCT at different skeletal sites as well as the recent technical developments including fast three-dimensional data acquisition and high resolution image acquisition and processing techniques, which may novel information about bone strength through analysis of trabecular microarchitecture.

Spinal QCT

The greatest advantages of spinal QCT for noninvasive bone mineral measurement lie in the high responsiveness and biomechanical importance of vertebral trabecular bone as well as in the large worldwide distribution of CT scanners (estimated 40, 000 worldwide). The method is usually applied to the spine to measure trabecular bone in consecutive vertebrae (usually 2 to 4 vertebrae out of T12 to L4) using commercial CT scanners and a bone mineral reference standard to calibrate each scan. Based on an initial lateral localized image, single 8–10 mm thick sections are obtained through the midplane of each of these vertebrae using a low-dose technique and the gantry angled parallel to the vertebral endplates. A region of interest (ROI) is manually positioned in the anterior portion of trabecular bone of the vertebral body for analysis [4, 10–12] (Fig. 1). In some approaches, this region of interest may be positioned automatically [13, 14]. For optimal reproducibility, the selection of scan plane and ROIs should be performed using computer-assisted localization to provide separate BMD measurements of trabecular bone, the cortical rim of the vertebral body, and integral bone [13, 14]. Care must be taken to exclude the basivertebral vein and sclerotic foci. The CT density of the selected area of interest within a slice through a vertebral body is measured in Houndsfield units (HU) (also known as CT number) where water = 0 HU and air = –1000 HU. Conversion to g/cm^3 is made by comparing the CT number of the trabecular bone to that of the compartments of the calibration standard. The calculated densities for the vertebrae are averaged and compared to those of a normal population [7, 10, 15]. Liquid calibration reference phantoms (e.g., the Cann-Genant standard) were initially used containing varying concentrations of dipotassium hydrogen phosphate (K_2HPO_4) [4]. Use of this type of phantom has a drawback of limited long-term stability of the solutions. Thus solid hydroxyapatite calibration phantoms have also come into widespread use.

Simultaneous calibration corrects to some extent for scanner instabilities, as well as for variable beam hardening depending on patient size and shape. Non-simultaneous calibration, in which an anthropomorphic tissue equivalent phantom is scanned after the patient, has also been investigated [16].

Recently some studies reported promising results on a new QCT technique in which paraspinal muscle and subcutaneous fat served for internal calibration [17, 18], however, only limited studies have been carried out to date.

The results from different types of calibration phantoms may not yield the same results and in longitudinal studies it is essential that the same reference phantom is used [19]. It is possible to change from a liquid to a solid calibration standard only if normative data are adjusted by a cross-calibration analysis [20–22]. Follow up measurements for a given individual subject should al-

Correspondence to: G. Guglielmi

124. Slemenda CW, Johnson CC (1988) Bone mass measurement: which site to measure. Am J Med 84: 643–645
125. Need AG, Nordin BEC (1990) Which bone to measure. Osteoporos Int 1: 3–6
126. Ross PD, Wasnich RD, Heilbrun LK, Vogel JM (1987) Definition of spine fracture threshold based upon prospective fracture risk. Bone 8: 271–278
127. Cummings SR, Black DM, Nevitt MC, Browner WS, Cauley JA, Genant HK, Mascioli SR, Scott JC, Seeley DG, Steiger P, Vogt TM and the Study of Osteoporotic Fracture Group (1990) Appendicular bone density and age predict hip fracture in women. J Am Med Assoc 263: 665–668
128. Black DM, Cummings SR, Genant HK (1992) Axial and appendicular bone density predict fractures in older women. J Bone Miner Res 6: 633–638
129. Cummings SR, Black DM, Nevitt MC, Browner W, Cauley J, Ensrund K, Genant HK, Palermo L, Scott J, Vogt TM for the study of Osteoporotic Fracture Research Group (1993) Bone density at various sites for prediction of hip fractures. Lancet 341: 72–75
130. Gardsell P, Johnell O, Nilsson BE, Gullberg B (1993) Predicting various fragility fractures in women by forearm densitometry: a follow-up study. Calcif Tissue Int 52: 348–353
131. Parfitt AM (1990) Interpretation of bone densitometry measurements; disadvantages of a percentage scale and a discussion of some alternatives. J Bone Miner Res 5: 537–540
132. World Health Organisation (1994) Assessment of fracture risk and its application to screening for postmenopausal osteoporosis. Technical report series 843, World Health Organization, Geneva
133. Kroger H, Heikkinen J, Laitinen K, Kotaniemi A (1992) Dual energy X-ray absorptiometry in normal women: a cross-sectional study of 717 Finnish volunteers. Osteoporos Int 2: 135–140
134. Looker AC, Wahner HW, Dunn WL, Calvo MS, Harris TB, Heyse SP, Johnston CC, Lindsay RL (1995) Proximal femur bone mineral levels of US adults. Osteoporos Int 5: 389–409
135. Simmons A, O'Doherty MJ, Barrington SF, Coakley AJ (1995) A survey of dual-energy X-ray absorptiometry (DEXA) normal reference ranges used within the UK and their effect on classification. Nucl Med Commun 16: 1041–1053
136. Dequeker J, Pearson J, Reeve J, Henley M, Bright J, Felsenberg D, Kalender W, Laval-Jeantet AM, Ruegsegger P, Adams J et al (1995) Dual-energy X-ray absorptiometry – cross-calibration and normative reference ranges for the spine; results of a European Community Concerted Action. Bone 17: 247–254
137. Pearson J, Dequeker J, Reeve J, Felsenberg D, Henley M, Bright J, Lunt M, Adams J, Diaz Curiel M, Galan F et al (1995) Dual energy X-ray absorptiometry of the proximal femur: normal European values standardised with the European Spine Phantom. J Bone Miner Res 10: 315–324
138. Pearson J, Ruegsegger P, Dequeker J, Henley M, Bright J, Reeve J, Kalender W, Felsenberg D, Laval-Jeantet AM, Adams JE et al (1995) European semi-anthropomorphic phantom for the cross-calibration of bone densitometers: assessment of precision, accuracy and stability. Bone Miner 27: 109–120
139. Ross PD, Davis JW, Wasnick RD, Vogel JM (1991) The clinical application of serial bone mass measurements. Bone Miner 12: 189–199
140. Verheij LF, Blokland JA, Papapoulos SE, Zwinderman AH, Pauwels EK (1992) Optimization of follow-up measurements of bone mass. J Nucl Med 33: 1406–1410
141. Gluer CC, Blake G, Lu Y, Blunt BA, Jergas M, Genant HK (1995) Accurate assessment of precision errors: how to measure the reproducibility of bone densitometry techniques. Osteoporos Int 5: 262–280
142. Wilson CR, Collier D, Carrera GF, Jacobson DR (1990) Acronym for dual-energy X-ray absorptiometry. Radiology 176: 875
143. Genant HK, Gluer CC, Faulkner KG, Majumdar S, Harris ST, Engelke K, van Kuijk C (1992) Acronyms in bone densitometry (letter). Radiology 184: 878

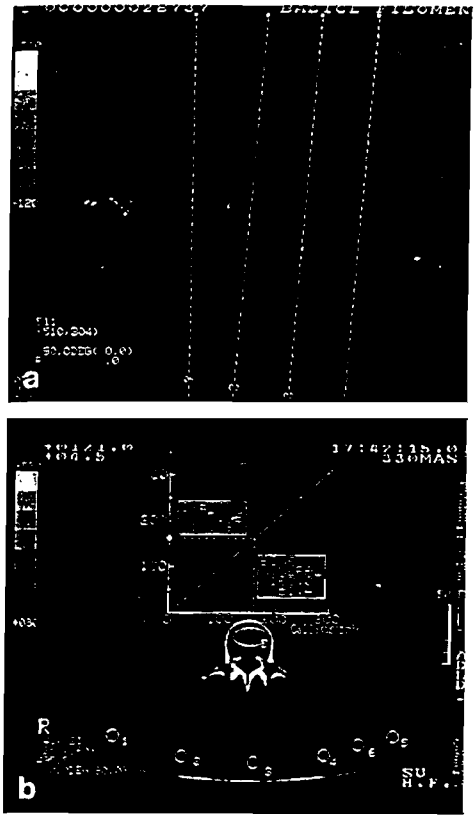

Fig. 1. a Quantitative Computed Tomography (QCT) of the lumbar spine. A lateral scout view is used to localize vertebrae. b An elliptical region of interest (ROI) including only trabecular bone, is used to determine vertebral bone mineral density (BMD). A mineral reference phantom based on calcium carbonate ($CaCO_3$), is part of the normal procedure to determine BMD

ways be carried out using the same phantom. If this cannot be done, duplicate measurement on the old and new standard need to be carried out on the same day to determine the offset.

The examination takes approximately 10–15 min and the effective dose is 60 μSv including 30 μSv for the location image.

QCT can be performed in single-energy (SEQCT) or dual-energy (DEQCT) modes, which differ in accuracy, precision, and radiation [23, 24). The presence of marrow fat within trabecular bone may cause the standard SEQCT technique to underestimate BMD by 10%–15% [25]. Provided that QCT scan are acquired at low effective energies (i.e. 80–90 kVp) the clinical relevance of the fat error is usually small however, given the use of age matched databases [26]. DEQCT techniques have been devised using either pre or postprocessing methods [27, 28]. Such techniques may improve accuracy, but with the penalty of poorer precision and practice [29, 30].

The in vivo precision and accuracy errors of QCT are approximately 2–4% and 4–15%, respectively [9, 24] and are generally higher than those observed for posteroanterior DXA of the spine and comparable with those of lateral DXA. However, QCT's ability to selectively assess the metabolically active and structurally important trabecular bone in the vertebral centrum results in the excellent ability to discriminate vertebral fracture and to measure bone loss, generally with better sensitivity than projectional methods such as DXA or DPA [6, 31–34].

Comparison of QCT and DXA

QCT has been shown to discriminate better between healthy women and those with osteoporosis than posteroanterior DXA [5]. To increase the sensitivity of DXA it has been suggested that BMD be measured with the patient in the lateral decubitus position [35]. There are several reasons for measuring bone mineral from a lateral projection in the vertebral body. Firstly, calcium deposition in the abdominal aorta, as well as degenerative and hypertrophic changes around the facet joints of the posterior compact bone elements of the vertebra (which are included in the standard PA spine scan), are projected outside the region of interest. Moreover, degenerative changes along the end plates, such as Schmorl's and Junghans's nodes and osteophytes, can often be excluded. Secondly, bone composition is not uniform throughout the vertebra. The vertebral body is the site of osteoporotic fractures, and its composition is predominantly trabecular bone. On the other hand, the posterior elements of the vertebrae mainly contain cortical bone and it is well known that the posterior portion of the vertebra does not play an important role in osteoporotic vertebral fractures. Lastly, bone loss with age and disease differs in trabecular and cortical bone. In fact, in oophorectomized women, the rate of bone loss in trabecular bone of the anterior vertebral body measured with QCT was twice that in the total vertebra. For all the reasons mentioned, previous studies have measured BMD with lateral DXA (L-DXA) [36–38]. Other studies have compared BMD decrements measured by PA-DXA, L-DXA and QCT in normal subjects and those with vertebral fractures [5, 6, 32, 39]. In a cross-sectional study of 108 postmenopausal women, Guglielmi et al. measured overall bone loss rates of 1.96%/year with QCT compared with 0.97%/year and 0.45%/year, respectively, for L-DXA and PA-DXA [6].

In summary, the great advantage of QCT over other densitometry methods is its ability to measure exclusively the high turnover trabecular bone. This accounts for the high sensitivity of the technique. Therefore, several authors have considered QCT as the method of choice in predicting fracture risk in the spine.

Measurement of BMD using volumetric CT images of the spine and hip

Spinal QCT is based on two-dimensional analysis of the trabecular bone compartment in 5 or 10-mm thick axial slices through the lumbar mid vertebral bodies. Although the single-slice approach is useful for spinal BMD quantification, three-dimensional approaches are optimal for analysis of highly complex structures, such

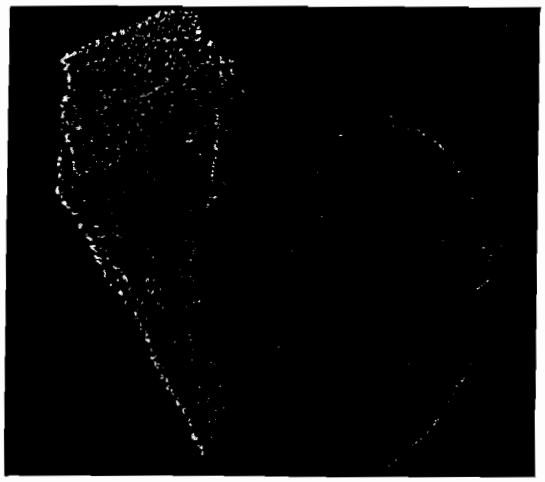

Fig. 2. Three-dimensional isosurface reconstruction of a femoral specimen, showing an intertrochanteric volume of interest overlaid on the data

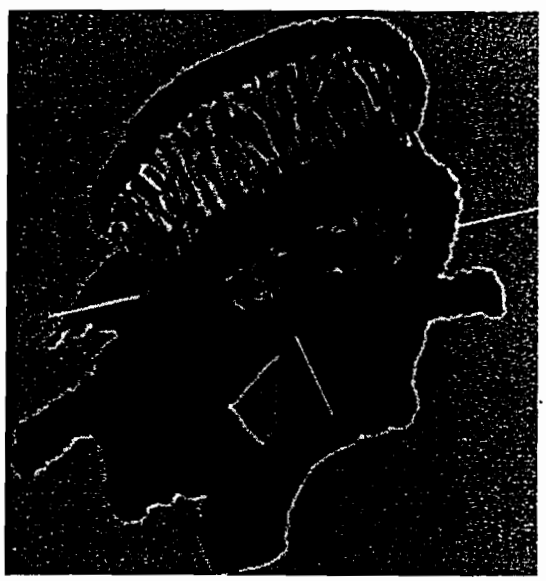

Fig. 3. Three dimensional isosurface reconstruction of a L1 vertebral body of a postmenopausal female volunteer. A region of interest encompassing most of the integral bone in the vertebral body (excluding endplates) is overlaid on the data

as the proximal femur. These volumetric techniques encompass the entire object of interest either with stacked-slice or spiral CT scans and can employ anatomic landmarks to automatically define coordinate systems for reformatting of the CT data into anatomically relevant projections.

Currently, quantitative analysis of the proximal femur is based on DXA technology, which provides an integral bone mass measurement which is normalized by the projected area, resulting in a size-dependent areal BMD [40, 41]. Extension of QCT to the proximal femur is desireable for both diagnostic and serial studies in that this technique can sample the highly-responsive trabecular bone compartment as well as provide a true volumetric density measurement.

Development of hip QCT techniques have been hindered by the acquisition time required to encompass the hip with a large number of slices, and by the need for specialized workstations capable of handling the large volume of image data. However, with the advent of helical CT systems equipped with inexpensive and powerful workstations, these obstacles have been greatly reduced, and femoral volumetric QCT should be clinically feasible, given the existence of appropriate image processing techniques to reproducibly delineate volumes of interest in the proximal femur. Several researchers have examined automated algorithms to accomplish this. Heitz et al. [42] has developed an femoral-neck-fixed coordinate system operated in conjunction with a second-derivative-based edge detection technique to determine VOIs (volumes of interest), while Sartoris et al. [43] and Bhasin et al. [44] have employed threshold-driven edge detection methods to isolate the entire compartment of trabecular bone in the proximal femur. Recently, Lang et al. [45] have presented an approach to semi-automatically define integral and trabecular VOIs in the femoral neck and intertrochanteric sub-regions (Fig. 2), as well as to measure geometric quantities such as the femoral neck cross-sectional area and cross-sectional moment of inertia. For trabecular BMD measurements, the in vivo precision of this method was found to range from 0.6 % to 1.1 % depending on the volume of interest assessed.

While there have relatively few efforts to develop proximal femur QCT for clinical use, a larger number of investigators have focused on establishing the relation between QCT measurements and biomechanical strength assessed in vitro. Several investigators have examined the relation between QCT density measures and femoral strength assessed in a loading configuration simulating a single-legged stance, and producing mostly fractures of the femoral neck [46–48]. In general, significant but relatively modest relationships ($r^2 = 0.4$–0.7) between BMD and femoral strength have been found [46–48]. Reasoning that most fractures are due to falls, Lotz and Hayes [49] developed a loading configuration which simulated a fall to the side, with impact on the posterolateral aspect of the greater trochanter. In this mode, which produced mostly intertrochanteric fractures, they measured a very high correlation of trabecular trochanteric BMD ($r^2 = 0.87$) with femoral strength. Lang et al. applied their analysis technique to scans of proximal femurs which were later fractured in both single-legged stance and fall-to-the-side modes [45]. These results confirmed those of Lotz and Hayes for trabecular BMD in the fall mode and found moderate correlations between BMD and single-legged stance fracture load, as did previous observers. However, when the stance-mode strength data were corrected for femoral-neck cross-sectional area and axis length, the BMD measurements (integral or trabecular) could explain $\simeq$ 90 % of the residual variance in the data.

Thus, based on good precision and strong correspondence of the BMD and geometry measurements to biomechnical strength measures, hip QCT shows potential for both diagnostic and serial assessments. The ad-

measures were adjusted for BMD, the difference was no longer statistically significant.

In summary, while the measures of trabecular structure described above may discriminate between fractured and non-fractured subjects, there is currently no evidence that these measures improve assessment of vertebral strength compared to BMD alone. This situation may change depending on technical improvements. In addition to diagnostic measurements, it is also of interest to explore the performance of these measures for longitudinal studies. It is possible that the representation of trabecular structure afforded by standard CT systems may be useful for clarifying the action of drug therapies.

Peripheral quantitative computed tomography

Technical aspects of pQCT

The two commercially distributed pQCT scanner types (XCT 900 and XCT 960, Stratec Electronic GmbH, Germany, and Densiscan, Scanco Medical, Switzerland), are second generation systems, using translate-rotate technique with a multi detector head for different acquisition angles. Only one (non-commercial) pQCT scanner prototype is known to use fan-beam rotation technique. Peripheral QCT scanners are generally limited to translate-rotate scanning technique due to the type of X-ray tubes that are desirable to be used. The tubes are operated in constant current mode without extensive cooling other than by an oil reservoir. The limited gantry space therefore also limits the size of the tubes [62]. The whole setup also has to meet stringent criteria considering the cost of the components [3, 62]. I-125 based systems became practically unimportant because of their limitations to objects of small diameters. Energy selection of the X-ray spectrum has to be adapted to the special requirements of quantitative bone scanning. Ideally, in a single energy mode it is found below 60 keV for best discrimination between fat/water and bone mineral. It has to be fairly above 30 keV because of the high absorption in thick tissue layers. Different filtering techniques are applied to achieve a small half band width of the spectrum (Fig. 4), such as a combination of Al, Cu and Ce [63–67]. Two-energy techniques in pQCT are practically not existing.

The calibration of pQCT systems is arbitralily. Several aspects may be considered. Bone consists of a certain amount of water and fat equivalent tissue and mineral compound. One may appropriately choose a ratio of fat/water simulating the relations in bone marrow. This usually leads to some type of resin for use as calibration material with different concentrations of hydroxyapatite added (Fig. 5). The resin may also be selected to simulate the density of water. In this case, true conditions may appear with negative mineral content, if bone marrow contains material less dense compared to water and the mineral content is very low. The calibration may also be based on dry bone. The Stratec machine uses the European Forearm Phantom (EFP)

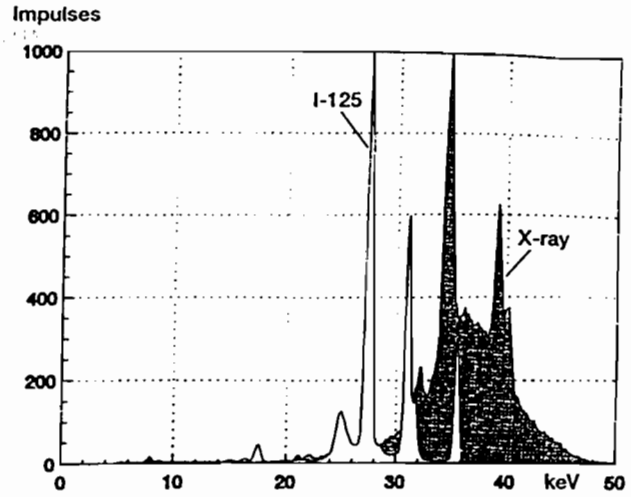

Fig. 4. Spectra of I-125 photon source and the X-ray source of the XCT 900, filtered with Al, Cu and Ce

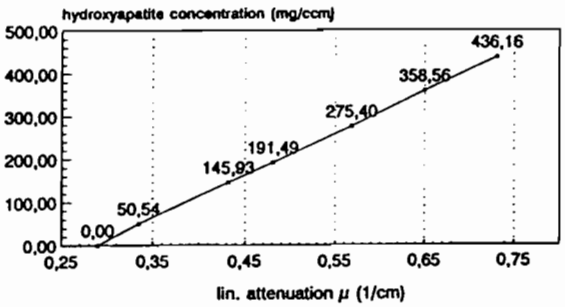

Fig. 5. Linearity of the XCT 900 pQCT system, calibrated with hydroxyapatite/resin phantoms

for calibration, which was developed for a multicenter trial [68, 69]. As this phantom uses water equivalent soft tissue simulating material, a calibration offset for the amount of fat found in vivo has to be added. In clinical use, accuracy does not play a significant role. However, for intercomparability, all systems must be equally calibrated or otherwise the exact offset must be known. Much different from planar absorptiometry systems, pQCT exhibited very high linearity within the range covered by the European Forearm Phantom and highly linear correction equations between the two pQCT systems of different manufacturers in the test [68, 69]. It should be noted that the difference between the XCT 900 device distributed in Europe and the XCT 960 system for the international distribution is only a 40 mg/ccm calibration offset. The XCT 960 is the only pQCT with an FDA approval. An increasingly important factor is the radiation exposure. Peripheral QCT has the lowest effective dose of all densitometric techniques (except SPA) exposing the forearm to 0.03 μSv, compared to 25 μSv of the abdomen scanned with axial QCT.

vent of helical CT systems and powerful but inexpensive computer workstations, in conjunction with the increased availability of CT scan time, should make this approach increasingly clinically attractive.

In the spine, the use of volumetric QCT measurements should impact precision more than discriminatory capability. Their potential to improve the precision of spinal measurements relates to the use of three-dimensional anatomic landmarks to guide the placement of volumes of interest and to the use of image alignment techniques to ensure that the volumes of interest are accurately repositioned in serial scans. Currently, single-slice QCT techniques are highly operator dependent, requiring careful slice positioning and angulation as well as careful ROI placement. In a volumetric approach, on the other hand, an image of the entire vertebral body is acquired, and the volumes of interest may be determined and repositioned in software. With a volumetric acquisition, it is possible to employ landmarks such as the vertebral endplates to determine the three-dimensional orientation of the vertebral body, thus removing the need for careful slice positioning by the operator, and improving the accuracy of the measurement in cases of pronounced lordotic or scoliotic curvature. It is also possible to define new trabecular and integral VOIs which contain most of the bone in the vertebral centrum, as shown in Fig. 3. Although measuring a larger volume of tissue may enhance precision, these new regions are highly correlated with the mid-vertebral sub-regions assessed with standard QCT techniques [50] and may not contain significant new information about vertebral strength. Consequently, volumetric studies of regional BMD, which examine specific sub-regions of the centrum [51] that may vary in their contribution to vertebral strength, and studies of the cortical shell [52], the condition of which may be important for vertebral strength in osteoporotic individuals, are of interest for future investigation.

High resolution imaging of trabecular micro-architecture using CT

The goal of high resolution CT techniques is to assess the arrangement of the trabeculae rather than the bone mass or density. Although the mean BMD assessed in a volume of interest is an important determinant of bone strength, there is evidence that the architecture of the trabeculae and the thickness of the cortical shell are determinants as well. Research approaches to assess the trabecular network involve both adaptation of existing clinical CT systems (spatial resolution $\simeq$ 500–700 μ) to this task as well as development of ultra-high-resolution μCT systems (20–200 μ) for scanning of bone specimens or of the peripheral skeleton, particularly at the distal radius and phalanges. This section will focus on the adaptation of existing body CT scanners for high-resolution measurements.

Several investigators have hypothesized that the status of the vertebral microarchitecture should be reflected in measurements of regional BMD. Sandor et al. presented a technique [53, 54] in which the trabecular bone in the mid-vertebral centrum was subdivided into small regions arranged in a radial pattern similar to a spider's web. BMD showed a characteristic regional distribution with maxima situated at the lateral and anterior portions of the vertebral body. These maxima showed the highest age-related BMD loss. Cody and Flynn developed a technique which assessed regional BMD [51, 55] in volumetric images of the vertebral body by distributing 18 cylindrical regions of interest through the vertebral centrum. These sub-volumes had high inter-correlations, and there was no specific regions which was more sensitive than the others in vertebral fracture prediction. However, in a later analysis, Flynn found that pattern classification methods [56] identified vertebral architectural density patterns that potentially provide enhanced fracture discrimination.

Reasoning that a high variation of the grey-scale values inside the QCT ROI was indicative of a robust trabecular architecture, Braillon et al. [57] suggested using the standard deviation of the BMD values as a parameter reflective of the trabecular structure in the lumbar vertebral bodies. Engelke et al. [58] applied this approach to 218 women, including both normal and vertebrally-fractured subjects. However, the results did not support the contention that the standard deviation could be used to improve vertebral fracture assessment over BMD alone. However, if higher radiation doeses and higher magnifications are employed to improve depiction of the trabecular structure than this technique may show more promise.

High-resolution thin-slice tomography performed with standard body CT scanners may be employed to better resolve the trabecular network. Such images typically have pixel sizes of 0.18–0.3 mm and slice thicknesses of 1–1.5 mm. The depiction of the trabeculae is limited by the spatial resolution of these systems, typically around 600 μ and the low radiation doses involved. While this imaging approach does not accurately represent the trabecular structure (trabecular thickness $\approx$ 100–150 μ and spacing $\approx$ 500–700 μ), it may be possible to extract some measures of trabecular texture. However, the results may vary substantially according to which image processing technique is used. Some investigational work using thin slice tomography has been published recently by Chevalier et al. [59]. They measured a feature termed the trabecular fragmentation index (length of the trabecular network divided by the number of discontinuities) to separate osteoporotic subjects from normal subjects. However, this index did not readily separate post menopausal osteoporotic women with vertebral fractures from normal or osteopenic subjects. A similar trabecular texture analysis approach was also reported by Ito et al. [60]. Wang et al. [61] applied a textural analysis (BV/TV, I.Th, N.Br) to a group of osteopenic women ($T_{DXA\ spine\ or\ hip} < -2.5$), containing a subset of vertebrally-fractured subjects. They found that these textural measures were moderately correlated to trabecular BMD ($r^2 = 0.55$–0.75), and also discriminated fractured and non-fractured subjects ($p < 0.03$), as did BMD. However, when the textural

Table 1. Reported in vivo and in vitro precision of pQCT devices for trabecular bone density in human bones, measured in mg/cm³

Authors	Precision CV %	Device	Method
Schneider [63]	1.7	SCT900	in vivo
Reiners [87]	0.8–1.5	SCT900	in vivo
Hosie [67]	1.26	SCT900	in vivo
Grampp [88]	0.9–2.1	XCT960	in vivo
Hangartner [89]	0.57	Prototyp	in vivo
Hosie [67]	0.5	OSCAR	in vivo
Wapniarz [90]	0.9	XCT900	in vitro
Guglielmi [91]	0.23	XCT900/ XCT960	in vitro

Precision of pQCT

According to the different purposes of pQCT scanners, the precision meets different levels. If time consuming multi-slice examinations are performed, a stack of consecutively spaced CT slices allows precise detection of the bone volume scanned at a previous session, provided that no modelling drift has changed the bone volume. This technique is based on a comparison of the cross sectional area, which is assumed to remain the same at the same cross section in relation to the bone axis. An interpolation algorithm allows fine-adjustment of the density result and changes therefore. This technique is used in the Densiscan machine and few research prototypes. Principly, the Stratec machine is capable to perform multislice analysis with interpolative calculation of the results, based on the same method. This technique is mainly used in animal studies and research studies in humans. In regular clinical application only single slice evaluation is used, due to the shorter scanning time. Despite justified criticism due to inadequate use of the single slice mode which may result in reduced precision, comprehensive means were provided to control precise location of a single CT slice in repeat measurements. This process has recently been fully operator independantly automated. The precision that can be achieved manually by trained operators is sufficient for follow-up measurements in normal clinical use and comparable with all other densitometry techniques (Table 1). In rapidly progressing diseases, modelling drift is likely to change the investigated bone volume considerably over time. Then, more or less sophisticated approaches to relocate the measurement site will not represent the expected changes. Undoubtfully, the Densiscan machine provides the best published in vivo precision figures in the hand of few experts. It remains open, if that would hold true under the conditions of a wide spread use, comparable to that of the Stratec scanner systems. A new development which is currently under clinical evaluation, the XCT 3000 system, offers several improvements over it's predecessors XCT 900 and XCT 960, eliminating substantial differences compared to the Densiscan.

Clinical evaluation of the pQCT technology

First clinical results have been reported in a small number of patients [3]. The instrumentation allowed monitoring of very small changes in density of the appendicular trabecular bone. Consecutive work proved the usefulness of the method to monitor very small changes of bone mineral mass in short periods of time either pharmacologically induced [70] or due to disease [71]. Only few investigations documented the significance of pQCT in comparison to other densitometry methods [63, 64]. It should also be mentioned that the clinical results obtained with the Densiscan have never been verified by other investigators. This is particularly true for the hypothesis stating a bimodal frequency of bone loss in a relatively small number of women in early menopause [71]. One would expect here a normal distribution at a larger number of cases.

In epidemiological use there are further requirements to make the pQCT method: (a) valuable for the diagnosis of osteoporosis, (b) to have comparable results among different sites and (c) comparable between different brands of machines.

This has been well noticed by the end of the 80s, when also other densitometry techniques appeared to be less comparable between different manufacturers. For the pQCT there were only few investigations known to show age distribution of trabecular density values at the radius or at the tibia in arbitrarily defined populations. Even at the same bone, namely the distal radius, the measurement sites were not exactly comparable because of the large variation of the radius along the axis and the slightly different site the investigators had chosen to measure the CT-slices. Therefore, in context with a large multicenter trial (COMAC-B.M.E), the standardisation committee first had to agree on a standardized measurement site before the study could be attempted. The COMAC-B.M.E. study included 7 Stratec XCT 900 scanners, 1 Stratec SCT 900 scanner and 2 Densiscan units. To achieve intercomparability of the different scanners, first a phantom had to be designed [69]. The EFP spanned most of the bone density values occuring in the radiuses of human subjects, including osteoporosis. The outcome of the study showed several important aspects for peripheral densitometers. It appeared that the older SPA technology performed less well than pQCT with regard to linearity and stability [68]. By means of the EFP, multi center data could be cross-calibrated to achieve a larger normal data base for healthy individuals, resulting in the first multi center data base for pQCT [72]. Along with German multi center data of normals [73], reliable data bases became available for comparison in clinical use as well as for comparison with regional differences in bone mineral content. Within the COMAC-B.M.E. study sensitivity and specificity analysis was attempted between the normative data and selected groups of osteoporotic diseases. The non significant differences among ROC-analyses showed that pQCT performed equally well in discrimation of fracture cases (hip and spine) as did all other densitometry techniques. Peripheral QCT there-

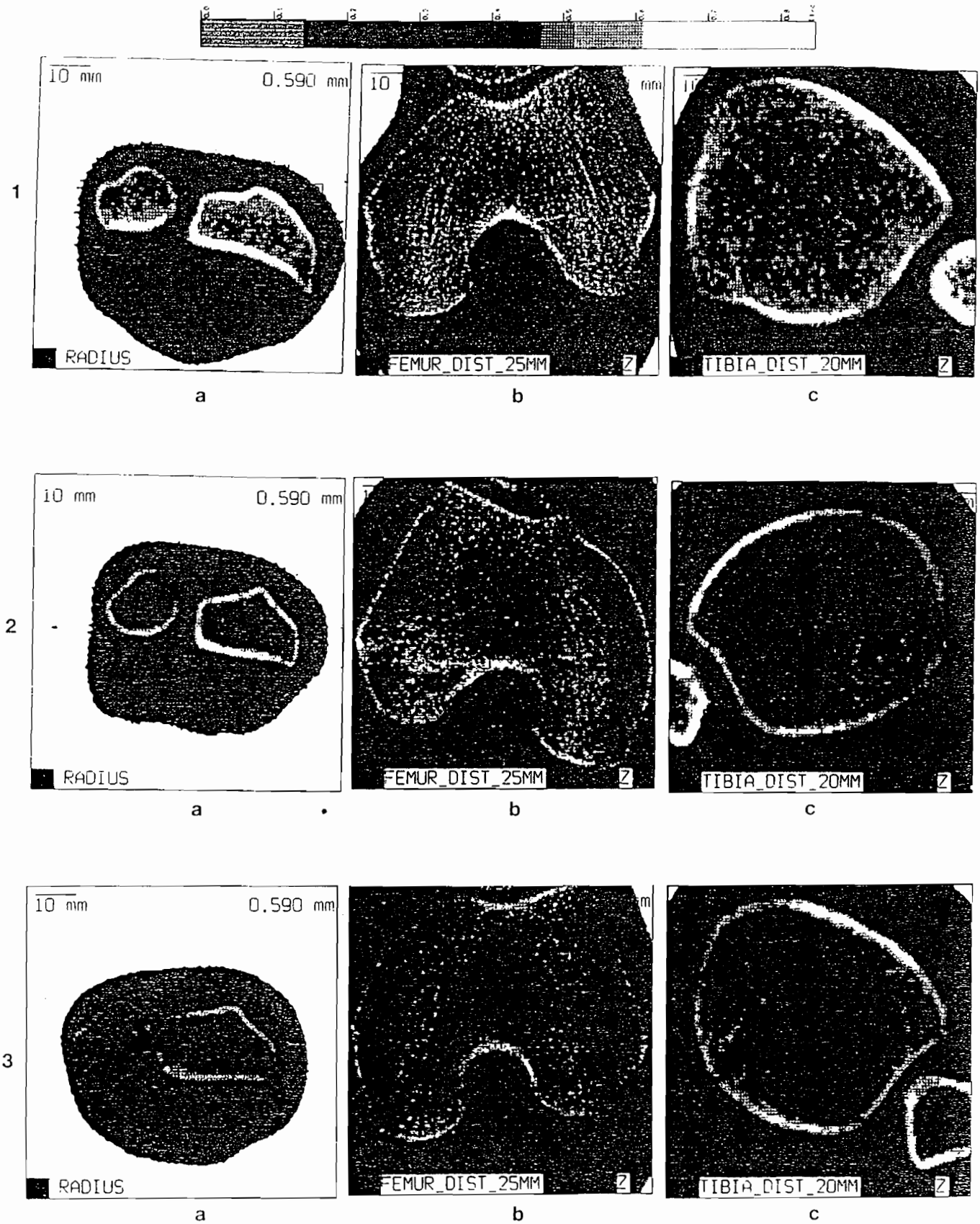

Fig. 6. Clinical examples of pQCT findings at **a** the distal forearm, **b** the distal femur, **c** the distal tibia in 1 a normal subject (24 y, female), 2 a patient with osteoporosis (70 y, female), 3 a patient with osteomalacia (72 y, female)

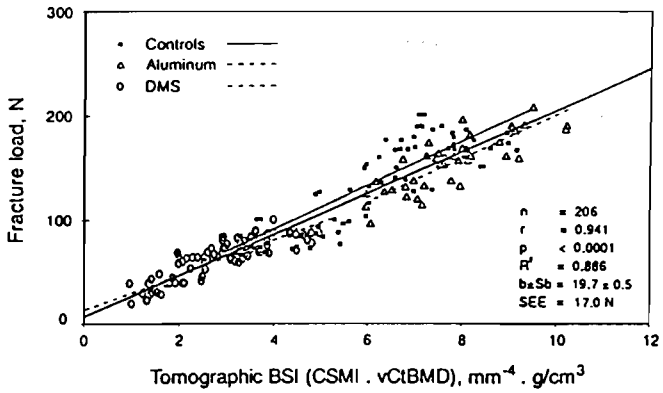

Fig. 7. Correlation between actual bending breaking force of rat femora either untreated (Controls) or treated with aluminum hydroxide (AL) or with dexamethasone (DMS) and the pQCT-assessed Bone Strength Index (BSI) (with kind approval from JL Ferretti). CSMI = cross sectional moment of inertia

fore may be the method of choice when evaluating generalized bone loss [74]. The ROC curves for the pQCT are very similar to the recent results of Takagi et al. [75]. Peripheral QCT has also impacted in the pediatric field and opened up a new clinical perspective in assessing bone mass and its development in children with different diseases [76, 77]. With new developments, such as the XCT 3000, investigations of further aspects of bone mineral and architectural changes at different sites using the same method (Fig. 6) are in progress.

Animal models assessed by pQCT

The specially built versions of the Stratec pQCT had a large impact on drug studies using animals. Predominantly pharmaceutical companies appreciated the advantages of the method [78, 79]. It was recognized that pQCT in small animals is an important addition to drug evaluation because it was found to be more sensitive than DXA and allows for shorter duration of experiments. This non-invasive method can reliably measure changes in cancellous and cortical bone mass in small animals over time. It should be viewed as a complimentary technique to static and dynamic histomorphometry, which does not replace either of these methods. A study of Sato et al. [80] showed a change of mineral density in a rat tibia to be 10 times larger as the precision of pQCT, whereas DXA failed due to edge detection problems. In the rat vertebra on the other hand, pQCT was unable to achieve acceptable precision in vivo due to positioning problems. In a study carried out by Jerome et al. [81] it was also reported that pQCT was potentially more sensitive than DXA, because it could seperate cancellous bone from cortical bone. Due to these results, pQCT potentially could allow the number of animals investigated and/or sacrificed to be reduced.

Noninvasive estimation of bone architecture

Different from all other methods, pQCT as a method capable of 3-dimensional imaging inherently bears the capability of providing information related to the architecture of bone. In addition, it allows to determine the material property by estimation of the bone mass per volume unit. It may hence be applied to noninvasive estimation of bone mechanical properties at organ level, beyond the possibilities of standard densitometry [82, 83]. Clinical application is currently evaluated by our group. Moreover, some sophisticated research machines even allow structural estimation at an almost microscopic level [84], simulating a noninvasive bone biopsy. Again, the wide spread use of the Stratec pQCT systems has opened part of these capabilities to a larger community of researchers. Excellent results have been obtained, correlating pQCT-assessed mechanical parameters, such as the second moment of inertia and it's derivatives (Fig. 7), with ultimate failure load [85]. Interesting in vivo correlations of noninvasively measured bone strength to clinically relevant fractures are to be expected. The most exciting advances are shown in pharmaceutical trials, demonstrating in vivo assessed changes of bone bending strength due to pharmacological interactions [86]. This approach is considered the most relevant with regard to desired improvement of the fracture threshold in individuals as the benefit of a drug application.

Conclusions

The introduction of pQCT has been the effort and the benefit of a small scientific community over the past 25 years. Successful commercialization has been achieved by researchers of Würzburg in cooperation with Stratec company. The measure for the high end at the technical side is still set by the Swiss group with Rüegsegger and coworkers, who also successfully commercialized their system. All groups together have set a new measure in densitometry, to overcome the restricted information provided by conventional techniques. The method is being widely used in health care systems in Europe and the Pacific Rim. It remains to be seen, based on the promising results in pharmaceutical research, whether it may also successfully take part in clinical trials and in the halth care system of North America, where DXA is still dominating.

The use of pQCT is very sensitive to immobilization and repositioning of the scanned object on one hand. On the other hand, it provides a look into separate bone compartments, offering more detailed variables as compared to any other densitometric method. At least in animal models, the first anticipations have been confirmed, that the look into metabolically more active bone compartments does provide earlier information about the onset of disease or therapy. There is no reason to believe that in humans different findings are to be expected.

References

1. Genant HK, Cann CE, Ettinger B, Gordan GS (1982) Quantitative computed tomography of vertebral spongiosa: a sensitive method for detecting early bone loss after oophorectomy. Ann Intern Med 97: 699–705
2. Guglielmi G, Glüer CC, Majumdar S, Blunt BA, Genant HK (1995) Current methods and advances in bone densitometry. Eur Radiol 5: 129–139
3. Rüegsegger P, Elsasser U, Anliker M, Gnehm H, Kind H, Prader A (1976) Quantification of bone mineralization using computed tomography. Radiology 121: 93–97
4. Cann CE, Genant HK (1980) Precise measurement of vertebral mineral content using computed tomography. J Comput Assist Tomogr 4: 493–500
5. Pacifici R, Rupich R, Griffin M, Chines A, Susman N, Avioli LV (1990) Dual energy radiography versus quantitative computed tomography for the diagnosis of osteoporosis. J Clin Endocrinol Metab 70: 705–710
6. Guglielmi G, Grimston SK, Fisher KC, Pacifici R (1994) Osteoporosis: diagnosis with lateral and posteroanterior dual X-ray absorptiometry compared with quantitative CT. Radiology 192: 845–850
7. Block JE, Smith R, Glüer CC, Steiger P, Ettinger B, Genant HK (1989) Models of spinal trabecular bone loss as determined by quantitative computed tomograhy. J Bone Miner Res 4: 249–257
8. Kalender WA, Klotz E, Süss C (1987) Vertebral bone mineral analysis: an integrated approach. Radiology 164: 419–423
9. Genant HK, Steiger P, Block JE, Glüer CC (1987) Quantitative computed tomography: Update 1987. Calcif Tissue Int 41: 179–186
10. Genant HK, Block JE, Steiger P, Glüer CC (1987) Quantitative computed tomography in the assessment of osteoporosis. In: Genant HK (ed) Osteoporosis update 1987. University of California Press, Berkeley, California, pp 49–71
11. Firooznia H, Golimbu C, Rafii M, Schwartz MS, Alterman ER (1984) Quantitative computed tomography assessment of spinal trabecular bone: II. In osteoporotic women with and without vertebral fractures. J Comput Tomogr 8: 99–103
12. Genant HK, Glüer CC, Steiger P, Faulkner KG (1992) Quantitative computed tomography for the assessment of osteoporosis. In: Computed Tomography of the body. Moss AA, Gamsu G, Genant HK (eds) Saunders, Philadelphia, pp 523–549
13. Kalender WA, Brestowsky H, Felsenberg D (1988) Bone mineral measurements: automated determination of the midvertebral CT section. Radiology 168: 219–221
14. Steiger P, Block JE, Steiger S, Heuck A, Friedlander A, Ettinger B, Harris ST, Glüer CC, Genant HK (1990) Spinal bone mineral density by quantitative computed tomography: effect of region of interest, vertebral level, and technique. Radiology 175: 537–543
15. Guglielmi G, Giannatempo GM, Blunt BA, Grampp S, Glüer CC, Cammisa M, Genant HK (1995) Spinal bone mineral density by quantitative computed tomography in a normal Italian population. Eur Radiol 5: 269–275
16. Cann CE (1987) QCT applications: comparison of current scanners. Radiology 162: 257–261
17. Boden SD, Goodenough DJ, Stockham CD, Jacobs E, Dina T, Allman RM (1989) Precise measurement of vertebra bone density using computed tomography without the use of an external reference phantom. J Digit Imag 2: 31–38
18. Gudmundsdottir H, Jonsdottir B, Kristinsson S, Johanesson A, Goodenough DJ, Sigurdsson G (1993) Vertebral bone density in Icelandic women using quantitative computed tomography without an external reference phantom. Osteoporos Int 3: 84–89
19. Suzuki S, Yamamuro T, Okumura H, Yamamoto I (1991) Quantitative computed tomography: comparative study using different scanners with two calibration phantoms. Br J Radiol 64: 1001–1006
20. Goodsitt MM (1992) Conversion relations for quantitative CT bone mineral density measured with solid and liquid calibration standards. Bone Miner 19: 145–148
21. Faulkner KG, Glüer CC, Grampp S, Genant HK (1993) Cross calibration of liquid and solid QCT calibration standards: corrections to UCSF normative data. Osteoporos Int 3: 36–43
22. Glüer CC, Engelke K, Jergas M, Hagiwara S, Grampp S, Genant HK (1993) Changes in calibration standards for quantitative computed tomography: recommendations for clinical practice. Osteoporos Int 3: 286–287
23. Genant HK, Boyd DP (1977) Quantitative bone mineral analysis using dual energy computed tomography. Invest Radiol 12: 545–551
24. Cann CE, Genant HK (1983) Single versus dual-energy CT for vertebral mineral quantification. J Comput Assist Tomogr 7: 551–552
25. Laval-Jeantet AM, Roger B, Bouysse S, Bergot C, Mazess RB (1986) Influence of vertebral fat content on quantitative CT density. Radiology 159: 463–466
26. Glüer CC, Genant HK (1989) Impact of marrow fat on accuracy of quantitative CT. J Comput Assist Tomogr 13: 1023–1035
27. Reinbold WD, Genant HK, Reiser UJ, Harris ST, Ettinger B (1986) Bone mineral content in early-postmenopausal osteoporotic women and postmenopausal women: comparison of measurements methods. Radiology 160: 469–478
28. Glüer CC, Reiser UJ, Davis CA, Rutt BK, Genant HK (1988) Vertebral mineral determination by quantitative computed tomography (QCT): accuracy of single and dual energy measurements. J Comput Assist Tomogr 12: 242–258
29. Pacifici R, Susman N, Carr PL, Birge SJ, Avioli LV (1987) Single and dual energy tomography analysis of spinal trabecular bone: a comparative study in normal and osteoporotic women. J Clin Endocrinol Metab 64: 209–214
30. Reinbold WD, Adler CP, Kalender WA, Lente R (1991) Accuracy of vertebral mineral determination by dual-energy quantitative computed tomography. Skeletal Radiol 20: 25–29
31. Cann CE, Genant HK, Kolb FO, Ettinger B (1985) Quantitative computed tomography for prediction of vertebral fracture risk. Bone 6: 1–7
32. Heuck A, Block J, Glüer CC, Steiger P, Genant HK (1989) Mild versus definitive osteoporosis: comparison of bone densitometry techniques using different statistical models. J Bone Miner Res 4: 891–899
33. Sambrook P, Barlett C, Evans R, Hesp R, Katz D, Reeve J (1985) Measurements of lumbar spine bone mineral: a comparison of dual photon absorptiometry and computed tomography. Br J Radiol 58: 621–624
34. Ross PD, Genant HK, Davis JW, Wasnich RD (1993) Predicting vertebral fracture incidence from prevalent fractures and bone density among non-black, osteoporotic women. Osteoporos Int 3: 120–126
35. Larnach TA, Boyd SJ, Smart RC, Butler SP, Rohl PG, Diamond TH (1992) Reproducibility of lateral spine scans using dual energy X-ray absorptiometry. Calcif Tissue Int 51: 255–258
36. Rupich R, Pacifici R, Griffin MG, Vered I, Susman N, Avioli LV (1990) Lateral dual energy radiography: a new method for measuring vertebral bone density: a preliminary study. J Clin Endocrinol Metab 70: 1768–1770
37. Slosman DO, Rizzoli R, Donath A, Bonjour JP (1990) Vertebral bone mineral density measured laterally by dual-energy X-ray absorptiometry. Osteoporos Int 1: 23–29
38. Reid IR, Evans MC, Stapleton J (1992) Lateral spine densitometry is a more sensitive indicator of glucocorticoid-induced bone loss. J Bone Miner Res 7: 1221–1225
39. Yu W, Glüer CC, Grampp S, Jergas M, Fuerst T, Wu CY, Lu Y, Fan B, Genant HK (1995) Spinal bone mineral assessment in postmenopausal women: a comparison between dual X-ray absorptiometry and quantitative computed tomography. Osteoporos Int 5: 433–439
40. Cummings S, Marcus R, Palermo L, Ensrud K, Genant HK (1994) Does estimating volumetric bone density of the femoral

neck improve the prediction of hip fracture? J Bone Miner Res 9: 1429–1432
41. Jergas M, Breitenseher M, Glüer CC, Yu W, Genant HK (1995) Estimates of volumetric bone density from projectional measurements improve the discriminatory capability of dual X-ray absorptiometry. J Bone Miner Res 10: 1101–1110
42. Heitz M, Kalender W (1994) Evaluation of femoral density and strength using volumetric CT and anatomical coordinate systems. Bone 25:S11
43. Sartoris DJ, Andre M, Resnick C, Resnick D (1986) Trabecular bone density in the proximal femur: quantitative CT assessment. Radiology 160: 707–712
44. Bhasin S, Sartoris DJ, Fellingham L, Zlatkin MB, Andre M, Resnick D (1988) Three-dimensional quantitative CT of the proximal femur: relationship to vertebral trabecular bone density in postmenopausal women. Radiology 167: 145–149
45. Lang T, Heitz M, Keyak J, Genant HK (1996) A 3D anatomic coordinate system for hip QCT. Osteoporos Int 6:S203
46. Esses SI, Lotz JC, Hayes WC (1989) Biomechanical properties of the proximal femur determined in vitro by single-energy quantitative computed tomography. J Bone Miner Res 4: 715–722
47. Alho A, Høiseth A, Torstein H (1989) Bone-mass distribution in the femur. Acta Orthop Scand 60: 101–104
48. Smith M, Cody DD, Goldstein S, Cooperman A, Matthews L, Flynn M (1992) Proximal femoral density and its correlation to fracture load and hip-screw penetration load. Clin Orthop 283: 244–251
49. Lotz JC, Hayes WC (1990) Estimates of hip fracture risk from falls using quantitative computed tomography. J Bone Joint Surg [Am] 72: 689–700
50. Lang T, Augat P, Heitz M, Genant HK (1996) Volumetric QCT of the Spine: comparison to single-slice QCT and DXA. J Bone Miner Res 11: 479
51. Cody DD (1991) Correlations between vertebral regional bone mineral density (rBMD) and whole bone fracture load. Spine 16: 146–154
52. Hangartner TN, Gilsanz V (1993) Measurement of cortical bone by computed tomography. Calcif Tissue Int 52: 160
53. Sandor T, Felsenberg D, Kalender W, Brown E (1991) Global and regional variations in the spinal trabecular bone: single and dual energy examinations. J Clin Endocrinol Metab 72: 1157–1168
54. Sandor T, Felsenberg D, Kalender W, Clain A, Brown E (1992) Compact and trabecular components of the spine using quantitative computed tomography. Calcif Tissue Int 50: 502–506
55. Cody DD, Flynn MJ, Vickers DS (1989) A technique for measuring regional bone mineral density in human lumbar vertebral bodies. Med Phys 16: 766–772
56. Flynn MJ, Cody DD (1993) The assessment of vertebral bone macroarchitecture with X-ray computed tomography. Calcif Tissue Int 53:S170–175
57. Braillon PM, Bochu M, Meunier PJ (1993) Quantitative computed tomography (QCT): a new analysis of bone quality in osteoporosis and osteomalacia. Calcif Tissue Int 52: 166
58. Engelke K, Grampp S, Glüer CC, Jergas M, Yang SO, Genant HK (1995) Significance of QCT bone mineral density and its standard deviation as parameters to evaluate osteoporosis. J Comp Assist Tomogr 19: 111–116
59. Chevalier F, Laval-Jeantet AM, Laval-Jeantet M, Bergot C (1992) CT image analysis of the vertebral trabecular network in vivo. Calcif Tissue Int 51: 8–13
60. Ito M, Ohki M, Hayashi K, Yamada M, Uetani M, Nakamura T (1995) Trabecular texture analysis of CT images in the relationship with spinal fracture. Radiology 194: 55–59
61. Wang X, Lang T, Heitz M, Ouyang X, Engelke K, Genant HK (1996) Comparison of spinal trabecular structure analysis and QCT spinal BMD: an in vivo, low-dose pilot study. J Bone Miner Res 11:S474
62. Hounsfield GN (1973) Computerized transverse axial scanning (tomography): Part 1. Description of System. Br J Radiol 46: 1016–1022
63. Schneider P, Börner W, Mazess RB, Barden H (1988) The relationship of peripheral to axial bone density. Bone Miner 4: 279–287
64. Stebler B, Rüegsegger P (1983) Kleincomputertomograph für quantitative Knochenuntersuchungen in den Extremitäten des Menschen. Biomedizinische Technik 28: 196–205
65. Rüegsegger P, Durand EP, Dambacher MA (1991) Localization of regional forearm bone loss from high resolution computed tomography images. Osteoporos Int 1: 76–80
66. Rüegsegger P, Durand EP, Dambacher MA (1991) Differential effects of aging and disease on trabecular and compact bone density of the radius. Bone 12: 99–105
67. Hosie CJ (1993) Measurements of trabecular bone density in the distal radius by two gamma ray computed tomography scanner. Physiol Meas 14: 269–276
68. Pearson J, Rüegsegger P, Dequeker J, Henley M, Bright J, Reeve J, Kalender W, Felsenberg D, Laval-Jeantet AM, Adams J, Birkenhäger JC, Fischer M, Geusens P, Hesch RD, Hyldstrup L, Jaeger P, Johnson R, Kröger H, Van Lingen A, Mitchel A, Reiners C, Schneider P (1995) European semianthropomorhic phantom for the cross-calibration of peripheral bone densitometers: assessment of precision, accuracy and stability. Bone Miner 27: 109–120
69. Rüegsegger P, Kalender W (1993) A phantom for standardization and quality control in peripheral bone measurements by pQCT and DXA. Phys Med Biol 38: 1963–1970
70. Hangartner TN, Overton TR, Harley CH, van den Berg L, Crockford PM (1985) Skeletal challenge: an experimental study of pharmacologically induced changes in bone density in the distal radius, using gamma-ray computed tomography. Calcif Tissue Int 37: 19–24
71. Müller A, Rüegsegger E, Rüegsegger P (1989) Peripheral QCT: a low-risk procedure to identify women predisposed to osteoporosis. Phys Med Biol 34: 741–749
72. Reeve J, Kröger H, Nijs J, Pearson J, Felsenberg D, Reiners C, Schneider P, Mitchell A, Rüegsegger P, Zander C, Dequeker J (1996) Radial cortical and trabecular bone densities standardized with the European Forearm Phantom. Calcif Tissue Int 58: 135–143
73. Schneider P, Butz S, Allolio B, Börner W, Klein K, Lehmann R, Petermann K, Tysarczyk-Niemeyer G, Wüster C, Zander C, Ziegler R, Reiners C (1995) Multicenter German reference data base for peripheral quantiative computer tomography. Technol Health Care 3: 69–73
74. Kröger H, Lunt M, Reeve J, Dequeker J, Adams JE, Birkenhager JC, Diaz-Curiel M, Felsenberg D, Hyldstrup L, Laval-Jeantet AM, Lips P, Louis O, Perez Cano R, Reiners C, Ribot C, Rüegsegger P, Schneider P, Braillon P, Pearson J (in press) Bone density reduction in various measurement sites in osteoporosis with fracture of spine and hip. The European quantitation of osteoporosis study. Osteoporos Int
75. Takagi Y, Fujii Y, Miyauchi A, Goto B, Takahashi K, Fujita T (1995) Transmenopausal change of trabecular bone density and structural pattern assessed by peripheral QCT in Japanese women. J Bone Miner Res 10: 1830–1834
76. Kruse K, Süss A, Büsse M, Schneider P (1987) Normal spongiosa density despite decreased secretion of monomeric calcitonin in children under anticonvulsant treatment with diphenylhydantoin and primidone. Acta Endocrinol 114: 53–54
77. Lettgen B, Jeken C, Reiners C (1994) Influence of steroid medication on bone mineral density in children with nephrotic syndrome. Pediatr Nephrol 8: 667–670
78. Rosen HN, Chen V, Cittadini A, Greenspan SL, Douglas PS, Mosese AC, Beamer WG (1995) Treatment with Growth Hormone and IGF-I in growing rats increases bone mineral content but not bone mineral density. J Bone Miner Res 10: 1352–1358
79. Gasser JA (1996) Assessing bone quantity by pQCT. Bone 17S:145–154
80. Sato M (1996) Comparative X-ray densitometry of bones from ovarectomized rats. Bone 17S:157–162

81. Jerome CP, Johnson CS, Lees CJ (1995) Effect of treatment for 3 months with human parathyroid hormone 1–34 pepetide in ovarectomized cynomolgus monkeys (Macaca fascicularis). Bone 17S:415–420
82. Faulkner KG, Glüer CC, Majumdar S, Lang P, Engelke K, Genant HK (1991) Non invasive measurements of bone mass, structure and strength. Current methods and experimental techniques. Am J Roentgenol 157: 1229–1237
83. Augat P, Reeb H, Claes LE (1996) Prediction of fracture load at different skeletal sites by geometric properties of the cortical shell. J Bone Miner Res 11: 1356–1363
84. Müller R, Hildebrand T, Rüegsegger P (1994) Non-invasive bone biopsy: a new method to analyse and display the three-dimensional structure of trabecular bone. Phys Med Biol 39: 145–164
85. Ferretti JL, Capozza RF, Mondelo N, Zanchetta JR (1993) Interrelationships between densitometric, geometric and mechanical properties of rat femora: inferences concerning mechanical regulation of bone modeling. J Bone Miner Res 8: 1389–1396
86. Ferretti JL, Gaffuri O, Capozza RF, Cointry G, Bozzini C, Olivera AM, Zanchetta JR, Bozzini CE (1995) Dexametasone effects on mechanical, geometric and densitometric proper of rat femur diaphyses as described by peripheral quantita computerized tomography and bending tests. Bone 16: 119-
87. Reiners C, Arnold B, Brust AS, Sonnenschein W (1990) Pr sion of bone mineral measurement with the new QCT scar Stratec SCT 900. J Nucl Med 31: 856–860
88. Grampp S, Lang P, Jergas M, Glüer CC, Mathur A, Engelk Genant HK (1995) Assessment of the skeletal status by qua tative peripheral computed tomography: short-term precis in-vivo and comparison to dual X-ray absorptiometry. J B Miner Res 10: 1566–76
89. Hangartner TN, Overton TR (1982) Quantitative meas ment of bone density using gamma-ray computed tomogra J Comput Assist Tomogr 6: 1156–1162
90. Wapniarz M, Lehmann R, Randerath R, Baedecker O, B decker S, John W, Klein K, Allolio B (1994) Precision of d X-ray absorptiometry and peripheral computed tomogra using mobile densitometry units. Calcif Tissue Int 54: 219–2
91. Guglielmi G, Giannatempo GM, Willnecker J, Cammisa (1996) Precision of peripheral QCT: impact on quality ass ance. Osteoporos Int 6: S81

Osteoporosis Int (1996) 6:43–49

Osteoporosis
International

Original Article

The Impact of Degenerative Conditions in the Spine on Bone Mineral Density and Fracture Risk Prediction

P. von der Recke[1], M. A. Hansen[1], K. Overgaard[2] and C. Christiansen[2]

[1]Department of Radiology, Glostrup Hospital, Glostrup; and [2]Center for Clinical and Basic Research, Ballerup, Denmark

Abstract. We examined the impact of degenerative conditions in the spine (osteophytosis and endplate sclerosis) and aortic calcification in the lumbar region on bone mineral content/density (BMC/BMD) measured in the spine and forearm by absorptiometry and on fracture risk prediction. The radiographs of 387 healthy postmenopausal women, aged 68–72 years, were assessed in masked fashion for the presence of osteophytosis, endplate sclerosis and aortic calcification in the region from L2 to L4. Vertebral deformities/fractures were assessed by different definitions. Osteophytes larger than 3 mm and in numbers of 3 or more resulted in a significantly (12%) higher spinal bone mass ($p<0.001$). Endplate sclerosis had a similar effect ($p<0.001$). In subjects with both degenerative conditions the BMC/BMD in the spine and forearm were significantly higher than in unaffected women (19% in the spine, 10% in the forearm; $p<0.001$). The spinal BMD values were significantly lower in fractured women if both degenerative conditions were absent ($p<0.001$), whereas fractured and unfractured women had similar values if degenerative conditions were present. Degenerative conditions did not alter the ability of forearm BMC to discriminate vertebral or peripheral fractures. Receiver operating characteristic (ROC) curves (true positive fraction versus false positive fraction) were generated for BMD of the lumbar spine and BMC of the forearm with regard to the discrimination between women with vertebral and peripheral fractures and healthy premenopausal women. The ROC curves for women without degenerative conditins were consistently above the curves for women affected by osteophytosis and endplate sclerosis in the lumbar spine ($p<0.001$). In conclusion, osteophytes and endplate sclerosis have a considerable influence on spinal bone mass measurements in elderly postmenopausal women and affect the diagnostic ability of spinal scans to discriminate osteoporotic women. Our data suggest that in elderly women, unless the spine is radiologically clear of degenerative conditions, a peripheral measurement procedure should be considered an alternative for assessment of bone mineral content/density.

Keywords: Bone densitometry; Degenerative conditions; Fracture risk; Osteophytosis; Osteoporosis

Correspondence and offprint requests to: Peter von der Recke, Center for Clinical & Basic Research, Ballerup Byvej 222, DK-2750 Ballerup, Denmark. Fax: 45 44 68 42 20.

Introduction

Osteoporosis is a major age-related disease affecting millions of women throughout the world. It is characterized by a decreased amount of bone and increased susceptibility to fracture. Bone mineral measurements in different skeletal areas are widely used to examine the future risk of osteoporotic fractures in postmenopausal women.

It has been intensely debated in which part of the skeleton the bone mass should be determined. The spinal bone mass seems to be more affected in several metabolic bone diseases than are areas with predominantly cortical bone [1,2] and osteoporotic patients often present with spinal crush fractures [2,3]. Measurements of the spinal bone mineral density (BMD), are, however, complicated because the vertebrae have an irregular shape and are surrounded by a thick layer of soft tissue. There is wide variability in body composition from one individual to another, and within the same

individual over time. Theoretically, degenerative conditions and aortic calcification in the area of interest may be other factors influencing the accuracy of spinal bone mass measurements.

A few studies have evaluated the influence of osteophytosis on spinal BMD with contradictory findings [4–8]. Two of these found in men that spinal osteophytosis gave falsely high values of BMD and thus camouflaged the extent of underlying osteoporosis [4,5]. In women, one study indicated no impact of osteophytosis on measurements of spinal BMD [6], whereas others have demonstrated the opposite [7,8]. The studies on aortic calcification, however, revealed consistently that this factor seems to have only minimal impact on BMD [4,9,10].

In the present study we reviewed previously published data [11] to investigate the influence of degenerative conditions in the region of the lumbar spine on spinal and forearm bone mineral content/density (BMC/BMD) in a large homogeneous group of elderly, otherwise healthy postmenopausal women. Furthermore, we examined the impact of these conditions on the discriminatory ability of bone mass measurements for osteoporotic fractures.

Materials and Methods

Subjects

We reviewed published data on a large study population of healthy postmenopausal women aged 68–72 years, applying an evaluation of degenerative conditions within the area of the lumbar spine. The women were recruited by questionnaires sent to all women in that age group residing in six municipalities near Glostrup Hospital. A total of 2009 questionnaires were sent out and 1522 were returned. In all, 788 fulfilled the primary selection criteria, which were: mobile; never suffering from coronary infarction, stroke, or malignancy; and not taking sex hormones or other drugs known to influence calcium metabolism. A total of 512 women attended a screening examination and of these a random sample of 387 women had a radiographic examination of the thoracolumbar spine [11].

A reference sample of 142 premenopausal women was included in the analysis. These women were healthy volunteers with no evidence of bone disease and no drug intake known to interfere with calcium metabolism. They were recruited during the same period as the target population.

Assessment of the Radiographs and Fractures

The participants were radiographed in the lumbar spine at the initial visit and 1 and 2 years. The lateral radiography was carried out under standardized conditions with a fixed film–focus distance of 1 m. All radiographs were assessed in masked fashion by the same experienced radiologist. The radiographs were evaluated independently for the presence of osteophytosis, endplate sclerosis and aortic calcification in the region from L2 to L4. Endplate sclerosis was registered as present or not and aortic calcification, if present, was registered as punctate or dense. The osteophytes were graded according to size (more or less than 3 mm) and numbers (from 1 to 6).

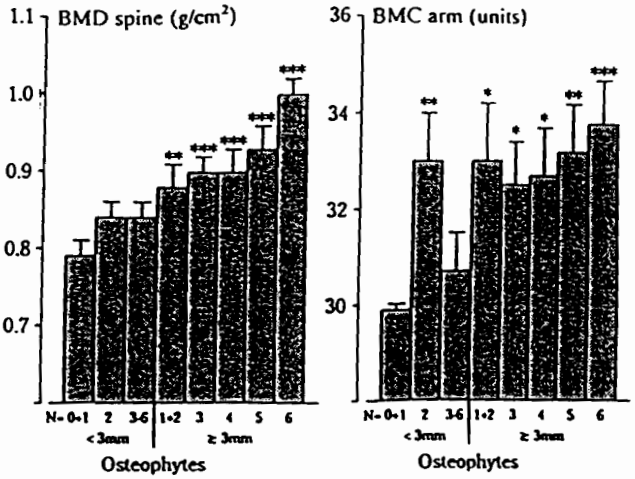

Fig. 1. Bone mineral density in the lumbar spine (BMDspine) and bone mineral content of the distal forearm (BMCarm) according to number (N) and size (<3 mm or ≥3 mm) of osteophytes (mean ± SEM). *$p<0.05$, **$p<0.01$, ***$p<0.001$ by analysis of covariance correcting for endplate sclerosis.

Figure 1 shows the spinal and forearm bone mass values according to numbers of osteophytes and size. Bone mass was generally unaffected by osteophytes smaller than 3 mm, whereas osteophytes above that size and in numbers of 3 or more resulted in a significantly higher bone mass both bone compartments ($p<0.001$). Only osteophytes of that size and quantity were therefore considered clinically significant.

Two quantitative methods – that of Kleerekoper et al. [12] and that of Melton et al. [13] – were used for assessment of the radiographs for vertebral deformities, and for both methods the anterior, midvertebral and posterior heights of the vertebrae were measured to the nearest millimetre by a transparent ruler. The intraobserver variation was 2.5% (range 1.5%–3.8%). In the method of Kleerekoper et al. [12] wedge deformities were basically defined as a reduction of at least 25% in anterior height as compared with posterior height; compression deformities had to have a reduction of at least 25% in posterior height as compared with that of adjacent vertebrae. In the method of Melton et al. [13] wedge and compression deformities were basically defined according to the same criteria as in the method of Kleerekoper et al. except that the reduction had to be at least 20%. Before these criteria were applied the height of each measurement was corrected by an adjustment factor that took into account the normal variation in vertebral shape and size throughout the spine between (1) the anterior and posterior heights and (2) the posterior heights and those of adjacent vertebrae.

The adjustments were based on data from 31 healthy early postmenopausal women who had no radiological evidence of vertebral deformities. Finally the radiographs were evaluated qualitatively by a traditional clinical assessment of atraumatic wedge or compression fractures. Peripheral fractures were ascertained through a medical history. All reported fractures were checked with medical records and the radiograph.

Measurement of Bone Mass

The BMD of the lumbar spine was measured by dual-energy X-ray absorptiometry (Hologic, model QDR-1000) [14]. This system uses a highly collimated dichromatic X-ray source (70 kVp and 140 HkV). The BMC is calculated in L2 to L4, including the intervertebral discs. BMC is expressed in grams after internal calibration, and BMD is calculated as BMC divided by the area of interest (g/cm^2). In our department the long-term precision in vivo is 1.5% [14]. The BMC of the distal forearm (BMCarm) was measured by single-photon absorptiometry with an ^{125}I source (3.7 GBq) with photopeak at 27 keV. In our department the long-term precision in vivo is 1% [15].

Statistical Analysis

Statistical analysis was performed using the statistical analysis system (SAS) program. The influence of endplate sclerosis, osteophytosis and aortic calcification on bone mass values was adjusted for body weight by analysis of covariance. The study population was divided into subgroups according to the presence of endplate sclerosis and/or osteophytes (presence of 3 or more osteophytes > 3 mm). Differences between subgroups in bone mass measurements were tested by one-way analysis of variance, and Student's *t*-test for paired and unpaired data was used when appropriate. All tests were two-tailed and $p<0.05$ was considered significant.

To compare the impact of degenerative changes on the discriminatory ability of different scanners, the individual BMC/BMD measurements were expressed in *T*-scores (i.e. differences between measurements expressed in standard deviations) relative to premenopausal women. In order to examine the impact of degenerative changes on discriminatory ability, receiver operating characteristic (ROC) curves [16,17] were generated for affected and unaffected women for both spinal and peripheral fractures. The ROC curve plots the true positive fraction (sensitivity) against the false positive fraction (1 − specificity) changing the cut-off level successively. The greater the area under the curve, the higher discriminatory ability between fractured and unfractured patients. The area under the ROC curves, standard errors and significance of differences of the area under the curves were calculated according to Hanley and McNeil [18,19].

Results

The gross morphology and values of bone mass measurements are given in Table 1 according to the presence of osteophytes, endplate sclerosis and aortic calcification. The groups were well matched with respect to morphology. The differences in spinal BMD between the women with and without osteophytosis and women with and without endplate sclerosis were 12% ($p<0.001$). The corresponding differences in forearm BMC constituted 8% for both the degenerative conditions ($p<0.001$). One hundred and fifty-eight women had aortic calcification alone, which did not affect bone mass at either of the two measuring sites. Body weight was lower in women with any of the three conditions than in women without ($p<0.01$). The data were therefore adjusted for weight, which did not significantly alter the results.

Figure 2 illustrates the relation of the spinal BMD and forearm BMC to the presence of osteophytosis and endplate sclerosis. Most women had both conditions ($n=137$), while 94 had endplate sclerosis alone and 32 women had osteophytes alone. In women with neither of the two degenerative conditions ($n=124$) the BMD values in the spine were 19% lower than in women with both conditions and 10% lower in the forearm ($p<0.001$), while women with either osteophytosis or endplate sclerosis had intermediate values. The 19%

Table 1. Gross morphology and baseline measurements of bone mass (mean±SD) according to degenerative conditions in the lumbar spine and aortic calcification

	Osteophytosis		Endplate sclerosis		Aortic calcification	
	Present	Absent	Present	Absent	Present	Absent
No. of patients	169	218	231	156	234	153
Height (cm)	160 ± 6	159 ± 6	160 ± 6	159 ± 6	159 ± 6	160 ± 6
Weight (kg)	68 ±11***	64 ±11	67 ±11*	64 ±11	65 ±11**	68 ±11
BMCarm (units)	33.6 ± 6.4***	30.9 ± 5.9	33.2 ± 6.4***	30.4 ± 5.7	31.6 ± 6.2	32.7 ± 6.3
BMDspine (g/cm^2)	0.95± 0.17***	0.82± 0.14	0.92± 0.18***	0.81± 0.13	0.87± 0.17	0.89± 0.17

BMCarm, bone mineral content of the distal forearm; BMDspine, bone mineral density of the lumbar spine.
*$p<0.05$, **$p<0.01$, ***$p<0.001$; Student's *t*-test for unpaired data.

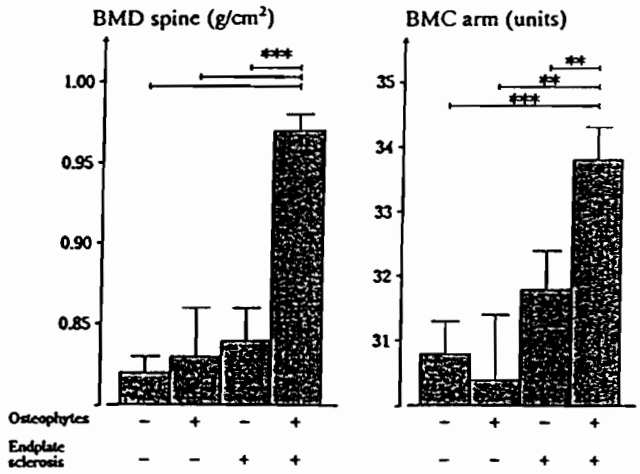

Fig. 2. Bone mineral density in the lumbar spine (BMDspine) and bone mineral content of the distal forearm (BMCarm) according to the existence of at least three osteophytes (≥3 mm in size) and/or endplate sclerosis (mean ± SEM). $^{*}p<0.05$, $^{**}p<0.01$, $^{***}p<0.001$ by analysis of covariance.

difference in the spine was significantly higher than the 10% difference in the forearm BMC ($p<0.001$).

Forty-two women had sustained a forearm fracture, 5 women a hip fracture and 9 women a humerus fracture. Defined by the method Melton et al. [13], the prevalence of spinal fractures was 16%; by the method of Kleerekoper et al. [12] 12%; and by clinical assessment 35%. Table 2 gives the spinal and forearm BMC/BMD values according to spinal fractures alone or in combination with peripheral fractures, and the presence of osteophytosis plus endplate sclerosis. The spinal BMD values were significantly lower in the group of women with fractures and without degenerative conditions ($p=0.001$), whereas fractured and unfractured women with the combination of osteophytosis and endplate sclerosis had similar values (NS). This was the case if the two quantitative methods (that of Kleerekoper et al. and that of Melton et al.) were used for the definition of spinal fractures, and both for spinal fractures alone and in combination with peripheral fractures. The presence of degenerative conditions did not affect the relation between BMC of the forearm and spinal fractures alone, whereas the forearm BMC was significantly lower in women with spinal plus peripheral fractures if degenerative conditions were not present ($p<0.01$–0.001). For clinically evaluated spinal fractures alone, the same pattern was seen for BMD of the spine, whereas the forearm BMC was significantly lower in fractured compared with non-fractured women regardless of degenerative conditions ($p<0.05$–0.001).

Figure 3 shows the ROC curves (true positive fraction versus false fraction) for BMD of the lumbar spine and BMC of the forearm with regard to the discrimination between women with spinal fractures (defined by the methods of Kleerekoper et al. and Melton et al.) or with peripheral fractures and healthy premenopausal women. For BMD of the lumbar spine, the curves for women without degenerative conditions were consistently above the curves for women affected by osteophytosis and endplate sclerosis in the area, for the discrimination of both spinal and peripheral fractures ($p<0.01$–0.001). For BMC of the distal forearm there was, however, no significant difference between women with and without degenerative conditions for the discrimination of fractures in general.

Discussion

In clinical research measurements of BMC/BMD are extensively used as a diagnostic tool and an index of skeletal response. Extraskeletal calcification has, however, been suggested to influence the measurement of BMC/BMD in the lumbar spine [4,5,7,8,20,21], but little has been published on its impact on the discriminatory ability of bone mass measurements for fractures. Studies in men have demonstrated that spinal osteophytosis gives falsely high values of spinal BMD and thus camouflages the extent of underlying osteoporosis [4,5].

Table 2. Relation between vertebral fractures (VF) (left) and VF plus peripheral fractures (PF) (right) and the presence of degenerative conditions (DC) in the lumbar spine, and spinal BMD and forearm BMC (mean ± SEM)

	DC	VF	*n*	BMDspine (g/cm²)	BMCarm (units)	VF+PF	*n*	BMDspine (g/cm²)	BMCarm (units)
Method of Kleerekoper et al. [12]	−	−	224	0.83±0.01	31.1±0.4	−	190	0.84±0.01	31.7±0.4
	−	+	26	0.78±0.03	30.8±1.1	+	60	0.78±0.02**	29.3±0.7**
	+	−	116	0.98±0.01	34.1±0.5	−	107	0.98±0.01	34.2±0.5
	+	+	21	0.91±0.03*	31.8±1.2	+	30	0.95±0.03	32.1±1.0
Method of Melton et al. [13]	−	−	213	0.84±0.01	31.3±0.4	−	182	0.84±0.01	31.9±0.4
	−	+	37	0.77±0.02**	30.2±0.9	+	68	0.78±0.02**	29.2±0.7***
	+	−	112	0.97±0.01	34.1±0.5	−	102	0.97±0.01	34.2±0.6
	+	+	25	0.96±0.03	32.7±1.1	+	35	0.99±0.03	32.6±1.0
Clinical assessment	−	−	164	0.84±0.01	31.7±0.4	−	140	0.85±0.01	32.2±0.5
	−	+	86	0.80±0.02*	30.1±0.6*	+	110	0.80±0.01**	29.8±0.5***
	+	−	89	0.98±0.02	34.9±0.6	−	81	0.97±0.02	35.0±0.6
	+	+	48	0.95±0.02	31.7±0.8**	+	56	0.97±0.02	31.9±0.8**

BMCarm, bone mineral content of the distal forearm; BMDspine, bone mineral density of the lumbar spine.
$^{*}p<0.05$, $^{**}p<0.01$, $^{***}p<0.001$; Student's *t*-test for unpaired data between fractured and unfractured women.

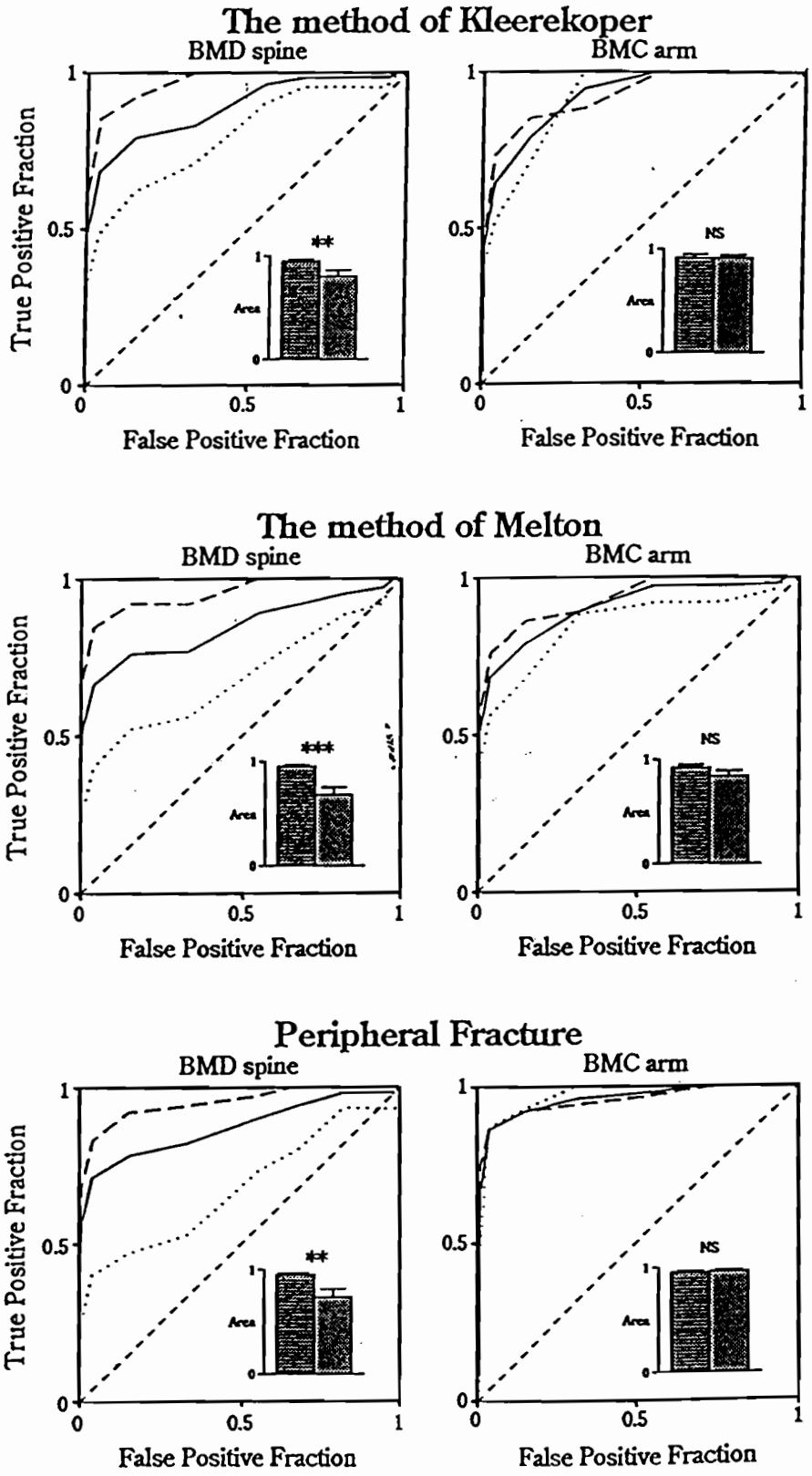

Fig. 3. ROC curves for discrimination between healthy premenopausal women and postmenopausal women with vertebral fractures (*top*, the method of Kleerekoper et al. [12]; *middle*, the method of Melton et al. [13]) and peripheral fractures (*bottom*) with (*dotted line*) or without (*dashed line*) degenerative conditions in the lumbar spine by measurements of BMDspine (*left*) and BMCarm (*right*). The histograms represent the relative magnitude of the areas (±SE) under the ROC curves. *Dark shading*, women unaffected by degenerative conditions; *light shading*, women affected by degenerative conditions. $^{**}p<0.01$; $^{***}p<0.001$; NS, not significant [18,19].

In women, the findings have been conflicting [6–8]. Confounding factors such as a wide age range including both pre- and postmenopausal women and different recruitment procedures may explain the discrepancy in results. Thus, men were recruited through hospital admission or as ambulatory patients [4,5], and women

through advertisement [6] or as osteoporotic patients with vertebral fractures [7]. The present study design eliminated several of these confounding factors. The selection procedure ensured a representative sample of healthy postmenopausal women, none of whom had diseases or took medication known to interfere with calcium metabolism, and the prevalence of fractures in a healthy population was given. The lumbar spine is an area with a high prevalence of degenerative conditions, i.e. spondylosis, disc disease which in addition to disc space narrowing and osteophytes results in reactive sclerosis of the vertebral body endplates [20]. It is well known that degeneration is maximal at the base of mobile segments of the spine immediately above a relatively rigid section, as is the case in the lower regions of the lumbar spine.

Previous studies in both men [4,5] and women [7,8] have focused primarily on the presence of osteophytes, but in the present study we also included endplate sclerosis. We found both osteophytic calcification and endplate sclerosis to have a considerable influence on the spinal BMD measures.

The presence of both types of degenerative change significantly influenced the ability of spinal measurements to discriminate between fractured and non-fractured women. This was the case both for peripheral fractures and for all three radiological methods of defining vertebral fractures. The discrepancy in prevalence of vertebral fractures between the applied methods illustrates the difficulty in defining vertebral deformities/fractures. The crucial problem is that no "gold standard" exists, which inevitably impedes a perfect approach to the accuracy of the diagnostic method. Thus, intergroup as well as individual comparisons can be obscured by degenerative changes in the lumbar spine and introduce errors into the evaluation of risk of osteoporosis. As low bone mass becomes more and more used as the most reliable predictor of the future risk of osteoporotic fractures [11], potential confounding factors should be realized. A large overlap in bone mass has been observed between fractured and unfractured women [11,22,23]. This overlap may in part be caused by the presence of degenerative conditions, resulting in falsely high spinal bone mass.

The present results indicate that the degenerative condition of osteoarthritis is a generalized phenomenon, affecting bone mass in both the axial and peripheral skeleton. This is in accordance with previous reports [6,7] which revealed a positive relation between femoral BMD and osteophytosis score. As in our study the peripheral bone mass (forearm) was affected to a lesser degree than the spinal BMD. This trend, however, implies that subjects who are prone to degenerative changes in the spine may also tend to have higher BMD throughout the skeleton. Earlier reports on patients with osteoarthritis have found increased BMD at sites remote from affected joints [24,25]. Furthermore, the incidence of osteoarthritis is significantly reduced in patients with proximal femur fractures [26]. The reason for these differences is not established, but subjects with osteoarthritis are heavier and stronger than controls and have supranormal fasting growth hormone levels [27]. Thus, the abnormalities underlying degenerative joint disease may have a systemic impact rather than being purely articular. In the same way, the higher spinal BMD in women with degenerative changes may to some extent be explained by this generalized phenomenon rather than by a local impact alone. Aortic calcification has no detectable effect on lumbar BMD [4,9,10]. This has been explained by the relatively low mineral density of vascular deposits [21]. One recent study [28] demonstrated that women with aortic calcification had lower BMD in the lumbar spine when measured with quantitative computed tomography (QCT) and in the femoral neck measured by dual-photon absorptiometry (DPA) when compared with women without degenerative changes and aortic calcification. However, they found no difference in the spine when measured by DPA in the anterior–posterior projection. Degenerative conditions of the lumbar spine affected the diagnostic ability of the spinal bone mass measurements for fractures, which was not the case for the forearm. Thus, the forearm measurement allowed discrimination between women with and without vertebral and peripheral fractures whether or not degenerative conditions were present.

We measured spinal BMC/BMD by DXA, but similar effects are found with systems using DPA [4,5] and with DXA systems with lateral scanning procedures [29]. To solve the problem it has been suggested that involved vertebra(e) should be eliminated from the spinal density analysis in cases of localized osteophytosis or disc disease. This, however, increases the methodological measurement error and is ienvitably impossible in practice in women with diffuse osteophytosis or degenerative disc disease at several levels. In the present study population of 70-year-old women the prevalence of significant degenerative changes in the area of interest was 35%. As a consequence, the diagnostic procedures would require every lumbar spine scan to be associated with a radiographic examination, increasing the costs and irradiation dose unnecessarily. Alternatively, the spinal measurement procedure could be replaced by a peripheral one (e.g. forearm or femur). In our study the bone mass was influenced twice as much in the spine as in the forearm, resulting in a larger diagnostic potential for the forearm measurement procedure.

In conclusion, osteophytic calcification and endplate sclerosis have a considerable influence on spinal bone mass measurements in elderly postmenopausal women and affect the diagnostic ability of spinal scans to discriminate osteoporotic women. Our data suggest that in elderly women, unless the spine is radiologically clear of degenerative conditions, a peripheral measurement procedure should be an alterative for assessment of bone mineral content/density.

References

1. Parfitt AM. Physiological and clinical significance of bone histomorphometric data. In: Recker RR, editor. Bone histomorphometry: techniques and interpretation. Boca Raton: CRC Press, 1983:143–223.
2. Melton LJ III. Epidemiology of fractures. In: Riggs BL, Melton LJ III, editors. Osteoporosis: etiology, diagnosis and management. New York: Raven Press, 1988:133–54.
3. Wasnich RD, Davis JW, Ross PD. Spine fracture risk is predicted by non-spine fractures. Osteoporosis Int 1994;4:1–5.
4. Orwoll ES, Oviatt SK, Mann T. The impact of osteophytic and vascular calcifications on vertebral mineral density measurements in men. J Clin Endocrinol Metab 1990;70:1202–7.
5. Drinka PJ, DeSmet AA, Bauwens SF, Rogot A. The effect of overlying calcification on lumbar bone densitometry. Calcif Tissue Int 1992;50:507–10.
6. Reid IR, Evans MC, Ames R, Wattie DJ. The influence of osteophytes and aortic calcification on spinal mineral density in postmenopausal women. J Clin Endocrinol Metab 1991;72:1372–4.
7. Masud T, Langley S, Wiltshire P, Doyle DV, Spector TD. Effect of spinal osteophytosis on bone mineral density measurements in vertebral osteoporosis. BMJ 1993;307:172–3.
8. Dawson Hughes B, Dellal GB. Effect of radiographic abnormalities on rate of bone loss for the spine. Calcif Tissue Int 1990;46:280–1.
9. Lie JT. The structure of the normal vascular system and its reactive changes. In: Jüergens JL, Spittell JA Jr, Fairbairn JF, editors. Peripheral vascular diseases. Philadelphia: Saunders 1980:65.
10. Silver MD. Cardiovascular pathology. New York: Churchill Livingstone, 1983:252.
11. Qvergaard K, Hansen MA, Riis BJ, Christiansen C. Discriminatory ability of bone mass measurements (SPA and DEXA) for fractures in elderly postmenopausal women. Calcif Tissue Int 1992;50:30–5.
12. Kleerekoper M, Parfitt AM, Ellis BI. Measurement of vertebral fracture rates in osteoporosis. In: Osteoporosis: proceedings of the International Symposium on Osteoporosis. Copenhagen, Denmark: Aalborg Stiftsbogtrykkeri, 1984:103–9.
13. Melton LJ III, Kan SH, Frye MA, Wahner HW, O'Fallon WM, Riggs BL. Epidemiology of vertebral fractures in women. Am J Epidemiol 1989;129:1000–11.
14. Hansen MA, Hassager C, Overgaard K, Marslew U, Riis BJ, Christiansen C. Dual-energy X-ray absorptiometry: a precise method of measuring bone mineral density in the lumbar spine. J Nucl Med 1990;31:1156–62.
15. Nilas L, Borg J, Gotfredsen A, Christiansen C. Comparison of single- and dual-photon absorptiometry in postmenopausal bone mineral loss. J Nucl Med 1985;26:1257–62.
16. Metz CE. Basic principles of ROC analysis. Semin Nucl Med 1978;8:283–98.
17. McNeil BJ, Keeler E, Adelstein SJ. Primer on certain elements of medical decision making. N Engl J Med 1975;293:211–5.
18. Hanley JA, McNeil BJ. The meaning and use of the area under a receiver operating characteristic (ROC) curve. Radiology 1982;143:29–36.
19. Hanley JA, McNeil BJ. A method of comparing the areas under receiver operating characteristic curves derived from the same cases. Radiology 1983;148:839–43.
20. Resnick D, Niwayama G. Degeneration disease of the spine. In: Resnick D, Niwayama G, editors. Diagnosis of bone and joint disorder. Philadelphia: Saunders, 1981:1374–80.
21. Pouilles JM, Tremollieres F, Louvet JP, Fournie B, Morlock G, Ribot C. Sensitivity of dual-photon absorptiometry in spinal osteoporosis. Calcif Tissue Int 1988;43:329–34.
22. Cummings SR. Are patients with hip fracture more osteoporotic? Review of the evidence. Am J Med 1985;78:487–94.
23. Gotfredsen A, Pødenphant J, Nilas L, Christiansen C. Discriminatory ability of total body bone-mineral measured by dual photon absorptiometry. Scand J Clin Lab Invest 1989;49:125–34.
24. Gevers G, Dequeker J, Geusens P, Nyssen-Behets C, Dhem A. Physical and histomorphological characteristics of iliac crest bone differ according to the grade of osteoarthritis at the hand. Bone 1989;10:173–7.
25. Roh YS, Dequeker J, Mulier JC. Cortical bone remodeling and bone mass in primary osteoarthritis of the hip. Invest Radiol 1973;8:251–4.
26. Wientroub S, Papo J, Ashkenazi M, Tardiman R, Weissman SL, Salama R. Osteoarthritis of the hip and fractures of the proximal femur Acta Orthop Scand 1982;53:261–4.
27. Dequeker J. The relationship between osteoporosis and osteoarthritis. Clin Rheum Dis 1985;11:271–96.
28. Banks LM, Lees B, Macsweeney JE, Stevenson JC. Effect of degenerative spinal and aortic calcification on bone density measurements in post-menopausal women: links between osteoporosis and cardiovascular disease? Eur J Clin Invest 1994;24:813–7.
29. Bjarnason K, Hassager C, Ravn P, Christiansen C. Early postmenopausal diminution of forearm and spinal bone mineral density: a cross-sectional study. Osteoporosis Int 1995;5:35–8.

Received for publication 8 March 1995
Accepted in revised form 22 August 1995

Giuseppe Guglielmi, MD • Susan K. Grimston, PhD • Keith C. Fischer, MD
Roberto Pacifici, MD

Osteoporosis: Diagnosis with Lateral and Posteroanterior Dual X-ray Absorptiometry Compared with Quantitative CT[1]

PURPOSE: To compare the diagnostic sensitivity of posteroanterior and lateral dual x-ray absorptiometry (PA-DXA, L-DXA, respectively) and quantitative computed tomography (CT).

MATERIALS AND METHODS: Among 108 women undergoing lumbar spine bone mineral density assessment, 66 were healthy (mean age, 52.9 years ± 1.2 [standard error of mean]) and 42 had osteoporosis (mean age, 66.9 years ± 1.2).

RESULTS: Although both L-DXA and PA-DXA correlated well with quantitative CT (r = .73 and .72, respectively; $P < .0001$), L-DXA correlated better than PA-DXA with age ($r = -.69$ and $-.50$, respectively; $P < .0001$). Women with osteoporosis showed higher bone loss with quantitative CT (1.33% per year) and L-DXA (0.3% per year) than with PA-DXA (0.07% per year). Logistic regression analysis indicated that quantitative CT and L-DXA but not PA-DXA are significant predictors of osteoporotic fractures. Receiver-operating-characteristic curve analyses showed L-DXA to have a sensitivity and specificity closer to those of quantitative CT than did PA-DXA.

CONCLUSION: Performance of L-DXA helped discriminate better than PA-DXA between healthy subjects and those with osteoporosis.

Index terms: Bones, absorptiometry, 32.12171 • Computed tomography (CT), quantitative, 33.12119, 33.56 • Osteoporosis, 33.12171, 33.56

Radiology 1994; 192:845–850

OSTEOPOROSIS is a common cause of vertebral and hip fractures. Although fracture occurrence depends on a variety of factors (eg, tendency to fall and bone quality [1,2]), bone mineral density (BMD) is an established, important predictor of risk of osteoporotic fracture (3–6). Several techniques have been developed for noninvasive measurement of axial BMD. Quantitative computed tomography (CT), dual-photon absorptiometry, and posteroanterior dual x-ray absorptiometry (PA-DXA) have been widely applied to diagnostic assessment of BMD and monitoring of changes in BMD due to treatment or progression of disease (7–11).

Quantitative CT has the ability to measure selectively the trabecular compartment of the vertebrae and has therefore been recognized as a sensitive method with which to assess BMD in patients with osteoporosis (12–15). Recently however, PA-DXA has gained widespread acceptance as a tool for assessing BMD on the basis of results from comparative studies that show PA-DXA to be more precise than either quantitative CT or dual-photon absorptiometry (16–18). More importantly however, acquisition of a PA-DXA scan involves a radiation exposure of only 2–3 mrem (19) compared with the 250–300-mrem exposure associated with quantitative CT (20,21) and allows for measurement of BMD at different skeletal sites (22–24). Although PA-DXA is a highly precise technique, with a 1% variation in short-term reproducibility studies (16,25,26), quantitative CT has been shown to help discriminate between healthy women and those with osteoporosis better than PA-DXA (27).

The better diagnostic sensitivity of quantitative CT compared with PA-DXA may be a result of the fact that PA-DXA quantifies not only the trabecular compartment of the vertebral body but also the posterior compact bone elements of the vertebra. In addition, any hypertrophic and degenerative change and/or vascular calcification, which commonly occur in women over the age of 60 years, are also included in the final result from PA-DXA (28).

To maximize the amount of trabecular bone and to minimize the amount of cortical bone and extravertebral calcification present in the area of interest, previous studies have measured BMD with lateral DXA (L-DXA) (29–33). In these studies, BMD was measured while the patient was in the lateral decubitus position. The lateral projection thus derived was shown to be more sensitive for detection of age-related bone loss than the projection derived from PA-DXA but resulted in poorer precision, possibly as a result of the positioning of the patients. Because of these results, an L-DXA scanner with a rotating C-arm has been developed that allows the patient to adopt the same supine position for both PA-DXA and L-DXA.

Results from preliminary studies suggest that a L-DXA scan obtained with the patient in the supine position provides significant improvement in precision (33,34) and accuracy. The present study was designed to assess the sensitivity of PA-DXA and L-DXA in the diagnosis of osteoporosis, with quantitative CT as the criterion measure. The role of L-DXA in detection of spinal bone loss was also studied.

MATERIALS AND METHODS

Subjects

Quantitative and DXA measurements were obtained in 108 white women who were seen at our center for osteoporosis

[1] From the Division of Bone and Mineral Diseases, Washington University School of Medicine, Department of Radiology, Jewish Hospital of St Louis, Mo. From the 1993 RSNA scientific assembly. Received December 16, 1993; revision requested February 16, 1994; revision received March 25; accepted April 13. Supported in part by a grant from Hologic, Inc, Waltham, Mass. Address reprint requests to G.G., Department of Radiology, Scientific Institute CSS, San Giovanni Rotondo FG, Italy.

Abbreviations: BMD = bone mineral density, DXA = dual x-ray absorptiometry, L-DXA = lateral DXA, PA-DXA = posteroanterior DXA.

screening. Women with known or suspected malignant disease or with secondary causes of osteoporosis were excluded. Only baseline spinal BMD studies were performed. A group of 66 healthy women (age, 26–73 years [mean, 52.9 years ± 1.4 [standard error of the mean]]) was established on the basis of results of medical history. In this study, menopause was defined as absence of menses for at least 6 months in women over the age of 35 years. The women had no history of fractures, low back pain, or height loss. None of them had any disease known to affect BMD or calcium metabolism. Their radiographs showed no evidence of vertebral fractures, spinal demineralization, arthritis, or scoliosis.

A second group of 42 subjects (age 49–83 years [mean, 66.9 years ± 1.2]) was classified as osteoporotic. All members of this group had experienced at least one but not more than four wedge or crush deformities of the vertebral bodies T-4 through L-5 and/or evidence of significant spinal demineralization identified on thoracolumbar spinal radiographs. A wedge deformity was considered to be present if the anterior vertebral cortex measured 85% or less of the posterior cortex on lateral spinal radiographs. A crush fracture consisted of an observable loss of both anterior and posterior height of at least 25% compared with intact adjacent vertebrae.

Table 1
T Test Comparisons between Healthy Subjects and Those with Osteoporosis

Variable	Group	
	Healthy (n = 66)	Osteoporotic (n = 42)
Age (y)	52.9 ± 1.4	66.9 ± 1.2*
Height (cm)	163.7 ± 0.8	161.9 ± 1.3
Weight (kg)	62.6 ± 1.6	58.4 ± 1.7
Years since menopause	8.5 ± 1.1	18.6 ± 1.4*
Quantitative CT (mg/cm³)	98.1 ± 3.8*	46.1 ± 3.2
PA-DXA (g/cm²)	0.888 ± 0.015*	0.739 ± 0.020
L-DXA (g/cm²)	0.617 ± 0.015*	0.452 ± 0.011
Volumetric L-DXA (g/cm³)	0.181 ± 0.004*	0.135 ± 0.004
Middle L-DXA (g/cm²)	0.548 ± 0.019*	0.373 ± 0.016
L-3 L-DXA (g/cm²)	0.612 ± 0.015*	0.461 ± 0.014

Note.—Numbers are mean ± standard error of mean.
* $P < .01$.

Table 2
Correlation Coefficients for Entire Subject Population

Factor	Quantitative CT	PA-DXA	L-DXA	L-3 L-DXA	Volumetric L-DXA	Middle L-DXA
Quantitative CT	...	.72	.73	.68	.71	.71
Age (y)	−.76	−.50	−.69	−.65	−.69	−.67

All correlations were significant at $P < .001$.

BMD Measurements

Single-energy quantitative CT of the L-1–L-3 segment of the lumbar spine was performed with a model 9800 CT scanner (GE Medical Systems, Milwaukee, Wis) according to the method of Cann and Genant (12), as previously described (35). Briefly, a phantom (Perspex; QCT Bone Mineral Analysis System, San Francisco, Calif) containing potassium phosphate standard was placed under the patient. Cursors were placed on the vertebral image to define 10-mm-thick transverse sections through the center of T-12, L-1, L-2, L-3, and L-4. Cross-sectional images of each uncompressed vertebra were obtained and used to position elliptical cursors in the trabecular area of each vertebral body. CT counts were then obtained for the selected vertebrae and for the standards. Spinal measurements were referenced to a calibration curve obtained from the standard and were expressed in milligrams per cubic centimeter. The short-term precision of this method, as assessed with multiple scans of human lumbar spine specimens obtained from cadavers, was 4.5%.

BMD measurements at L-DXA (L-2–L-4) with the patient in the supine decubitus position and at PA-DXA (L-1–L-4) were made with a model QDR-2000 densitometer (Hologic, Waltham, Mass), with use of standard procedures supplied by the manufacturer for scanning and analysis that were similar to those described previously (27,29,36–38). The densitometer is a 32-detector fan-beam DXA device that uses pulsed x-ray sources and employs an internal calibration system previously described by Stein et al (39) and multiple detector arrays that offer increased scanning speed and improved spatial resolution along the y axis (40). We used the manufacturer's recommended settings of "array spine" for the posteroanterior projection for L-1–L-4 and "array supine lateral fast" for the lateral projection for L-2–L-4. All measurements were taken on the same day for each subject.

All fractured vertebral bodies (n = 68) identified on lateral thoracolumbar spine radiographs were excluded from data analysis. Since superimposition of pelvic bone to L-4 occurred in 14% of our patients (15 of 108) and superimposition of ribs to L-2 occurred in 100% of cases reported by others (41,42) (167 and 55 patients, respectively), we also analyzed L-DXA measurements restricted to L-3 (L-3 L-DXA). The middle central area of vertebral bodies L-2–L-4 (middle L-DXA), as proposed by the manufacturers, was also included in the measurement data file for each subject. The results of L-DXA, L-3 L-DXA, and middle L-DXA measurements were expressed in grams per square centimeter. A volumetric BMD (volumetric L-DXA) (calculated by dividing the lateral BMD by the average width of that vertebra measured from the posteroanterior projection) was also determined and results expressed in grams per cubic centimeter. Total L-DXA scanning time was approximately 2 minutes. The long-term precision (coefficient of variation) of PA-DXA and L-DXA, as evaluated by calculating the coefficient of variation of daily scanning of the spine phantom for a period of 270 days, was 0.40% and 0.50%, respectively.

Statistical Analysis

Group mean values were compared with a two-tailed Student t test. Linear regression was performed to determine relationships between quantitative CT, PA-DXA, L-DXA, volumetric L-DXA, middle L-DXA, L-3 L-DXA, and age. Analysis of covariance was performed to correct for any effect of age on each of the BMD measurements and to compare the slopes of the regressions of BMD with age. Predicted quantitative CT and PA-DXA and L-DXA values for age were calculated by regression of quantitative CT, PA-DXA, and L-DXA with age from our results in healthy subjects. Forward stepwise regression analysis was performed to determine the most important predictor(s) of BMD. Standard z scores were determined to adjust for differences in age and unit of measurement and to convert the raw score deviation from predicted normal units into standard deviation units.

Logistic regression analysis was performed to compare the ability of each technique to help discriminate between healthy women and those with osteoporosis. A forward stepwise selection approach was used with the likelihood ratio as the criterion statistic. As a further test of predictive power, receiver-operating-characteristic curves of each technique were generated (LABROC1 software; Metz C, Department of Radiology, University of Chicago, Ill) (43). The areas under the curves were compared as previously described (44,45).

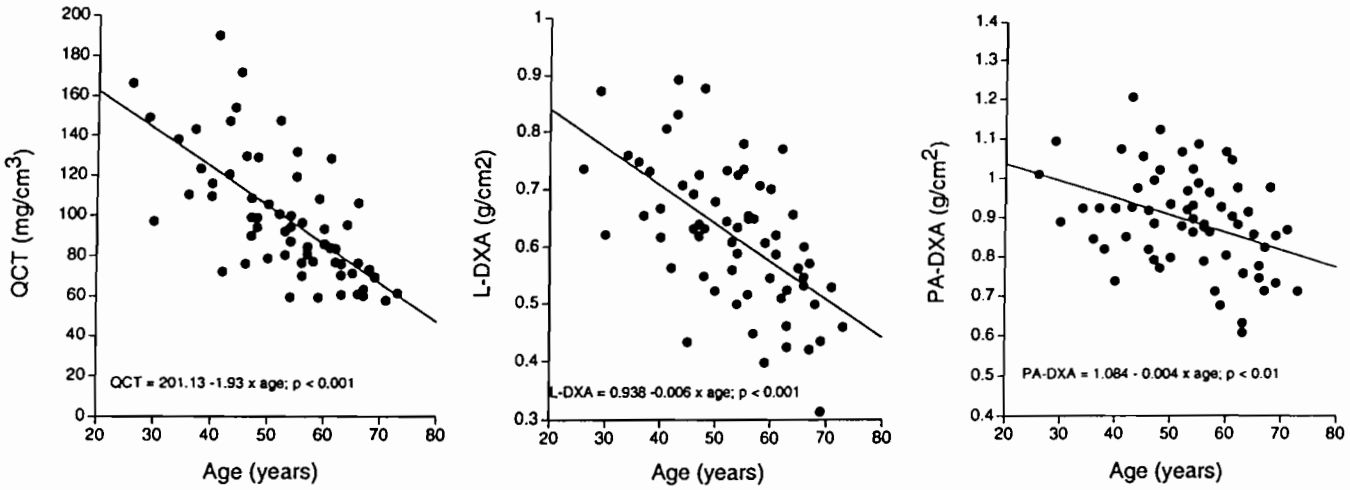

1. 2. 3.

Figures 1–3. (1) Linear regression of BMD measured with quantitative CT (*QCT*) with age for healthy subjects ($n = 66$). (2) Linear regression of BMD measured with L-DXA with age for healthy subjects ($n = 66$). (3) Linear regression of BMD measured with PA-DXA with age for healthy subjects ($n = 66$).

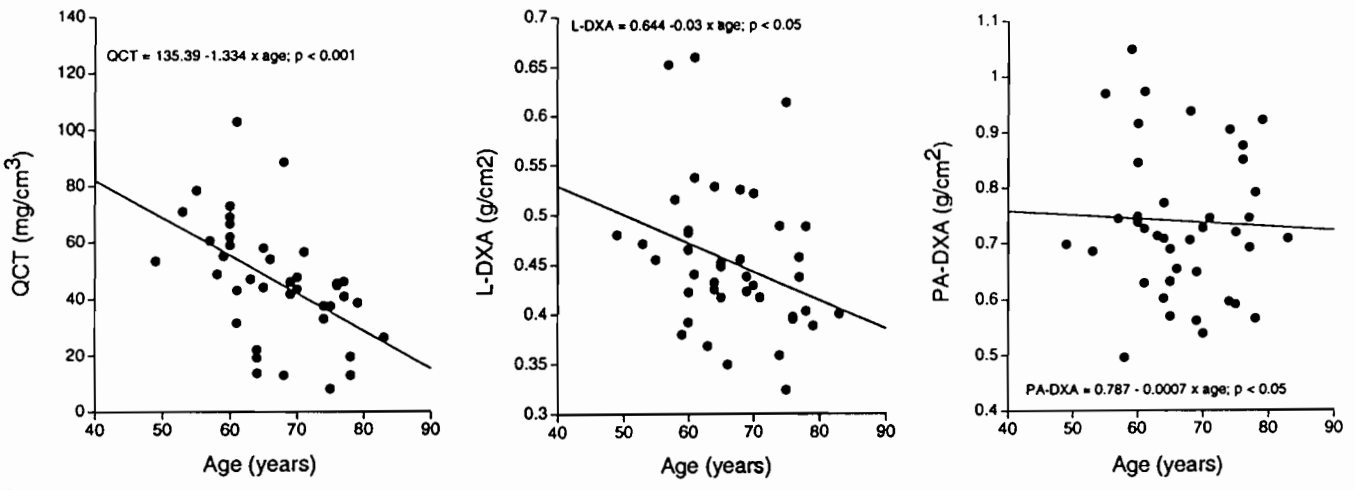

4. 5. 6.

Figures 4–6. (4) Linear regression of BMD measured with quantitative CT (*QCT*) with age for subjects with osteoporosis ($n = 42$). (5) Linear regression of BMD measured with L-DXA with age for subjects with osteoporosis ($n = 42$). (6) Linear regression of BMD measured with PA-DXA with age for subjects with osteoporosis ($n = 42$).

RESULTS

Women with osteoporosis were significantly older and longer past menopause than healthy women (Table 1). Analysis of covariance with age and years since menopause did not affect the significant differences noted in BMD.

In the total study population, findings at both L-DXA ($r = 0.73$, $P < .001$) and PA-DXA ($r = .72$, $P < .001$) correlated well with findings at quantitative CT. Moreover, findings at quantitative CT ($r = -.76$) and L-DXA ($r = .69$) correlated better with age than findings at PA-DXA ($r = .50$) (Table 2). The best-fitting curve was linear, and the correlation was independent of years since menopause. In the healthy women, a more significant linear decrease in BMD with age was found when measured with both quantitative CT and L-DXA than with PA-DXA (Figs 1–3).

The rate of bone loss, calculated from each regression curve, was 1.96% per year ($P < .001$) with quantitative CT, 0.97% per year ($P < .001$) with L-DXA, and 0.45% per year ($P < .01$) with PA-DXA. The women with osteoporosis had significant bone loss with quantitative CT (2.89% per year) and with L-DXA (0.66% per year) but not with PA-DXA (0.10% per year) (Figs 4–6).

Forward stepwise regression analyses indicated age to be the single most important predictor of BMD in both healthy subjects and those with osteoporosis. However, BMD measured with PA-DXA was not significantly associated with age in subjects with osteoporosis (Table 3).

To investigate further the ability of quantitative CT, L-DXA, and PA-DXA to help discriminate between healthy subjects and those with osteoporosis, the BMD of patients with osteoporosis was expressed as a deviation from the predicted value for that age (z score). The subjects with osteoporosis had a larger ($P < .05$) z score with quantitative CT (-1.69 ± 0.67) and L-DXA (-1.35 ± 0.60) than with PA-DXA (-1.21 ± 1.06).

Attempts to increase the sensitivity of L-DXA by correcting for vertebral height (measured with PA-DXA) to provide an estimate of true volumetric density (volumetric L-DXA) and by restricting analysis to the middle central area of the vertebral body (middle L-DXA) were not successful in increasing diagnostic sensitivity (Table 2). In addition, restriction of the analysis to the third lumbar vertebra exclu-

sively to overcome any error associated with overlapping of rib and/or pelvis on L-2 and L-4, respectively, did not improve the diagnostic sensitivity of L-DXA.

Results of logistic regression analysis indicated both quantitative CT and L-DXA but not PA-DXA to be significant predictors of osteoporotic fracture ($P < .01$). In contrast, volumetric L-DXA, middle L-DXA, and L-3 L-DXA were not significant predictors of osteoporotic fracture. A similar finding was derived from analysis of receiver-operating-characteristic curves (Fig 7). The curves for fracture prediction (areas under curve: quantitative CT = 0.9518 ± 0.0228, L-DXA = 0.8741 ± 0.0332, PA-DXA = 0.7931 ± 0.0446) showed L-DXA to have a sensitivity and specificity higher than those of PA-DXA ($P < .05$) but lower than those of quantitative CT ($P < .05$).

Table 3
Regression Equations for Each Measurement Technique on Age for Healthy and Osteoporotic Groups

Group	Equation	*r*	*P*
Healthy (n = 66)	QCT = 201.13 − 1.93 × age	−.69	<.001
Osteoporotic (n = 42)	QCT = 135.39 − 1.334 × age	−.52	<.001
Healthy (n = 66)	PA-DXA = 1.084 − 0.004 × age	−.34	<.01
Osteoporotic (n = 42)	PA-DXA = 0.787 − 0.0007 × age	−.04	ns
Healthy (n = 66)	L-DXA = 0.938 − 0.006 × age	−.56	<.001
Osteoporotic (n = 42)	L-DXA = 0.644 − 0.003 × age	−.31	<.05

Note.—ns = not significant, QCT = quantitative CT.

DISCUSSION

DXA provides a convenient, noninvasive method of measuring skeletal BMD and is now widely used for assessment of patients thought to be at risk for osteoporosis and for quantification of results due to treatment or progression of disease. To assess the sensitivity of DXA, a number of studies have been conducted to compare measurements at DXA with a generally accepted criterion measure of BMD, quantitative CT (9,16–18). In general, results indicated that scans obtained with PA-DXA do not help discriminate between healthy subjects and those with osteoporosis as well as quantitative CT does.

The major reason for the reduced discriminatory power of PA-DXA is the fact that it is not possible to measure the trabecular bone of the vertebral body selectively (27). To overcome this limitation, attempts were made to measure BMD by obtaining a lateral projection, which was accomplished by placing patients in a lateral decubitus position. The major limitation associated with this method was the difficulty in patient repositioning. The precision error of L-DXA performed with the patient in the lateral decubitus position has been assessed in several previous studies and found to range between 2.8% and 5.9% (29,34). These factors limit the performance of L-DXA with the patient in the lateral decubitus position in longitudinal studies, in which reliable patient positioning is critical. The development of a new L-DXA scanner with a rotating C-arm allows paired posteroanterior and lateral spine scanning to be performed without repositioning the patient. However, limited information is available concerning the ability of L-DXA performed with the patient in the supine position to help discriminate between healthy subjects and those with osteoporosis (46).

In the present study, the BMD of the lumbar vertebrae was measured with quantitative CT, PA-DXA, and L-DXA in a population of healthy women and women with clinically diagnosed osteoporosis. We have found that normal BMD values and rate of bone loss with age were similar to those reported previously by Pacifici et al (35) and others (40,46,47). The BMD values of the osteoporotic group were also representative of the BMD values for a general osteoporotic population (Table 1).

BMD measured at PA-DXA and L-DXA correlated significantly with BMD measured at quantitative CT in the mixed population of healthy subjects and those with osteoporosis. However, when patients were divided into separate groups, findings at PA-DXA could not significantly help predict the variability in BMD with age in subjects with osteoporosis (Table 3). In contrast, the relationship between BMD as measured with L-DXA and age was significant for both healthy subjects and those with osteoporosis. These results were similar to those reported previously on the basis of direct comparison of results with L-DXA and PA-DXA (29).

In a previous study, Rupich et al demonstrated that supine positioning allowed inclusion of L-3 and L-4 but exclusion of L-2 in a lateral lumbar scan (42). These recommendations were based on analysis of the frequency of overlap of the pelvic bone and rib on the vertebrae. In the present study, restriction of the area of interest to L-3 (L-3 L-DXA) or the middle highly trabecular region of the vertebrae (middle L-DXA) or use of the width of the vertebrae to estimate true volumetric density (volumetric L-DXA) did not significantly improve the sensitivity of L-DXA. These findings are in agreement with those recently reported by others (46,48). This suggests that the superimposition of pelvic bone to L-4, which occurred in 14% of our cases, and superimposition of the ribs to L-2, which is known to occur in all patients (42), does not significantly affect BMD measurements with DXA. Presumably, this is a result of the fact that the error generated by superimposition of bone is of the same magnitude as that generated by reduction in the size of the area of interest.

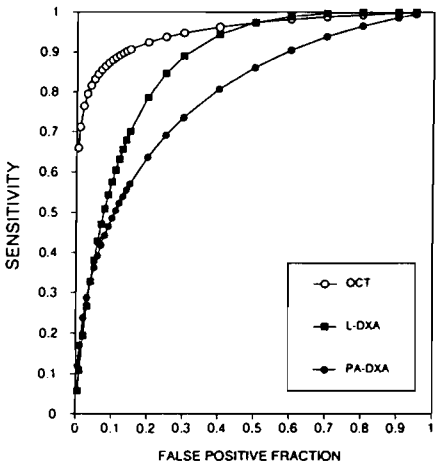

Figure 7. Receiver-operating-characteristic curves for quantitative CT (*QCT*), PA-DXA, and L-DXA.

Rate of bone loss per year, estimated from generated regression equations, was higher with quantitative CT than with L-DXA and much higher with L-DXA than with PA-DXA (Table 3). This result corresponds to results of previous studies, which showed age-related bone loss to be greater when estimated with L-DXA than with PA-DXA (30,38,46). In the present study, we extended these observations by using findings at quantitative CT as a criterion against which findings at PA-DXA

and L-DXA were compared. This allowed for evaluation of sensitivity in the measurement of BMD.

The choice of treatment modalities for osteoporosis often depends on the diagnostic sensitivity of screening procedures. In the present study, receiver-operating-characteristic curves were generated for each BMD measurement technique and were compared in terms of diagnostic sensitivity. With this procedure, L-DXA was shown to be superior to PA-DXA but inferior to quantitative CT in terms of accurate differentiation between fracture and nonfracture. These results are in agreement with those of Ott et al (49), who found quantitative CT to be superior to dual-photon absorptiometry, and those of Finkelstein et al (46), who reported that L-DXA is superior to PA-DXA. Surprisingly, the results of the current study also showed better performance for both quantitative CT and PA-DXA than was previously reported in a similar study from our group (35). However, the difference in diagnostic sensitivity between the two techniques was similar in this and the previous study.

To test further the ability of each technique to help differentiate between osteoporotic and normal bone, a logistic regression approach was used. Logistic regression analysis is appropriate under conditions in which either a positive or negative diagnosis is possible. In logistic regression, a direct estimate is made of the probability of an event (or diagnosis). In the present study, subjects were classified as either having osteoporosis or being healthy. With use of forward stepwise logistic regression, only BMD measurements obtained with quantitative CT and L-DXA were significant predictors of osteoporosis. The close association between findings at L-DXA and at quantitative CT probably relates to similarities in the specific bone regions measured with the two techniques.

In conclusion, findings in this study demonstrate that the diagnostic sensitivity of L-DXA is between that of PA-DXA and quantitative CT. Moreover L-DXA is potentially more sensitive than quantitative CT to errors due to anatomic abnormalities or degenerative processes of the spine. However, the decreased radiation exposure and cost of L-DXA compared with quantitative CT suggest that L-DXA is a valid alternative to quantitative CT in the clinical setting. ■

Acknowledgments: The authors thank Vincent Lowett, ARTT, for performing the DXA measurements for this study and Peter Steiger, PhD, of Hologic, Inc, Waltham, Mass, for providing technical assistance regarding the model QDR-2000 densitometer.

References

1. Parfitt AM. Trabecular bone architecture in pathogenesis and prevention of fracture. Am J Med 1987; 82(suppl 1b):68–72.
2. Recker RR. Low bone mass may not be the only cause of skeletal fragility in osteoporosis. Proc Soc Exp Biol Med 1989; 191: 272–274.
3. Cummings SR, Black DM, Rubin SM. Lifetime risk of hip, Colles', or vertebral fracture and coronary heart disease among white postmenopausal women. Arch Intern Med 1989; 149:2445–2448.
4. Genant HK, Block JE, Steiger P, Glüer CC, Ettinger B, Harris S. Appropriate use of bone mineral densitometry. Radiology 1989; 170:817–822.
5. Kleerekoper M, Nelson DA, Peterson EL, Tilley BC. Outcome variables in osteoporotic trials. Bone 1992; 13(suppl):29–34.
6. Cummings SR, Black DM, Nevitt MC, et al. Bone density at various sites for prediction of hip fractures. Lancet 1993; 341:72–75.
7. Goodwin PN. Methodologies for the measurement of bone density and their accuracy and precision. Semin Nucl Med 1987; 17:293–304.
8. Cann CE. Quantitative CT for the determination of bone mineral density: a review. Radiology 1988; 166:509–522.
9. Hansen MA, Hassager C, Overgaard K, Marslew U, Riis BJ, Christiansen C. Dual energy x-ray absorptiometry: a precise method of measuring bone mineral density in the lumbar spine. J Nucl Med 1990; 31: 1156–1162.
10. Glüer CC, Steiger P, Selvidge R, Elliesen-Kliefoth K, Hayashi C, Genant HK. Comparative assessment of dual-photon absorptiometry and dual energy radiography. Radiology 1990; 174:223–228.
11. Ostlere SJ, Gold RH. Osteoporosis and bone density measurements methods. Clin Orthop 1991; 271:149–163.
12. Cann CE, Genant HK. Precise measurement of vertebral mineral content using computed tomography. J Comput Assist Tomogr 1980; 4:493–500.
13. Genant HK, Steiger P, Block JE, Glüer CC, Ettinger B, Harris ST. Quantitative computed tomography: update 1987. Calcif Tissue Int 1987; 41:179–186.
14. Steiger P, Block JE, Steiger S, et al. Spinal bone mineral density measured with quantitative CT: effect of region of interest, vertebral level, and technique. Radiology 1990; 175:537–543.
15. Genant HK, Faulkner KG, Glüer CC. Measurements of bone mineral density: current status. Am J Med 1991; 91(suppl 5B):49–53.
16. Pacifici R, Rupich RC, Vered I, et al. Dual energy radiography (DER): a preliminary comparative study. Calcif Tissue Int 1988; 43:189–191.
17. Sartoris DJ, Resnick D. Dual energy radiographic absorptiometry for bone densitometry: current status and prospective. AJR 1989; 152:241–246.
18. Ho CP, Kim RW, Schaffler MB, Sartoris DJ. Accuracy of dual-energy radiographic absorptiometry of the lumbar spine: cadaver study. Radiology 1990; 176:171–173.
19. O'Malley M, Kenrick AJ, Sartoris DJ. Axial bone density in rheumatoid arthritis: comparison of dual-energy projection radiography and dual-photon absorptiometry. Radiology 1989; 170:501–505.
20. Cann CE. Low-dose CT scanning for quantitative spinal mineral analysis. Radiology 1981; 160:469–478.
21. Heuck HF, Block J, Glüer CC, Steiger P, Genant HK. Mild versus definite osteoporosis: comparison of densitometry techniques using different statistical models. J Bone Miner Res 1989; 4:891–900.
22. Borders J, Keer E, Sartoris DJ. Quantitative dual-energy radiographic absorptiometry of the lumbar spine: in vivo comparison with dual-photon absorptiometry. Radiology 1989; 170:129–131.
23. Black DM, Cummings SR, Genant HK, Nevitt MC, Palermo L, Browner W. Axial and appendicular bone density predict fractures in older women. J Bone Miner Res 1992; 7:633–638.
24. Mazess R, Collick B, Trempe J, Barden H, Hanson J. Performance evaluation of a dual-energy x-ray bone densitometer. Calcif Tissue Int 1989; 44:228–232.
25. Lees B, Stevenson JC. An evaluation of dual-energy x-ray absorptiometry and comparison with dual-photon absorptiometry. Osteoporos Int 1992; 2:146–152.
26. Sievänen H, Oja P, Vuori I. Precision of dual-energy x-ray absorptiometry in determining bone mineral density and content of various skeletal sites. J Nucl Med 1992; 33:1137–1142.
27. Pacifici R, Rupich RC, Griffin MG, Chines A, Susman N, Avioli LV. Dual energy radiography versus quantitative computer tomography for the diagnosis of osteoporosis. J Clin Endocrinol Metab 1990; 70:705–710.
28. Haddaway MJ, Davie MW, McCall IW. Bone mineral density in healthy normal women and reproducibility of measurements in spine and hip using dual-energy x-ray absorptiometry. Br J Radiol 1992; 65: 213–217.
29. Rupich RC, Pacifici R, Griffin MG, Vered I, Susman N, Avioli LV. Lateral dual energy radiography: a new method for measuring vertebral bone density: a preliminary study. J Clin Endocrinol Metab 1990; 70: 1768–1770.
30. Slosman DO, Rizzoli R, Donath A, Bonjour JP. Vertebral bone mineral density measured laterally by dual-energy x-ray absorptiometry. Osteoporos Int 1990; 1:23–29.
31. Mazess RB, Gifford CA, Bisek JP, Barden HS, Hanson JA. DEXA measurement of spine density in the lateral projection: methodology. Calcif Tissue Int 1991; 49: 235–239.
32. Reid IR, Evans MC, Stapleton J. Lateral spine densitometry is a more sensitive indicator of glucocorticoid-induced bone loss. J Bone Miner Res 1992; 7:1221–1225.
33. Slosman DO, Rizzoli R, Donath A, Bonjour JP. Bone mineral density of lumbar vertebral body determined in supine and lateral decubitus: study of precision and sensitivity (abstr). J Bone Miner Res 1992; 7:397.
34. Devogelaer JP, Baudoux C, Nagant de Deuxchaisnes C. Lack of precision of the lumbar-BMD measurements with the QDR-1000/W when the patients are lying in a lateral position. Presented at the Ninth Bone Densitometry Workshop, Traverse City, Mich, September 4–6, 1992.
35. Pacifici R, Susman N, Carr PL, Birge SJ, Avioli LV. Single and dual energy tomography analysis of spinal trabecular bone: a comparative study in normal and osteoporotic women. J Clin Endocrinol Metab 1987; 64:209–214.
36. Devogelaer JP, Baudoux C, Nagant de Deuxchaisnes C. Reproducibility of BMD measurements on the QDR-2000, Hologic, Inc. Presented at the Ninth Bone Densi-

tometry Workshop, Traverse City, Mich, September 4–6, 1992.
37. Sabin MA, MacLaughlin SM, Blake GM, Fogelman I. A study of the accuracy of lateral and volumetric spinal bone density measurements with the Hologic QDR-2000. Presented at the Ninth Bone Densitometry Workshop, Traverse City, Mich, September 4–6, 1992.
38. Harper KD, Wilkinson WE, Lobaugh B, King ST, Drezner MK. Supine lateral dual-energy x-ray absorptiometry of the spine provides improved diagnostic sensitivity. Presented at the Ninth Bone Densitometry Workshop, Traverse City, Mich, September 4–6, 1992.
39. Stein JA, Lazewatsky JL, Hochberg AM. Dual energy x-ray bone densitometer incorporating an internal reference system (abstr). Radiology 1987; 165(P):313.
40. Steiger P, Wahner HW. Instruments using fan beam geometry. In: Wahner HW, Fogelman I, eds. The evaluation of osteoporosis: dual energy x-ray absorptiometry in clinical practice. London, England: Dunitz, 1993; 75–87.
41. Uebelhart D, Duboeuf F, Meunier PJ, Delmas PD. Lateral dual-photon absorptiometry: a new technique to measure the bone mineral density at the lumbar spine. J Bone Miner Res 1990; 5:525–531.
42. Rupich RC, Griffin MG, Pacifici R, Avioli LV, Susman N. Lateral dual-energy radiography: artifact error from rib and pelvic bone. J Bone Miner Res 1992; 7:97–101.
43. Metz CE. ROC methodology in radiologic imaging. Invest Radiol 1986; 21:720–733.
44. Hanley JA, McNeil BJ. The meaning and use of the area under a receiver operating characteristic (ROC) curve. Radiology 1982; 143:29–36.
45. Hanley JA, McNeil BJ. A method of comparing the areas under receiver operating characteristic curves derived from the same cases. Radiology 1983; 148:839–843.
46. Finkelstein JS, Cleary RL, Butler JP, et al. A comparison of lateral versus anterior-posterior spine dual energy x-ray absorptiometry for the diagnosis of osteopenia. J Clin Endocrinol Metab 1994; 78:724–730.
47. Slosman DO, Casez JP, Pichard C, et al. Assessment of whole-body composition with dual-energy x-ray absorptiometry. Radiology 1992; 185:593–598.
48. Harper KD, Lobaugh B, King S, Drezner M. Supine lateral dual energy x-ray absorptiometry (DXA) of the spine: superior technique to assess bone loss (abstr). J Bone Min Res 1993; 8:A355.
49. Ott SM, Kilcoyne RF, Chesnut CH. Ability of four different techniques of measuring bone mass to diagnose vertebral fractures in postmenopausal women. J Bone Min Res 1987; 2:201–210.

European Journal of Clinical Investigation (1994) **24**, 813–817

Effect of degenerative spinal and aortic calcification on bone density measurements in post-menopausal women: links between osteoporosis and cardiovascular disease?

L. M. BANKS, B. LEES,* J. E. MACSWEENEY & J. C. STEVENSON* Department of Diagnostic Radiology, Royal Postgraduate Medical School and *Wynn Institute for Metabolic Research, London, UK

Received 31 August 1993 and in revised form 25 March 1994; accepted 28 March 1994

Abstract. The effect of spinal degenerative changes and aortic calcification on bone mineral density measurements was studied in 115 healthy early post-menopausal women. Lateral lumbar spine radiographs and quantitative computer tomography images were used to determine the presence and severity of aortic calcification and degenerative changes in the lumbar spine. Women with spinal degenerative calcification had higher spine bone density when measured by dual photon absorptiometry compared to those without calcification ($P < 0{\cdot}01$), but this was not reflected by the quantitative computer tomography or the proximal femur bone densities, suggesting that spinal calcification artefactually increases spinal bone density when measured by dual photon techniques. Women with aortic calcification had significantly lower quantitative computer tomography and proximal femur bone density compared to those without calcification (both $P < 0{\cdot}05$). These women may be at increased risk for both osteoporosis and cardiovascular disease, suggesting a common aetiological factor such as oestrogen deficiency.

Keywords. Aortic calcification, bone density, cardiovascular disease, osteophytes, osteoporosis.

Introduction

Dual photon techniques are now widely used in the measurement of bone density (BMD) in the lumbar spine and the proximal femur [1–3]. A number of centres [4–8] have assessed the apparent increase in anteroposterior (AP) spinal BMD measurements caused by degenerative osteoarthritic changes and aortic calcification when using dual photon absorptiometry (DPA) and dual energy X-ray absorptiometry (DXA) techniques. This apparent increase is due to the fact that these techniques measure an integral of cortical and trabecular bone and thus may include any extra-osseous calcification. None of these studies have compared BMD measurements by QCT with those by DPA or DXA. With QCT, a cross-sectional image is taken at the mid-vertebral level and localization of a region of interest (ROI) within the vertebral body permits a measurement of solely trabecular BMD [9]. Since this method of measuring BMD is not subject to the influence of extraneous calcification and degenerative changes, QCT could theoretically be regarded as the 'gold standard'. The development of lateral DXA scanning of the lumbar vertebral bodies has been suggested as a technique for circumventing some of these problems by avoiding any extraneous calcification that might influence the BMD values [10]. The aim of this study was to assess the influence of degenerative change and extra osseous calcification, as demonstrated on radiographs and QCT, on DPA BMD measurements in a group of healthy early post-menopausal women.

Correspondence: Linda M. Banks, Department of Diagnostic Radiology, Royal Postgraduate Medical School, Hammersmith Hospital, Du Cane Road, London W12 ONN, UK.

Patients and methods

The study group comprised of 115 normal, healthy, Caucasian, post-menopausal women recruited for participation in a placebo-controlled, double-blind therapeutic study of the prevention of post-menopausal bone loss. The age range of the group was 49–64 years with a mean age (±SD) of 56 ± 4·1 years. The women were all within 12 years of their menopause with a mean time since menopause (±SD) of 5 ± 2·8 years.

Menopausal status was supported in each case by elevated gonadotrophin levels. None of the women were taking, or had taken in the previous 6 months, any form of medication that might affect bone mineral metabolism.

DPA measurements of the lumbar spine (AP) and proximal femur (femoral neck and Ward's triangle) were made using a Lunar DP3 (Lunar Corporation, Madison, WI, USA). QCT measurements of the lumbar spine were made using a Siemens Somatom 2 CT scanner (Siemens, Erlangen, Germany). L2-L4 was scanned by both techniques. All of the volunteers had lateral lumbar spine radiographs on the same day

as the BMD measurements. The precision of the DPA measurements was 1·3% for the lumbar spine, 1·9% for the femoral neck and 2·3% for the Ward's triangle region [11]. The DPA measurements were acquired and analysed by the same operator (BL). The QCT precision was 2·2% [9] and scans were performed and analysed by the same operator (LB). The QCT images were assessed for the presence of aortic calcification by a single observer (LB). A region of interest (ROI) was drawn around the aorta and those with an average Hounsfield Unit (HU) at one or more QCT levels (12 mm per vertebrae) of 40–75 HU were classified mild, 76–120 HU moderate and > 120 HU severe. From the lateral lumbar spine radiographs, the presence of osteophytes, aortic calcification, apophyseal joint changes and other extraneous calcifications was assessed by an experienced radiologist (JMcS). The severity of these changes were classified subjectively as mild, moderate or severe. These assessments were made without the knowledge of the BMD values.

From the radiographic and QCT findings, the women were initially classified into two groups, those with or without (group 1) any form of degenerative calcification. Those women with calcification present were further subdivided into one of three groups: group 2—only spinal degenerative calcification present (e.g. osteophytes, apophyseal joint changes, end-plate sclerosis) (Fig. 1A); group 3—only aortic calcification present (Fig. 1B); group 4—both spinal degenerative and aortic calcification present (Fig. 1C). This further subdivision allowed the effect of different types of calcification on BMD measurements to be examined.

Statistical analyses

Analysis of variance with linear contrasts was used to examine differences between group means in patient characteristics. Analysis of covariance was used to examine differences in mean bone density measurements using age, time since menopause, height and weight as covariates.

Results

From the radiographic and QCT images, 68 women were found to have some type of calcification present and 47 women had no visible calcification (group 1). The demographic data of these two groups are shown in Table 1. DPA spine BMD measurements were significantly greater in the group with calcification compared to the women with no calcification (group 1) even after adjusting for age, time since menopause, height and weight (Table 1).

Of the 68 women with calcification present either on the radiographs or the QCT images, 23 were found to have spinal degenerative calcification only (group 2), 23 had aortic calcification only (group 3) and 21 had both spinal degenerative and aortic calcification (group 4). One woman with calcification observed on her QCT image could not be assigned to a group as radiographs were not available. The demographic data for these three groups are also shown in Table 1.

Figure 1. (A) Example of group 2. Lateral lumbar spine radiograph showing a moderate osteophyte on L3 and mild osteophyte on L4 (arrowed). (B) Example of group 3. Lateral lumbar spine radiograph showing aortic calcification at level of L1-L4 of moderate severity (moderate = 80–120 HU). (C) Example of group 4. Lateral lumbar spine radiograph showing both severe spinal degenerative changes and moderate aortic calcification.

The BMD measurements for the women with no calcification were compared with each group with calcification (Table 1). After adjusting the data for

Table 1. Patient demographic and BMD data (mean±SD)

	Group 1	Calcification group	Group 2	Group 3	Group 4
n	47	68†	23	23	21
Age (years)	54·6 (3·6)	57·1 (4·1)**	57·4 (4·1)**	56·4 (4·1)	57·7 (4·0)**
Time since menopause (years)	4·3 (2·4)	5·9 (2·8)**	6·0 (3·1)*	5·4 (2·6)	6.4 (2·8)**
Height (cm)	161·3 (6·6)	161·7 (5·1)	161·5 (4·7)	161·6 (4·7)	161·7 (5·4)
Weight (kg)	62·3 (7·1)	62·6 (7·9)	63·8 (8·4)	61·7 (9·0)	62·1 (5·7)
QCT (mg/cm³)	107 (24)	99 (22)	103 (19)	91 (21)*	101 (23)
DPA-spine (g/cm)	1·086 (0·129)	1·129 (0·140)*	1·152 (0·117)**	1·045 (0·094)	1·183 (0·158)**
DPA-femoral neck (g/cm)	0·842 (0·104)	0·825 (0·084)	0·843 (0·095)	0·784 (0·076)*	0·847 (0·067)
DPA-Ward's triangle (g/cm)	0·726 (0·124)	0·710 (0·105)	0·726 (0·113)	0·672 (0·099)	0·728 (0·092)

Group 1, women with no calcification; calcification group = all women with calcification (†total $n = 68$ but X-rays unavailable in one patient); Group 2, women with spinal calcification only; Group 3, women with aortic calcification only; Group 4, women with spinal and aortic calcification. Analysis of covariance between group 1 and groups with calcification with age, time since menopause, height and weight as covariates; $^*P < 0.05$, $^{**}P < 0.01$.

age, time since menopause, height and weight, the mean QCT BMD was significantly lower in group 3 compared to group 1 ($P < 0.05$) and BMD was also significantly reduced in the femoral neck ($P < 0.05$). The mean DPA spine BMD was significantly increased in group 2 and group 4 (both $P < 0.01$), but this was not observed in the QCT BMD measurement or the DPA femoral neck and Ward's triangle measurement.

The radiographs showed the presence of apophyseal joint changes in 13 (11%) of the women and osteophytes were seen in 38 (33%). Other extraneous calcifications such as sclerosis of the end-plates were seen on the radiographs of four women (4%). On the radiographs, aortic calcification was observed in 19 (17%) of the women compared to 45 (39%) noted on the QCT images. The distribution of the severity of each type of calcification is summarized in Fig. 2. Mild and moderate calcification was more common than the severe type of calcification.

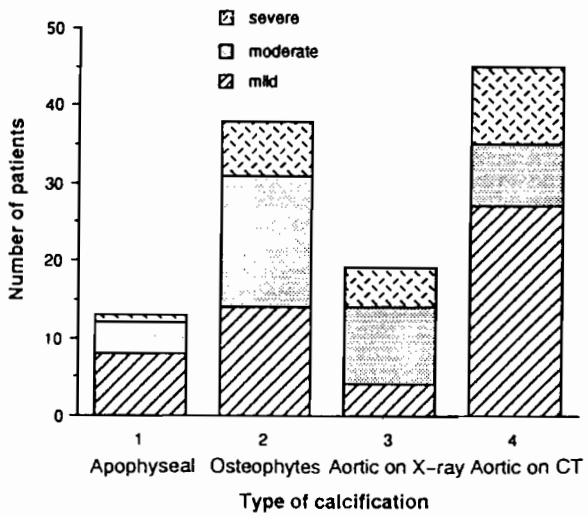

Figure 2. Distribution of the severity of calcification seen on QCT scans and radiographs.

Discussion

In agreement with the findings of others [4–7] we found that degenerative changes in the spine have a more significant effect than aortic calcification on AP DPA spine measurements. However, a number of new observations arise from our study. We have shown that even in a healthy population of early post-menopausal women entering a clinical trial, over half the women (59%) had some type of spinal degenerative change. We found that the women with calcification were older in terms of both chronological and menopausal age compared to the women with no calcification confirming other studies [5,12]. However, as far as we are aware, no other study has examined the effects of time since menopause on degenerative change in relation to BMD.

The women with aortic calcification alone had a significantly lower QCT BMD compared with women with no calcification and this was also reflected in the DPA proximal femur BMD measurements. Reid *et al.* [5] found no effect of aortic calcification on spine BMD in normal women. Others [4,6,7,12] have found significant increases in spine BMD but these were most pronounced when severe calcification was present. One explanation for our finding of reduced BMD in women with aortic calcification is that the other studies measured spine BMD by dual photon techniques only, whereas we measured BMD by QCT which does not include extraneous calcification in its measurement. In the other studies, a reduction in BMD in the proximal femur was not observed, but this may be due to differences in the age and gender of the populations studied. Knight *et al.* [13] have suggested that where osteoarthritis of the hip is present proximal femur BMD may be increased compared with projected control values. A higher incidence of early aortic calcification was found on QCT images (39%) compared with that found on radiographs (17%). The incidence of aortic

calcification found on the radiographs was similar to that reported by Elkeles [14] who found an incidence of 13% on radiographs of women aged between 50 and 60 years. The improvement in detection of aortic calcification using QCT images instead of radiographs was due to the superior spatial resolution of computed tomography images.

We found that women with aortic calcification also have a high incidence of osteopenia, as reported previously [15–17]. In these early studies, low bone mass was determined using radiographs of the spine and hand, and the presence of aortic calcification was noted on radiographs of the spine. Using more accurate techniques our study confirms these early observations. Frye *et al.* [12] demonstrated a significant negative correlation between the number of calcified aortic plaques and spine BMD by DPA in an age-adjusted random sample of 200 women. Some workers have suggested that the high incidence of aortic calcification with low bone mass occurs purely by chance as both conditions worsen with age [16]. However, Browner *et al.* showed that women with lower BMD have a higher mortality from cardiovascular disease (CVD), especially strokes [18]. Witteman *et al.* [19] found that, after adjustment for age and other indicators of CVD risk, women with a natural menopause had a 3·4 times higher risk of atherosclerosis (determined by radiographic detection of calcified deposits in the aorta) than premenopausal women. Similarly, after adjustment for age, the risk of osteoporotic fracture (determined by BMD measurements) is also increased after the menopause [20]. It is possible that these women are more at risk for both osteoporosis and CVD, suggesting a common aetiological factor such as oestrogen deficiency. We were surprised that we did not find a reduced bone density in the group with both aortic and spinal calcification as we did in the group with aortic calcification only. One explanation for this might be that where degenerative changes in the spine are present there are reactive sclerotic changes of the bone causing an increase in bone density in cortical and trabecular bone [21].

As a group, the women with degenerative calcification had higher DPA spine BMD measurements although this was not reflected by the QCT or DPA proximal femur BMD measurements, suggesting that this was not a true increase in BMD but that spinal degenerative calcification was artefactually affecting the measurement. This confirms other studies [4–8], although the extent to which BMD is affected varies according to the age and gender of the population studied. The degenerative changes found in this population were mostly of the mild to moderate category. Accordingly, when studying an older population these changes may become more severe [12,19,22]. These influences on BMD are important to consider when measuring BMD using DPA or by the more recent DXA technology, especially in longitudinal studies where such degenerative changes may progress and mask 'true' changes in BMD. The use of QCT for measuring BMD will certainly circumvent these problems but this technique is not as widely available as DPA and DXA. It has been suggested that lateral DXA scanning may also avoid problems caused by degenerative change. However, the precision of lateral measurements is generally poorer than that of AP [23] but Slosman *et al.* [24] showed that precision may be increased by altering the technique from decubitus to supine lateral scanning.

In conclusion, we found that the majority of healthy post-menospausal women entering a clinical trial had some type of spinal degeneration or aortic calcification. Spinal degenerative calcification artefactually increased DPA spinal BMD measurements. The presence of aortic calcification was associated with reduced BMD, suggesting increased atheromatous disease risk in patients at risk from osteoporosis.

Acknowledgments

We would like to thank Dr Christopher Walton of the Wynn Institute for Metabolic Research for statistical advice.

References

1 Wahner HW, Dunn WL, Mazess RB *et al.* Dual photon Gd^{153} absorptiometry of bone. Radiology 1985;156:203–5.
2 Stein JA, Hochberg AM, Lazewatsky L. Quantitative digital radiography for bone mineral analysis. In: Dequeker JV, Geusens P, Wahner HW, eds. Bone Mineral Measurements by Photon Absorptiometry: Methodological Problems. Louvain: Leuven University Press, 1987:411–14.
3 Mazess RB, Collick B, Trempe J, Barden H, Hanson J. Performance evaluation of a dual-energy X-ray bone densitometer. Calcif Tissue Int 1989;44:228–32.
4 Orwoll ES, Oviatt SK, Mann T. The impact of osteophytic and vascular calcification on vertebral mineral density measurements in men. J Clin Endocrinol Metab 1990;70:1202–7.
5 Reid IR, Evans MC, Ames R, Wattie DJ. The influence of osteophytes and aortic calcification on spine mineral density in postmenopausal women. J Clin Endocrinol Metab 1991;72:1372–4.
6 Krølner B, Berthelsen B, Nielsen SP. Assessment of vertebral osteopenia. Comparison of spinal radiography and dual photon absorptiometry. Acta Radiol Diag 1982;23:517–21.
7 Pouilles JM, Tremollieres F, Louvet JP, Fournie B, Morlock G, Ribot C. Sensitivity of dual-photon absorptiometry in spinal osteoporosis. Calcif Tissue Int 1988;43:329–34.
8 Masud T, Langley S, Wiltshire P, Doyle DV, Spector TD. Effect of spinal osteophytosis on bone mineral density measurements in vertebral osteoporosis. BMJ 1993;307:172–3.
9 Banks LM, Stevenson JC. Modified method of spinal computed tomography for trabecular bone mineral measurements. J Comput Assist Tomogr 1986;10:463–7.
10 Mazess RB, Gifford CA, Bisek JP, Barden HS, Hanson JA. DEXA measurement of spine density in the lateral projection: 1. Methodology. Cal Tiss Int 1991;49:235–9.
11 Lees B, Stevenson JC. An evaluation of dual-energy X-ray absorptiometry and comparison with dual-photon absorptiometry. Osteoporosis Int 1992;2:146–52.
12 Frye MA, Melton LJ, Bryant SC *et al.* Osteoporosis and calcification of the aorta. Bone and Mineral 1992;19:185–94.
13 Knight SM, Ring EFG, Bhalla AK. Bone mineral density and osteoarthritis. Ann Rheum Dis 1992;51:1025–6.

14 Elkeles A. A comparative radiological study of calcified atheroma in males and females over 50 years of age. Lancet 1957;2:714–5.
15 Marum GJ. Roentgenographic observations in age: atrophy and osteoporosis of the spine. Radiology 1946;37:220–6.
16 Anderson JB, Barnett E, Nordin BEC. The relation between osteoporosis and aortic calcification. Br J Radiol 1964;37:910–2.
17 Boukhris R, Becker KL. Calcification of the aorta and osteoporosis: A roentgenographic study. JAMA 1972;219:1307–11.
18 Browner WS, Seeley DG, Vogt TM, Cummings SR. Non-trauma mortality in elderly women with low bone mineral density. Lancet 1991;338:355–8.
19 Witteman JCM, Kok FJ, Van Saase JLCM, Valkenberg HA. Aortic calcification as a predictor of cardiovascular mortality. Lancet 1986;2:1120–2.
20 Slemenda C, Hui SL, Loncope C, Johnson CC. Sex steroids and bone mass: a study of changes about the time of the menopause. J Clin Invest 1987;80:1261–9.
21 Resnick D, Niwayama G. Articular disease. In: Resnick D, Niwayama G, eds. Diagnosis of Bone and Joint Disorders. Philadelphia: WB Saunders, 1988:1480–561.
22 Ross PD, Wasnich RD, Vogel RD. Magnitude of artifact errors in spine dual-photon absorptiometry measurements. In: Christiansen C, Johansen JS, Riis BJ, eds. Osteoporosis 1987. Viborg, Denmark: Norhaven A/S 1987:389–91.
23 Lilley J, Walters BG, Heath DA, Drolc Z. *In vivo* and *in vitro* precision for bone density measurements by dual-energy X-ray absorptiometry. Osteoporosis Int 1991;1:141–6.
24 Slosman DO, Rizzoli R, Donarth A, Bonjour JP. Bone mineral density of lumbar vertebral body determined in supine and lateral decubitus. Study of precision and sensitivity. J Bone Miner Res 1992;7 (Suppl, 1):S192.

JOURNAL OF BONE AND MINERAL RESEARCH
Volume 16, Number 5, 2001

Perspective

Inaccuracies Inherent in Dual-Energy X-Ray Absorptiometry In Vivo Bone Mineral Density Can Seriously Mislead Diagnostic/Prognostic Interpretations of Patient-Specific Bone Fragility

H.H. BOLOTIN[1,2] and H. SIEVÄNEN[3]

INTRODUCTION

SINCE ITS advent, noninvasive dual-energy X-ray absorptiometric (DXA) in vivo measurement of bone mineral density (BMD) has been accepted almost universally as the methodology of choice in the field of clinical bone fragility. More specifically, DXA generally is considered to be the prime, reliable assessor of the osteopenic/osteoporotic condition[1-6] of bone fracture propensity,[6-9] of correlations of measured BMD with fracture failure load of bones,[10-17] and of the efficacy of remedial bone therapies.[18-26] DXA also is held to be the standard against which newer, emerging alternative methods of bone quality assessment are evaluated.[27,28]

However, despite the near ubiquitous clinical use of DXA-measured in vivo BMD and the widespread reliance on it, recently attention has been drawn to the prospect that BMD, per se, may not be the primary determinant of bone fracture risk. Reports of large reductions in vertebral fracture rates attributed to antiresorptive therapy, but without commensurate accompanying increases in BMD,[20,22,24,29,30] have prompted suggestions[7,31] that BMD may not be homologous with bone strength and that other nondensity particulars may be as, or more, important in this respect.

Notwithstanding the importance of the foregoing, certainly one of the most fundamental issues relevant to all aspects of bone densitometry and fragility studies and resultant in vivo diagnostic/prognostic interpretations relates to the growing number of investigations that have shown DXA-derived in vivo BMD to be subject to sizable inherent systematic inaccuracies that may adversely influence measurement outcomes.[32-39] Clearly, the extent of such in vivo BMD inaccuracies and the dependence of them on soft-tissue anthropometric particulars are of salient import for patient-specific clinical DXA measurements.[38,39] Such BMD inaccuracies could seriously compromise the integrity of measurements undertaken to diagnose, monitor, and evaluate the osteopenic/osteoporotic condition and predictive bone fragility of any individual patient. Were this the case, reliance on DXA-derived BMD measurement values could lead to misinterpretations and erroneous assessments of the efficacy and/or quantitative effectiveness of drug and other therapeutic regimens intended to ameliorate the osteoporotic condition.[32-41] Moreover, should large in vivo BMD inaccuracies pertain, clinical DXA investigations undertaken to delineate specific anthropometric, dietary, and/or therapeutic factors which may prove biologically causal or remedially effective in altering BMD and bone fracture propensity, could yield tenuous and/or misleading conclusions.[38-41]

These concerns are underscored by the findings of a considerable number of investigations: in situ/in vitro cadaveric DXA studies,[10,11,17,42] absorptiometrically realistic phantom DXA studies,[40] simulation studies of replicated clinical in vivo bone-site particulars,[38-41] and fundamental quantitative analyses of DXA methodology.[34,43] Collectively, these observations and results may be seen to con-

[1]Department of Medical Radiations Science, RMIT University, Bundoora, Victoria, Australia.
[2]School of Physics, University of Melbourne, Victoria, Australia.
[3]The Bone Research Group, UKK Institute, Tampere, Finland.

stitute a formidable case for reevaluation of the reliability and accuracy of DXA-measured in vivo BMD.

For these reasons, it is important to highlight and evaluate the evidence substantiating the presence of inherent clinical inaccuracies in DXA-measured in vivo BMD, assess the demonstrated extent of these inaccuracies, and draw attention to some of the consequential effects of these inaccuracies on bone densitometry in the clinical context.

EVIDENCE OF SIZABLE INHERENT DXA IN VIVO BMD INACCURACIES

Origin of inherent systematic DXA in vivo BMD inaccuracies

Inherent systematic inaccuracies in DXA BMD derive from the known inapplicability of planar DXA methodology to bone sites comprised of more than two absorptiometrically distinguishable components in the entire scan region of interest (ROI); the "two-component DXA limitation."[32-35,37-39] Yet, all in vivo bone sites are comprised of bone material, intraosseous soft tissue of some unspecified red/yellow marrow compositional mix, and some combination of lean muscle tissue and fat external to the bone that together constitute at least four absorptiometrically disparate components in the DXA scan ROI. Therefore, it is clear that in vivo bone-site reality does not and cannot strictly conform to or satisfy the two-component DXA restriction.[38] This shortcoming is further exacerbated in any patient-specific case by the inability of DXA to assess the necessary particulars of the bone marrow composition. Further, in vivo DXA can neither determine the fat component (and its degree of inhomogeneity) within the lean extraosseous tissue along any X-ray path traversing bone material nor determine the quantitative extent to which the two-component DXA limitation fails to be satisfied in any given in vivo bone-site scan.

A most serious consequence of the violation of this intrinsic two-component DXA limitation is the under- or overestimation of BMD. This is so because DXA methodology erroneously and unavoidably attributes to bone material any difference between the X-ray absorptiometric characteristics of the specific bone marrow composition and the particular extraosseous soft-tissue composition within the particular bone-scan ROI of a given patient.[38-40] This is the case even when these soft tissues are homogeneously constituted throughout their separate, respective, intra- and extraosseous domains (e.g., even when fat is distributed uniformly throughout the lean muscle tissue in the ROI external to the bone). For this reason, the DXA in vivo BMD measurement must be inherently inaccurate to some indeterminate extent for any given patient, and, in general, the DXA scan will necessarily result in a measured value of BMD that differs from the true value.[38] (In the present context, the true value of BMD denotes that which would have been measured were there no DXA BMD measurement inaccuracies.)

Results of anatomically realistic simulation studies of vertebral and femoral in vivo DXA scans

Based on the comprehensively developed analytic underpinnings of DXA,[38] an extensive series of quantitative simulation studies of typical DXA in vivo lumbar vertebral and proximal femoral sites have been reported[38-40] in which the full ranges of anatomically realistic BMD and soft-tissue anthropometrics encountered clinically within the scan ROI were represented. These studies showed that, even for cases in which the extraosseous tissues in the bone-scan ROI are homogeneously constituted and uniformly distributed, patient-specific in vivo BMD inaccuracies readily exceeding ±20% (i.e., some two SDs of age-moderated, population-based, normative BMD data) can be anticipated. This is particularly so for postmenopausal women, the elderly, and the osteopenic/osteoporotic—the very groups for which it is most important that in vivo DXA gauge BMD accurately. In addition, these studies showed, both quantitatively and qualitatively, that the well-documented correlations between percent body fat mass/body mass/body mass index (BMI) and DXA-measured in vivo BMD[5,43-52] seem unlikely to be of bone-biological origin, but, instead, appear fully consistent with being manifestations of inherent DXA in vivo BMD inaccuracies unaccompanied by any true BMD changes.[39] At the same time, and again based on DXA in vivo inaccuracies induced by changes in soft-tissue habitus, these simulation studies also provide a realistically credible explanation for the apparent lack of expected BMD increases with remedial antiresorptive therapy regimens.[41]

DXA scans of absorptiometrically realistic phantoms replicating bone material, marrow, fat, and lean muscle tissue compositions

Norland XR-26 (Norland Corp., Fort Atkinson, WI, USA), Lunar DPX-α (Lunar Corp., Madison, WI, USA), and Hologic QDR-1000 (Hologic, Waltham, MA, USA) DXA instruments were each used to carry out the same extensive set of BMD scans of 150 different phantom arrays. The phantom assemblies were comprised of materials specially formulated and fabricated to span the anthropometric ranges of BMD and intra- and extraosseous soft-tissue compositions encountered clinically.[40] Additionally, the X-ray attenuation coefficients of all relevant in vivo tissues were matched virtually exactly by their respective phantom representations across the full DXA X-ray energy range. To establish conditions most favorable for DXA BMD measurements, all phantom arrays had identical overall dimensions, all intra- and extraosseous phantom materials were separately absorptiometrically homogeneous throughout their respective domains in the scan ROI, and the geometry of the phantom arrays were effectively ideal for bone-edge detection algorithms incorporated in each of the DXA instruments used.[40] The results of these studies—effectively identical for all three of these widely used DXA instruments—corroborated in every respect the inherent systematic DXA BMD inaccuracies found in the extensive

quantitative simulation studies described previously[38,39] and those carried out for each of these phantom arrays.[40]

These foregoing findings can be summarized fairly as follows. DXA-measured in vivo BMD inaccuracies are very much patient specific, because the magnitude of the BMD value extracted from a given DXA measurement depends on: (i) the exact specifications of the bone marrow composition, (ii) the detailed composition of the extraosseous soft tissue, and (iii) the true (not measured) value of BMD (i.e., proportional to the average thickness of bone material along all X-ray paths traversing the given bone-site) actually pertaining within the specific scan ROI of each given patient.[40] It is the case that (a) for any given extraosseous soft-tissue composition in the scan ROI, the more yellow the bone marrow the more DXA underestimates true BMD; (b) for any given bone marrow composition, the smaller the proportion of fat in the extraosseous lean tissue the more the DXA-measured BMD underestimates the true value; and (c) for any given marrow and extraosseous soft-tissue compositions, the smaller the true BMD at any particular bone site, the greater is the DXA over- or underestimate of it. Thus, for any individual with low true BMD, more yellowish bone marrow and leaner soft-tissue habitus (postmenopausal, osteopenic, osteoporotic, and elderly persons), these inherent inaccuracies in DXA could lead to measured BMD values that are sizable over- or underestimates of the true BMD value, the extent of which depends most particularly on the patient-specific soft-tissue anthropometrics in the scan ROI of the given bone sites(s) that were interrogated.

This being the case, it must be noted that bone marrow is one of the most labile of soft tissues[53-56] and that the extraosseous soft-tissue composition within the DXA scan ROI varies considerably from bone site to bone site and for any selected bone site may vary over time in any given patient and from patient to patient. For these reasons, it can be expected that the inaccuracies inherent in DXA in vivo methodology may result in seemingly arbitrary (if not capricious) BMD values being extracted from the measurements. Thus, for postmenopausal, osteopenic, osteoporotic, and elderly individuals (generally lower true BMD, more yellowish marrow, and often leaner than the normal population), these inaccuracies may readily give rise to underestimates of true BMD as large as 20–30%.[38-40]

Results of in situ/in vitro cadaveric studies

A number of carefully detailed cadaveric studies[10,11,17,36,42] have provided incisive evidence of large inaccuracies in specimen-specific (patient-specific) DXA BMD measurements. Of these, the in vitro investigation of Kuiper et al.[36] showed quite conclusively that the BMD values obtained from DXA measurements of excised human cadaveric femoral neck specimens, immersed in a water bath after removal of all external soft tissues ("denuded"), were consistently smaller when the given bone specimen was scanned with the intraosseous marrow intact than when measured again after the marrow was removed and replaced by water. The latter arrangement constitutes a reasonably close approximation to a two-component DXA scan ROI. Further, the differences in these paired, carefully standardized DXA-measured BMD values tended to be greater the higher the percent of fat in the original bone marrow (determined by chemical analysis of the extracted marrow). These observations are in excellent agreement with the findings of the analytic simulation and phantom studies described previously[38-41]; they display (and confirm) the established[41] trend and extent of inherent DXA BMD inaccuracies induced by the different absorptiometric properties of the various pertaining bone marrow compositions.

Comparison of the findings of the cadaveric bone fragility studies of Lochmüller et al.[10] and Bouxsein et al.[11] serves to exemplify and illustrate sizable DXA-measured BMD inaccuracies directly attributable to variations in specimen-specific soft-tissue composition particulars within the scan ROI of their respective studies. The former workers scanned vertebrae L2–L4 only in situ, the latter obtained BMD values of the femoral trochanteric region only ex situ (DXA-scanned in a water bath with marrow intact). In both studies, the fracture failure load of the corresponding excised and denuded cadaveric bone (marrow intact) was determined after the DXA measurement. The overall BMD versus fracture failure load correlation coefficient found in the in situ study[10] was small (r^2 = 0.23), which was somewhat lower than reported by others,[28,57] but marginally higher than that reported by Bjarnason et al.[17] This is to be compared with the femoral in vitro work of Bouxsein et al.[11] in which the much higher value of r^2 = 0.90 pertained. A number of other similar studies[12-16] of fracture failure load versus DXA in vitro BMD measurements of denuded cadaveric lumbar vertebral and proximal femoral bone specimens also yielded generally higher correlation coefficients (r^2 values) than did the in situ works of Lochmüller et al.[10] and Bjarnason et al.[17] In the context of the analytical underpinnings of DXA,[38] the generally smaller r^2 values found in the in situ studies can be seen as due principally to the more sizable and varied DXA BMD inaccuracies expected in these cases. This is anticipated as generally broader absorptiometric disparities between the compositions of the extraosseous fat/lean muscle tissue and the intraosseous red/yellow marrow combinations would pertain in situ (and in vivo) than would be the case between the various bone marrow compositions within the excised, denuded specimens and the standardized water bath in the in vitro scans.[12] Thus, because the DXA in vitro BMD measurements of denuded cadaveric bone specimens in the works of Bouxsein et al.[11] and others[12,17,42] tend to approach two-component scan ROIs to a greater extent than do DXA in situ (in vivo) BMD situations, the in vitro BMD values are tacitly taken in these studies as the better approximations to true BMD values.

The illuminating study by Svendsen et al.[42] on the impact of soft-tissue composition on in vivo accuracy of DXA-measured BMD is of particular importance in this regard. These investigators compared the DXA-measured BMD values of in situ and in vitro lumbar vertebral specimens (L2–L3 and L2–L4 in lateral and anteroposterior [AP] projections, respectively), forearm, and five proximal femoral regions of 14 cadavers. Exactly the same vertebral bone specimens were DXA-measured in a standardized orientation in both the in situ and the in vitro facets of their

investigation, the in vitro scans being of excised, denuded specimens immersed in a 71.4% wt/wt water/ethanol bath. The linear regression analysis of their corresponding in situ versus in vitro BMD values yielded overall accuracy in the standard estimate of errors (SEE%) for the L2–L4 vertebrae of 5.3% and 9.7% for the AP and lateral scans, respectively. The analogous SEE% found for the various femoral sites ranged from about 3% to about 11%. Nevertheless, it is important in the present context to note that their data displayed several individual, specimen-specific inaccuracies exceeding 20% in these 14 cadaveric cases, some of the largest of which pertained to vertebral specimens displaying DXA in vitro BMD values in the lower ranges. The trend and extent of these specimen-specific BMD inaccuracies are fully consistent with and complementary to other observations and findings already summarized above.

Cadaveric studies by Bjarnason et al.,[17] in which biomechanical measurements were made of 32 individual vertebrae from the same 14 cadavers used in the earlier work of Svendsen et al.,[42] clearly display large specimen-specific inaccuracies in DXA-derived BMD. These later workers[17] compared the measured fracture failure load of each of the 32 individual vertebrae with BMD values obtained from separate AP and lateral DXA scans of the same vertebra both in situ and in vitro. Although their analyses and discussion focused on overall linear regression-derived dependencies of DXA-measured BMD and bone fragility, the format of their published data provides a one-to-one correspondence between the in situ and in vitro (denuded specimens in a 71.4% water/ethanol, wt/wt, bath) BMD values of each of these vertebral specimens (see in vitro vs. in situ data in Fig. 2 of Bjarnason et al.[17]). The present Fig. 1 displays these in situ/in vitro comparisons extracted from their lateral and AP scan results,[17] respectively. Despite the limited number of different combinations of body soft tissue and bone marrow compositions, which only 14 in situ cadavers unavoidably represent, Fig. 1A, nevertheless, clearly shows that the DXA-measured BMD values obtained from lateral scans of these vertebrae exhibited measurable, sizable differences between the in situ and in vitro measurements of the same vertebra in 30 of these 32 cases. More than half of these BMD disparities (inaccuracies) exceeded 10%, 5 of the 30 reflected inaccuracies greater than 20%; and one displayed a measured in situ versus in vitro BMD difference of ~53%. It is of particular interest that in their lateral scan cases (Fig. 1A), 11 of the inaccuracies constituted overestimates of BMD and 19 were underestimations, whereas in their AP scans of the same vertebrae (Fig. 1B), almost the reverse pertained for these same vertebrae, with 20 overestimates and 11 underestimates of BMD. The results of the analytic, simulation, and phantom studies[34,38–41] strongly suggest that the observed reversal in the in situ versus in vitro over- and underestimates in the lateral and AP DXA-measured BMD of these same 32 vertebrae arose from in situ differences in: (i) the ratio of the areal densities of extraosseous fat and lean muscle tissue (the particular body soft-tissue composition external to the bone) and (ii) any inhomogeneities in the distribution of fat through the lean muscle tissue within the ROI of each of these two alternative scans.

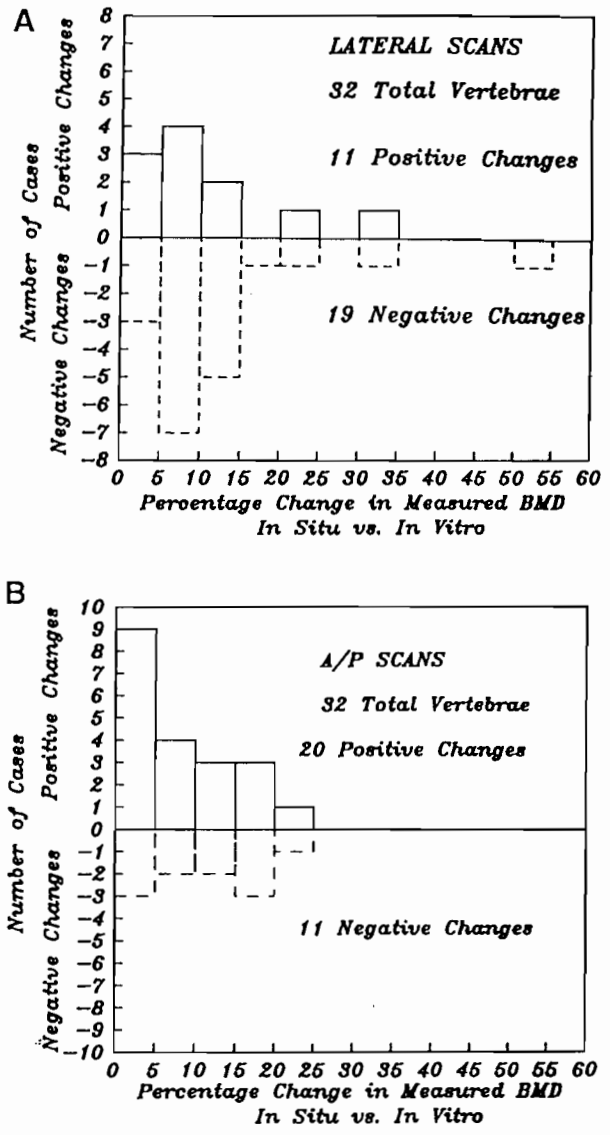

FIG. 1. Percentage differences between DXA measured in situ and in vitro BMD values for (A) lateral scans and (B) AP scans for each of the 32 vertebrae excised from 14 cadavers, as extracted from the results reported by Bjarnason et al.[17] Displayed in groupings of 5% BMD differences are the number of cases out of 32 that the in situ DXA BMD values separately overestimate (positive inaccuracy) and underestimate (negative inaccuracy) the BMD values meted in vitro in the two alternative scans.

DISCUSSION

First, it should be noted that the term "true BMD" is used here to designate that value of BMD that would have been extracted from a standardized DXA scan were no BMD inaccuracy associated with the measurement, while "measured BMD" is that value extracted from an actual standardized DXA scan of the same bone site.

The extensive evidence of sizable inherent systematic inaccuracies in DXA-measured in vivo BMD displayed in the results of a considerable number of relevant and perti-

nent investigations makes it clear that DXA-measured BMD is not necessarily synonymous with true BMD. As such, it would appear necessary and prudent that the distinction between measured and true BMD values be circumspectively considered before definitive conclusions are educed from any DXA-based assessments of BMD, bone fragility, the osteopenic/osteoporotic condition, and/or the effectiveness of antiresorptive drugs or other remedial therapies in any given patient case. These cautionary qualifications are wholly consistent with but extend considerably beyond the conclusion of Marshall et al.[8] that the DXA measurement of BMD should not be relied on to identify those individuals who will develop a future fracture.

This stricture should not be ignored in any given study in which regression analysis is relied on to interrogate trends, relationships, and/or correlations between DXA-derived BMD values and any other given measured parameter (e.g., bone fracture propensity, BMI, body fat mass, body lean tissue mass, therapeutic regimen effectiveness, etc.). The same wariness may be attached justifiably to those DXA-based findings relating BMD to fracture failure load, which have indicated the causative dependence of measured BMD on bone fragility to be less positive than expected from particular antiresorptive drug therapies. Such circumspection appears warranted in light of the realistic prospect that outcomes may, in fact, be distorted artifactually because of measured rather than true BMD being the associated factor in each of these studies. For example, the lack of observed BMD changes expected from antiresorptive therapy may not necessarily imply that BMD is not a good measure of bone fragility or strength, but only that measured BMD, due to the inherent and sizable DXA in vivo inaccuracies, may not be.[41] Similarly, the relationship between BMI, body soft-tissue composition, etc., and DXA in vivo BMD measurements[5,43–52] can be attributed more to these anthropometric features affecting the measured BMD values than to some related biologically causal mechanism affecting true BMD.[39,41]

From the evidence presented, it is clear that patient-specific DXA-measured in vivo BMD inaccuracies can readily exceed ±20% or more in individual cases without any available clinical means to identify these cases. From this perspective, it is therefore reasonable to question the reliability of DXA-measured changes in vertebral BMD to gauge the effectiveness of therapeutic drugs for any given person. Conversely, but not without similar underpinnings, such treatment regimens as hormone replacement therapy, antiresorptive drugs, etc. may, if evaluated primarily on DXA in vivo BMD measurements, be judged erroneously to be either of exaggerated efficacy or of unexpected inadequacy. This follows from the very real prospect that one or another of these therapies might induce relatively modest changes in (i) bone marrow composition[41,53,54] and/or (ii) the particular distribution and proportions of fat within the lean extraosseous tissue in the local bone-site vicinity sufficient to cause patient-specific DXA-measured BMD to either over- or underestimate true BMD. Changes in both bone marrow and extraosseous body composition accompanying aging[55,56] also can lead to analogous uncertainties and ambiguities.

Indeed, even some of instances of weaker than expected correlation coefficients relating fracture failure loads[10,12,14,16,17,28] with DXA-measured in vitro BMD of cleansed, excised cadaveric vertebrae might very well have a related origin. From the present perspective, these DXA measurements may be seen as having been influenced as much or more by the absorptiometric disparity between the in vitro bath (in which each specimen was scanned) and that of the particular intact or residual bone marrow within the given vertebra than to a weak relationship between true BMD and fracture failure load. Going yet a step further, one also might question the extent to which "biological" variability (± ~20% about the mean) in the population-based, age-matched normative DXA BMD data is due to natural variations in true BMD values among individuals and to what degree it may be due more to person-to-person variations in the soft-tissue anthropometrics of the normal population. If traced to the latter, it might largely help explain the number of false-negative osteoporotic diagnoses of those persons known by other means to be osteoporotic, but whose measured BMD values fall within the ±2 SD band of the DXA-based in vivo BMD normative data. Thus, if true BMD were a reasonably good gauge of bone fragility (as it might well be), evidence in support of it might actually be obscured by the very DXA methodology now used to mete it.

The ramifications of inherent systematic DXA in vivo BMD inaccuracies are clearly wide-ranging and potentially serious. For this reason, it would not be unwarranted to view patient-specific bone fragility interpretations based on this methodology with considerable circumspection and/or to advocate reassessment of much of the existing "conventional wisdom," which now rests on DXA in vivo bone densitometry.

REFERENCES

1. Dunn WL, Wahner HW 1994 Commercial instruments available for bone mineral measurements. In: Wahner HW, Fogelman I (eds.) The Evolution of Osteoporosis: Dual Energy X-Ray Absorptiometry in Clinical Practice. Martin Dunitz, Ltd., London, UK, pp. 35–48.
2. Wahner HW, Dunn WL, Brown ML, Morin RL, Riggs BL 1988 Comparison of dual-energy X-ray absorptiometry for bone mineral measurements of the lumbar spine. Mayo Clin Proc 63:1075–1084.
3. Genant HK, Engelke K, Fuerst T, Gluer C-C, Grampf S, Harris ST, Jergas M, Lang T, Lu Ying, Majumdar S, Mathur A, Takada M 1996 Noninvasive assessment of bone mineral and structure: State of the art. J Bone Miner Res 11:707–730.
4. Jergas M, Breitenseher M, Gluer C-C, Yu W, Genant HK 1995 Estimates of volumetric bone density from projectional measurements improve the discriminatory capability of dual X-ray absorptiometry. J Bone Miner Res 10:1101–1110.
5. Ravn P, Cizza G, Bjarnason NH, Thompson F, Daley M, Wasnich RD, McClung M, Hosking D, Yates AJ, Christiansen C, for the Early Postmenopausal Intervention Cohort (EPIC) Study Group 1999 Low body mass index is an important risk factor for low bone mass and increased bone loss in early postmenopausal women. J Bone Miner Res 14:1622–1627.
6. Hansen MA, Overgaard K, Riis BJ, Christiansen C 1991 Role of peak bone mass and bone loss in postmenopausal osteoporosis: 12 year study. BMJ 303:961–964.

7. Hui SL, Slemenda CW, Johnston CC 1989 Baseline measurement of bone mass predicts fracture in white women. Ann Intern Med **111**:355–361.
8. Marshall D, Johnell O, Wedel H 1996 Meta-analysis of how well measures of bone mineral density predict occurrence of osteoporotic fracture. BMJ **312**:1254–1259.
9. Cummings SR, Black DM, Nevitt MC, Browner W, Cauley J, Ensrud K, Genant HK, Palermo L, Scott J, Vogt TM, for the Study of Osteoporotic Fractures Research Group 1993 Bone density at various sites for prediction of hip fractures. Lancet **341**:72–75.
10. Lochmüller E-M, Eckstein F, Kaiser D, Zeller JB, Landgraf J, Putz R, Steldinger R 1998 Prediction of vertebral failure loads from spinal and femoral dual-energy x-ray absorptiometry, and calcaneal ultrasound: An in situ analysis with intact soft tissue. Bone **23**:417–424.
11. Bouxsein ML, Coan BS, Lee SC 1999 Prediction of the strength of the elderly proximal femur by bone mineral density and quantitative ultrasound measurements of the heel and tibia. Bone **25**:49–54.
12. Courtney AC, Wachtel EF, Myers ER, Hayes WC 1994 Effects of loading rate on strength of the proximal femur. Calcif Tissue Int **55**:53–58.
13. Courtney AC, Wachtel EF, Myers ER, Hayes WC 1995 Age-related reductions in the strength of the femur tested in a fall-loading configuration. J Bone Joint Surg Am **77**:387–395.
14. Pinilla TP, Boardman KC, Bouxsein ML, Myers ER, Hayes WC 1996 Impact direction from a fall influences the failure load of the proximal femur as much as age-related bone loss. Calcif Tissue Int **58**:231–235.
15. Bouxsein ML, Courtney AC, Hayes WC 1995 Ultrasound and densitometry of the calcaneus correlate with the failure loads of cadaveric femurs. Calcif Tissue Int **56**:99–103.
16. Cheng XG, Lowet G, Boonen S, Nicholson PHF, Brys P, Nus J, Dequeker J 1997 Assessment of the strength of proximal femur in vitro: Relationship to femoral bone mineral density and femoral geometry. Bone **20**:213–218.
17. Bjarnason K, Hassager C, Svendsen OL, Stang H, Christiansen C 1996 Anteroposterior and lateral spinal DXA for the assessment of vertebral body strength: Comparison with hip and forearm measurement. Osteoporos Int **6**:37–42.
18. Kiel DP, Felson DT, Anderson JJ, Wilson PWF, Moskowitz MA 1987 Hip fracture and the use of estrogens in postmenopausal women: The Framingham Study. N Engl J Med **317**: 1169–1174.
19. Riggs BL, Hodgson SF, O'Fallon WM, Chao EYS, Wahner HW, Muhs JM, Cedel SL, Melton LJ III 1990 Effect of fluoride treatment on the fracture rate in postmenopausal women with osteoporosis. N Engl J Med **322**:802–809.
20. Lufkin EG, Wahner HW, O'Fallon WM, Hodgson SF, Kotowicz MA, Lane AW, Judd HL, Caplan RH, Riggs BL 1992 Treatment of postmenopausal osteoporosis with transdermal estrogen. Ann Intern Med **117**:1–9.
21. Liberman UA, Weiss SR, Broll J, Minne HW, Quan H, Bell NH, Rodriguez-Portales J, Downs RW Jr, Dequeker J, Favus M, Seeman E, Recker RR, Capizzi T, Santora AC, Lombardi A, Shah RV, Hirsch LJ, Karpf DB, for the Alendronate Phase III Osteoporosis Treatment Study Group 1995 Effect of oral alendronate on bone mineral density and the incidence of fractures in postmenopausal osteoporosis. N Engl J Med **333**: 1437–1443.
22. Black DM, Cummings SR, Karpf DB, Cauley JA, Thompson DE, Nevitt MC, Bauer DC, Genant HK, Haskell WL, Marcus R, Ott SM, Torner JC, Quandt SA, Reiss TF, Ensrud KE, for the Fracture Intervention Trial Research Group 1996 Randomised trial of effect of alendronate on risk of fracture in women with existing vertebral fractures. Lancet **348**:1535–1541.
23. Hosking D, Chilver CED, Christiansen C, Pavn P, Wasnich R, Ross P, McClung M, Balske A, Thompson D, Daley M, Yates J, for the Early Postmenopausal Intervention Cohort Study Group 1998 Prevention of bone loss with alendronate in postmenopausal women under 60 years of age. N Engl J Med **338**:485–492.
24. Ettinger B, Black DM, Mitlak BH, Knickerbocker RK, Nickelsen T, Genant HK, Christiansen C, Delmas PD, Zanchetta JR, Stakkestad J, Gluer C-C, Krueger K, Cohen FJ, Eckert S, Ensrud KE, Avioli LV, Lips P, Cummings SR, for the Multiple Outcomes of Raloxifene Evaluation (MORE) Investigators 1999 Reduction of vertebral fracture risk in postmenopausal women with osteoporosis treated with Raloxifene: Results from a 3-year randomized clinical trial. JAMA **282**:637–645.
25. Eastell R 1998 Treatment of postmenopausal osteoporosis. N Engl J Med **338**:736–746.
26. Meunier PJ 1999 Evidence-based medicine and osteoporosis: A comparison of fracture risk reduction data from osteoporosis randomised clinical trials. Int J Clin Practice **53**:122–129.
27. Bauer DC, Gluer CC, Genant HK, Stone K 1995 Quantitative ultrasound and vertebral fracture in postmenopausal women. J Bone Miner Res **10**:353–358.
28. Cheng XG, Nicholson PHF, Boonen S, Lowet G, Brys P, Aerssens J, Van Der Perre G, Dequeker J 1997 Prediction of vertebral strength in vitro by spinal bone densitometry and calcaneal ultrasound. J Bone Miner Res **10**:1721–1728.
29. Chapuy MC, Ariot ME, Duboeuf F, Brun J, Crouzet B, Arnaud S, Delmas PD, Meunier PJ 1992 Vitamin D3 and calcium to prevent hip fractures in the elderly women. N Engl J Med **327**:1637–1642.
30. Cummings SR, Black DM, Thompson DE, Applegate WB, Barrett-Connoner EA, Musliner TA, Palermo L, Prineas R, Rubin SM, Scott JC, Vogt T, Wallace R, Yates AJ, LaCroix AZ, for the Fracture Intervention Trial Research Group 1998 Effect of alendronate on risk of fracture in women with low bone density but without vertebral fractures. JAMA **280**:2077–2082.
31. Faulkner KG 2000 Bone matters: Are density increases necessary to reduce fracture risk? J Bone Miner Res **15**:183–187.
32. Webber CE 1987 The effect of fat on bone mineral measurements in normal subjects with recommend values of bone, muscle, and fat attenuation coefficients. Clin Phys Physiol Meas **8**:143–148.
33. Farrell TJ, Webber CE 1989 The error due to fat inhomogeneity in lumbar spine bone mineral measurements. Clin Phys Physiol Meas **10**:57–64.
34. Sorenson JA 1990 Effects of nonmineral tissues on measurements of bone mineral content by dual-photon absorptiometry. Med Phys **17**:77–84.
35. Tothill P, Avenell A, Reid RM 1994 Precision and accuracy of measurements of whole-body bone mineral comparisons between Hologic, Lunar and Norland dual-energy X-ray absorptiometers. Br J Radiol **67**:1210–1217.
36. Kuiper JW, Van Kuijk C, Grashius JL, Ederveen AGH, Schutte HE 1996 Accuracy and influence of marrow fat on quantitative CT and dual-energy X-ray absorptiometry measurements of the femoral neck in vitro. Osteoporos Int **6**:25–30.
37. Antonacci MD, Hanson DS, Hegeness MH 1996 Pitfalls in the measurement of bone mineral density by dual energy X-ray absorptiometry. Spine **21**:87–91.
38. Bolotin HH 1998 Analytic and quantitative exposition of patient-specific systematic inaccuracies inherent in planar DXA-derived in vivo BMD measurements. Med Phys **25**:139–151.
39. Bolotin HH 1998 A new perspective on the causal influence of soft tissue composition on DXA-measured in vivo bone mineral density. J Bone Miner Res **13**:1739–1746.
40. Bolotin HH, Sievänen H, Grashius JL, Kuiper JW, Järvinen TLN 2001 Inaccuracies inherent in patient-specific DXA bone

mineral density measurements: Comprehensive phantom-based evaluation. J Bone Miner Res **16**:417–426.
41. Bolotin HH 2001 Inaccuracies inherent in DXA in vivo bone mineral densitometry may flaw osteopenic/osteoporotic interpretations and mislead assessments of anti-resorptive therapy effectiveness. Bone (in press).
42. Svendsen OL, Hassager C, Skodt V, Christiansen C 1995 Impact of soft tissue on in vivo accuracy of bone mineral measurements in the spine, hip, and forearm: A human cadaver study. J Bone Miner Res **10**:868–873.
43. Compston JE, Laskey MA, Croucher PI, Coxon A, Dreitzman S 1992 Effect of diet-induced weight loss on total body bone mass. Clin Sci **82**:429–432.
44. Reid IR, Ames R, Evans MC, Sharpe S, Gamble G, France JT, Lim TM, Cundy TF 1992 Determinants of total body regional bone mineral density in normal postmenopausal women—a key role for fat mass. J Clin Endocrinol Metab **75**:45–51.
45. Reid IR, Plank LD, Evans MC 1992 Fat mass is an important determinant of whole body bone density in premenopausal women but not in men. J Clin Endocrinol Metab **75**:770–782.
46. Compston JE, Bhambhani M, Laskey MA, Murphy S, Khaw KT 1992 Body composition and bone mass in postmenopausal women. J Clin Endocrinol (Oxf) **37**:426–431.
47. Reid IR, Ames R, Evans MC, Sharpe SJ, Gamble GD 1994 Determinants of the rate of bone loss in normal postmenopausal women. J Clin Endocrinol Metab **79**:950–954.
48. Reid IR, Evans MC, Ames RW 1994 Volumetric bone density of the lumbar spine is related to fat mass but not lean mass in normal postmenopausal women. Osteoporos Int **4**:362–367.
49. Aloia JR, Vaswani A, Ma R, Flaster E 1995 To what extent is bone mass determined by fat-free or fat-mass? Am J Clin Nutr **61**:1110–1123.
50. Salamone LM, Glynn N, Black D, Epstein RS, Palermo L, Meilahn E, Kuller LH, Cauley JA 1995 Body composition and bone mineral density in premenopausal and early perimenopausal women. J Bone Miner Res **10**:1762–1768.
51. Glynn NW, Meilahn EN, Charron M, Anderson SJ, Kuller LH, Cauley JA 1995 Determinants of bone mineral density in older men. J Bone Miner Res **10**:1769–1777.
52. Salamone LM, Cauley JA, Black DM, Simkin-Silverman L, Lang W, Gregg E, Palermo L, Epstein RS, Kuller LH, Wing R 1999 Effect of a lifestyle intervention on bone mineral density in premenopausal women: A randomized trial. Am J Clin Nutr **70**:97–103.
53. Custer RP 1974 Chapter 2: An Atlas of the Blood and Bone Marrow. Saunders, Philadelphia, PA, USA, pp. 33–42.
54. Minaire P, Edouarde C, Arlot M, Meunier PJ 1984 Marrow changes in paraplegic patients. Calcif Tissue Int **36**:338–340.
55. Glowacki J 1995 Influence of age on human marrow. Calcif Tissue Int **35**(Suppl 1):S50–S51.
56. Ricci C, Cova M, Kang YS, Yang A, Rohmouni A, Scott WW, Zerhouni EA 1990 Normal age-related pattern of cellular and fatty bone marrow distribution in the axial skeleton: MR imaging study. Radiology **177**:83–88.

Address reprint requests to:
Professor Emeritus H.H. Bolotin, Ph.D., D.Sc.
School of Physics
University of Melbourne
Victoria 3010, Australia

DXA in obese patients: are normal values really normal?

Jean M. Weigert, MD and Christopher E. Cann, PhD, Imaging Center of West Hartford, CT and University of California, San Francisco, CA.

Measurements of areal bone density (gm/cm2) in obese patients are reported increased in the spine and proximal femur compared to age-matched controls when DXA is used. This has been attributed to the increased mechanical forces placed on the weightbearing skeleton in obese patients or the possibility of increased circulating estrogen from aromatization in the body fat. Variability in overlying tissue composition is known to affect the results of studies using DXA but is not included in reports. One reason may be that even though the possible inaccuracies have been determined in studies in vitro or in phantoms, little in vivo data exist comparing bone densitometry by DXA with bone density measured using techniques that are not affected by the composition of overlying tissue.

We measured BMD of the spine and proximal femur of 6 obese women and 18 matched control women using DXA and 3DQCT. The 3D QCT analysis included a compensation for body size to normalize QCT results to the UCSF normal database. T-scores based on age 30 were used to compare the clinical results. In obese vs. control, T-scores were DXA SP 0.3+-1.9 vs. -2.6+-.9, DXA FN -0.5+-0.8 vs. -3.1+-0.6, QCT SP -2.8+-1.1 vs. -3.0+-0.8. In obese women, T-score QCT=0.7 T-score DXA –2.9 (r=0.96). 2/6 obese women had thoracic vertebral compressions.

These results of this study suggest that DXA of both the spine and hip overestimate BMD in obese women and the results should be interpreted with caution. In addition, alternate BMD modalities not affected by the overlying soft tissue should be considered as primary modalities for the diagnosis of osteoporosis in these patients.

The NEW ENGLAND JOURNAL of MEDICINE

One Year of Alendronate after One Year of Parathyroid Hormone (1–84) for Osteoporosis

Dennis M. Black, Ph.D., John P. Bilezikian, M.D., Kristine E. Ensrud, M.D., M.P.H., Susan L. Greenspan, M.D., Lisa Palermo, M.A., Trisha Hue, M.A., Thomas F. Lang, Ph.D., Joan A. McGowan, Ph.D., Clifford J. Rosen, M.D., for the PaTH Study Investigators

ABSTRACT

Background Since the use of parathyroid hormone as a treatment for osteoporosis is limited to two years or less, the question of whether antiresorptive therapy should follow parathyroid hormone therapy is important. We previously reported results after the first year of this randomized trial comparing the use of full-length parathyroid hormone (1–84) alone, alendronate alone, or both combined. In the continuation of this trial, we asked whether antiresorptive therapy is required to maintain gains in bone mineral density after one year of therapy with parathyroid hormone (1–84).

Methods In the data reported here, women who had received parathyroid hormone (1–84) monotherapy (100 μg daily) in year 1 were randomly reassigned to one additional year with either placebo (60 subjects) or alendronate (59 subjects). Subjects who had received combination therapy in year 1 received alendronate in year 2; those who had received alendronate monotherapy in year 1 continued with alendronate in year 2. Bone mineral density at the spine and hip was assessed with the use of dual-energy x-ray absorptiometry and quantitative computed tomography (CT).

Results Over two years, alendronate therapy after parathyroid hormone therapy led to significant increases in bone mineral density in comparison with the results for placebo after parathyroid hormone therapy, a difference particularly evident for bone mineral density in trabecular bone at the spine on quantitative CT (an increase of 31 percent in the parathyroid hormone–alendronate group as compared with 14 percent in the parathyroid hormone–placebo group). During year 2, subjects receiving placebo lost substantial bone mineral density.

Conclusions After one year of parathyroid hormone (1–84), densitometric gains appear to be maintained or increased with alendronate but lost if parathyroid hormone is not followed by an antiresorptive agent. These results have clinical implications for therapeutic choices after the discontinuation of parathyroid hormone.

Source Information

From the Departments of Epidemiology and Biostatistics (D.M.B., L.P., T.H.) and Radiology (T.F.L.), University of California, San Francisco; the Department of Medicine, College of Physicians and Surgeons, Columbia University, New York (J.P.B.); the Departments of Medicine and Epidemiology, Minneapolis Veterans Affairs Medical Center and University of Minnesota, Minneapolis (K.E.E.); the University of Pittsburgh Medical Center, Pittsburgh (S.L.G.); the National Institute of Arthritis and Musculoskeletal and Skin Diseases, National Institutes of Health, Bethesda, Md. (J.A.M.); and the Maine Center for Osteoporosis Research, St. Joseph Hospital, Bangor (C.J.R.).

Address reprint requests to Dr. Black at the University of California, San Francisco, San Francisco Coordinating Center, 74 New Montgomery St., Suite 600, San Francisco, CA 94105, or at dblack{at}psg.ucsf.edu .

1: Arthritis Rheum. 2002 May;46(5):1292-7.

Quantitative computed tomography of the lumbar spine, not dual x-ray absorptiometry, is an independent predictor of prevalent vertebral fractures in postmenopausal women with osteopenia receiving long-term glucocorticoid and hormone-replacement therapy.

Rehman Q, Lang T, Modin G, Lane NE.

University of California, San Francisco, CA 94143, USA.

OBJECTIVE: To determine which measurement of bone mineral density (BMD) predicts vertebral fractures in a cohort of postmenopausal women with glucocorticoid-induced osteoporosis. METHODS: We recruited 114 subjects into the study. All had osteopenia of the lumbar spine or hip, as demonstrated by dual x-ray absorptiometry (DXA), and were receiving long-term glucocorticoids and hormone replacement therapy (HRT). Measurements of BMD by DXA of the lumbar spine, hip (and subregions), and forearm (and subregions), quantitative computed tomography (QCT) of the spine and hip (n = 59), and radiographs of the thoracolumbar spine were performed on all subjects to assess prevalent vertebral fractures. Vertebral fracture prevalence, as determined by morphometry, required a >or=20% (or >or=4-mm) loss of vertebral body height. Demographic information was obtained by questionnaire. Multiple regression and classification and regression trees (CART) analyses were used to assess predictors of vertebral fracture. RESULTS: Twenty-six percent of the study subjects had prevalent fractures. BMD of the lumbar spine, total hip and hip subregions, as measured by QCT, but only the lumbar spine and total hip, as measured by DXA, were significantly associated with prevalent vertebral fractures. However, only lumbar spine BMD as measured by QCT was a significant predictor of vertebral fractures. CART analysis showed that a BMD value <0.065 gm/cm(3) was associated with a **7-fold higher risk of fracture** than a BMD value >or=0.065 gm/cm(3).CONCLUSION: In postmenopausal women with osteoporosis induced by long-term glucocorticoid treatment who are also receiving HRT, **BMD of the lumbar spine as measured by QCT, but not DXA, is an independent predictor of vertebral fractures.**

PMID: 12115236 [PubMed - indexed for MEDLINE]

Diagnostic Imaging
November 2001

Bone Density

Imaging use grows as osteoporosis treatment becomes common

Radiologists move from plain film to DXA scanners and QCT to assess early signs of fracture risk

By Virginia J. Griswold, M.D.

Osteoporosis is no longer regarded as a disease only of postmenopausal women, and it is no longer an accepted consequence of aging. While the National Institutes of Health consensus development panel on osteoporosis prevention, diagnosis, and therapy reported that the condition is a major health threat, it added that it is no longer considered age- or sex-dependent and described it as largely preventable.[1]

Developments that have contributed to this new approach include the introduction of nonhormonal therapy, low-dose image-based bone mineral density (BMD) methods, and the use of fracture-risk comparison-based BMD calculations based on a young healthy adult peak peer group rather than an aged-matched peer group. Other influences include international research and consensus based on relative fracture risk estimates and treatment outcome. In addition, the Bone Mass Measurement Act (BMMA) of 1998 stabilized reimbursement, making BMD exams a covered benefit by Medicare carriers for four specified groups of patients:

- estrogen-deficient women deciding about hormone replacement therapy;
- patients with vertebral abnormalities or radiographic osteopenia needing diagnosis of spinal osteoporosis for possible therapy;
- patients receiving long-term glucocorticoid therapy in order to adjust therapy dosage; and
- patients with primary hyperparathyroidism who might be candidates for surgery.

Osteoporosis is a critical disease facing the aging population, and is one of the most important disorders encountered in clinical practice. More than 28 million people in the U.S. suffer from osteoporosis, but in the past, the diagnosis was often not made until a fracture had occurred.

The lifetime risk of hip fracture in women is greater than the sum of the lifetime risk of developing breast, endometrial, and ovarian cancer. Of patients who have fractured a hip, 50% are subsequently unable to walk unassisted and 15% to 20% will die within a year. The cost of hip fractures alone is expected to reach $62 billion by 2020.

loss of early menopause as well as to the response to therapy, which is frequently first seen in trabecular bone.

In the U.S., 1.8 million fractures are attributed to osteoporosis annually: roughly 700,000 vertebral fractures, 300,000 hip fractures, 250,000 distal forearm fractures, and 300,000 fractures of other limbs.[9,10] Worldwide, fractures from osteoporosis occurring each year are projected to increase to 6.3 million in 2050 from 1.7 million in 1990.[11,12]

Men At Risk

Each year men suffer one-third of all the hip fractures that occur, and the lifetime risk of hip fracture in men is greater than that of prostate cancer. Age-adjusted mortality for men with hip fractures is about twice that of women: as high as 30% in the first three months and 50% within a year.[13]

In addition to hip fracture, men also experience painful and debilitating fractures of the spine, wrist, and other bones due to osteoporosis.[14] Two million men in the U.S. have osteoporosis, and another three million or more are at risk. Yet despite the large number of men affected, osteoporosis in men remains underdiagnosed, underreported, and inadequately researched. By ignoring evidence of osteopenia on plain films in males, providers are doing a disservice to patients who will subsequently have serious consequences. Research interest in male bone loss is growing, however.

Densitometry Techniques

When viewed by the unaided eye, plain skeletal radiographs have never been useful for quantifying bone density. Approximately 40% loss of bone mineral must be present to be readily apparent, but no true quantification can be made. The two most commonly used methods for bone densitometry are DXA and QCT.

DXA uses two different photon energies simultaneously to separate the influence of soft tissues and bone and accurately measure bone density. The source of the photon energy is an x-ray tube. The x-ray beam must be narrowed by using k-edge filters or alternating energies to produce the two distinct photoelectric peaks necessary.

Originally, DXA scanners used rectilinear pencil-beam technology. These gave way to fan-array scanners, and scan times have been reduced from a few minutes to as short as 30 seconds. Radiation exposure is extremely low. Expressed in skin entry doses, radiation exposures for an AP spine or femur study are 2 to 5 mrem. The biologically important effective dose or whole-body equivalent dose is 0.1 mrem.[15] At 1 meter from the finely collimated fanbeam source, the radiation scatter is the same as background, which allows the scanners to be placed in rooms without lead shielding in the walls. The operator requires no protection other than distance from the x-ray beam.

The most important advance with DXA has been marked improvement in precision. Reproducibility resulting in short-term precision has been reported as low as 0.9% for the AP lumbar spine and 1.4% for the femoral neck. Newer machines can also perform supine AP and lateral images of the thoracolumbar spine (T4 to L4) with fine detail using a single-source beam in seconds to either look for compression fractures or perform morphometric measurements of each vertebra for signs of subtle loss of vertebral body height.

Because DXA has been found in prospective studies to predict fracture risk, it has become the

gold standard in densitometry exams.

QCT studies use a phantom reference standard containing Ca_2HPO_4, which is placed underneath the patient during the study. A scout view is taken for localization, then an 8 to 10-mm-thick slice is taken through the midbody of two or more vertebral bodies. A region of interest within the anterior portion of the vertebral body is analyzed for bone density and compared with the phantom. It is reported out as mg/cm^3 Ca2HPO4 equivalents, a volumetric value.

QCT measures the trabecular bone of vertebral bodies and avoids problems inherent in the AP spine DXA exams: inclusion of cortical-rich bone from the posterior processes, bone spurs, sclerosis from degenerative disk disease, and incorporation of aortic vascular calcifications. The result is a three-dimensional trabecular density unlike the two-dimensional cortical and trabecular densities reported with DXA.

QCT requires 20 minutes and the skin dose is generally 100 to 300 mrem, although only a small portion of marrow is irradiated during a study of the spine. The effective dose or whole-body equivalent dose from this highly collimated exam is generally in the range of 30 mrem. The localizer scan that precedes the actual QCT study will add 3 mrem to the effective dose. These values are acceptable in the context of natural background radiation of approximately 20 mrem per month or 27 mrem for one-view chest x-ray. Doses are higher (70 mrem) when using newer spiral CT scanners.

The accuracy of QCT is affected by the presence of marrow fat. Because marrow fat increases with age, error in the accuracy of spine QCT measurements increases as the patient ages.

As has been shown in prevalence studies of osteoporotic fractures, QCT can distinguish normal from osteoporotic individuals as well as or better than DXA. Fractures are rare above 110 mg/cm^3 and extremely common below 60 mg/cm^3. Because QCT measures only trabecular bone, which is known to be more metabolically active than cortical bone, rates of change using QCT tend to be greater than those observed with AP spine studies performed with DXA.

Peripheral DXA units can measure bone density of the distal radius and ulna and the calcaneus, and dedicated peripheral QCT scanners are available to evaluate the forearm.

Ultrasound densitometry units for screening of the calcaneus are known as quantitative ultrasound (QUS). Although these units may be acceptable for screening populations, applying T-score criteria to them is probably ill-advised. T-score is the number of standard deviations above or below the peak BMD for young adult females or males. Any detectable bone loss would probably warrant a central site examination.

Diagnostic Guidelines

Osteoporosis can be diagnosed before fractures by measuring bone density, according to the World Health Organization's 1994 definitions. The WHO study defined osteopenia and osteoporosis in a multinational group of postmenopausal white females using DXA. A panel of 16 international experts in the field of osteoporosis noted that a cutoff value of bone density more than 2.5 SDs below the average value for healthy young women would label 30% of their study group as having osteoporosis at some skeletal site (see table). Fifty percent or more of these women had sustained a fracture of the spine, femur, forearm, humerus, or pelvis.[6] Although these guidelines were not originally intended to be applied to women of other racial background or to men, this concept and grading system has been applied in clinical practice in the absence of any other diagnostic guidelines for these groups as well.

Radiologists are uniquely positioned to recognize many of the patients who need screening or quantification of bone mass loss based on increased appreciation of osteopenia/osteoporosis on the plain films they review. Many of these patients may otherwise go undetected until a severe fracture occurs. A large proportion of female patients receiving other imaging from radiology departments, such as mammography or ultrasound, also should be screened for osteopenia. Screening peripheral densitometry units are already used in some mobile mammography units.

CT bone densitometry has a role in densitometry, especially in patients who fail to get reasonable results in the spine with DXA. In addition, DXA scanners are now using larger numbers of detectors to become more imaging-based. Many states require the technologist operating the DXA scanner to be a qualified radiology technologist. In some states, Medicare carriers and other insurance carriers require that the scans be interpreted by radiologists.

Dr. Griswold *is an assistant clinical professor of radiology at the University of California, San Francisco.*

References

1. NIH consensus development panel on osteoporosis prevention, diagnosis, and therapy. JAMA 2001;285(6):785-795.
2. Johnson CC, Melton LJ, Lindsay R, Eddy DM. Clinical indications for bone mass measurements. A report from the scientific advisory board of the National Osteoporosis Foundation. J Bone Miner Res 1989;4:52.
3. Cummings SR, Black DM, Nevitt MC, et al. Bone density at various sites for prediction of hip fractures. Lancet 1993; 341:72-75.
4. Melton L, Atkinson E, O'Fallon W, et al. Long-term fracture prediction by bone mineral assessed at different sites. J Bone Miner Res 1993;8:1227-1233.
5. Gardsell P, Johnell O, Nilsson BE, Gullberg B. Predicting various fragility fractures in women by forearm bone densitometry:a follow-up study. Calcif Tissue Int 1993;52:348-353.
6. The WHO Study Group. Assessment of fracture risk and its applications to screening for postmenopausal osteoporosis. Switzerland: World Health Organization, 1994. WHO Technical Reports Series Geneva: WHO.
7. Miller PD, Bonnick SL, Rosen CJ. Consensus of an international panel on the clinical utility of bone mass measurements in the detection of low bone mass in the adult population. Calcif Tissue Int 1996;58:207-214.
8. Hodgson SF, Johnston CC Jr. Introduction to guidelines: AACE clinical practice guidelines for the prevention and treatment of postmenopausal osteoporosis. Endocr Pract 1996 2:155-171.
9. Consensus Development Conference: diagnosis, prophylaxis and treatment of osteoporosis. Am J Med 1993;94:646-650.
10. Kanis JA, Melton LJ III, Christiansen C, et al. The diagnosis of osteoporosis. J Bone Miner Res 1994;9:1137-1141.
11. Kanis JA, Delmas P, Burckhardt P, et al. Guidelines for diagnosis and management of osteoporosis. Osteoporosis Int 1997;7:390-406.
12. Compston JE, Cooper C, Kanis JA. Bone densitometry in Clinical pratice. BMJ 1995;310:1507-10.
13. Legrand E, Chappard D, Pascaretti C, et al. Trabecular bone microarchitecture, bone mineral density and vertebral fractures in male osteoporosis. JBMR 2000;15:13-19.
14. Mattei JP, Arniaud D, Tonolli I, Roux H. Aetiologies of male osteoporosis: identification procedures. Clin Rheum 1994;13(1):447-452.
15. Bonnick SL, Miller PD. Bone Densitometry in Clinical Practice: Application and

ORIGINAL ARTICLE

ACTA RADIOLOGICA

Effect of Spinal Degenerative Changes on Volumetric Bone Mineral Density of the Central Skeleton as Measured by Quantitative Computed Tomography

G. GUGLIELMI, I. FLORIANI, V. TORRI, J. LI, C. VAN KUIJK, H. K. GENANT & T. F. LANG

Department of Radiology, Scientific Institute Hospital "Casa Sollievo della Sofferenza", San Giovanni Rotondo, Italy; Biometry and Data Management Unit, Scientific Institute "Mario Negri", Milan, Italy; Department of Radiology, Academic Medical Center, University of Amsterdam, The Netherlands, Osteoporosis and Arthritis Research Group, University of California San Francisco, Calif., USA

Guglielmi G, Floriani I, Torri V, Li J, van Kuijk C, Genant HK, Lang TF. Effect of spinal degenerative changes on volumetric bone mineral density of the central skeleton as measured by quantitative computed tomography. Acta Radiol 2005;46:000–000

Purpose: To evaluate the impact of degenerative changes due to osteoarthritis (OA) at the spine on volumetric bone mineral density (BMD) as measured by volumetric quantitative computed tomography (vQCT).

Material and Methods: Eighty-four elderly women (mean age 73 ± 6 years), comprising 33 with vertebral fractures assessed by radiographs and 51 without vertebral fractures, were studied. Trabecular, cortical, and integral BMD were examined at the spine and hip using a helical CT scanner and were compared to dual X-ray absorptiometry (DXA) measurements at the same sites. OA changes visible on the radiographs were categorized into two grades according to severity. Differences in BMD measures obtained in the two groups of patients defined by OA grade using the described radiologic methods were compared using analysis of variance. Standardized difference (effect sizes) was also compared between radiologic methods.

Results: Spinal trabecular BMD did not differ significantly between OA grade 0 and OA grade 1. Spinal cortical and integral BMD measures showed statistically significant differences, as did the lumbar spine DXA BMD measurement (13%, $P=0.02$). The QCT measurements at the hip were also higher in OA 1 subjects. Femoral trabecular BMD was 13–15% higher in OA grade 1 subjects than in OA grade 0 subjects. The cortical BMD measures in the CT_TOT_FEM and CT_TROCH ROI's were also higher in the OA 1 subjects. The integral QCT BMD measures in the hip showed difference between grades OA 1 and 0. The DXA measurements in the neck and trochanter ROI's showed smaller differences (9 and 11%, respectively). There were no statistically significant differences in bone size.

Conclusion: ~~There is no evidence~~ supporting that trabecular BMD measurements by QCT are influenced by OA. Instead, degenerative changes have an effect on both cortical and ~~integral QCT, and on DXA at the lumbar spine and the hip.~~ For subjects with established OA, assessment of BMD by volumetric QCT may be suggested.

Key words: Bone mineral density; dual X-ray absorptiometry; hip; osteoarthritis; spine; volumetric QCT

Giuseppe Guglielmi, M.D., Department of Radiology, Scientific Institute Hospital "Casa Sollievo della Sofferenza", Viale Cappuccini, IT-71013 San Giovanni Rotondo, Italy (fax. +39 0882 453861, e-mail. guglielmi_g@hotmail.com)

Accepted for publication 15 December 2004

Osteoarthritis (OA) refers to the stress-related skeletal response to age-related deterioration of articular structures (2). Along with osteoporosis, OA is an age-related condition with a significant impact on the elderly population (19). Several studies have addressed the relationship between OA and osteoporosis, but have yielded conflicting results. More recent studies of BMD in large

Taylor & Francis
Taylor & Francis Group

DOI ???

BMD measurements

DXA

PA-DXA was performed at lumbar spine (L2–L4) with a Norland XR 26 scanner (Norland Instruments, Fort Atkinson, Wisc., USA) using standard procedures supplied by the manufacturer for scanning and analysis. The in vivo reproducibility of the measurement in our laboratory was 1.0% CV (15). At the hip site, DXA BMD was evaluated at three femoral sites: neck (NECK), Ward's triangle (WT), and great trochanter (TROCH), with an in vivo precision of 2.1, 3.5, and 2.4% CV, respectively.

Helical CT

Volumetric QCT was performed in all subjects at the hip and spine using a spiral CT scanning protocol (Prospeed; G.E. Medical Systems, Milwaukee, Wisc., USA) and image analysis protocols described previously (14, 15). For the spine scan, the patient was positioned supine on the CT table, with a solid bone mineral reference phantom (Image Analysis, Columbia, Ky., USA) beneath the patient's lower back. After location of the L1 and L2 vertebrae on a lateral scout-view of the spine, these levels were encompassed with 3-mm slices at 80 kVp/180mA, pitch=1. Following the spinal measurement, the phantom was centered beneath the patient's hips, and an anteroposterior scout-view of the pelvis was obtained. A region located between the superior aspect of the femoral head and the inferior aspect of the lesser trochanter was scanned with 3-mm-thick slices, with 120 kVp, 150 mA and pitch=1. CT images were transferred to a Sun Ultra 1 Workstation and processed to extract measures of BMD. The processing-task included calibration of the CT images from the native scanner Hounsfield Units to equivalent density (mm/cc) of calcium hydroxyapatite, and determination of trabecular, cortical and integral ROIs from the volumetric CT scans of the spine and proximal femur. The spinal trabecular ROIs included an elliptical region defined on the anterior portion of the central 10 mm of the vertebral body (2D_TRAB), and a region of similar shape (3D_TRAB) centered on the mid-vertebral level but encompassing 70% of the volume between the vertebral endplates. The spinal integral ROIs included regions approximately matched to the bone volumes imaged by PA DXA (SIM_AP), and lateral DXA (SIM_LAT). The SIM_AP region included all of the vertebral bone except for the transverse processes and the vertebral endplates. A spinal cortical region (3D_CORT) encompassed the cortical rim of the vertebral body in a volume that was spatially matched to the SIM_LAT region. Spinal regions are displayed in Fig. 1. The femoral ROIs included volumes of trabecular, cortical, and integral regions of bone approximately matched to the femoral neck (CT_NECK) and total femur (CT_TOT_FEM) regions imaged on Lunar DXA systems (15). These regions are depicted in Fig. 2.

Statistical Analysis

A statistical analysis program (SAS Institute, Cary, N.C., USA) was utilized to compute mean values and standard deviations (SD) for each variable, as well as to test the hypothesis of no difference significance between means of the groups of subjects with OA grade 0 and OA grade 1. The one-way analysis of variance was utilized to verify the influence of OA degenerative changes on BMD measurements after correction for age, body weight, and height. Agreement between the two radiologists was calculated using kappa statistics (κ).

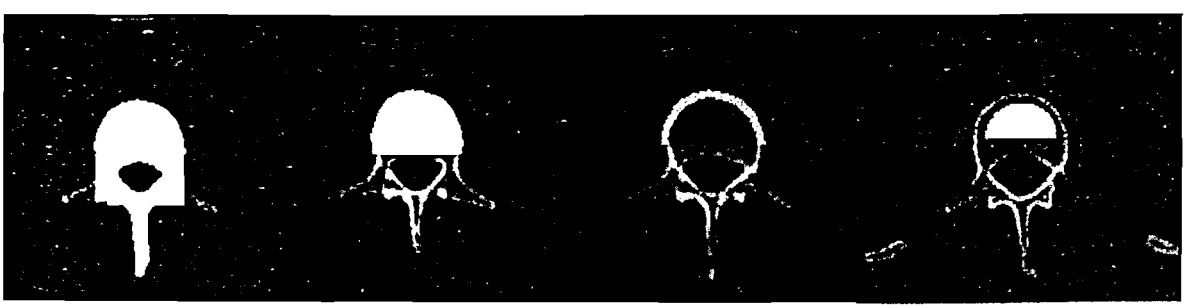

Fig. 1. Spinal QCT regions of interest included regions approximately matched to the bone volumes imaged by PA-DXA (SIM-AP), and lateral (SIM-LAT). The SIM-AP region included all of the vertebral bone except for the tranverse processes, and the SIM-LAT region excluded all of the posterior elements but not the vertebrae endplates. The spinal CORT –cortical- region encompassed the cortical rim of the vertbral body. The spinal TRAB –trabecular- region encompassed 70% of the volume of the vertebral body.

Table 2. BMD measurements obtained with QCT and DXA in the study population with degenerative changes (OA) grade 0 (none or mild) and grade 1 (moderate or severe) in different regions at the lumbar spine and femoral neck

Region	OA grade 0 Mean BMD±SD (n=29)	OA grade 1 Mean BMD±SD (n=22)	P value
2D QCT ellpt (mg/cm^3)	84.5923±28.3461	92.4722±22.6527	0.2901
2D QCT plld (mg/cm^3)	88.6466±28.0591	96.8301±23.0564	0.2716
2D QCT intg (mg/cm^3))	174.447±33.9509	192.821±32.0954	0.0558
3DQCT trab (mg/cm^3)	87.1599±24.3462	97.271±21.1815	0.1271
3DQCT cort (mg/cm^3)	159.82±32.182	184.342±36.9079	0.0147
Min CSA	862.232±170.965	920.689±190.355	0.2551
Max CSA	1597.3±202.71	1686.31±275.416	0.2099
3D QCT neck cort (mg/cm^3)	342.577±31.7901	353.651±29.2318	0.2083
3D QCT neck trab (mg/cm^3)	124.42±29.3643	140.031±38.4988	0.1066
3D QCT neck intg (mg/cm^3)	230.249±32.1726	256.43±48.6094	0.025
3D QCT troch cort (mg/cm^3)	403.966±59.3549	437.439±44.8451	0.032
3D QCT troch trab (mg/cm^3)	108.198±23.4454	125.166±43.8878	0.0816
3D QCT troch intg (mg/cm^3)	241.041±46.9756	286.459±68.8525	0.0073
3D QCT tot cort (mg/cm^3)	373.481±35.1036	394.508±34.737	0.0384
3D QCT tot trab (mg/cm^3)	115.808±23.7902	133.25±39.7959	0.0571
3D QCT tot intg (mg/cm^3)	232.586±39.9741	269.975±55.6144	0.0074
AP-DXA LS (g/cm^2)	0.853±0.171994	0.9635±0.152565	0.0211
AP-DXA neck (g/cm^2)	0.680034±0.109226	0.738091±0.095536	0.0531
AP-DXA troch (g/cm^2)	0.610517±0.094834	0.677273±0.117651	0.0294
AP-DXA ward (g/cm^2)	0.595414±0.130268	0.604909±0.133893	0.8

Discussion

A common finding in the spine of the elderly is OA, which refers to the deterioration of articular structures resulting from mechanical stress (1). OA causes changes in the spine that can be detected by radiographs (4, 11). OA changes in the spine, such as disk space narrowing, sclerosis, and osteophytosis, can influence BMD measurements. Several studies have investigated the impact of vertebral osteophytes on BMD measurements, each showing that the presence of osteophytes increased the measured BMD (17, 18). OA includes not only osteophytes at vertebrae, but also other changes at vertebral bodies, spinal processes, and facet joint. BMD results may be influenced when any of these changes occur within the region of BMD measurement (18). For this reason, QCT may have an advantage in the assessment of BMD because it can evaluate the trabecular bone of the vertebral body which should not be influenced by OA, as well as the cortical and integral bone (1, 12). Furthermore, using our volumetric QCT technique, we could also examine the trabecular and cortical bone in the hip, providing BMD measurements that are independent of bone size.

The results we found for spinal OA are in agreement with previous publications. In fact the influence of OA on PA-DXA and the influence of OA on cortical BMD assessed by both DXA and QCT have been reported by Yu et al. (21) and Ito et al. (12), respectively. In particular, Yu et al. confirmed the impact of vertebral osteophytes but also found that disk narrowing, sclerosis, and osteophytes at other sites in the spine elevated PA-DXA BMD compared to women without OA changes. They also evaluated the impact of OA on lateral-DXA, the mid-lateral ROI (mL-DXA), and

Table 3. Comparison of standardized BMD measurements obtained with QCT and DXA in different regions at the lumbar spine and femoral neck

Type of contrast	Effect size	95% LCI	95% UCI	P value
2DQTC ellpt (mg/cm3) vs. APDXA LS	−0.366	−1.162	0.430	0.368
2DQCT plld (mg/cm3) vs. APDXA LS	−0.354	1.151	0.442	0.384
2DQCT intg (mg/cm3) vs. APDXA LS	−0.118	−0.919	0.683	0.773
3DQCT trab (mg/cm3) vs. APDXA LS	−0.232	−1.030	0.567	0.570
3DQCT cort (mg/cm3) vs. APDXA LS	0.041	−0.765	0. 846	0.921
3DQCT neck cort (mg/cm3) vs. APDXA neck	−0.197	−0.991	0.597	0.627
3DQCT neck trab (mg/cm3) vs. APDXA neck	−0.094	−0.890	0.702	0.817
3DQCT neck intg (mg/cm3) vs. APDXA neck	0.092	−0.709	0.893	0.822
3DQCT troch cort (mg/cm3) vs. APDXA troch	−0.010	−0.812	0.792	0.980
3DQCT troch trab (mg/cm3) vs. APDXA troch	−0.130	−0.929	0.669	0.750
3DQCT troch intg (mg/cm3) vs. APDXA troch	0.155	−0.653	0.962	0.707

11. Iannuzzi L, Dawson N, Zein N, et al. Does drug therapy slow radiographic deterioration in rheumatoid arthritis? N Engl J Med 1983;309:1023–8.
12. Ito M, Hayashi K, Yamada M, Uetani M, Nakamura T. Relationship of osteophytes to bone mineral density and spinal fracture in men. Radiology 1993;189:497–502.
13. Jergas M, Breitenseher M, Gluer CC, Yu W, Genant H. Estimates of volumetric density from projectional estimates improve the discriminatory capability of dual X-ray absorptiometry. J Bone Miner Res 1995;10:1101–10.
14. Lang TF, Li J, Harris ST, Genant HK. Assessment of vertebral bone mineral density using volumetric quantitative CT. J Comput Assist Tomogr 1999;23:130–7.
15. Lang TF, Guglielmi G, van Kuijk C, De Serio A, Cammisa M, Genant HK. Measurement of bone mineral density at the spine and proximal femur by volumetric quantitative computed tomography and dual-energy X-ray absorptiometry in elderly women with and without vertebral fractures. Bone 2002;30:247–50.
16. Nevitt MC, Lane NE, Scott JC, et al. Radiographic osteoarthritis of the hip and bone mineral density. The Study of Osteoporotic Fractures Research Group. Arthritis Rheum 1995;38:907–16.
17. Nilas L, Gotfredsen A, Riis B, Christiansen C. The diagnostic validity of local and total bone mineral measurements in postmenopausal osteoporosis and osteoarthritis. Clin Endocrinol 1986;25:711–20.
18. Orwoll E, Oviatt S, Mann T. The impact of osteophytic and vascular calcifications on vertebral mineral density measurements in men. J Clin Endocrinol Metab 1990;70:1202–7.
19. Pogrund H, Makin M, Robin G, Menczel J, Steinberg R. Osteoporosis of the spine, pelvis and hand: a comparative study in a femoral neck fracture series. Clin Orthop 1979;139:156–63.
20. Reid I, Evans M, Ames R, Wattie D. The influence of osteophytes and aortic calcification on spinal mineral density in postmenopausal women. J Clin Endocrinol Metab 1991;72:1372–4.
21. Yu W, Gluer CC, Grampp S, et al. Spinal bone mineral assessment in postmenopausal women: a comparison between dual X-ray absorptiometry and quantitative computed tomography. Osteoporos Int 1995;5:433–9.

Original Article

How Often Does Lateral Spine DXA Detect Low Bone Mass in Patients with Both Normal PA Spine and Hip?

Michael Maricic, MD,[1] John Tesser, MD,[2] Zhao Chen, PHD,[3] Pamela Lund, MD,[4] and Oscar Gluck, MD[2]

[1]Arizona Arthritis Center, University of Arizona, Tucson, AZ; [2]Arizona Rheumatology Center, Phoenix, AZ; [3]Arizona Prevention Center, University of Arizona, Tucson, AZ; and [4]Department of Radiology, University of Arizona, Tucson, AZ

Abstract

The clinical utility of lateral bone mineral density (BMD) measurement for the diagnosis of osteoporosis remains controversial. Since both posterior–anterior (PA) spine and hip scans are universally performed, the true clinical utility of lateral dual-energy X-ray absorptiometry (DXA) should lie in its ability to detect low bone mass independent of both PA spine and hip. We examined lateral, PA and hip BMDs in 2134 referred Caucasian females aged 25–89 using the Hologic 2000. Compared only to PA scans, the additional percentages of women with very low BMD (*T*-score below –2.5 utilizing the National Health and Nutrition Examination Survey [NHANES] III normative database) on lateral were 7.3, 16.4, 28.2, 33.7, and 26.2% for age groups 25–49, 50–59, 60–69, 70–79, and 80–89, respectively. When the results from both PA and total hip measurements were combined, lower but still significant percentages were found: 5.4, 14.9, 24.4, 26.6, and 17.8% for age groups 25–49, 50–59, 60–69, 70–79, and 80–89, respectively. Utilizing the original Hologic normative database, the additional yield in women with a non-osteoporotic PA spine and femoral neck was quite low: 4.6, 8.5, 13.3, 10.0, and 2.5% for women age 25–49, 50–59, 60–69, 70–79, and 80–89, respectively. Thus, the lateral scans now add more additional patients into the very low BMD category. Whether the relationship to future fracture risk of low BMD and *T*-scores on lateral is similar to that of PA spine remains to be established.

Key Words: Bone densitometry; lateral BMD; osteoporosis; postmenopausal women.

Introduction

Until a prospective study examining the relationship of bone mineral density (BMD) and *T*-scores to relative fracture risk for the supine lateral dual-energy X-ray absorptiometry (DXA) is performed, the true clinical utility of this test will not be known. One potential value of lateral DXA may lie in its ability to exclude artifacts resulting from osteophytes and aortic calcification seen on posterior–anterior (PA), thereby providing a more accurate representation of vertebral BMD. Also, lateral DXA measures more predominant trabecular bone, which might increase the sensitivity of detecting early menopausal bone loss. Studies have demonstrated a higher association of BMD with age and with Quantitative Cat Scan (QCT) values on lateral DXA compared to PA *(1–3)*. These studies have suggested that lateral DXA is comparable to QCT and more sensitive than PA for the detection of low bone mass, and is more highly associated with fractures than PA BMD *(3)*. However, other studies comparing *Z*-scores of fracture patients to those without frac-

Address correspondence to Dr. Michael Maricic, Arizona Orthritis Center, University of Arizona, Tucson, AZ 85724. E-mail: maricic@u.arizona.edu

Journal of Clinical Densitometry, vol.1, no. 3, 251–257, Fall 1998

1094–6950/98/1:251–257/$9.75

tures have suggested that the diagnostic sensitivity of lateral DXA is no better or worse than PA *(4–6)*. This discrepancy may be owing to variability of the populations examined or to the high accuracy error on lateral spine DXA caused by uncertainty in the soft tissue baseline *(7,8)* and overlapping of ribs in front of L_2 and pelvis anterior to L_4.

Owing to the finding of higher sensitivity for the detection of low bone mass with aging in studies comparing lateral to PA DXA, it is widely held that lateral DXA may have its greatest clinical utility in the very elderly. However, since DXA of the hip is routinely performed along with the PA spine in clinical practice, the increasing prevalence of osteoporosis in the hip with aging might actually diminish the additional yield and potential clinical importance of the lateral in the very elderly.

Therefore, the major utility of low lateral BMD is likely to occur only in patients with normal values on both hip and PA scans. To date, most studies have reported the discrepancy between lateral and PA. The uniqueness of this study is the determination of the additional pickup of low BMD on lateral not seen on PA nor hip.

Last year, Hologic replaced their normative hip database with the National Health and Nutrition Examination Survey (NHANES) III database, which has a lower average peak bone mass for hip regions. As a consequence, without changes in hip BMD, an individual's *T*-score at the total hip, and especially at the femoral neck, would be increased based on the NHANES III database in comparison with the original Hologic database. This will result in a reduced number of people with osteoporosis at the hip and an increase in the potential utility of lateral DXA measurements among the older population. Therefore, we also examined how the switch to the NHANES III database affected the additional pickup of low bone mass on lateral scans.

Materials and Methods

Subjects

All subjects in the study were white female patients between ages 25–89 referred for bone densitometry either at the University of Arizona Medical Center in Tucson or at the Arizona Rheumatology Center in Phoenix from 1993 to 1996. At each center, lateral spines were performed routinely, in addition to PA and hip, as standard clinical protocol. Therefore, neither Institutional Review Board (IRB) approval nor informed consent was obtained for the added lateral scan. Since this was a retrospective, and not a prospective study, the only information recorded on patients was age, ethnicity, and body size. Chart review for complete medical or fracture history was not performed on any subject. Among the study subjects (n = 2134), 52% of scans were performed in Phoenix, and the rest in Tucson. All clinical information was treated confidentially, and only patients' identification numbers were used in the study.

Bone Mineral Density (BMD)

BMD of the PA spine (L_{1-4}), lateral spine (L_{2-4}), and total hip were measured with the Hologic QDR-2000, Waltham, MA, which has a C-arm for performing supine lateral scans. At each center, PA and lateral spine and hip scans were performed routinely as standard clinical protocol.

Each patient's regional scans were performed on the same day. Standard proce-

Table 1. Characteristics of the Study Population

Age groups	25–49 Yr $n = 369$ mean ± SD	50–59 Yr $n = 470$ mean ± SD	60–69 Yr $n = 603$ mean ± SD	70–79 Yr $n = 574$ mean ± SD	80–89 Yr $n = 118$ mean ± SD
Age (yr)	42.6 ± 6.7	54.6 ± 2.5	64.9 ± 2.7	73.9 ± 2.4	83.0 ± 2.3
PA spine-BMD (g/cm^2)	0.956 ± 0.161	0.924 ± 0.151	0.874 ± 0.157	0.844 ± 0.170	0.818 ± 0.191
Lateral spine-BMD (g/cm^2)	0.733 ± 0.110	0.679 ± 0.111	0.620 ± 0.114	0.578 ± 0.111	0.549 ± 0.118
Total Hip-BMD (g/cm^2)	0.833 ± 0.145	0.808 ± 0.129	0.756 ± 0.133	0.704 ± 0.134	0.645 ± 0.126
Weight (kg)	64.6 ± 20.2	66.9 ± 16.4	66.0 ± 15.9	62.1 ± 14.4	58.8 ± 9.4
Height (mm)	1557.5 ± 349.4	1606.9 ± 201.7	1585.3 ± 243.7	1565.4 ± 256.1	1564.2 ± 164.0

dures supplied by the manufacturer for scanning and analysis were followed. Both densitometers in Tucson and Phoenix utilized fan beam scanning, using the "array spine" for the PA scan and the "array fast lateral" for the lateral scan. Calibration with the manufacturer's spine phantom and quality-control analysis are performed at each site daily. Crosscalibration of the two scanners was conducted by repeatedly (10 times) measuring a same spine phantom at both centers. No systematic difference in the measurements was found between the two scanners ($p = 0.86$).

Statistical Analysis

Results of age, BMDs, height, and weight were expressed as mean ± 1 standard deviation (SD). *T*-scores for each hip scan were calculated from both the original Hologic and NHANES normative databases. *T*-scores for each PA and lateral spine scan were calculated from the Hologic normative database only, since the PA and lateral spine normative databases were not changed by the new software sent to all Hologic users in early 1997.

This article will refer to lateral *T*-scores >–1 as normal, those between –1 and –2.5 as "low BMD" and *T*-scores <–2.5 as "very low BMD," rather than use the terms osteopenia and osteoporosis, since this later terminology was not specifically developed for lateral scans. The percentages of women with normal BMD, low BMD (osteopenia), and very low BMD (osteoporosis) in each age group (10-yr interval) were calculated for lateral, PA spine, and hip scans. To examine the additional yield of the lateral in determining very low BMD, the percentages of women with very low BMD picked up by lateral, but not by PA alone, or not by either PA or hip (based on either the old Hologic hip normative database or the NHANES III data) were also computed. All the statistical analyses were done on SPSS (version 7.0).

Results

The general characteristics of each age group in the study population is presented in Table 1. There is a continued decrease in mean BMD at all the regional scan sites with age. The percentage of subjects in each age group being classified as having normal (*T*-score >–1), low BMD (*T*-score =–1 to –2.5), and very

Table 2. Percentages of Women with Normal, Low, and Very Low BMD

Age groups	25–49 Yr $n = 369$	50–59 Yr $n = 470$	60–69 Yr $n = 603$	70–79 Yr $n = 574$	80–89 Yr $n = 118$
Lateral spine (%)					
Normal (T>–1)	37.1	19.4	9.6	6.1	3.4
Low (T = –1 to –2.5)	49.1	54.9	41.5	27.5	24.6
Very low (T<–2.5)	13.8	25.7[b]	48.9[b]	66.4[b]	72.0[b]
PA spine (%)					
Normal (T>–1)	52.8	43.2	33.0	27.4	24.6
Low (T = –1 to –2.5)	33.3	40.6	41.0	37.1	26.3
Very low (T>–2.5)	13.8	16.2	26.0	35.5	49.2
Total hip (%)[a]					
Normal (T>–1)	52.6	45.1	30.2	19.5	7.6
Low (T = –1 to –2.5)	39.3	47.2	52.9	52.3	45.8
Very low (T<–2.5)	7.9	7.7	16.9	28.2	46.6

[a]Using the NHANES III data to calculate T-scores.
[b]McNemar's Test (lateral spine vs. PA spine): $p < 0.001$

Table 3. Agreement Between PA Spine Measurement and Lateral Spine Measurement

Age groups	25–49 Yr	50–59 Yr	60–69 Yr	70–79 Yr	80–89 Yr
κ	0.386	0.310	0.323	0.335	0.411

low BMD or osteoporosis (T-score <–2.5) is displayed in Table 2. On PA DXA, 16.2% of the age group 50–59 had osteoporosis, and this increased to 49.2% in the age group 80–89. Before age 60, very few women had osteoporosis at the total hip. The percentage increased with age and reached a peak of 46.6% in the age group of 80–89. Except in the group 25–49 yr old, the lateral scan picked up a significantly greater number of those with very low BMD than the PA scan (McNemar's Test $p < 0.001$).

The overall correlation between PA and lateral BMD was 0.67 ($p < 0.001$). The rate of BMD loss per year on PA spine (0.37%) was less than on lateral (0.47%). Therefore, the difference between PA and lateral BMD increases with age ($r = 0.11$, $p < 0.001$).

Table 3 shows the agreement between PA scan and lateral scan in detecting very low BMD. The κ test showed that the association between lateral scans and PA scans was statistically significant for every age group. However, the degree of the agreement was only fair *(9)* (0.31–0.40).

Figure 1 shows the additional pickup (percentages) in patients with a T-score below –2.5 on lateral without osteoporosis on the PA spine scan alone, and in patients without osteoporosis on either the PA spine and total hip scans (utilizing both NHANES III and the old Hologic hip normative databases). Since some patients with osteoporosis on lateral did not have osteoporosis on PA and/or hip, the additional diagnostic pickup is not a simple subtraction of the numbers shown in Table 2. Utilizing the current NHANES III database, performing lateral DXA in patients with normal PA scans may add an additional 7.3, 16.4, 28.2, 33.2, and 26.2% of women into the very low BMD (or osteoporosis) category for women age 25–49, 50–59, 60–69, 70–79 and 80–89 respectively. In those with nonosteoporotic PA and total hip scans, the additional yields of very low BMD on lateral measurements were reduced to 5.4, 14.9, 24.4, 26.6 and 17.8% for women age 25–49, 50–59, 60–69, 70–79 and 80–89, respectively. Therefore, even though the difference between PA and lateral BMD increases with age, the additional yield of lateral scans does not increase indefinitely in the very elderly. After age 80, it decreases owing to the increasing percentage of women with osteoporosis at the hip.

Utilizing the original Hologic hip normative database, the additional pickup on lateral (in those with nonosteoporotic PA and total hip scans) is even lower: 4.7,

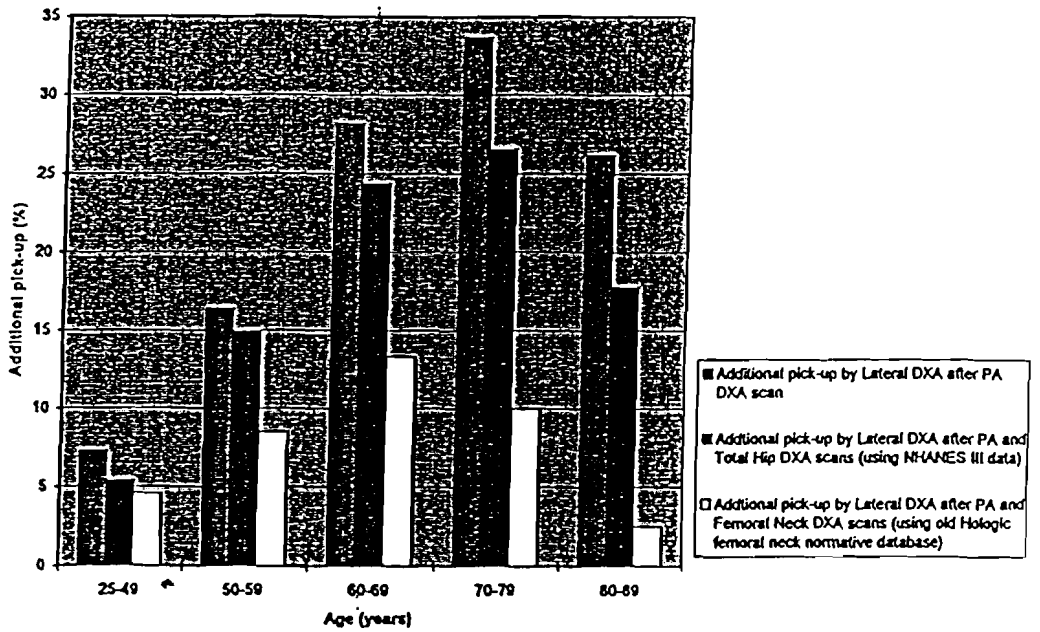

Fig. 1. Additional percentage of women with very low BMD (*T*-score <–2.5) at lateral DXA among different age groups

14.1, 21.4, 21.5, and 11.0% for women age 25–49, 50–59, 60–69, 70–79, and 80–89, respectively. If one utilized the femoral neck as the region of interest for the hip (which was the common practice), the additional yield after both PA spine and femoral neck was very low: 4.6, 8.5, 13.3, 10.0, and 2.5% for women age 25–49, 50–59, 60–69, 70–79, and 80–89, respectively. As demonstrated in Fig. 1, the additional yield in diagnosing very low BMD on lateral scans has increased substantially since changing from the femoral neck (Hologic database) to the total hip (NHANES III database).

Discussion

Since the potential utility of finding low BMD on the lateral scan is likely to be greatest in the absence of low BMD at other sites, the most important clinical question is whether low BMD is present on lateral in patients with normal hips and PA spines, and not only with normal PA spines. Although PA and lateral spine BMD are highly correlated, there is a statistically significant higher percentage of women over age 50 with a *T*-score below –2.5 on lateral compared to PA scan (range 16.4–33.7%). In women over age 50 who did not have osteoporosis on either PA spine or hip, the additional pickup of very low BMD on lateral scans is slightly lower, but still significant (14.9–26.6%).

The potential clinical utility of performing lateral DXA may have been increased as a result of changing the old Hologic hip database and femoral neck region of interest with the NHANES III total hip. The same individual would now be less likely to be diagnosed as being osteoporotic at the hip, increasing the additional pickup by the lateral.

From a cost-effective standpoint, in addition to the all-important relationship of lateral *T*-scores to future fracture risk, one important question is who should have a lateral scan performed. Our results

challenge the concept that the utility of the lateral increases in the very elderly population. Although the discrepancy between PA and lateral measurements increases with age, the additional pickup of low BMD on lateral not seen on PA spine or hip was actually reduced among women in their 80s (17.8%) compared with women in their 60s (24.4%) and 70s (26.6%), owing to the fact that the percentage of patients with osteoporosis at the hip sharply increased over age 80. The additional yield of finding very low BMD on lateral in women age 80–89 was not much different than in women age 50–59 (14.9%).

There are several limitations of this study:

1. Because this is a retrospective study of a referred population, complete fracture history was not obtained. Therefore the crucial question of the relationship of lateral spine BMD to fracture risk in this population is unknown.
2. Likewise, since we did not have complete clinical data, we are unable to determine whether the additional pickup on Lateral (after PA and hip) of very low bone mass in women age 25–49 (5.4%) and in women age 50–59 (14.9%) is owing to estrogen deficiency, or other factors, such as corticosteroid use, hyperthyroidism, and so forth. Such a study should be performed to determine if these younger patients with specific risk factors should have lateral scans, even when both PA and hip are normal.
3. Precision errors for lateral scans have been reported to be in the range of 2–4% *(10)*. Since ours is a retrospective study, the reproducibility for lateral scan and analysis for all technicians at each site is not known. The extent to which measurement and analysis errors affect our results is unknown.

In summary, the discovery of low BMD (and *T*-score) on lateral DXA not found on either PA spine or hip is significant among women over 50. However, even if low lateral BMD is found to be a predictor of future fracture risk, from a cost-effective standpoint, it might be best to reserve this scan only for those with a nonosteoporotic hip or PA spine.

References

1. Duboeuf F, Pommet R, Meunier PJ, Delmas PD. 1994 Dual-energy x-ray absorptiometry of the spine in anteroposterior and Lateral projections. Osteoporosis Int 4:110–116.
2. Finkelstein JS, Cleary RL, Butler JP, Antonelli R, Mitlak BH, Deraska DJ, et al. 1994 A comparison of Lateral versus anterior-posterior spine dual energy x-ray absorptiometry for the diagnosis of osteopenia. J Clin Endocrinol Metab 78:724–730.
3. Guglielmi G, Grimston SK, Fischer KC, Pacifici R. 1994 Osteoporosis: diagnosis with Lateral and posteroanterior dual X-ray absorptiometry compared with quantitative CT. Radiology 192:845–850.
4. Uebelhart D, Duboeuf F, Meunier PJ, Delmas PD. 1990 Lateral dual-photon absorptiometry: A new technique to measure the bone mineral density at the lumbar spine. J Bone Miner Res 5:525–531.
5. Del Rio L, Pons F, Huguet M, Setoain FJ, Setoain J. 1995 Anteroposterior versus Lateral bone mineral density of spine assessed by dual x-ray absorptiometry. Eur J Nuclear Med 22:407–412.
6. Raymaker JA, Hoekstra O, van Putten J. 1986 Osteoporotic fracture prevalence and bone mineral mass measured with CT and DPA. Skeletal Radiol 15:191–197.
7. Tothill P, Avenell A. 1994 Errors in dual-energy x-ray absorptiometry of the lumbar spine owing to fat distribution and soft tissue thickness during weight changes. Br J Radiol 67:71–75.
8. Edmondston SJ, Singer KP, Price RI, Breidahl PD. 1993 Accuracy of Lateral dual energy x-ray absorptiometry for the determination of bone mineral content in the thoracic and lum-

bar spine: an *in-vitro* study. Br J Radiol 66:309–313
9. Landis JR, Koch GG. 1977 The measurement of observer agreement for categorical data. Biometrics 33:159–174.
10. Mazess RB, Barden HS, Eberle RW, Denton MD. 1995 Age changes of spine density in Posterior-Anterior and Lateral projections in normal women. Calcif Tissue Int. 56:201–205.

RELATIVE FRACTURE RISK ESTIMATES BY ODDS RATIOS FOR QCT*

	ODD RATIOS	
QUARTILE	QCT	PA DPA
1	1	1
2	2.5	0.4
3	5.7	2.8
4	10.5	3.8

BMD to double Odds Ratio: QCT = -19.3 mg/cc; DPA = - 0.15 g/cm^2

*Heuck et al, Mild versus Definite Osteoporosis: Comparison of BMD Techniques J. Bone Mineral Res. 4:891-899, 1989.

BMD Values for FX and Non-FX patients by QCT and PA DXA

	QCT(mg/cc)	PA DXA (g/cm2)
Grampp, Genant et al (`96)		
FX Mean	72.0	0.79
Non FX Mean	106.0	0.90
% decrement	31.5%	12.0%
Pacifici et al (`90)		
FX Mean	59.3	0.69
Non FX Mean	94.5	0.81
% decrement	37.0%	15.0%
Smith et al(`94)		
FX Mean	33.0	0.73
Non FX Mean	73.0	0.84
% decrement	54.8%	13.1%
Guglielmi et al (`94)		
FX Mean	46.1	0.74
Non FX Mean	98.1	0.89
% decrement	53.0%	16.8%
Average % decrement	44.2	14.2

% decrement ratio (QCT/PA DXA) ≅ 3.1

DISCRIMINATION OF FRACTURED AND NON-FRACTURED POSTMENOPAUSALWOMEN BY PA DXA, LATERAL DXA AND QCT

	Odds Ratios	*Annual Loss %*
PA DXA	2.4	0.30
LAT DXA	2.6	0.58
QCT	4.3	1.18

Genant et al. 11th Int. BMD Conference Sept. 1995

DISCRIMINATION OF MILD FROM DEFINITIVE FRACTURES IN OSTEOPOROTIC PATIENTS *

	QCT mg/cm^3	PA DPA g/cm^2
Mild Deformity	90 ± 25	0.89±.16
Definitive Fracture	72 ± 21	0.79±.14
% Decrement (Mild/Defin.)	- 20	-11

*Heuck et al, Mild versus Definite Osteoporosis: Comparison of BMD Techniques. J. Bone Mineral Res. 4: 891-899, 1989.

EFFECTIVE DOSE

Natural Background / Year	2400 µS
Return Transatlantic Flight	80 µS
Lateral Lumbar X-Ray	700 µS
DXA Lumbar	1 µS
Lateral Lumbar Topogram CT	30 µS
BMD with QCT	30 µS
Dental X-Ray	50 µS
Chest X-Ray	100 µS

Kalendar, Osteoporosis Intl. (1992) 2:82-87